



TECHNISCHE UNIVERSITÄT MÜNCHEN

Fakultät für Medizin

**T cell activation versus tolerance induction in
islet autoimmunity**

Isabelle Daniela Serr

Vollständiger Abdruck der von der Fakultät für Medizin der Technischen Universität München zur Erlangung des akademischen Grades eines Doktors der Naturwissenschaften genehmigten Dissertation.

Vorsitzender: Prof. Dr. Percy A. Knolle

Prüfer der Dissertation:

1. Prof. Dr. Anette-Gabriele Ziegler
2. Prof. Dr. Martin Hrabé de Angelis
3. Prof. Dr. Ludger Klein

Die Dissertation wurde am 02.08.2017 bei der Technischen Universität München eingereicht und durch die Fakultät für Medizin angenommen.

2.3 Cell staining and flow cytometry	- 27 -
2.4 Proliferation assays	- 28 -
2.5 Tetramer stainings.....	- 28 -
2.6 Generation of insulin-specific CD4 ⁺ T cell clones.....	- 28 -
2.7 HLA-DQ8 peptide-binding assay.....	- 29 -
2.8 <i>In vitro</i> Treg induction assay	- 29 -
2.9 DNA bisulfite conversion and methylation analysis.....	- 30 -
2.10 Reconstitution of NSG mice and <i>in vivo</i> Treg induction.....	- 30 -
2.11 Expression analysis of mRNAs and miRNAs	- 30 -
2.12 <i>In vitro</i> Treg suppression assay.....	- 30 -
2.13 <i>In vitro</i> TFH precursor cell induction assay.....	- 31 -
2.14 Histopathological analysis and immunofluorescent staining of pancreas sections	- 32 -
2.16 Statistics.....	- 32 -
3. Results: Publications originating from this thesis.....	- 33 -
3.1 Summary of publications.....	- 33 -
3.2 Type 1 diabetes vaccine candidates promote human Fox3(+) Treg induction in humanized mice	- 35 -
3.2.1 Supplementary information.....	- 36 -
3.2.2 Authors' contributions	- 37 -
3.3 miRNA92a targets KLF2 and PTEN to promote human T follicular helper precursors in T1D islet autoimmunity	- 38 -
3.3.1 Supplementary information.....	- 39 -
3.3.2 Authors' contributions	- 40 -
4. Discussion.....	- 42 -
5. References.....	- 53 -
Danksagung.....	- 80 -

List of abbreviations

AGO2	Argonaute 2
Akt	Protein kinase B
aAPC	Artificial antigen presenting cell
APC	Antigen presenting cell
Ascl2	Achaete-scute homologue 2
Bcl6	B cell lymphoma 6
BCR	B cell receptor
CCR	C-C chemokine receptor
CD	Cluster of differentiation
CD25	High-affinity IL2 receptor alpha chain
CXCR	C-X-C chemokine receptor
CpG	5'-C-phosphate-G-3'
Ctla4	Cytotoxic T lymphocyte antigen 4
DC	Dendritic cell
dsRNA	Double stranded RNA
EAE	Experimental autoimmune encephalomyelitis
Foxp3	Forkhead box protein 3
Foxo	Forkhead box protein O
GAD	Glutamic acid decarboxylase
GC	Germinal center
HLA	Human leukocyte antigen
HSC	Hematopoietic stem cell
IA2	Insulinoma antigen 2

IAA	Insulin autoantibodies
ICOS	Inducible T cell costimulator
IL	Interleukin
IL2Rg	Interleukin 2 receptor gamma chain
i.p.	intra peritoneal
IPEX	Immunedysregulation polyendocrinopathy enteropathy X-linked syndrome
KLF2	Krueppel-like factor 2
MHCII	Major histocompatibility complex class II
miRNA	microRNA
mTOR	Mammalian target of rapamycin
NFAT5	Nuclear factor of activated T cells 5
NOD	Non-obese diabetic
NSG	NOD Scid IL2Rg knockout
PBMC	Peripheral blood mononuclear cell
PD1	Programmed cell death 1
PHLPP2	PH domain and leucine rich repeat protein phosphatase 2
PI3K	Phosphatidylinositol-3-kinase
Pri-miRNA	Primary miRNA
Prkdc	Protein kinase, DNA activated, catalytic polypeptide
PSGL-1	P-selectin glycoprotein ligand 1
PTEN	Phosphatase and tensin homolog
RISC	RNA induced silencing complex
RNAi	RNA interference
Ror α	retinoid-related orphan receptor alpha

SAP	SLAM-associated-protein
Scid	Severe combined immunodeficiency
siRNA	silencer RNA
Sirpa	Signal regulatory protein alpha
S1PR1	Sphingosin 1 phosphate receptor 1
TCR	T cell receptor
T1D	Type 1 Diabetes
TFH cell	T follicular helper cell
TGF β	Transforming growth factor beta
Treg	regulatory T cell
TSDR	Treg specific demethylated region
UTR	Untranslated region
VNTR	Variable number of tandem repeats
ZnT8	Zinc transporter 8

Publications included in this thesis

Peer-reviewed publications:

Type 1 diabetes vaccine candidates promote human Foxp3(+)Treg induction in humanized mice

Isabelle Serr, Rainer W. Fürst, Peter Achenbach, Martin G. Scherm, Füsün Gökmen, Florian Haupt, Eva-Maria Sedlmeier, Annette Knopff, Leonard Shultz, Richard A. Willis, Anette-G. Ziegler and Carolin Daniel. *Nature Communications* 2016;7:10991.

miRNA92a targets KLF2 and PTEN to promote human T follicular helper precursors in T1D islet autoimmunity

Isabelle Serr, Rainer W. Fürst, Verena B. Ott, Martin G. Scherm, Alexei Nikolaev, Füsün Gökmen, Stefanie Kälin, Stephanie Zillmer, Melanie Bunk, Benno Weigmann, Nicole Kunschke, Brigitta Loretz, Claus-Michael Lehr, Benedikt Kirchner, Bettina Haase, Michael Pfaffl, Ari Waisman, Richard A. Willis, Anette-G. Ziegler and Carolin Daniel. *Proceedings of the National Academy of Sciences* 2016;113(43):E6659–E6668.

Publications not included in this thesis

Peer-reviewed publications:

A miRNA181a/NFAT5 axis links impaired T cell tolerance induction with autoimmune Type 1 diabetes

Isabelle Serr, Martin G. Scherm, Adam M. Zahm, Jonathan Schug, Victoria K. Flynn, Markus Hippich, Stefanie Kälin, Maike Becker, Peter Achenbach, Alexei Nikolaev, Katharina Gerlach, Nicole Kunschke, Brigitta Loretz, Claus-Michael Lehr, Benedikt Kirchner, Melanie Spornraft, Bettina Haase, James Segars, Christoph Küper, Ralf Palmisano, Ari Waisman, Richard A. Willis, Wan-Uk Kim, Benno Weigmann, Klaus H. Kaestner, Anette-Gabriele Ziegler and Carolin Daniel. *Science Translational Medicine* under revision.

Treg vaccination in autoimmune type 1 diabetes

Isabelle Serr, Benno Weigmann, Randi Kristina Franke and Carolin Daniel. *Biodrugs* 2014;28(1):7-16.

Summary

Defects in immune tolerance are critical triggers of autoimmune Type 1 Diabetes (T1D). A better understanding of their molecular basis is therefore pivotal for the development of novel therapeutic strategies aimed at limiting autoimmune activation and progression. CD25⁺Foxp3⁺ regulatory T cells (Tregs) are the main mediators of peripheral T cell tolerance and their *de novo* induction is a long envisioned goal for the restoration of tolerance in autoimmunity. However, the exact requirements, especially for human Treg induction, are ill defined. Therefore, we aimed here to investigate the antigen-specific induction of human Tregs *in vitro* and *in vivo* in a humanized mouse model. The highly variable progression to symptomatic T1D which ranges from a few months to more than two decades in children underscores the plasticity in mechanisms regulating immune activation versus immune tolerance. T cells from children at a pre-symptomatic stage of the disease, who are autoantibody positive but have not yet progressed to symptomatic T1D, therefore offer a valuable resource for studying signaling pathways involved in aberrant immune activation versus immune tolerance. In this thesis, we sought to analyze mechanisms of aberrant immune activation during the early heterogeneous phase of the disease. Here, focus was set on T follicular helper (TFH) cells, a cell type important for antibody production by B cells. Additionally, we aimed at studying miRNAs that might be involved in regulating aberrant immune activation or impairments in T cell tolerance, because of their ability to regulate complex cellular states. Using novel insulin-specific tetramer reagents, we show here, that children with recent activation of islet autoimmunity display decreased frequencies of insulin-specific CD25⁺Foxp3⁺ regulatory T cells (Tregs), which are important mediators of immunological tolerance. Likewise, we observe increased frequencies of T follicular helper (TFH) precursor cells in these children with recent activation of islet autoimmunity. These effects are however reversed in children with longterm autoimmunity, meaning with autoantibodies for more than 10 years without developing the symptomatic disease, supporting the concept of inducing regulatory T cells or limit immune activation to delay the progression to symptomatic T1D. In the context of this thesis, we demonstrate that human Treg induction requires subimmunogenic stimulation with a strong agonistic ligand for the T cell receptor (TCR). We show that strong agonistic insulin variants are able to induce human Tregs from naïve T cells *in vitro* and *in vivo* in a humanized mouse model and that the induced Tregs are stable and functional. Concerning the underlying mechanisms, we demonstrate that the enhanced frequencies of TFH cells in children with recent activation of islet autoimmunity are mediated by an increased abundance of miRNA92a and identify krueppel-like factor 2 KLF2 as a novel target of this miRNA. Most importantly, we demonstrate that the inhibition of miRNA92a by an antagomir can reduce insulinitis scores and autoantibody titers as well as immune activation in non-obese diabetic (NOD) mice *in vivo*. The data presented here contribute to the understanding of requirements for efficient Treg induction as well as to the mechanistic basis of aberrant immune activation and defective

tolerance in islet autoimmunity. Additionally, the introduced novel tetramer reagents and humanized mice are new tools that will help to improve clinical trial readouts, as well as the evaluation of translatability of new reagents to the human disease.

Zusammenfassung

Defekte in der Immuntoleranz sind wichtige Auslöser für Typ 1 Diabetes (T1D). Ein detaillierteres Verständnis der zugrunde liegenden molekularen Mechanismen ist daher essentiell zur Entwicklung von neuen Therapieansätzen zur Hemmung der Aktivierung und des Fortschreitens der Autoimmunität. CD25⁺Foxp3⁺ regulatorische T-Zellen (Tregs) sind entscheidende Vermittler der peripheren zellulären Immuntoleranz und ihre *de novo* Induktion ist ein seit langem angestrebtes Ziel zur Wiederherstellung der Toleranz bei Autoimmunität. Allerdings ist über die genauen Voraussetzungen für die *de novo* Induktion von Tregs, insbesondere im humanen System, nur wenig bekannt. Deshalb war es unser Ziel, die antigen-spezifische Induktion von humanen Tregs *in vitro* und *in vivo* in einem humanisierten Mausmodell zu untersuchen. Die starke Varianz in der Zeit bis zur Entwicklung des symptomatischen T1D, die in Kindern zwischen wenigen Monaten und mehr als zwei Jahrzehnten betragen kann, betont die Plastizität in Mechanismen, die Immunaktivierung und Immuntoleranz regulieren. T-Zellen von Kindern in einem prä-symptomatischen Stadium der Krankheit, die Autoantikörper positiv, aber noch nicht zur symptomatischen Krankheit fortgeschritten sind, bieten daher eine wertvolle Ressource zur Untersuchung von Signalwegen, die in der Immunaktivierung versus Immuntoleranz involviert sind. In dieser Arbeit wollten wir die Mechanismen der abnormen Immunaktivierung während dieser frühen, heterogenen Phase der Krankheit untersuchen. Hier haben wir unseren Fokus auf T folliculäre Helfer (TFH) Zellen gesetzt, einem Zelltyp, der für die Antikörperproduktion durch B-Zellen essentiell ist. Zusätzlich zielten wir darauf ab, miRNAs zu untersuchen, die an der Regulation der abnormen Immunaktivierung oder der gestörten Immuntoleranz beteiligt sind, wegen ihrer Fähigkeit komplexe zelluläre Zustände zu regulieren. Mithilfe von neuen insulin-spezifischen Tetramer-Reagenzien zeigen wir hier, dass Kinder mit kürzlich eingetretener Aktivierung der Inselautoimmunität, eine verringerte Frequenz an insulin-spezifischen Tregs aufweisen. Ebenso sehen wir in den Kindern mit kürzlich eingetretener Aktivierung der Inselautoimmunität eine erhöhte Frequenz von TFH Vorläuferzellen. Diese Effekte sind allerdings umgekehrt in Kindern mit Langzeit Inselautoimmunität, die Autoantikörper für mehr als 10 Jahre aufweisen, ohne die symptomatische Krankheit zu entwickeln, was das Konzept der Induktion von insulin-spezifischen Tregs zur Verhinderung des Fortschreitens zum symptomatischen T1D unterstützt. Im Zusammenhang dieser Dissertation zeigen wir, dass die Induktion von humanen Tregs die Gabe von stark-agonistischen Liganden für den T-Zell Rezeptor (TCR) unter subimmunogenen Bedingungen benötigt. Wir zeigen, dass stark-agonistische Insulinvarianten Tregs aus naiven humanen T-Zellen induzieren können, *in vitro* und *in vivo* in einem humanisierten Mausmodell und, dass die induzierten Tregs stabil und funktionell sind. Bezüglich der zugrunde liegenden Mechanismen zeigen wir, dass der Anstieg in TFH Zellen in Kindern mit kürzlich eingetretener Aktivierung der Inselautoimmunität durch eine erhöhte Expression der miRNA92a hervorgerufen wird und wir identifizieren Krueppel-like factor 2 (KLF2) als ein neues Target von miRNA92a. Darüber

hinaus zeigen wir, dass die Hemmung der miRNA92a mittels eines antagomirs zu einer Reduktion des Insulitis Scores und der Insulin Autoantikörper Titer, sowie der Immunaktivierung im non-obese diabetic (NOD) Mausmodell *in vivo* führt. Die hier präsentierten Daten tragen zu einem detaillierteren Verständnis der Voraussetzungen für die Induktion von humanen Tregs, sowie der Mechanismen von abnormer Immunaktivierung und gestörter Immuntoleranz in Inselautoimmunität bei. Zusätzlich werden die hier eingeführten neuen Tetramer-Reagenzien und humanisierten Mäuse zu einer Verbesserung der Auswertung von klinischen Studien, sowie der Bewertung der Nutzbarkeit von neuen Reagenzien für den humanen T1D beitragen.

1. Introduction

1.1 Immunological self-tolerance

Already in the beginning of the 20th century, Paul Ehrlich proposed, that the immune system generally avoids a reaction against the body's own structures, a phenomenon he called "horror autotoxicus" (Ehrlich, 1906). This discrimination of self versus non-self is acquired early during development and maintained throughout life mainly in two ways: recessive and dominant tolerance. Recessive tolerance happens during T cell development in the thymus to eliminate self-reactive T cell receptors (TCRs) that develop during somatic rearrangement (Kappler et al., 1987; Kisielow et al., 1988). If an autoreactive T cell escapes negative selection, a second mechanism, called dominant tolerance, will help to tame their autoreactive response. The main mediators of dominant tolerance are CD4⁺CD25⁺ regulatory T cells (Tregs) (Sakaguchi et al., 1995; Thornton and Shevach, 1998).

1.1.1 Regulatory T cells execute dominant tolerance

Tregs develop in the thymus (Apostolou et al., 2002; Jordan et al., 2001) or can be induced from naïve T cells in the periphery (Apostolou and von Boehmer, 2004; Kretschmer et al., 2005; Verginis et al., 2008). Tregs are characterized by a high expression of the high-affinity α chain of the interleukin 2 (IL2) receptor (CD25) (Sakaguchi et al., 1995; Thornton and Shevach, 1998) and the expression of their master transcription factor Forkhead box protein 3 (Foxp3). Foxp3 is the Treg lineage specifying factor and is essential for Treg development and function (Fontenot et al., 2003; Fontenot et al., 2005; Hori et al., 2003; Khattri et al., 2003; Roncador et al., 2005). Tregs obtain the capacity to tame their autoreactive counterparts in various ways: They can inhibit T cell responses directly by killing their effector T cell counterparts via secretion of lytic enzymes, such as granzyme B (Cao et al., 2007; Gondek et al., 2005), they can secrete immunosuppressive cytokines like IL10 (Asseman et al., 1999; Kearley et al., 2005) or transforming growth factor β (TGF β) (Fahlén et al., 2005; Green et al., 2003), and they can disrupt the metabolic environment of the effector T cells. For example Tregs can deprive their surroundings from IL2, a cytokine which is crucial for CD4⁺T cell responses, via the high expression of CD25 (Pandiyan et al., 2007). Most importantly, Tregs can also modulate the activity of antigen-presenting cells (APCs) (Misra et al., 2004; Onishi et al., 2008). Since Treg mediated suppression does not necessarily require cell contact, Tregs are able to not only inhibit T cells with the same antigen specificity, but also other T cells in their proximity, a process called bystander suppression (Miller et al., 1991).

A tight regulation of the immune system is of great importance in order to, on the one hand, ensure protective immune responses against foreign antigens like viruses or bacteria, but on the other hand avoid immune reactions against self-antigens. The failure of the immune system to discriminate self from non-self structures leads to the development of autoimmune

diseases, characterized by an immune reaction of the body directed against self-antigens. The essential role of Tregs in regulating immune responses is evidenced by the lethal autoimmune phenotype of mice with the Scurfy mutation in the *Foxp3* gene (Brunkow et al., 2001) and similar mutations in the human gene leading to the fatal autoimmune disorder immunodysregulation polyendocrinopathy enteropathy X-linked syndrome (IPEX) (Bennett et al., 2001).

1.2 Autoimmune diseases – the failure of immunological self-tolerance

There are more than 80 diseases known which have an autoimmune character. According to the National Institutes of Health all autoimmune diseases combined affected 23.5 million US citizens in 2012 and the incidence is rising (National Institute of Environmental Health Sciences, 2012). Autoimmune diseases can be separated into diseases with a systemic or organ-specific autoimmune reaction. The most common organ-specific autoimmune diseases are Type 1 Diabetes (T1D), Multiple Sclerosis and Rheumatoid Arthritis.

T1D is one of three diseases included in the term diabetes, the other two being Type 2 Diabetes and Gestational Diabetes. In T1D the immune system attacks and destroys the insulin-producing β cells in the islets of Langerhans in the pancreas. T1D is also known as juvenile diabetes, because the disease onset is usually very early in life. Intensive research is focused on finding a treatment or preventive measurement for T1D, however to date, individuals suffering from the disease require lifelong insulin-replacement therapy and are at high risk of developing secondary complications such as blindness, heart diseases and kidney problems. In 2015 half a million people worldwide were affected by T1D with 86.000 new cases every year and this incidence is rising by 3% every year (International Diabetes Federation, 2015). This incidence increase is especially dramatic in children below the age of 5 years, with a doubling in the number of new cases being predicted from 2005 to 2020 (Patterson et al., 2009).

1.2.1 Immunopathogenesis of human Type 1 Diabetes

T1D risk has an environmental and a genetic component. Environmental factors that have been proposed to influence T1D development are among others certain viruses, microbial stimulation and the diet early in life (summarized in (Rewers and Ludvigsson, 2016)).

It is apparent, that in T1D a combination of environmental and genetic factors make up the risk for disease development. However, the genetic component contributes extensively to the risk, indicated by the around 10 times increased risk in children with a first-degree relative with T1D, depending on which family member is affected (Bonifacio et al., 2004; Hemminki et al., 2009; Ziegler and Nepom, 2010). The strongest contributor to the genetic risk for T1D is the human leucocyte antigen (HLA) class II, with the genotype HLA-DR4; HLA-DQ8

accounting for the highest risk (Nerup et al., 1974; Singal and Blajchman, 1973; Todd et al., 1987; Ziegler and Nepom, 2010). In children with a family history of T1D the risk can rise up to 30% if this genotype is present, depending on the family member already affected by T1D (Aly et al., 2006; Schenker et al., 1999; Ziegler and Nepom, 2010). Even in children without a family history of T1D the risk to develop T1D can rise to 5% if this genotype is present (Emery et al., 2005; Ziegler and Nepom, 2010). In the general Caucasian population the HLA-DR4; HLA-DQ8 genotype is present in around 2.3% of the children born in the US and 39% of diabetic patients with disease onset before age 20 harbor the HLA-DR4; HLA-DQ8 genotype (Lambert et al., 2004; Ziegler and Nepom, 2010).

Genome wide association studies have identified several variants in gene loci other than the HLA locus associated with T1D (Barrett et al., 2009; Todd et al., 2007). The highest contributor is the insulin locus, where a variation in the variable number of tandem repeats (VNTR) 5' of the insulin gene is responsible for higher expression in the thymus and a reduced risk for T1D development (Pugliese et al., 1997; Vafiadis et al., 1997).

Already in the beginning of the 1970s and 1980s researchers have highlighted that in T1D there is a long pre-symptomatic phase marked by the presence of islet autoantibodies and that these autoantibodies are powerful tools for risk assessment in T1D (Bonifacio et al., 1990; Bottazzo et al., 1974; Gorsuch et al., 1981). By now, islet autoantibodies against four islet autoantigens have been identified and are used for predictive purposes: insulin (Palmer et al., 1983), glutamic acid decarboxylase (GAD) (Baekkeskov et al., 1990), insulinoma-antigen 2 (IA2) (Lan et al., 1994; Rabin et al., 1994) and zinc transporter 8 (ZnT8) (Wenzlau et al., 2007). Using a prospective follow-up from birth cohort, Anette-Gabriele Ziegler and colleagues have shown in 2013 that the lifelong risk for T1D development approaches 100% if two or more autoantibodies are present (Ziegler et al., 2013).

These findings have paved the way for a proposed new staging of the disease, where the presence of multiple autoantibodies without clinical symptoms is included in the disease diagnosis as pre-symptomatic T1D (Insel et al., 2015). The time of progression from autoantibody development (so-called 'seroconversion') to clinical symptoms is very heterogeneous and can range from a few months in some children (so-called fast progressors) to more than a decade in others (so-called slow progressors) (Ziegler et al., 2013). However, currently very little is known about the mechanisms underlying this heterogeneity.

The identification of children with a pre-symptomatic disease allows the study of mechanisms of islet autoimmunity before the onset of the symptomatic disease, a time when the targets of the autoimmune attack to a large extent are destroyed already. Specifically, the heterogeneity in the disease progression offers a tool to study mechanisms of aberrant

immune activation versus T cell tolerance. As one T cell type involved in the promotion of immune activation, T follicular helper (TFH) cells were studied in the context of this thesis.

1.2.2 Immune effector mechanisms in Type 1 Diabetes: T follicular helper cells

TFH cells are a subset of CD4⁺T cells that are defined by the expression of their master transcription factor B-cell lymphoma 6 (Bcl6) (Johnston et al., 2009; Nurieva et al., 2008; Yu et al., 2009), the C-X-C chemokine receptor type 5 (CXCR5) (Breitfeld et al., 2000; Kim et al., 2001; Schaerli et al., 2000) and by the secretion of their effector cytokine IL21 (Avery et al., 2010; Linterman et al., 2010; Zotos et al., 2010). The expression of CXCR5 together with a low expression of C-C chemokine receptor 7 (CCR7) enables these T cells to enter the B cell follicle of the lymph node (Hardtke et al., 2005; Haynes et al., 2007), where they take part in the germinal center (GC) reaction, helping B cells to undergo class switch recombination and to produce high-affinity antibodies (Breitfeld et al., 2000; Johnston et al., 2009; Kim et al., 2001; Nurieva et al., 2008; Schaerli et al., 2000; Yu et al., 2009).

Because of their requirement for functional humoral immune responses, TFH cells play a major role in the clearance of infections (Harker et al., 2011) and are important for long-lasting vaccinations (Bentebibel et al., 2013). Since autoantibodies are a hallmark of many autoimmune diseases, TFH cells have been studied in the context of autoimmunity. Recently, Rupert Kenefeck and colleagues have demonstrated in a transgenic TCR model, that the transfer of TFH cells from diabetic mice to healthy recipients can induce diabetes (Kenefeck et al., 2015). Furthermore, increased IL21 production by CD4⁺T cells and increased frequencies of circulating TFH precursors have been demonstrated in patients with T1D (Ferreira et al., 2015). However, all of these studies focused on patients with established T1D, a point where most of the pancreatic β cells, the targets of the immune attack in T1D, are destroyed already. Data on the involvement of TFH cells in disease progression and initiation is lacking.

TFH cells have been studied extensively in animal models, yet their differentiation in humans is still poorly understood. One major challenge in the study of human TFH cells is their primary point of action in the lymph nodes and limited access in the blood. Studies by He *et al.* have demonstrated, that a CXCR5⁺CCR7^{low} programmed cell death 1 (PD1)^{high} TFH precursor population circulates in the blood (He et al., 2013). These cells are CD45RA⁻, indicating an antigen-experienced, memory state. CXCR5⁺CCR7^{low}PD1^{high}TFH precursors can be readily reactivated and help to produce high-affinity antibodies in response to infections and their frequency in the blood correlates with the frequency of active TFH cells in the lymph nodes (He et al., 2013). Therefore, circulating CXCR5⁺CCR7^{low}PD1^{high}TFH precursors offer a good opportunity to study TFH responses in health and disease.

In 2011, Morita *et al.* have described three subsets of circulating CXCR5⁺TFH cells, termed Th1-like, Th2-like and Th17-like TFH cells, which display a T helper-like profile and produce similar cytokines as their T helper cell counterparts, although to a lesser extent (Morita et al.,

2011). These precursors can be distinguished by the combination of expression of CXCR3 and CCR6, with Th1-like TFH cells being CXCR3⁺CCR6⁻, Th2-like TFH cells being CXCR3⁻CCR6⁻ and Th17-like TFH cells being CXCR3⁻CCR6⁺ (Morita et al., 2011). These subsets are distinct in their ability to provide B cell help: whereas Th1-like TFH cells are unable to provide B cell help, Th2-like and Th17-like TFH cells are able to do so, although impacting differentially on class switching (Morita et al., 2011).

The differentiation of TFH cells is a highly complex process, involving several differentiation steps and factors. When a naïve T cell gets activated via its TCR during an immune response, it can induce the TFH program by upregulating Bcl6, CXCR5 and inducible T cell costimulator (ICOS) and induce IL21 production (Deenick et al., 2010; Goenka et al., 2011; Langenkamp et al., 2003). Further characteristics of these early TFH cells are the upregulation of PD1, downregulation of CCR7 and downregulation of P-selectin glycoprotein ligand 1 (PSGL-1) (Deenick et al., 2010; Odegard et al., 2008; Poholek et al., 2010). Achaete-scute homologue 2 (Ascl2), another transcription factor important for early TFH cell development, was recently identified. It was highlighted in mouse studies that Ascl2 expression can induce CXCR5 expression in CD4⁺T cells and that the upregulation of Ascl2 will precede Bcl6 expression (Liu et al., 2014).

Bcl6 is transiently induced by stimulation with IL6, IL21 and ICOS signaling (Choi et al., 2011a; Nurieva et al., 2008; Nurieva et al., 2009). ICOS upregulates *Bcl6* by relieving the repression of *Bcl6* via forkhead box protein O1 (Foxo1) (Stone et al., 2015). Alternatively, Foxo1 repression of *Bcl6* can also be relieved by degradation via the E3 ubiquitin ligase ITCH (Xiao et al., 2014). Consequently, TFH differentiation is dependent on low levels of Foxo1.

ICOS is additionally required in TFH cells to induce the production of IL21 (Odegard et al., 2008) and is furthermore involved in the migration of TFH cells to the B cell follicle via the interaction with ICOS-ligand on B cells (Xu et al., 2013). TFH function is largely dependent on ICOS signaling via phosphatidylinositol-3-kinase (PI3K) (Gigoux et al., 2009; Rolf et al., 2010) which in turn is negatively regulated by the phosphatase and tensin homolog (PTEN) and the PH domain and leucine rich repeat protein phosphatase 2 (PHLPP2) (Brognard et al., 2007; Stambolic et al., 1998).

The interaction with follicular B cells will induce further maturation of TFH cells, like the upregulation of SLAM-associated-protein (SAP), which is indispensable for TFH function in the GC reaction. The continuous stimulation with antigen, in the follicles provided by follicular B cells, is important to maintain high levels of Bcl6 and the TFH cell phenotype (Baumjohann et al., 2013b; Choi et al., 2011b; Choi et al., 2013), therefore circulating TFH precursors express only low levels of Bcl6 (Hale et al., 2013; He et al., 2013).

In 2013, Dirk Baumjohann and colleagues and Seung Goo Kang and colleagues independently reported a new important component of the TFH differentiation program.

They demonstrated, that the microRNA17~92 (miRNA17~92) cluster is essential for normal TFH development and function (Baumjohann et al., 2013a; Kang et al., 2013).

1.2.3 The role of miRNAs in the regulation of immune activation in Type 1 Diabetes

MiRNAs are small, ~22nt long, non-coding RNAs which are part of the RNA interference (RNAi) pathway (Grishok et al., 2001). In contrast to other RNAs involved in this pathway, namely small interfering RNAs (siRNAs), miRNAs are transcribed from the genome and not derived from endogenous or exogenous double stranded RNA (dsRNA) (Zamore et al., 2000).

Primary miRNAs (pri-miRNA) are cleaved into stem-loop structured pre-miRNAs in the nucleus by an RNA cleavage enzyme called Drosha (Lee et al., 2003). After export to the cytoplasm, the hairpin structure is cleaved by the enzyme Dicer into two complementary strands (Hutvagner et al., 2001; Ketting et al., 2001). One strand is subsequently incorporated into the so-called RNA-induced silencing complex (RISC) (Hammond et al., 2000; Hutvagner and Zamore, 2002).

The RISC complex consists of the mature miRNA and several protein components, most importantly Argonaute 2 (AGO2) (Hammond et al., 2001). The miRNA complementarily binds the 3' untranslated region (UTR) of its target mRNAs with a specific ~7nt long seed sequence, thereby guiding the RISC complex to its target (Lewis et al., 2003). Binding of the RISC to the target mRNA induces translational repression (Olsen and Ambros, 1999) or degradation of the mRNA (Bagga et al., 2005; Lim et al., 2005), depending on the degree of complementarity with the miRNA (Haley and Zamore, 2004; Martinez and Tuschl, 2004) and the properties of the Argonaute protein in the RISC complex (Liu et al., 2004; Meister et al., 2004).

Only recently it has become evident, that miRNA-mediated regulation of target expression is more complex than previously assumed. The group of Shobha Vasudevan has published several studies highlighting that, in dependence of cellular state and function, miRNAs can also lead to a translational upregulation of their targets (Bukhari et al., 2016; Truesdell et al., 2012; Vasudevan, 2012; Vasudevan and Steitz, 2007; Vasudevan et al., 2007).

MiRNAs usually have a multitude of targets and induce rather modest regulation (Baek et al., 2008; Selbach et al., 2008). This enables miRNAs to regulate complex cellular states rather than single targets and makes them suitable candidates for immune modulating therapies.

MiRNAs have been demonstrated to be involved in T cell differentiation and function (Cobb et al., 2006; Cobb et al., 2005). In the context of this thesis focus was set on miRNAs that are potentially involved in the aberrant immune activation in pre-symptomatic T1D.

First of all, the miRNA17~92 cluster was studied, because of its essential role in TFH differentiation (Baumjohann et al., 2013a; Kang et al., 2013). The cluster transcribes six mature miRNAs: miRNA17, miRNA18a, miRNA19a, miRNA19b, miRNA20a and miRNA92a. This

miRNA cluster might be of interest to study in autoimmune diseases, since its overexpression leads to autoimmunity and autoantibody production (Xiao et al., 2008). MiRNA17~92 regulates TFH differentiation and migration to the B cell follicles together with Bcl6. This occurs, on the one hand, by repressing TFH inappropriate subset genes like *retinoid-related orphan receptor α* (*Rora*) and, on the other hand, by regulating signaling through ICOS and PI3K/protein kinase B (Akt) (Baumjohann et al., 2013a; Kang et al., 2013). Two validated targets of the miRNA17~92 cluster are PTEN and PHLPP2 (Jiang et al., 2010; Xiao et al., 2008), the former counteracting the function of PI3K (Stambolic et al., 1998) and the latter dephosphorylating Akt (Brognard et al., 2007). Although a lot of research has been conducted on the regulation of TFH cell differentiation by miRNA17~92 in mouse models, very little is known about TFH differentiation in humans, especially in the context of autoimmune T1D.

Another miRNA potentially important for aberrant immune activation is miRNA181a. This miRNA has been reported to regulate the sensitivity to the TCR stimulus in developing lymphocytes in the thymus in murine models (Li et al., 2007). Therefore, it could potentially be an important signaling intermediate regulating aberrant immune activation versus T cell tolerance in mature T cells in autoimmune settings such as T1D.

1.2.4 Lessons from murine models of Type 1 Diabetes

The non-obese diabetic (NOD) mouse is the model of choice for studying T1D in a murine setting. NOD mice develop spontaneous diabetes with immune infiltration of the islets and autoimmune destruction of the β cells (Makino et al., 1980). The disease in the NOD mouse shows many similarities to that in man, including the presence of insulin autoantibodies (Pontesilli et al., 1987). In the NOD mouse, unlike in the human disease, females are predominantly affected, with 80% of females having developed diabetes at 30 weeks of age opposed by only 20% of males (Makino et al., 1980). In these mice the risk to develop T1D is associated to a high degree with the major histocompatibility complex class II (MHCII), with the NOD MHCII IA^{g7} (further referred to as IA^{g7}) being the high risk genotype (Hattori et al., 1986; Prochazka et al., 1987).

Insulin is an essential autoantigen in the NOD mouse. This was highlighted by the abrogation of disease development in NOD mice lacking the Insulin 1 and Insulin 2 genes (Nakayama et al., 2005) and the tolerogenic effect of transgenic overexpression of preproinsulin 2 (Jaekel et al., 2004). In mice, the autoimmune response is focused on an IA^{g7}-restricted insulin epitope of the B chain comprising residues 9-23 (B:9-23), since 90% of islet infiltrating T cell clones recognize this peptide in the context of IA^{g7} (Alleva et al., 2001; Daniel et al., 1995b)

The IA^{g7} displays a polymorphism that influences the binding affinity to the insulin B:9-23 epitope. A change in position 57 of the β chain from arginine to serine disrupts the usually present hydrogen bond to position 76 of the α chain and leaves an unopposed positive

charge at position p9 of the binding pocket. This positive charge is met by an also positively charged arginine at position 22 of the peptide, making the interaction unstable and weak (Stadinski et al., 2010a).

This inefficient presentation of the insulin B:9-23 peptide by the MHCII leads to a weak interaction with the insulin-specific TCR of autoreactive T cells in the thymus and thereby promotes their escape from negative selection (Wucherpfennig and Sethi, 2011). In addition, a weak agonistic ligand for the TCR is unable to efficiently induce Tregs in the periphery and thereby also limits dominant tolerance.

Even though polyclonal Treg frequencies were found to be rather unaltered in the NOD mouse (Mellanby et al., 2007; You et al., 2005), as well as in human T1D (Brusko et al., 2007; Brusko et al., 2005; Lindley et al., 2005), evidence is accumulating pointing towards a contribution of defects in Treg function or stability to T1D. In the human disease, this is highlighted by the identification of polymorphisms associated with increased T1D risk in genes relevant for Treg maintenance and function like *Il2ra* (Vella et al., 2005) and *cytotoxic T Lymphocyte associated protein 4 (Ctla4)* (Nistico et al., 1996).

Tregs can be generated *de novo* in the peripheral immune system and bear therapeutic potential, since their antigen-specific induction promises high safety compared to general immunosuppressive treatments. However, the exact requirements for optimal antigen-specific induction of functional and stable Tregs need further investigation.

1.2.5 Strategies for *de novo* T cell tolerance induction

Functional Tregs are stable, which is maintained by a complete demethylation of the Treg specific demethylated region (TSDR) of the *Foxp3* locus. In contrast, effector T cells have a completely methylated TSDR. (Floess et al., 2007; Polansky et al., 2008)

The most common protocol for the induction of Tregs *in vitro* is the stimulation of naïve T cells via the TCR in the presence of TGF β . However, these *in vitro* induced Tregs are not stable, have a methylated TSDR and do not resemble *ex vivo* Tregs (Floess et al., 2007; Polansky et al., 2008).

Research in mouse models demonstrated that Tregs can be efficiently induced in the peripheral immune system *in vivo*, even in the absence of TGF β . For this process to be most efficient, a strong agonistic ligand for the TCR is needed, supplied under subimmunogenic conditions, avoiding general immune activation. From these studies it has become evident, that a weak interaction of the agonistic ligand with the TCR could not be compensated for by higher dose of the ligand (Daniel et al., 2011; Daniel et al., 2010; Gottschalk et al., 2010; Gottschalk et al., 2012; Kretschmer et al., 2005).

To overcome the problematic inefficient antigen-presentation of the insulin B:9-23 by the IA^{g7}, insulin variants, so-called mimetopes, which have an altered amino acid sequence, were developed based on work from John Kappler's group (Stadinski et al., 2010b). His laboratory demonstrated that the exchange of the positively charged arginine at position 22 to the negatively charged glutamic acid increases the binding of the peptide to the IA^{g7} (Crawford et al., 2011; Stadinski et al., 2010b). An additional alteration at position 21 was included, based on the presence of so-called type A and type B T cells in the pancreatic infiltrates of NOD mice. These T cells are specific for the insulin B:9-23 epitope but differ in their preference of the TCR contact residue, which is situated at position p8 of the MHCII binding pocket (Crawford et al., 2011).

Carolin Daniel and colleagues applied a combination of these insulin mimetopes to young NOD mice by osmotic minipumps to achieve subimmunogenic doses. This treatment led to a significant improvement of insulin-specific Treg induction when compared to the natural insulin B:9-23 epitope and was also suited to halt the progression to T1D development in these mice for 40 weeks and longer. The treatment was furthermore accompanied by increased frequencies of insulin-specific Tregs in the pancreatic lymph nodes and directly in the pancreas (Daniel et al., 2011).

An efficient insulin-specific Treg induction in NOD mice was however limited to young mice, with moderate or low levels of autoantibodies (Daniel et al., 2011). In mice with a strong immune reaction, indicated by high autoantibody titers, most of the insulin-specific T cells are already activated (Daniel et al., 2011).

The group of Matthias Merkenschlager has demonstrated that Tregs can also be induced in a TGF β independent manner by limiting the activity of the PI3K/Akt/mammalian target of rapamycin (mTOR) pathway, either by premature withdrawal of the TCR stimulus, or by inhibition of either PI3K, Akt or mTOR (Sauer et al., 2008). PI3K is activated via the costimulatory CD28 pathway (Garçon et al., 2008) and leads itself to the phosphorylation of Akt. Akt activates mTOR, which in turn phosphorylates Foxo proteins like Foxo1 and Foxo3a, resulting in their exclusion from the nucleus, where they are needed for *Foxp3* induction. Therefore, Tregs are dependent on high expression of molecules that counteract the PI3K/Akt/mTOR pathway, such as PTEN (Delgoffe et al., 2013; Ouyang et al., 2010; Sauer et al., 2008). The strong engagement of the PI3K/Akt/mTOR pathway in activated T cells is therefore believed to be one mechanism that limits Treg induction in previously activated T cells (Sauer et al., 2008). To potentially also improve Treg induction in settings of ongoing autoimmune activation, it is important to better understand mechanisms of aberrant immune activation during islet autoimmunity.

1.3 Current strategies for the prevention or treatment of Type 1 Diabetes

To date, many clinical trials and research efforts are focusing on the prevention and treatment of T1D. In this regard, increasing interest is focused on antigen-specific strategies, as they promise higher safety compared to the alternative general immune suppression.

Preventive strategies can be classified into three major categories: primary, secondary and tertiary prevention. Primary prevention means the prevention of seroconversion in children genetically at risk for T1D. Secondary prevention aims at the prevention of the progression to symptomatic T1D in children with multiple autoantibodies and tertiary prevention is the preservation of residual β cell function in patients with T1D.

With insulin as the antigen, three trials have been already conducted with the aim of secondary prevention: The Diabetes Prevention Trial-1 (DPT-1) (Skyler et al., 2005), the Intranasal Insulin Trial I (Harrison et al., 2004) and the Intranasal Insulin for Prevention of T1D Trial (Nanto-Salonen et al., 2008). All of these studies showed no or only limited clinical benefit. Recently, the Pre-POINT study was completed, a randomized trial aiming at primary prevention using oral insulin administration in children with genetic susceptibility for T1D (Bonifacio et al., 2015). The Pre-POINT study group reported an increase in insulin-responsive T cells with regulatory features in children treated with oral insulin, compared to the placebo control group, accompanied by no events of hypoglycemia, autoantibody development or T1D development (Bonifacio et al., 2015).

Combined, these studies demonstrate that successful antigen-specific tolerance induction is strongly dependent on the choice of antigen, the route of administration and especially the time point of intervention. Interestingly the human high-risk HLA-DQ8 shows striking structural similarity to the IA^{g7} of the NOD mouse with the identical problem of the disrupted hydrogen bond and the positively charged p9 position of the binding groove. Since the insulin B:9-23 is identical in its sequence in mouse and man this suggests similar antigen-presentation events involved in the development of human and murine T1D (Lee et al., 2001b). It will be of great importance to investigate the exact requirements for the insulin-specific induction of stable and functional Foxp3⁺Tregs, also in the human setting. To gain a better understanding of the human immune system and to enable improved translatability, novel model systems that bridge the gap between mouse models and the human disease will be essential.

1.4 Humanized mouse models for translational research

One major challenge for the development of novel therapeutic and preventive strategies in T1D is the limited translatability of findings from the NOD mouse model to human disease

(summarized in (Atkinson and Leiter, 1999)). Even though the NOD mouse model shows high levels of similarity to human T1D (Makino et al., 1980; Pontesilli et al., 1987), differences in the physiology of the pancreatic islets (Steiner et al., 2010), as well as differences in the immune system (summarized in (Mestas and Hughes, 2004)) between mouse and man, might lead to difficulties in the translation between the two species.

Since the discovery of the protein kinase, DNA activated, catalytic polypeptide (*Prkdc*) severe combined immunodeficiency (*scid*) mutation (abbreviated as *Prkdc^{scid}*) (Bosma et al., 1983), mice harboring this mutation have been engrafted with human hematopoietic tissues (McCune et al., 1988), hematopoietic stem cells (HSCs) (Lapidot et al., 1992) or peripheral blood mononuclear cells (PBMCs) (Mosier et al., 1988) in order to study the human immune system *in vivo*. The *scid* mutation disables TCR and B cell receptor (BCR) rearrangement and therefore leads to a loss of functional T and B cells (Schuler et al., 1986).

Because of the very low reconstitution efficacy in these early models, extensive research has led to the development of several humanized mouse models, differing in the background strain, the immunodeficiency mutations and the material used for engraftment (summarized in (Shultz et al., 2007)). It has become evident, that the most efficient reconstitution with human immune cells is achieved in the NOD.Cg-*Prkdc^{scid}IL2rg^{tm1Wjl}* (NSG) mouse (Ishikawa et al., 2005; Ito et al., 2002; Shultz et al., 2005). These are NOD mice with the *Prkdc^{scid}* mutation and an additional mutation leading to the knockout of the *IL2 receptor γ chain* (*IL2rg*). The *IL2ry* is a common chain for various cytokine receptors (namely the receptors for IL2, IL4, IL7, IL9, IL15, IL21) and crucial for their signaling (Asao et al., 2001; Giri et al., 1994; Kondo et al., 1994; Kondo et al., 1993; Noguchi et al., 1993; Russell et al., 1994; Russell et al., 1993; Takeshita et al., 1992). The absence of signaling through these cytokine receptors greatly impairs immune functionality and especially NK-cell development (Cao et al., 1995; DiSanto et al., 1995; Ohbo et al., 1996), a cell population that has been associated with impaired human cell engraftment in early humanized models (Christianson et al., 1996). The NOD mouse background has additional advantages, since NOD-*scid* mice harbor additional defects in innate immunity (Shultz et al., 1995) and further support human cell engraftment due to a polymorphism in the *Sirpa* gene, encoding the signal regulatory protein- α (*Sirp α*) (Strowig et al., 2011; Takenaka et al., 2007). *Sirp α* is expressed on macrophages and its interaction with CD47 on hematopoietic cells prevents phagocytosis of the body's own or transplanted hematopoietic cells (Blazar et al., 2001; Okazawa et al., 2005; Oldenborg et al., 2000). It has been demonstrated by Takenaka and colleagues in 2007 that the *Sirpa* polymorphism of the NOD mouse leads to improved binding to human CD47, thereby supporting human cell engraftment in NOD-*scid* mice (Takenaka et al., 2007).

Importantly, NSG mice develop a diverse T cell repertoire, comparable to the human repertoire in its complexity (Marodon et al., 2009). However, the selection of T cells in the thymus on murine MHCII molecules might be problematic when studying human disease

settings that rely on the recognition of antigens presented by human antigen presenting cells (APCs) on HLA molecules. Therefore, novel mouse strains deficient for murine MHCII and transgenically overexpressing human HLA molecules (HLA-DR4 (Covassin et al., 2011) and HLA-DQ8) have been developed.

These models promise to be a helpful tool for defining requirements for efficient human Treg induction *in vivo*. The very early onset of pre-symptomatic T1D, with the peak incidence of seroconversion between nine months and two years of age (Giannopoulou et al., 2015; Ziegler and Bonifacio, 2012), remains a major challenge, especially for primary prevention efforts. Since the Treg induction efficacy is limited in an already activated immune setting, it will be crucial to find regimens that will reduce immune activation and open a window of opportunity for T cell tolerance induction, also at later stages of the disease.

1.5 Objectives

Antigen-specific tolerization strategies are a promising tool to implement the vision of preventing T1D due to their safe and specific mode of action. In this regard, insulin mimetopes have been used successfully in the NOD mouse model to prevent the development of T1D. However, the exact conditions for efficient and stable Treg induction in a human setting are not known.

Therefore, the first objective of this thesis was to study as a proof of principle, the antigen-specific induction of human Foxp3⁺Tregs in the setting of a human immune system *in vivo*. Specifically, it was the goal to investigate the use of insulin mimetopes for Foxp3⁺Treg induction in the human setting *in vitro* and in humanized mice *in vivo*.

The requirement of limited immune activation for efficient Treg induction is a major challenge for antigen-specific tolerization strategies for T1D, since the peak incidence of seroconversion is very early in life. The heterogeneity in the time of progression from seroconversion to symptomatic disease implies differences in immune activation and T cell tolerance in children at risk to develop T1D. However, the underlying mechanisms of this heterogeneity are poorly understood. A better understanding of the mechanisms regulating the aberrant immune activation in this early pre-symptomatic phase of the disease is essential in order to find new regimens that will limit immune activation and open a window of opportunity for antigen-specific tolerance induction, also after onset of the autoimmune process.

Therefore, the second objective of this thesis was to study mechanisms of aberrant immune activation in the early heterogeneous phase of T1D. Here, the focus was set on TFH cells due to their capacity to provide help to B cells to produce high-affinity antibodies.

Additionally, as a third objective, miRNAs were studied, because of their ability to regulate complex cellular states. Specifically, miRNAs that might be involved in regulating aberrant immune activation or impairments in T cell tolerance were studied in the context of this thesis.

2. Methods

2.1 Human subjects, blood samples and cell isolation

Blood samples were collected from first degree relatives of T1D patients, who consented to the Munich Bioresource project (approval number #5049/11, approval committee: Technische Universität München, Munich, Germany). The age of seroconversion (development of islet autoantibodies) had been documented for all patients in previous prospective follow-up from birth studies. Blood collection was performed using sodium heparin tubes and the volume was in accordance with EU guidelines (maximum 2.4 ml/kg of body weight).

The stratification of the subjects was based on the time of presence or absence of multiple islet autoantibodies (without the development of symptomatic T1D): no autoimmunity = islet autoantibody negative; recent onset of islet autoimmunity = multiple islet autoantibodies for less than 5 years; persistent autoimmunity = multiple islet autoantibodies for more than 5 but less than 10 years; longterm autoimmunity = multiple islet autoantibodies for more than 10 years. Additionally, children with onset of symptomatic T1D before the age of 5 years (fast progressor) and patients with longterm symptomatic T1D for 45 years were studied. The investigators were not blinded for the group allocations of the different children.

PBMCs were isolated via density centrifugation over Ficoll Paque (GE Healthcare). Human CD4⁺T cells were isolated from PBMC samples by negative magnetic activated cell sorting (MACS) enrichment using the EasySep Human CD4 T Cell enrichment kit (Stem Cell) or by positive enrichment using CD4 Microbeads human (Miltenyi Biotec) according to the instructions. Autologous dendritic cells (DCs) were isolated via MACS enrichment using the Blood DC Isolation Kit II human (Miltenyi Biotec). B cells were isolated from the flow through of positive CD4 enrichments using CD19 Microbeads human (Miltenyi Biotec).

Umbilical cord blood (UCB) was obtained immediately after delivery from healthy full-term newborns in citrate phosphate dextrose and provided through the DKMS Cord Blood Bank of the University Hospital Dresden (Germany) or from the Institute of Diabetes Research, Klinikum rechts der Isar, Technische Universität München (approval number #5293/12, Technische Universität München, Munich, Germany).

The HLA genotype was determined based on a fast genotyping protocol described previously (Nguyen et al., 2013).

PBMCs were isolated from UCB samples and HSCs were purified using the Diamond CD34+ Isolation Kit human (Miltenyi Biotec).

2.2 Mice and murine cell isolation

All mice were bred and maintained group-housed on a 12-h/12-h light dark cycle at 25°C with food and water ad libitum under specific pathogen free conditions at the animal facility of Helmholtz Zentrum München, Munich, Germany, according to the Institutional Animal Committee Guidelines. Ethical approval for all mouse experimentations has been received by the District Government of Upper Bavaria, Munich, Germany (approval numbers: #55.2-1-54-2532-81-12 and 55.2-1-54-2532-84-12). The investigators were not blinded to group allocation during the *in vivo* experiments or to the assessment of experimental endpoints.

NOD.Cg-Prkdc^{scid} H2-Ab1^{tm1Gru} Il2rg^{tm1Wjl} Tg(HLA-DQA1,HLA-DQB1)1Dv//Sz mice were developed by and obtained from Leonard Shultz at the Jackson Laboratory (JAX strain number 026561).

NOD.129X1(Cg)-*Foxp3*^{tm2Tch}/DvsJ and NOD/ShiLtJ mice were obtained from the Jackson Laboratory (JAX strain number 025097 and 001976). Insulin autoantibodies were determined with ELISA as described previously (Babaya et al., 2009). To determine levels of insulin autoantibodies (IAA) in NOD mice, a Protein A/G radiobinding assay based on ¹²⁵I-labeled recombinant human insulin was applied as previously described (Achenbach et al., 2009).

Cells were isolated from lymph nodes and spleen by gentle grinding through a 70 µm cell strainer. CD4⁺T cells were purified by MACS enrichment using a CD4-Biotin antibody (BD Biosciences) and Streptavidin Microbeads (Miltenyi Biotec).

Pancreata were digested for 4-7 min at 37°C using collagenase V (1 mg/ml) in PBS with 0.1 mM HEPES and 0.1% BSA.

White adipose tissue was digested for 10 min at 37°C using collagenase II (4 mg/ml) in PBS with 0.5% BSA and 10 mM CaCl₂.

For *in vivo* inhibition of miRNA92a, IAA⁺NOD mice or reconstituted NSG mice were injected intra peritoneally (i.p.) with 10 mg/kg custom-designed *in vivo* LNA miRNA92a antagomir (Exiqon) on day 0, day 2 and day 6. Analysis was performed on day 7. Additional experiments were performed in IAA⁺NOD mice for 14 days with injections of miRNA92a antagomir every second day.

2.3 Cell staining and flow cytometry

Cells were stained for 30 min on ice in Hanks buffer supplemented with 5% FCS and 10 mM HEPES after treatment with Fc blocking reagent (BD Bioscience). The antibodies and clones that were used for the stainings can be found in the publications provided in this thesis.

For intracellular staining of Foxp3 and Ki67 cells were fixated and permeabilized using the Foxp3 staining buffer set (eBioscience), stained for 30 min on ice and washed three times afterwards.

Cells were acquired and sorted on a BD FACS Aria III cell sorting system with FACS Diva software and optimal compensation and gain settings. Dead cells were excluded based on forward and sideward scatter and staining with sytox blue or red (Life Technologies) or Fixable viability dye eFlour450 (eBioscience). Analysis was performed using FlowJo software version 7.6.1 (TreeStar Inc.).

2.4 Proliferation assays

Naïve CD4⁺CD25⁻T cells or HLA-DQ8-restricted insulin-specific T cell clones were labelled with CFSE (1 µM) for 3-4 minutes at 37°C and washed with PBS. The cells were seeded in X-Vivo15 medium, complemented with 10% human serum (Invitrogen), penicillin-streptomycin (50 µg/ml) and 2 mM glutamin into 96-well plates and stimulated with peptides (detailed information on peptide sequences can be found the publications provided in this thesis). For peptide-presentation either autologous DCs or T cell depleted PBMCs were added to the culture. Analysis of CFSE dilution and CD25 expression was performed after 5 days of stimulation.

2.5 Tetramer stainings

Insulin-B-chain-10-23-mimotope based Tetramer reagents were obtained from Richard A. Willis from the NIH tetramer core facility (Atlanta, USA). For the identification of human HLA-DQ8-restricted insulin-specific CD4⁺T cells, tetramers based on ins.mim.1 (14E-21G-22E) and ins.mim.4 (14E-21E-22E) were used. For the identification of murine IA^{g7}-restricted insulin-specific CD4⁺T cells, tetramers were based on ins.mim.2 (21G-22E) and ins.mim.3 (21E-22E). CD4⁺T cells were stained with tetramer reagents in 10 µl RPMI medium with 5% human serum (human stainings, or FCS for murine stainings) for 1 hour at 37°C with gentle agitation every 20 minutes. Afterwards, surface antibodies were added directly and cells were stained for 30 minutes on ice. Dead cell staining was performed before analysis of the cells.

Control tetramers, fused to irrelevant peptides, were used to verify the specificity and virtually no tetramer⁺CD4⁺T cells were detected with the control tetramers.

2.6 Generation of insulin-specific CD4⁺T cell clones

Naïve T cells (CD4⁺CD25⁻) were CFSE-labelled (as described in 2.4) and stimulated in 96-well plates with 230 µg/ml artificial APCs (aAPCs) for 7 days. aAPCs were used, to make sure that the cells were stimulated only with peptides presented by HLA-DQ8. The generation of aAPCs was described previously (Maus et al., 2003). Specifically, anti-HLA-DQ antibodies (SPV-L3,

Abcam) were coated onto antibody-coupling beads (Dynabeads Antibody coupling kit, Life Technologies) at 20 µg/mg beads, followed by coupling with unlabeled HLA-DQ8 tetramers (ins.mim.1 and ins.mim.4 or control tetramer based, 3 µg per 1×10^7 beads). After 7 days, cells were analyzed on the BD FACS Aria III and one single CFSE^{dim}CD4⁺T cell was sorted into each well of a 96-well plate prefilled with irradiated feeder cells (CD4-depleted PBMCs from a DQ8⁺ and a DQ8⁻ donor and EBV-transformed B cells from the Riken cell Bank, Japan) in X-vivo medium with 30 µg/ml anti-CD3 (Okt3, BioLegend), 20 U/ml IL2 and 10 ng/ml IL4 (both from Peprotech). For expansion IL21 (10 ng/ml), IL15 (10 ng/ml) and IL7 (0.1 ng/ml, all from Peprotech) were added additionally. Cells were split into 48-well plates after 2 weeks and tested for antigen-specificity by restimulation with the natural insulin B:9-23 epitope or mimetopes at 0.1 – 10 µg/ml in the presence or absence of anti-DQ blocking antibody (SPV-L3, abcam, 10 µg/ml) for 48 hours and analyzed for CD25 upregulation.

2.7 HLA-DQ8 peptide-binding assay

HLA-DQ8 binding analysis of the 4 mimetopes was performed according to previously described procedures (Ettinger and Kwok, 1998; Sidney et al., 2013; Yang et al., 2014). Specifically, the FITC labelled GAD 253-265^{R255F} peptide was used as an indicator peptide at 10 µM together with thrombin cleaved HLA-DQ8 monomers (provided by the NIH tetramer core facility, Richard A. Willis) at 0.4 µM and increasing concentrations of competitor peptides (natural insulin B:9-23 epitope, ins.mim.1-4) or MPI 185-204 as a binding control. Indicator peptide and monomers without competitor peptide served as a positive control and for background analysis the binding reaction was performed without monomers. The binding reaction was performed for 48h at 37°C and captured on anti-HLA-DQ (SPV-L3, Abcam, 15 µg/ml) pre-coated plates. Detection was performed using anti-FITC HRP antibodies (Abcam, 1:1000) and TMB substrate (BD Bioscience). Fluorescence was measured on an Epoch plate reader (Biotech) at 405 and 450 nm. Binding curves were fitted by nonlinear regression using log transformed x values ($x^{1/4}$ test peptide concentration) with the one-site competitive binding model to extract IC50 values (Prism software, v.6.04, GraphPad Software).

2.8 *In vitro* Treg induction assay

Human naïve CD4⁺CD45RA⁺CD45RO⁻CD25⁻CD127⁺T cells were sort purified on the BD FACS Aria III cell sorting system and stimulated in 96-well plates. For polyclonal Treg induction, plates were pre-coated with 5 µg/ml anti-CD3 (UCHT1, Biolegend) and 5 µg/ml anti-CD28 (CD28.1, Biolegend). For insulin-specific Treg induction the cells were stimulated with ins.mim.1 and ins.mim.4, presented by autologous CFSE-labelled DCs. 100 U/ml IL2 was added to the culture medium. To mimic subimmunogenic conditions *in vitro*, the cells were pipetted into new uncoated wells, or the T cells were sort-purified from DCs as CFSE^{dim} after 18h. T cells were cultured without stimulation for additional 36h prior to analysis.

To analyze Treg stability CD25^{high}CD127^{low} Tregs were sort-purified from Treg induction assays and restimulated with anti-CD3 and anti-CD28 antibodies for 54h and Foxp3 expression was analyzed.

2.9 DNA bisulfite conversion and methylation analysis

Lysis and bisulfite conversion of the sorted Foxp3⁺T cells were combined, due to the low cell numbers and performed with the EpiTect Plus LyseAll Bisulfite Kit (Qiagen) or the EZ DNA Methylation-Direct Kit (Zymo Research), according to the instructions. A combination of MS-HRM and Pyrosequencing analysis was performed, as previously described (Baron et al., 2007; Floess et al., 2007). Primers were designed with the PyroMark Assay Design Software 2.0 (Qiagen) to cover the area of differential methylation in the first *Foxp3* intron initially reported by Baron et al. (Baron et al., 2007) (primer sequences can be found in the publications provided in this thesis). Methylation results are presented as the mean of all 5'-C-phosphate-G-3' (CpG)-sites analyzed.

2.10 Reconstitution of NSG mice and *in vivo* Treg induction

Two-week old immunodeficient murine MHCII-deficient HLA-DQ8 transgenic NOD.Cg-*Prkdc^{scid}Il2rg^{tm1Wjl}* (NSG) mice were reconstituted with 50.000 CD34⁺HSCs injected *i.v.* in 50 μ l PBS. The mice were sex-matched to the HSC donor and donors were HLA-DQ8⁺. Reconstitution efficacy was tested after 8 weeks based on murine and human CD45 expression in peripheral blood. *In vivo* Treg induction experiments were performed at week 20 post-reconstitution based on previously described protocols (Daniel et al., 2011). Specifically, osmotic minipumps transfusing continuous and minute amounts of peptide (ins.mim.1 and ins.mim.4, 5 μ g/d) for 14 days were implanted subcutaneously. Treg induction was analyzed in various tissues and peripheral blood by FACS analysis as indicated in 2.2.

2.11 Expression analysis of mRNAs and miRNAs

Cells were sort-purified and RNA extraction was performed using the miRNeasy Micro Kit (Qiagen), or, in the case of very low cell numbers, cDNA was synthesized directly using the SMARTer ultra low input RNA Kit for Sequencing-v3 (Takara Clontech) according to the instructions. Previously isolated RNA was transcribed into cDNA using the iScript cDNA Synthesis Kit (BioRad) and qPCR analysis was performed on a CFX96 real time system (Biorad) in combination with SsoFast Evagreen Supermix (Biorad) and QuantiTect Primer Assays (Qiagen). Levels of Histone and 18s rRNA were used for normalization.

2.12 *In vitro* Treg suppression assay

CD4⁺CD3⁺CD127^{low}CD25^{high}Tregs were sort-purified (in control experiments Treg identity of CD4⁺CD3⁺CD127^{low}CD25^{high}T cells was confirmed by intracellular staining for Foxp3) from

lymph nodes and spleens of humanized mice and expanded for six days by polyclonal stimulation with α CD3 and α CD28 at 1 μ g/ml each in the presence of IL-2 (500 U/ml) and 2×10^5 irradiated CD4⁻ feeder cells. On day 6 conventional sort-purified CD4⁺CD3⁺CD127⁺CD25⁻T cells (expanded accordingly with 50 U/ml IL2) and expanded Tregs were sort-purified to remove the remaining feeder cells and conventional T cells (responder cells) were labeled with CFSE (0.25 μ M). Treg cells and conventional T cells were rested for 16 hours in the absence of IL2 to force them into synchronous resting states and further cultured at different ratios (responder: Tregs 1:0; 1:2; 1:4 and 1:8) for three days in the presence of α CD3 and α CD28 [1 μ g/ml each]. On day 3 responder cell proliferation was assessed by dilution of the CFSE label. Suppression of responder cell proliferation is shown in % suppression of the proliferation of the responder cells stimulated in the absence of Tregs.

For insulin-specific suppression assays, induced Tregs from humanized mice were sorted-purified as indicated above and insulin-specific T cell clones were used as effector cells as described above. The cells were stimulated either with insulin mimetopes [100 ng/ml] or the natural insulin B:9-23 epitope [10 μ g/ml].

Additional experiments were performed using effector T cells from T1D individuals and polyclonal stimulation as outlined above.

2.13 *In vitro* TFH precursor cell induction assay

Human naïve T cells (sort-purified as CD3⁺CD4⁺CD45RA⁺CD45RO⁻CXCR5⁻) and memory B cells (sort-purified as CD20⁺CD27⁺) were cocultured at a ratio of 1:1 and stimulated with 5 μ g/ml anti-CD3 (Okt3, Biolegend) and anti-CD28 (CD28.2, Biolegend) for 5 days in the presence of a miRNA92a mimic or antagomir. MiRNA92a mimic (miRCURY LNA microRNA Mimic; Exiqon) or antagomir (miRCURY LNA microRNA Antagomir; Exiqon) were loaded onto PLGA-coated nanoparticles at a ratio of 1:50 by mixing and incubation at room temperature for 30 minutes. The loaded nanoparticles were added to the culture at a final concentration of mimic of 0.75 ng/ μ l per 100,000 cells ("high"), 0.375 ng/ μ l per 100,000 cells ("medium") or 0.1875 ng/ μ l per 100,000 cells ("low"). The miRNA92a antagomir loaded nanoparticles were added at a final antagomir concentration of 2 ng/ μ l per 100,000 cells. As a control a negative control miRNA mimic or antagomir, which was found to have no homology to any known miRNA or mRNA in mouse, rat and human, were added to the cultures. Cells were analyzed on a BD FACS AriaIII cell sorting system for expression of CXCR5, PSGL-1, PD1 and CCR7. In some experiments IL-6 and IL-21 were added to the culture at 50 ng/ml or cells were stimulated with PMA/Ionomycin (PMA 50 ng/ml, Ionomycin 1 μ g/ml) 12h prior to analysis. In some experiments a PTEN inhibitor (SF1670, 325 nM) or a PI3K inhibitor (LY494002, 10 μ M) were added to the cultures. The miRNA92a-krueppel-like factor 2 (KLF2) target site blocker or control TSB (custom designed by Exiqon) were loaded onto PLGA-coated nanoparticles as described above and added to the culture at a final concentration of 2 ng/ μ l per 100,000

cells. The nanoparticles were developed and tested by the research group of Claus-Michael Lehr at the Helmholtz Center for Pharmaceutical Research, Saarland. Further information on the preparation and characterization can be found in the publications provided in this thesis.

2.14 Histopathological analysis and immunofluorescent staining of pancreas sections

Pancreata were embedded with TissueTek O.C.T. Compound and frozen on dry ice. Serial sections were prepared and stained with hematoxylin and eosin in the lab of Benno Weigmann at the Kussmaul Campus of the University of Erlangen. Insulitis scoring was performed as previously described (Jaeckel et al., 2004; Krishnamurthy et al., 2006). The researches were blinded for group allocations. Serial sections were sent to the lab of Ari Waisman at the Johannes-Gutenberg Universität, Mainz and stained for immunofluorescent analysis. Rabbit-anti-mouse insulin antibodies (Cell Signaling), rat-anti-mouse CD4 (Becton, Dickinson and Company) and rat-anti-mouse Foxp3 antibodies (eBioscience) were used as primary antibodies. Donkey-anti-rabbit^{Alexa647} antibodies (Dianova), goat-anti-rat^{AlexaFluor488} (Dianova) and goat-anti-rat^{bio} (Becton, Dickinson and Company) were used as secondary antibodies and combined with TSA Cyanine3 amplification (PerkinElmer). Nuclei were counterstained with HOECHST 33342 dye (Invitrogen). Negative control slides were incubated with secondary antibodies only. Cells were analyzed by confocal microscopy (Olympus).

2.16 Statistics

Results are presented as the mean and standard error of the mean (s.e.m.) or as percentages, where appropriate. For normal distributed data the Student's t test was used. The Student's t test for unpaired values was used to compare means between independent groups and the Student's t test for paired values was used to compare values for the same sample or subject tested under different conditions. For data that was not normally distributed, the nonparametric Wilcoxon signed-ranks test was applied. Group size estimations were based upon a power calculation to yield minimally an 80% chance to detect a significant difference in the respective parameter of $P < 0.05$ between the relevant groups. The significance level was determined as a two-tailed P value of <0.05 . Statistical significance is shown as * $P < 0.05$, ** $P < 0.01$, *** $P < 0.001$, or not significant ($P > 0.05$). Statistical analyses were performed using the programs GraphPad Prism 6 and the Statistical Package for the Social Sciences (SPSS 19.0; SPSS, Inc.).

3. Results: Publications originating from this thesis

3.1 Summary of publications

Type 1 diabetes vaccine candidates promote human Foxp3(+)Treg induction in humanized mice: Serr et al. 2016

In this publication we investigated the requirements for human Treg induction. We demonstrate that subimmunogenic doses of a strong agonistic TCR ligand can efficiently induce human Tregs *in vitro* and *in vivo* in a HLA-DQ8 transgenic murine MHCII deficient humanized mouse model. We used strong agonistic variants of the insulin B:9-23 epitope supplied by osmotic minipumps for Treg induction in these mice and observed increased frequencies of Tregs. We furthermore show that the induced Tregs are stable and functional. Moreover, we use novel HLA-DQ8-restricted insulin B:9-23 specific tetramer reagents based on the strong agonistic variants of the insulin B:9-23 epitope to identify insulin-specific Tregs in children at different stages of islet autoimmunity. We show that children with recent activation of islet autoimmunity display decreased frequencies of insulin-specific Tregs. In contrast, Treg frequencies in children with longterm islet autoimmunity without progression to symptomatic disease are comparable to those in children without islet autoantibodies, supporting the concept of insulin-specific Treg induction for the prevention of T1D progression. In summary, this publication shows as a proof of principle that subimmunogenic doses of strong agonistic TCR ligands are able to induce human Tregs *in vitro* and *in vivo* and might help to better define Treg induction strategies for the prevention of islet autoimmunity.

miRNA92a targets KLF2 and the phosphatase PTEN signaling to promote human T follicular helper precursors in T1D islet autoimmunity: Serr et al. 2016

In this second publication we were interested to investigate differences in the aberrant immune activation in children with different durations of islet autoimmunity. We focused on TFH precursor cells, since they are important mediators in (auto)-antibody production and are therefore an important effector T cell population in autoimmunity. Here, we identify insulin-specific as well as polyclonal TFH precursor cells to be increased during recent activation of islet autoimmunity, whereas the frequencies of TFH precursors in children with longterm islet autoimmunity are similar to those in children without islet autoantibodies. During recent activation of islet autoimmunity we identify Th2-like TFH cells to be specifically increased. Concerning the molecular mechanism underlying these differences, we observe miRNA92a to be differentially regulated between children with or without islet

autoantibodies and we show a positive correlation between miRNA92a expression and TFH precursor cell frequencies in the blood. In TFH induction assays a miRNA92a mimic increased, while a miRNA92a antagomir inhibited TFH induction. Specifically we identify negative regulators of T cell activation like CTLA4, Foxo1 and PTEN to be negatively regulated by miRNA92a. Additionally, we identify KLF2 as a novel target of miRNA92a and show that the downregulation of KLF2 by miRNA92a is essential for TFH precursor cell induction. Most importantly, a miRNA92a antagomir improved insulinitis scores and decreased immune activation in insulin autoantibody positive NOD mice in vivo. In summary, this publication provides evidence for the involvement of TFH cells and miRNA92a in the aberrant immune activation in pre-symptomatic T1D and proposes miRNA92a as possible drug candidate for the prevention of islet autoimmunity.

3.2 Type 1 diabetes vaccine candidates promote human Foxp3(+) Treg induction in humanized mice

Isabelle Serr, Rainer W. Fürst, Peter Achenbach, Martin G. Scherm, Füsün Gökmen, Florian Haupt, Eva-Maria Sedlmeier, Annette Knopff, Leonard Shultz, Richard A. Willis, Anette-G. Ziegler and Carolin Daniel.

Published in

Nature Communications 2016 March 15;7:10991. doi:10.1038/ncomms10991.

Permission:



RightsLink®



Title: Type 1 diabetes vaccine candidates promote human Foxp3+Treg induction in humanized mice
Author: Isabelle Serr, Rainer W. Fürst, Peter Achenbach, Martin G. Scherm, Füsün Gökmen et al.
Publication: Nature Communications
Publisher: Nature Publishing Group
Date: Mar 15, 2016
Copyright © 2016, Rights Managed by Nature Publishing Group

Creative Commons

The article for which you have requested permission has been distributed under a Creative Commons CC-BY license (please see the article itself for the license version number). **You may reuse this material without obtaining permission from Nature Publishing Group, providing that the author and the original source of publication are fully acknowledged**, as per the terms of the license. For license terms, please see <http://creativecommons.org/>

ARTICLE

Received 26 Jun 2015 | Accepted 9 Feb 2016 | Published 15 Mar 2016

DOI: 10.1038/ncomms10991

OPEN

Type 1 diabetes vaccine candidates promote human Foxp3⁺ Treg induction in humanized mice

Isabelle Serr^{1,2}, Rainer W. Fürst^{2,3}, Peter Achenbach^{2,3}, Martin G. Scherm^{1,2}, Füsün Gökmen^{1,2}, Florian Haupt^{2,3}, Eva-Maria Sedlmeier^{2,3}, Annette Knopff^{2,3}, Leonard Shultz⁴, Richard A. Willis⁵, Anette-Gabriele Ziegler^{2,3} & Carolin Daniel^{1,2}

Immune tolerance is executed partly by Foxp3⁺ regulatory T (Treg) cells, which suppress autoreactive T cells. In autoimmune type 1 diabetes (T1D) impaired tolerance promotes destruction of insulin-producing β -cells. The development of autoantigen-specific vaccination strategies for Foxp3⁺ Treg-induction and prevention of islet autoimmunity in patients is still in its infancy. Here, using human haematopoietic stem cell-engrafted NSG-HLA-DQ8 transgenic mice, we provide direct evidence for human autoantigen-specific Foxp3⁺ Treg-induction *in vivo*. We identify HLA-DQ8-restricted insulin-specific CD4⁺ T cells and demonstrate efficient human insulin-specific Foxp3⁺ Treg-induction upon subimmunogenic vaccination with strong agonistic insulin mimetopes *in vivo*. Induced human Tregs are stable, show increased expression of Treg signature genes such as *Foxp3*, *CTLA4*, *IL-2R α* and *TIGIT* and can efficiently suppress effector T cells. Such Foxp3⁺ Treg-induction does not trigger any effector T cells. These T1D vaccine candidates could therefore represent an expedient improvement in the challenge to induce human Foxp3⁺ Tregs and to develop novel precision medicines for prevention of islet autoimmunity in children at risk of T1D.

¹Institute for Diabetes Research, Independent Young Investigator Group Immune Tolerance in Type 1 Diabetes, Helmholtz Diabetes Center at Helmholtz Zentrum München, Heidemannstrasse 1, 80939 München, Germany. ²Deutsches Zentrum für Diabetesforschung (DZD), Ingolstädter Landstrasse 1, 85764 München, Germany. ³Institute for Diabetes Research, Helmholtz Diabetes Center at Helmholtz Zentrum München, Klinikum rechts der Isar, Technische Universität München, Heidemannstrasse 1, 80939 München, Germany. ⁴The Jackson Laboratory, 600 Main Street, Bar Harbor, Maine 04609, USA. ⁵Emory Vaccine Center, NIH Tetramer Core Facility, 201 Dowman Drive, Atlanta, Georgia 30322, USA. Correspondence and requests for materials should be addressed to C.D. (email: carolin.daniel@helmholtz-muenchen.de).

Type 1 diabetes (T1D) afflicts millions of people worldwide and is a severe chronic autoimmune disease characterized by the progressive loss of self-tolerance to insulin-producing pancreatic β -cells¹. The incidence of T1D is rising dramatically especially in young children². T1D and other autoimmune diseases are thought to develop when T cells with specificity for weakly binding T-cell receptor (TCR) agonists, which may include self-antigens, evade thymic negative selection and then mount a peripheral autoimmune attack^{3–7}. In children, the appearance of multiple islet autoantibodies indicates the onset of islet autoimmunity (pre-T1D)⁸. Insulin autoantibodies are often the first to appear thereby highlighting the contribution of insulin in initiating T1D autoimmunity⁹.

Regulatory T (Treg) cells are pivotal in preventing autoimmunity. Impairments in Treg numbers, function and induction critically contribute to autoimmune destruction in T1D. Tregs are characterized by the expression of the high-affinity interleukin-2 (IL-2) receptor α -chain (*IL-2R α*) and the X-linked gene forkhead box P3 (*Foxp3*), encoding the transcription factor Foxp3, which acts as a lineage specification factor for the development and function of CD4⁺CD25⁺Tregs^{10–13}. The essential function of human Foxp3⁺Tregs to avoid autoimmunity is illustrated by the fatal autoimmune disease IPEX (immunodysregulation, polyendocrinopathy, enteropathy and X-linked syndrome), which is caused by mutations in the *Foxp3* gene.

Foxp3⁺Tregs have attracted attention as they can ‘tame’ their autoreactive counterparts by direct contact-dependent inhibition of antigen-presenting cells (APCs) and effector T cells or by releasing inhibitory cytokines such as TGF β or IL-10. Tregs maintain their regulatory functions for a long period of time even in the absence of antigens that induced their generation and are stable and transferable¹⁴, thereby permitting the prospective induction of these cells to prevent unwanted immunity. We are focusing on novel strategies using optimized variants of critical autoantigens for Foxp3⁺Treg induction since Tregs bear the promise of specifically targeting the harmful effects of peripheral autoreactive T cells to control autoimmunity such as that observed in T1D while preserving the ability of the immune system to fight off infections^{15–18}. Optimal *in vivo* induction of stable murine Foxp3⁺Tregs requires the subimmunogenic delivery of strongly agonistic TCR ligands to naive CD4⁺T cells^{16,17,19–21}. By contrast, even high immunogenic doses of weakly agonistic ligands fail to induce stable Foxp3⁺Tregs^{17,22}. The most efficient Foxp3⁺Treg induction is achieved in T cells that proliferated least extensively¹⁹. Specific Foxp3⁺Treg induction in the context of autoimmunity could allow modulating the immune response for clinical benefit while limiting long-term immune suppression.

T1D mouse models as non-obese diabetic (NOD) mice showed that insulin functions as an essential autoantigen^{23,24}. In humans and mice, T cell responses to insulin are highly focused on a human leukocyte antigen (HLA)-DQ8- or murine IA^{g7}-restricted segment of the insulin-B-chain comprising residues 9–23 and the human epitope is identical to that of mouse insulin^{25–27}. Initial murine studies using subimmunogenic delivery of natural insulin B-chain epitopes show only a limited Treg induction efficacy and a slight delay in T1D progression¹⁷. As one possible means to explain the poor efficacy of Treg induction by natural insulin B-chain epitopes in murine T1D, it has been indicated that the insulin-B-chain peptide is presented by I-A^{g7} in a low-affinity binding register, which results in weak-agonistic activity of the peptide presented by the major histocompatibility complex (MHC)II (refs 7,28). To efficiently induce insulin-specific Foxp3⁺Tregs that could interfere with the development of T1D in NOD mice, we devised a strongly agonistic mimetope of the natural insulin-B-chain-epitope (21E-22E) with improved

MHCII-binding⁷ and showed that its sub-immunogenic delivery promoted efficient Foxp3⁺Treg induction and T1D protection for 40 weeks and longer¹⁷. Importantly, crystal structures of the human T1D susceptibility HLA-DQ8 allele and the homologous molecule in NOD mice, I-A^{g7}, reveal striking structural overlap between the MHC-peptide binding pockets²⁹, which suggests similar peptide presentation events of insulin-epitopes in human T1D. Accordingly, a recent study provides evidence that insulin B:9-23-reactive CD4⁺T cells are present in the peripheral blood of T1D patients and that the immunogenic register of this peptide has low-affinity binding to HLA-DQ8 (ref. 30). Moreover, T1D risk may be related to how an *HLA-DQ* genotype determines the balance of T-cell inflammatory versus regulatory responses to insulin, having implications for insulin-specific therapies to prevent T1D (ref. 31).

Currently, the majority of strategies approved by the FDA for autoimmune diseases have focused on non-antigen-specific immune suppression. Although this was found to be partially effective in inhibiting autoreactivity, these compounds have numerous side effects and long-term treatment remains challenging. Strategies that promote autoantigen-specific Treg induction will permit the specific blockade of the deleterious effects of autoimmune destruction while maintaining the ability of the immune system to clear non-autoantigens. While promising results have been obtained in mice, in man the development of autoantigen-specific Foxp3⁺Treg induction strategies is still in its infancy. It is currently unclear whether concepts established for efficient murine *in vivo* Foxp3⁺Treg induction will be translatable to the human immune system, especially in the context of autoimmune diseases such as T1D. Further studies are needed that provide mechanistic insights for the *in vivo* induction of human autoantigen-specific Foxp3⁺Tregs. As an excellent accessible system permitting predictive *in vivo* immunology research, here we used human haematopoietic stem cell (HSC)-engrafted NOD-Scid-IL2-receptor- γ -chain knockout (NSG)-HLA-DQ8 transgenic mice and newly established autoantigen-specific Treg induction.

We provide first direct evidence that a set of two novel human insulin mimetopes promotes human Foxp3⁺Treg induction in human-HSC-engrafted NSG-HLA-DQ8 transgenic mice *in vivo*. Such induced Tregs from humanized mice are stable over prolonged periods of time, present with robust suppressive capacities and harbour high abundance of Treg signature genes such as *Foxp3*, *CTLA4*, *IL-2R α* and *TIGIT* in the absence of effector T-cell responses. These T1D vaccine candidates could critically contribute to the development of efficient autoantigen-specific Treg induction strategies for prevention of islet autoimmunity in children at risk of developing T1D.

Results

Agonistic activity of insulin mimetopes in CD4⁺T cells.

To define optimal conditions for human insulin-specific Foxp3⁺Treg induction we tested agonistic activities of four insulin-B-chain-10-23 mimetopes. Peptide selections were made first based on the finding that insulin-B:10-23 peptide variants with a mutation of arginine (R) to glutamic acid (E) at position 22 and/or including a change to glycine (G) at position 21 (ins.mim.2 = 21G-22E; ins.mim.3 = 21E-22E) were more potent in stimulating murine insulin-specific CD4⁺T cells^{7,17,28} and stimulated human insulin-specific CD4⁺T cells^{30,31}. The use of either E or G at position 21 was included based on findings in NOD mice that insulin B:9–23-specific CD4⁺T cells can be divided into types A and B T cells. Both recognize the peptide bound to IA^{g7} in register 3. However, type A T cells prefer the

glutamic acid at position 21 as TCR-binding residue while type B cells prefer glycine 21 (ref. 28).

Second, we set up two novel human insulin mimetopes with mutations at position 22 to glutamic acid (E) together with position 21 being E or G and an additional mutation of position 14 from alanine (A) to glutamic acid (E) (ins.mim.1 = 14E-21G-22E; ins.mim.4 = 14E-21E-22E). The mutation at position 14 was included since structural analyses of a human insulin-peptide-HLA-DQ8 complex had suggested that glutamic acid (=E) is preferred over alanine at the first MHC-anchor²⁹ (Supplementary Fig. 1 for peptide sequences).

Proliferative responses were assessed using polyclonal CFSE-labelled CD4⁺T cells from eight islet autoantibody positive HLA-DQ8⁺ children. Comparisons were made upon stimulation with either the natural insulin-B-chain-epitope or a set of insulin-B-chain mimetopes or as controls left untreated. When the proportion of cells with diluted CFSE-label was determined, the insulin mimetopes showed increased stimulatory capacities when compared with the natural insulin-B-chain epitope (unstimulated: 6.2 ± 0.2 versus insulin B:9-23: 6.4 ± 0.3 versus insulin mimetopes: 13.7 ± 1.4 CFSE^{dim}CD45RO⁺CD25⁺T cells in % of CD4⁺T cells, *P* < 0.01, Fig. 1).

Moreover, a combination of ins.mim.1 = 14E-21G-22E and ins.mim.4 = 14E-21E-22E resulted in significantly enhanced stimulation when compared with ins.mim.2 = 21G-22E and ins.mim.3 = 21E-22E either in CD4⁺T cells from non-diabetic children with ongoing islet autoimmunity (Fig. 1d, *P* < 0.01) or without autoimmunity (Supplementary Fig. 2).

Ex vivo identification of human insulin-specific Tregs. Next, based on their enhanced stimulatory potential, agonistic activity and in accordance with identified crystal structures²⁹ we employed 14E-21G-22E (ins.mim.1) and 14E-21E-22E (ins.mim.4) for the development of insulin-specific HLA-DQ8-tetramers. CD4⁺T-cell enrichment before flow cytometric enumeration distinctly increased sensitivity of detection of insulin-specific CD4⁺T cells. Virtually no tetramer⁺CD4⁺T cells were detected with the HLA-DQ8 control tetramers and by using CD4⁺T cells from an HLA-DQ8-negative donor (Fig. 2a,b). By contrast, insulin mimetope-specific CD4⁺T cells were readily identified *ex vivo* using HLA-DQ8 insulin mimetope-specific tetramers, and frequencies of tetramer⁺CD4⁺T cells were correlated with CD3 expression (second right and right plots in Fig. 2b).

To permit for the first time the direct *ex vivo* identification of human HLA-DQ8-restricted insulin-specific Foxp3⁺Tregs we used pre-enriched CD4⁺T cells and newly developed settings to combine tetramer stainings with multiparameter flow cytometry and intracellular Foxp3 staining (Fig. 2c).

To verify the specificity of the tetramer⁺CD4⁺T cells for the insulin mimetope and insulin B:9-23 itself, tetramer⁺ cells were sort-purified and expanded in a polyclonal fashion. Re-stimulation of CD4⁺T cells with the insulin mimetopes induced rapid proliferation, as determined by dilution of the CFSE label (Fig. 2d). The CD4⁺T cells likewise responded to the natural insulin B:9-23 epitope, albeit to a lesser extent (right plot in Fig. 2d).

Insulin-specific Foxp3⁺Tregs and autoimmune progression. HLA-DQ8-restricted insulin mimetope-specific CD4⁺T cells were identified in children without and with various durations of islet autoimmunity (disease categories: no autoimmunity: islet autoantibody negative, recent activation: multiple islet autoantibodies for <5 years and long-term autoimmunity: multiple islet autoantibodies >10 years, Fig. 3a,c). Likewise

such T cells were found in children with recent-onset or longterm T1D (Supplementary Fig. 3). At least 8 × 10⁶ and up to 40 × 10⁶ cells were acquired and HLA-DQ8-restricted insulin mimetope-specific CD4⁺T cells were detected in a range of 0.001–0.01% of CD4⁺T cells (see summary graph in Fig. 3c). These frequencies of insulin mimetope-specific CD4⁺T cells are in accordance with the range that has been estimated for islet-antigen-specific CD4⁺T cells, for example for proinsulin₇₆₋₉₀-specific CD4⁺T cells the frequency has been estimated to be ~1 in 300,000 PBMCs^{32,33}. Phenotyping of HLA-DQ8-restricted insulin mimetope-specific CD4⁺T cells revealed an increase in the frequency of cells with a memory phenotype according to the duration of islet autoimmunity (Fig. 3d).

In young at-risk children, T1D can develop within several months of the appearance of autoantibodies. However, it may take more than a decade in some children^{8,9}, supporting the concept of episodes of successful immune tolerance. Of interest, frequencies of insulin mimetope-specific Foxp3⁺Tregs were significantly lower in children with recent onset of autoimmunity than in children without autoimmunity (no autoimmunity versus recent onset of autoimmunity: 1.9 ± 0.9 versus 0.5 ± 0.4% of Tet⁺CD4⁺T cells, *P* < 0.05, Fig. 3e). We identified enhanced frequencies of insulin mimetope-specific Foxp3⁺Tregs in non-diabetic children with longterm autoimmunity (long-term autoimmunity versus recent onset of autoimmunity: 11.7 ± 0.9 versus 0.5 ± 0.4 Foxp3⁺Tregs as a % of Tet⁺CD4⁺T cells, *P* < 0.001, Fig. 3e), indicative of at least periods of successful ongoing immune regulation in such children. To further support a critical role of insulin mimetope-specific Tregs in delaying progression of islet autoimmunity to clinically overt T1D, frequencies of insulin mimetope-specific Tregs were found to be severely reduced in children with newly diagnosed T1D and a very early disease manifestation (age at diagnosis ≤ 5 years) (Fig. 3e). These findings underscore the rationale of inducing autoantigen-specific Tregs for delaying T1D progression.

Agonistic activity of insulin mimetopes in CD4⁺T-cell clones.

To determine agonistic activities of the individual insulin mimetopes we generated HLA-DQ8-restricted insulin mimetope-specific CD4⁺T-cell clones from children without islet autoimmunity or with various durations of islet autoimmunity. For the stimulation of human CD4⁺T cells and T-cell cloning we used HLA-DQ8 insulin mimetope-specific artificial APCs expressing insulinB:chain-10-23-mimetopes (14E-21G-22E (ins.mim.1) and 14E-21E-22E (ins.mim.4)) which were established using antibody-coupling beads, DQ-antibodies³⁴ and unlabelled insulin mimetope-specific HLA-DQ8-tetramers. CD4⁺T cells responding to stimulation with insulin mimetope-specific artificial APCs were single-cell-sorted as CFSE^{dim}CD25^{high}CD4⁺T cells. In control experiments using HLA-DQ8-expressing artificial APCs fused to irrelevant peptides no dilution of the CFSE-label was observed (Supplementary Fig. 4).

Insulin-specificity in growing CD4⁺T-cell clones was confirmed upon stimulation with insulin mimetopes in the presence or absence of DQ-blocking antibodies, analysed flow-cytometrically by CD25 upregulation (Fig. 4a,b) and confirmed by analyses of the highest CD25 levels (CD25⁺⁺⁺ levels, Fig. 4c,d and Supplementary Fig. 5). All tested CD4⁺T-cell clones also responded to the natural insulin B:9-23 epitope albeit to a lower extent (Fig. 4e,f and Supplementary Fig. 5). These data show that T cells cloned from CD4⁺T cells responding to insulin-B-chain-10-23 mimetopes are likewise specific for the

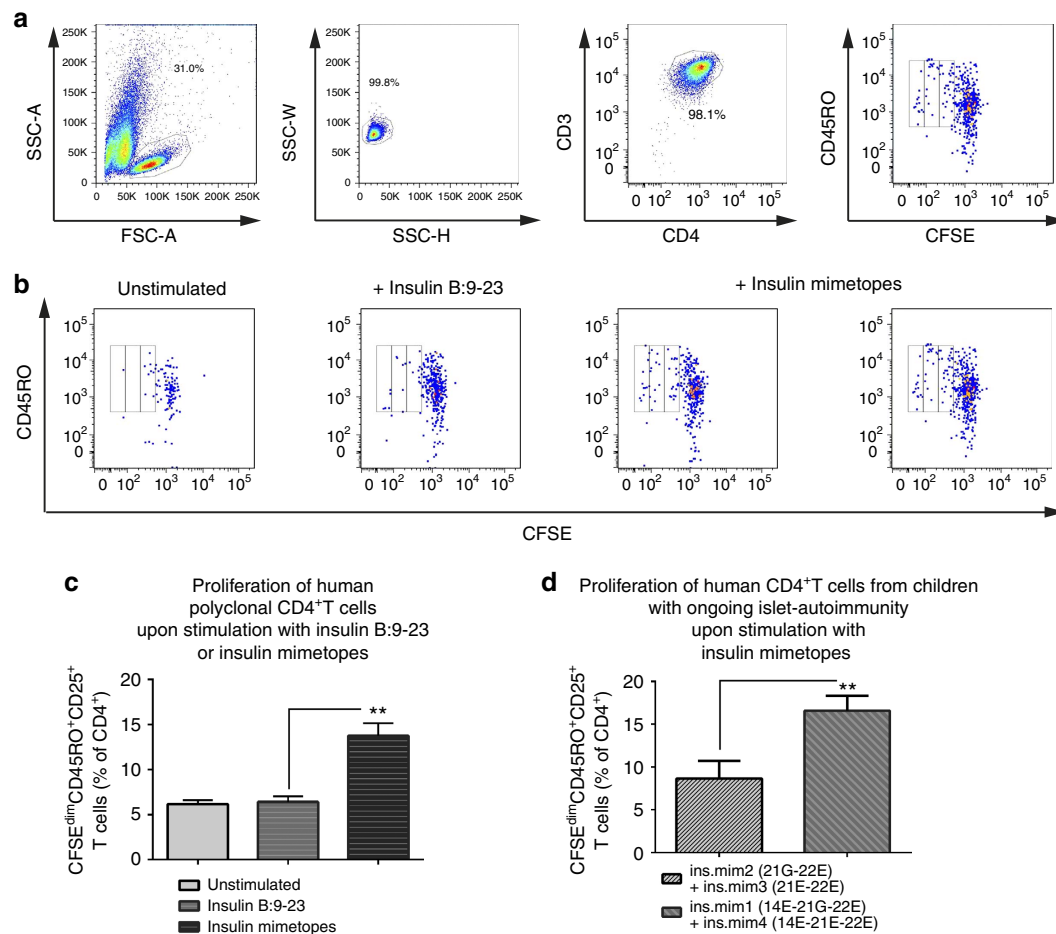


Figure 1 | Agonistic activity of insulin mimetopes in human polyclonal CD4⁺T cells required for Foxp3⁺Treg induction. (a) Representative FACS plots for the identification of proliferating human polyclonal CD4⁺CD3⁺T cells by CFSE-dilution in CD45RO⁺CD4⁺CD25⁺T cells (left to right). **(b)** Representative FACS plots of CFSE-dilution profiles from human polyclonal CD4⁺T cells purified from children with or without pre-T1D either left untreated, stimulated with the natural insulin B:9-23 epitope (1 μg ml⁻¹) or a set of four insulin-B-chain-10-23-mimetopes (shown are two staining examples of cells stimulated with ins.mim.2 = 21G-22E; ins.mim.3 = 21E-22E; ins.mim.1 = 14E-21G-22E; ins.mim.4 = 14E-21E-22E, final concentration at 1 μg ml⁻¹). Proliferating CFSE^{dim}CD4⁺CD25⁺CD45RO⁺T cells were considered as responding T cells. **(c)** Percentages of divided human CFSE^{dim}CD4⁺CD25⁺CD45RO⁺T cells. Bars represent the means ± s.e.m. (n = 8) from duplicate wells of eight children performed in four independent experiments. **P < 0.01 (Student's t-test). **(d)** Percentages of divided human CFSE^{dim}CD4⁺CD45RO⁺T cells upon stimulation with a combination of ins.mim.2 = 21G-22E; ins.mim.3 = 21E-22E or a combination of ins.mim.1 = 14E-21G-22E; ins.mim.4 = 14E-21E-22E. Bars represent the means ± s.e.m. (n = 6) from duplicate wells of six children done in three independent experiments. **P < 0.01 (Student's t-test).

natural insulin B:9-23 epitope (Fig. 4e,f and Supplementary Fig. 5).

The set of four insulin-B-chain-10-23 mimetopes was used to assess their individual proliferative capacities (ins.mim.2 = 21G-22E; ins.mim.3 = 21E-22E; ins.mim.1 = 14E-21G-22E; ins.mim.4 = 14E-21E-22E) in generated insulin-specific CD4⁺T-cell clones (Fig. 4g). The stimulatory potential of the individual insulin mimetopes is shown in fold of the stimulation achieved with the natural insulin B:9-23 epitope. Irrespective of the presence or duration of autoimmunity (Fig. 4g) all insulin-variants were superior in stimulating insulin-specific CD4⁺T-cell clones. In particular ins.mim.4 (ins.mim.4 = 14E-21E-22E) presented with a significantly enhanced stimulatory capacity (P < 0.05) when compared with ins.mim.2 (ins.mim.2 = 21G-22E) and ins.mim.3 (ins.mim.3 = 21E-22E). A summary of the stimulatory capacities of all tested insulin-specific CD4⁺T-cell clones is outlined in Fig. 4g. These findings are in accordance with our observations obtained from competitive *in vitro* HLA-DQ8 binding assays (Fig. 4h) where ins.mim.4 presented with the highest affinity to HLA-DQ8

(IC₅₀ = 0.9 μM) when compared with ins.mim.3 (IC₅₀ = 2.1 μM), ins.mim.2 (IC₅₀ = 6.3 μM), ins.mim.1 (IC₅₀ = 3.2 μM) and the natural insulin B:9-23 epitope (IC₅₀ = 14.8 μM).

Human insulin-specific Foxp3⁺Treg induction *in vitro*. In agreement with their enhanced stimulatory potential, agonistic activity, in reference to identified categories of types A and B T cells²⁸ and in accordance with identified crystal structures²⁹ we used ins.mim.1 (14E-21G-22E) and ins.mim.4 (14E-21E-22E) to determine human insulin-specific Foxp3⁺Treg induction. We set up human *in vitro* Foxp3⁺Treg induction mimicking subimmunogenic TCR stimulation^{16,35}. We developed a protocol for human insulin-specific Foxp3⁺Treg induction without TGFβ using premature withdrawal of TCR stimulation building up on murine studies³⁵. Highly pure human naive CD4⁺T cells isolated from children with or without islet autoimmunity (Fig. 5a-c; disease categories: no autoimmunity, recent activation of autoimmunity and longterm autoimmunity) were used as a starting population (Supplementary Fig. 6 for gating example of

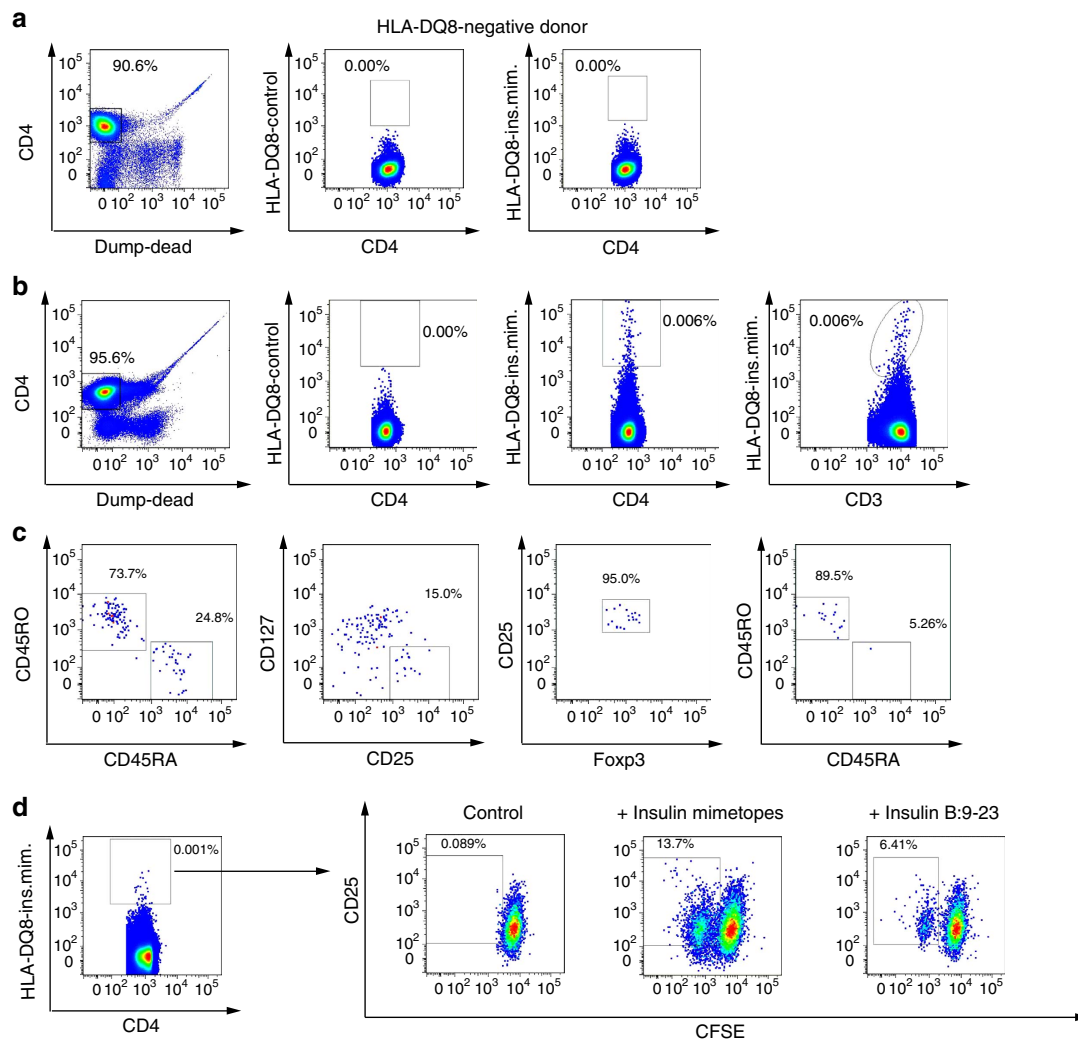


Figure 2 | Ex vivo identification of human HLA-DQ8-restricted insulin-specific regulatory T cells. Human CD4⁺T cells were analysed by FACS, first gating on live, CD14⁻, CD19⁻, CD8a⁻, CD11b⁻, CD4⁺ (left; **a,b**) and CD3⁺, followed by examination of tetramer binding. (**a**) Representative FACS plots for the direct ex vivo identification of HLA-DQ8-restricted insulin-specific CD4⁺T cells. Control staining was performed to assess the quality and specificity of the tetramer staining using a combination of two control tetramers fused to irrelevant peptides (centre) or using CD4⁺T cells from an HLA-DQ8-negative individual (right). (**b**) Representative FACS plots for the quality of HLA-DQ 8-restricted insulin-specific tetramer staining gating against CD4 (centre) and CD3 (right). (**c**) Representative FACS plots for the phenotypic characterization of HLA-DQ8-restricted insulin-specific CD4⁺T cells based on CD45RA versus CD45RO expression (memory status) and of insulin-specific Foxp3⁺Tregs based on CD127^{low}CD25^{high} and Foxp3^{high} expression. (**d**) Re-stimulation of sorted and purified tetramer⁺ CD4⁺T cells (example plot on the left) either left untreated (= control, left) or stimulated with insulin mimetopes (ins.mim.1,2,3,4 at final 10 ng ml⁻¹, middle plot), or with insulin B:9-23 (100 ng ml⁻¹, right), as assessed by analysing the dilution of the CFSE label and CD25 expression.

human naive CD4⁺T cells). For antigen presentation during Treg induction autologous dendritic cells (DCs) were purified from PBMCs by depletion of CD14⁺ and CD19⁺ cells and subsequent positive selection of CD304⁺ plasmacytoid DCs and CD1c⁺ and CD141⁺ myeloid DCs.

We compared the *in vitro* Treg induction activity of the natural insulin-B-chain epitope with ins.mim.1 (14E-21G-22E) and ins.mim.4 (14E-21E-22E) (Fig. 5a–c). The combination of ins.mim.1 = 14E-21G-22E and ins.mim.4 = 14E-21E-22E showed best Treg induction as assessed by analysis of induced CD127^{low}CD25^{high}Foxp3^{high}Tregs. Optimal Treg induction activity was seen in children without ongoing autoimmunity (insulin mimetope (ins.mim.1 + 4 final at 0.001 ng ml⁻¹): 53.9 ± 16.0 versus insulin-B-chain-epitope (0.001 ng ml⁻¹): 0.0; $P < 0.05$ or (0.01 ng ml⁻¹): 7.7 ± 6.4% of CD127^{low}CD25^{high}CD4⁺T cells, Fig. 5a).

Stability of human Foxp3⁺Tregs induced *in vitro*. Next, we characterized human Treg stability upon their induction using sub-immunogenic (limited) TCR stimulation^{16,35}. Sub-immunogenic TCR stimulation significantly increased frequencies of induced CD127^{low}CD25^{high}Foxp3^{high}CD4⁺Tregs compared with non-sub-immunogenic (continuous) TCR stimulation (limited TCR versus continuous TCR stimulation: 42.5 ± 2.7 versus 6.9 ± 1.9 Foxp3^{high}Tregs as % of CD127^{low}CD25^{high} cells, $P < 0.01$, Fig. 6a,b). Importantly, when we re-stimulated the previously induced CD127^{low}CD25^{high}Tregs, the frequency of Foxp3^{high}Tregs was significantly higher when the cells were previously stimulated by limited TCR conditions than cells previously stimulated by continuous TCR conditions (40.3 ± 3.8 versus 9.4 ± 3.2 Foxp3^{high}Tregs as % of CD127^{low}CD25^{high} cells) (Fig. 6c,d). These data support the concept that a subimmunogenic TCR

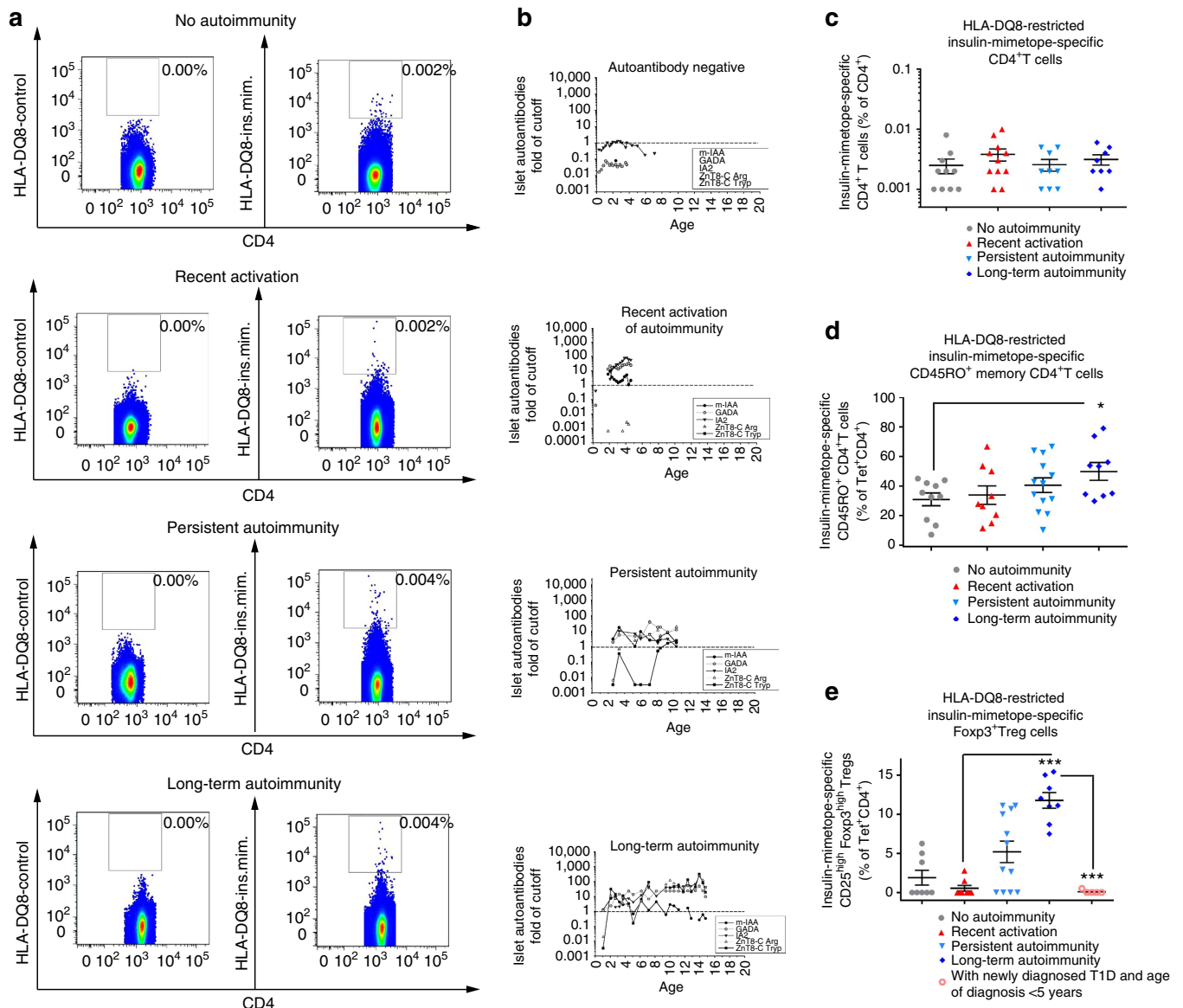


Figure 3 | Frequency of insulin mimetope-specific Foxp3⁺ Tregs in children with recent onset of islet autoimmunity. (a) Representative set of FACS plots for the identification of HLA-DQ8-restricted insulin mimetope-specific CD4⁺ T cells with control (left) and insulin mimetope-specific tetramer (right) staining using CD4⁺ T cells purified from *HLA-DQ8⁺* children without autoimmunity (islet autoantibody negative), with recent onset of autoimmunity (recent activation = multiple autoantibodies for ≤5 years), persistent autoimmunity (multiple autoantibodies for >5 to ≤10 years) and longterm autoimmunity (multiple autoantibodies >10 years without T1D). (b) Representative autoantibody profiles shown as the fold cutoff value for each disease stage. (c) Frequency of HLA-DQ8-restricted insulin-specific tetramer⁺ CD4⁺ T cells in children without autoimmunity (islet autoantibody negative, *n* = 10), with recent onset of autoimmunity (recent activation = multiple autoantibodies for ≤5 years, *n* = 9), persistent autoimmunity (multiple autoantibodies for >5 to ≤10 years, *n* = 13), and long-term autoimmunity (multiple autoantibodies >10 years without T1D, *n* = 10). (d) Frequency of HLA-DQ8-restricted insulin-specific memory tetramer⁺ CD45RO⁺ CD4⁺ T cells in children without autoimmunity (islet autoantibody negative, *n* = 10), with recent onset of autoimmunity (recent activation = multiple autoantibodies for ≤5 years, *n* = 9), persistent autoimmunity (multiple autoantibodies for >5 to ≤10 years, *n* = 13), and longterm autoimmunity (multiple autoantibodies >10 years without T1D, *n* = 10). (e) Frequency of HLA-DQ8-restricted insulin-specific tetramer⁺ CD127^{low} CD25^{high} CD4⁺ Foxp3^{high} Tregs in children without autoimmunity (islet autoantibody negative, *n* = 8), with recent onset of autoimmunity (multiple autoantibodies for ≤5 years, *n* = 8), persistent autoimmunity (multiple autoantibodies for >5 to ≤10 years, *n* = 12), longterm autoimmunity (multiple autoantibodies for >10 years, *n* = 5), or newly diagnosed type 1 diabetes with very early disease manifestation (age at diagnosis ≤5 years, *n* = 5). Data are presented as the mean ± s.e.m. from 10 independent experiments. **P* < 0.05 and ****P* < 0.001 (Student's *t*-test).

stimulus during human Treg induction *in vitro* confers increased stability of Foxp3^{high} Tregs.

Insulin-specific CD4⁺ T cells in NSG-HLA-DQ8 mice. To determine the conditions for human insulin-specific Foxp3⁺ Treg

induction in the context of a human immune system *in vivo* murine MHCII-deficient NSG-HLA-DQ8 transgenic mice were reconstituted 2 weeks after birth with human HSCs purified from fresh umbilical cord blood from six *HLA-DQ8⁺* donors. Such reconstituted NSG-HLA-DQ8 mice showed high engraftment efficiency 8 weeks post reconstitution in

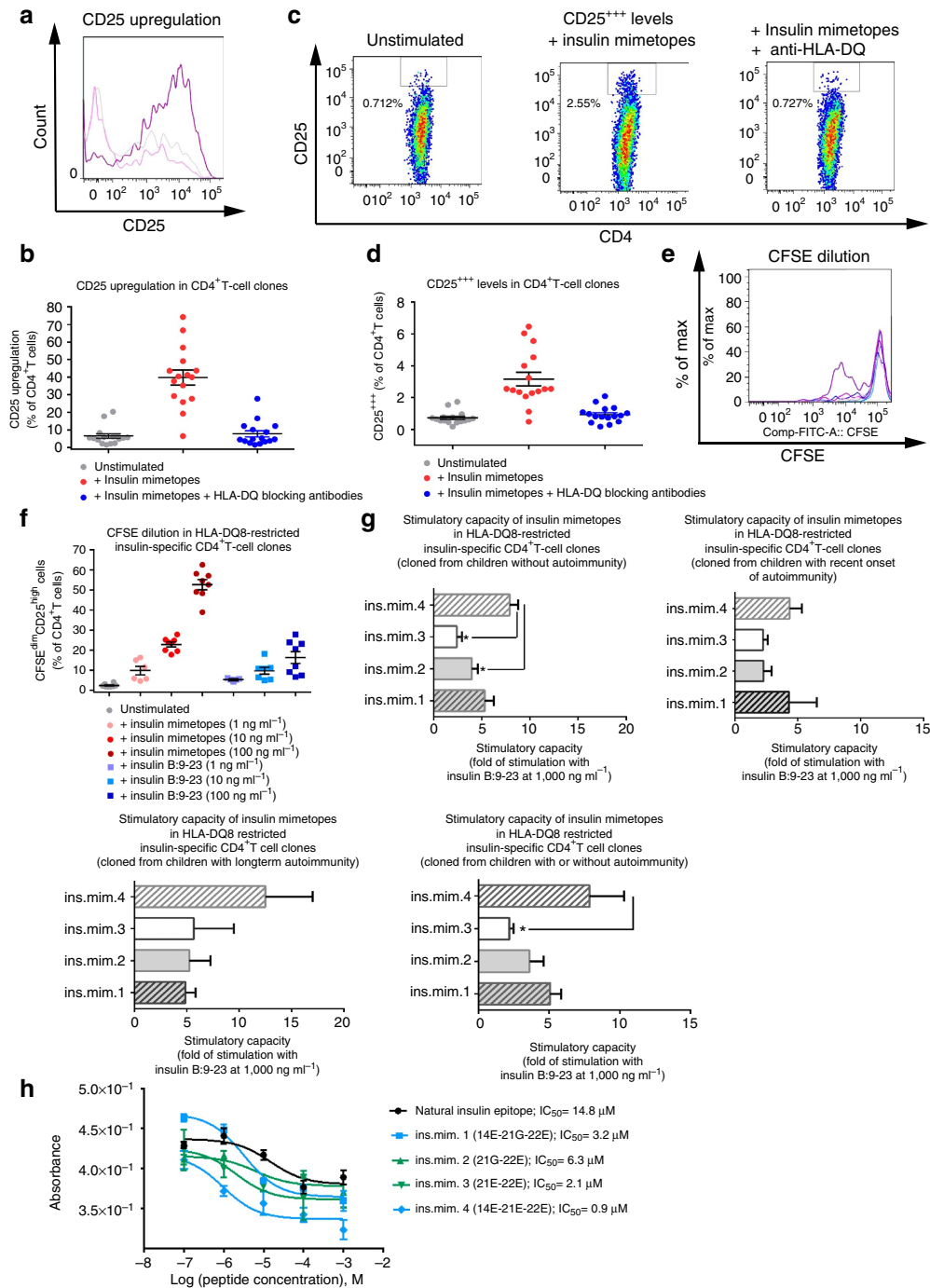


Figure 4 | Agonistic activity of insulin mimetopes in human insulin-specific CD4⁺T-cell clones. (a) CD25 upregulation in CD4⁺T-cell clones left untreated or upon stimulation with insulin mimetopes (ins.mim.1,2,3,4 at 100 ng ml⁻¹) with or without DQ-blocking antibodies (grey line: unstimulated control; dark pink line: + insulin mimetopes; light pink line: + insulin mimetopes + HLA-DQ blocking antibodies). (b) Summary graph for a. 16 CD4⁺T-cell clones: four from three subjects without ongoing autoimmunity; five from four subjects with recent onset of autoimmunity, seven from five individuals with long-term autoimmunity. (c) CD25⁺⁺⁺ levels of an insulin-specific CD4⁺T-cell clone left unstimulated (left plot), stimulated with insulin mimetopes (middle plot) or with insulin mimetopes + HLA-DQ blocking antibodies (right plot). (d) Summary graph for c. Numbers of clones tested as in b. (e) CFSE-dilution profiles from insulin-specific CD4⁺T-cell clones (grey line: unstimulated; light blue line: + insulin B:9-23 epitope (1 ng ml⁻¹); blue line: + insulin B:9-23 epitope (10 ng ml⁻¹); dark blue line: + insulin B:9-23 epitope (100 ng ml⁻¹); light pink line: + insulin mimetopes (1 ng ml⁻¹); pink line: + insulin mimetopes (10 ng ml⁻¹); dark pink line: + insulin mimetopes (100 ng ml⁻¹)). (f) Summary graph for e. Eight CD4⁺T-cell clones have been tested: two from two subjects without ongoing islet autoimmunity, two from two individuals with recent onset of autoimmunity, four from three individuals with long-term autoimmunity. (g) Summary graphs of stimulatory capacities of ins.mim.2 = 21G-22E; ins.mim.3 = 21E-22E; ins.mim.1 = 14E-21G-22E; ins.mim.4 = 14E-21E-22E (100 ng ml⁻¹) in T-cell clones shown in fold of the stimulatory potential of the insulin B:9-23 (1,000 ng ml⁻¹). Numbers of clones tested as in b. (b,d,f,g) Data represent the means ± s.e.m. 16 clones (b,d,g) or eight clones (f) have been tested. *P < 0.05 (Student's t-test). (h) In vitro binding of insulin B:9-23, ins.mim.1 (14E-21G-22E), ins.mim.2 (21G-22E), ins.mim.3 (21E-22E) and ins.mim.4 (14E-21E-22E) to HLA-DQ8. Competitive binding assays were carried out using a FITC-labelled reference GAD65 peptide and increasing concentrations of unlabelled insulin epitopes and mimetopes.

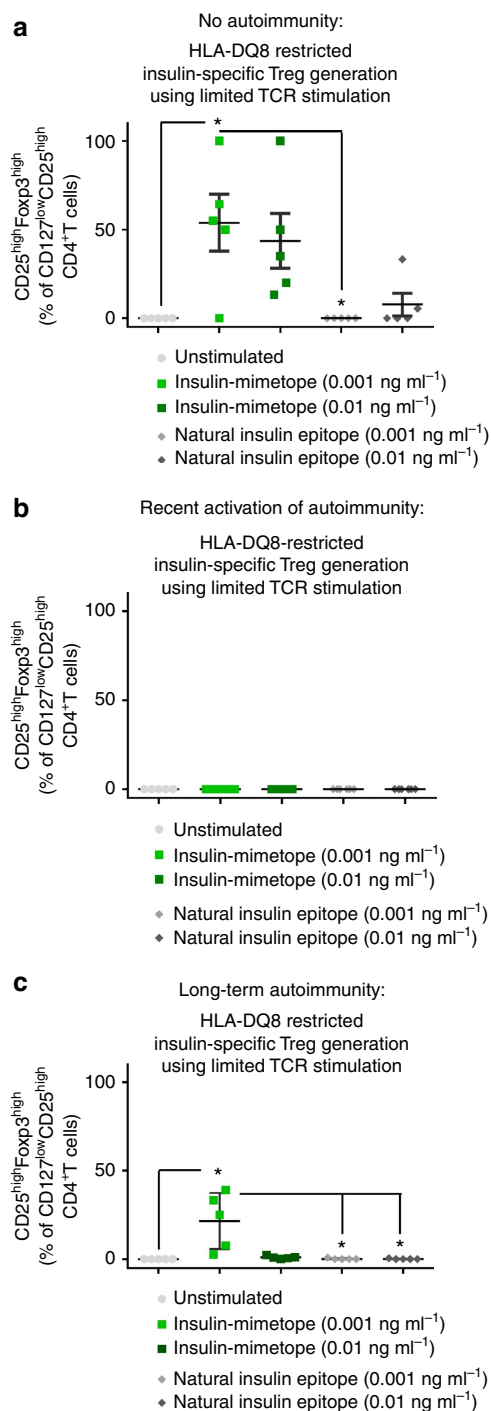


Figure 5 | Human insulin-specific Foxp3⁺ Treg induction using insulin mimetopes and subimmunogenic TCR stimulation. Comparison of human Treg induction potential of insulin mimetopes (ins.mim.1 = 14E-21G-22E; ins.mim.4 = 14E-21E-22E) and the natural insulin-B-chain 9-23 epitope using limited TCR stimulation in the presence of autologous CD304⁺ plasmacytoid, CD1c⁺ and CD141⁺ myeloid dendritic cells *in vitro* and human naive CD4⁺ T cells purified from children with or without ongoing islet autoimmunity (no autoimmunity, $n = 5$ per group (a)); recent activation of autoimmunity, $n = 6$ per group (b)); long-term autoimmunity, $n = 5$ per group (c)) from duplicate wells done in five independent experiments. Tregs were identified as CD4⁺CD3⁺CD127^{low}CD25^{high} T cells and then verified by intracellular staining for Foxp3. * $P < 0.05$ (Student's *t*-test).

peripheral blood (human CD45⁺ leukocytes = 73.5 ± 5.1%, Fig. 7). When analysed at 20 weeks post reconstitution NSG-HLA-DQ8 mice presented with successful CD4⁺T-cell development in pooled spleen and lymph nodes (3.9 ± 0.4% of human CD45⁺ leukocytes, Fig. 8, $n = 8$ from two independent experiments) and peripheral blood (Supplementary Fig. 7) in accordance with previous studies³⁶. Upon reconstitution we likewise identified in those animals other immune subsets, for example, human CD8⁺T cells and B cells (Supplementary Fig. 8).

To characterize insulin mimetope-specific CD4⁺T cells we used insulin-HLA-DQ8-tetramers. Of note, we identified HLA-DQ8-restricted insulin mimetope-specific CD4⁺T cells indicating successful positive selection on human HLA-DQ8 molecules in those humanized mice (0.2 ± 0.2 of human CD4⁺T cells, Fig. 8). Expression levels of tetramer⁺CD4⁺T cells correlated with CD3. No tetramer⁺CD4⁺T cells were detected with the control tetramers. Two-third of the insulin-specific CD4⁺T-cell fraction were in a naive CD45RA⁺ state (Fig. 8c, middle plot) therefore suitable for Foxp3⁺Treg induction. HLA-DQ8-restricted insulin-specific CD4⁺T cells were likewise identified in peripheral blood but not in CD4⁺T cells purified from white adipose tissues (WATs) (Supplementary Fig. 9).

Human insulin-specific Foxp3⁺ Treg induction *in vivo*. To determine human insulin-specific Foxp3⁺Treg induction *in vivo* using subimmunogenic TCR stimulation reconstituted NSG-HLA-DQ8 mice were subcutaneously implanted with osmotic mini-pumps infusing minute amounts of insulin mimetopes (5 µg per day for 14 days). Based on optimal CD4⁺T-cell development vaccination was done at 20 weeks post reconstitution. In accordance with their enhanced stimulatory potential as identified in insulin-specific CD4⁺T-cell clones (Figs 1 and 4) and optimal *in vitro* Treg induction (Fig. 5) we chose a combination of ins.mim.1 = 14E-21G-22E and ins.mim.4 = 14E-21E-22E for *in vivo* Foxp3⁺Treg induction.

Human CD127^{low}CD25^{high}Tregs were identified in humanized NSG-HLA-DQ8 mice in peripheral blood and spleen (Fig. 9a,b). Treg identity within CD127^{low}CD25^{high}T cells was verified by intracellular staining for Foxp3 (Fig. 9c).

Three weeks after subimmunogenic vaccination with insulin mimetopes humanized NSG-HLA-DQ8 mice showed significantly increased frequencies of human CD127^{low}CD25^{high}Tregs (Fig. 9d, + PBS: CD127^{low}CD25^{high}Tregs: 2.8 ± 0.4% versus + insulin mimetopes: CD127^{low}CD25^{high}Tregs: 10.2 ± 1.0%; $P < 0.001$). Upon application of insulin mimetopes we also identified HLA-DQ8-restricted insulin-specific CD127^{low}CD25^{high}Tregs (Supplementary Fig. 10).

Moreover, when CD4⁺T cells were isolated from pancreatic islets we identified increased frequencies of CD127^{low}CD25^{high}Tregs in NSG mice that had received insulin mimetopes for Treg induction in contrast to control animals treated with PBS (Supplementary Fig. 11).

Next, when we analysed Ki67 expression in insulin mimetopes treated NSG mice, we observed a higher proliferative potential of CD127^{low}CD25^{high}Tregs purified from lymph nodes when compared with peripheral blood and pancreatic islets (Supplementary Fig. 12).

Signatures of induced Tregs in NSG-HLA-DQ8 mice. Upon *in vivo* Foxp3⁺Treg induction insulin-specific CD4⁺T cells purified from spleens of humanized NSG-HLA-DQ8 mice presented with enhanced Foxp3 abundance as seen from quantitative PCR with reverse transcription analyses thereby further supporting the concept of insulin mimetope-specific tolerance induction (Fig. 10a). Analyses of human Treg signature

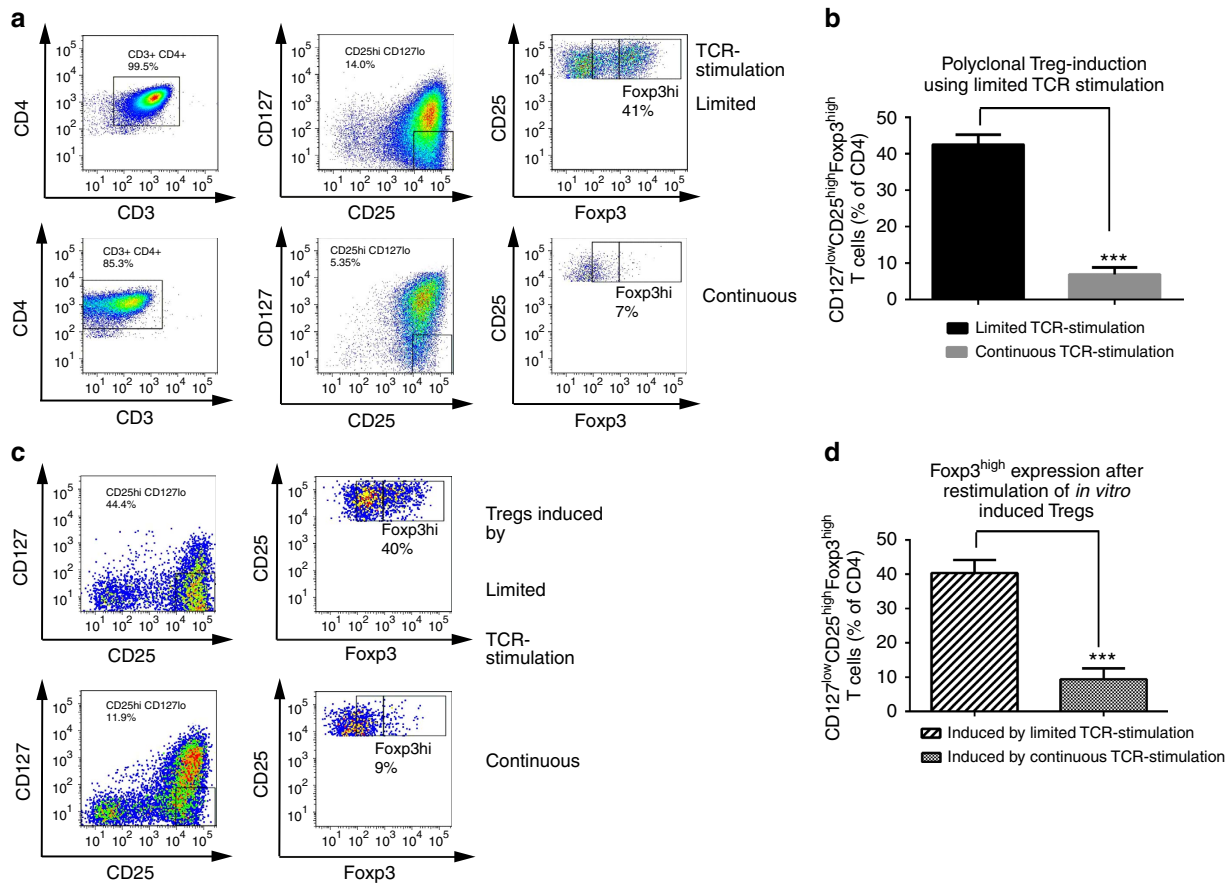


Figure 6 | Stability of human Foxp3⁺ Tregs induced by sub-immunogenic TCR stimulation *in vitro*. (a) Polyclonal induction of Tregs by limited TCR stimulation *in vitro*. Representative FACS plots of limited (12 h) and continuous (54 h) TCR stimulation. (b) Frequency of Foxp3^{high} Tregs induced by limited or continuous TCR stimulation. Data are presented as the mean \pm s.e.m. ($n = 5$) of duplicate wells in five individual experiments. *** $P < 0.001$ (Student's t -test). (c) Stability of Tregs induced by limited or continuous TCR stimulation *in vitro*. Representative FACS plots prepared after re-stimulation of CD127^{low} CD25^{high} Tregs that had been previously induced by continuous or limited polyclonal TCR stimulation to assess Treg stability. (d) Frequency of induced Tregs following re-stimulation. Data are presented as the mean \pm s.e.m. ($n = 5$) of duplicate wells in five individual experiments. *** $P < 0.001$ (Student's t -test).

genes^{37,38} revealed enhanced abundance of *CTLA4* and *IL-2R α* which impact Treg physiology. In addition, we observed significantly increased abundance of *TIGIT* which has been reported as important for Treg suppressive function^{39,40} and *RTKN2* which was shown to share the unique Treg signature expression pattern while its functional role in Treg biology remains largely undefined³⁷ (Fig. 10a). Upon subimmunogenic vaccination with insulin mimetopes we did not observe any significant changes in *IKZF2* encoding Helios, nor in *ENTPD1* (encoding CD39, a Treg effector molecule⁴¹). Moreover, no upregulation of T effector cell genes such as *IL-17R α* and *IL-21* was seen (Supplementary Fig. 13, abundance of *NFATc2*, *ROR γ t*, *T-bet* and *IFN γ* were below the lower limit of detection).

Stability of human Foxp3⁺ Tregs induced *in vivo*. To assess the methylation status of the *Foxp3* CNS2 region (Treg-specific demethylated region (TSDR)-PCR and pyrosequencing (Supplementary Fig. 14). The TSDR region is critically involved in maintaining long-term stability of *Foxp3* expression^{42,43}. We first evaluated the *Foxp3* TSDR methylation status in *ex vivo* human CD4⁺ T cell/Treg populations from male and female donors (Supplementary Fig. 15a,b). Because of the fact that the *Foxp3* gene is X-linked, levels of *Foxp3* TSDR methylation were higher in T cells from female compared with male donors.

Next, we found that upon Foxp3⁺ Treg induction *in vivo* human CD127^{low}CD25^{high}Foxp3^{high} Tregs purified from spleens and lymph nodes of humanized NSG-HLA-DQ8 mice presented with a demethylated TSDR region (Supplementary Fig. 15c). The methylation status of such Tregs from humanized mice induced by application of insulin mimetopes was as low as levels seen in *ex vivo* human Foxp3^{high} Treg populations (Supplementary Fig. 15). In contrast, the TSDR region from naive CD4⁺ T cells of such humanized NSG mice was completely methylated (Supplementary Fig. 15c).

To further assess the stability of human Tregs induced upon subimmunogenic TCR stimulation *in vivo*, humanized NSG-HLA-DQ8 mice were maintained for 6 months upon Treg induction. After 6 months humanized NSG mice that had received insulin mimetopes for Foxp3⁺ Treg induction presented with significantly enhanced abundance of *Foxp3*, *CTLA4*, *IL-2R α* and *TIGIT* compared with control animals (Supplementary Fig. 16a). Moreover, 6 months after subimmunogenic vaccination no upregulation of T effector cell genes had occurred (Supplementary Fig. 16b). In accordance, CD4⁺ T cells from such humanized NSG mice also harboured reduced abundance of *IL-17R α* , *IL-21* and *IFN γ* when compared with control animals, (Supplementary Fig. 16b, abundance of *NFATc2*, *ROR γ t* and *T-bet* remained below the lower limit of detection).

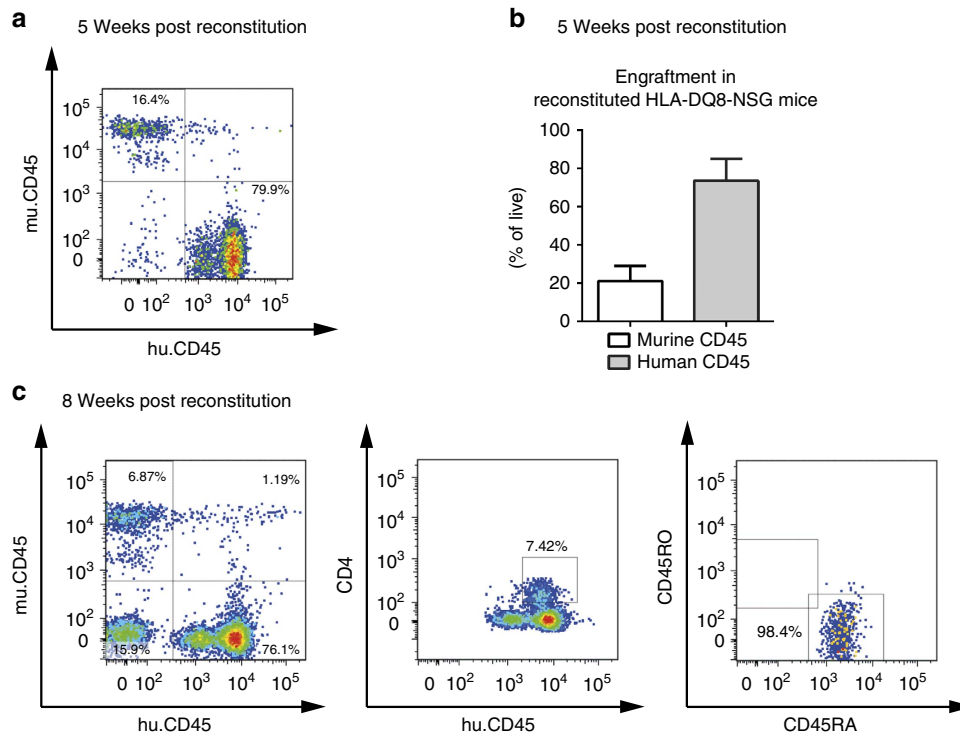


Figure 7 | Engraftment efficiency of reconstituted NSG-HLA-DQ8 transgenic mice. (a) NSG-HLA-DQ8 mice that had been reconstituted with human HSCs at 2 weeks after birth were first analysed for the engraftment of a human immune system 5 weeks later in peripheral blood. A representative FACS plot is shown to assess engraftment efficiency based on murine versus human CD45 expression levels. (b) Summary graphs for identified murine versus human CD45⁺ cells in peripheral blood five weeks after reconstitution; $n = 8$ from two independent experiments. (c) Representative set of FACS plots 8 weeks post engraftment to confirm human immune cell subsets based on murine versus human CD45 as assessed in peripheral blood. Human CD4 and activation status of human CD4⁺ T cells using CD45RA and CD45RO expression.

These findings are in accordance with data obtained in murine T1D. We purified CD4⁺T cells from pancreatic lymph nodes of 40-week-old NOD Foxp3-GFP reporter mice that had either received the natural insulin-B-chain epitope or insulin mimetope (ins.mim.3 = 21E-22E) for Treg induction at the age of 4–6 weeks. Using two fluorescent insulin mimetope-specific IA^{B7}-tetramers (21G-22E- and 21E-22E-tetramer)²⁸ we showed that NOD mice that had received the insulin mimetope and were still diabetes-free presented with significantly increased frequencies of insulin-specific Foxp3⁺Tregs (7.2 ± 1.8 versus $20.2 \pm 1.7\%$ of insulin-specific CD4⁺T cells, $P < 0.01$, Supplementary Fig. 17).

Moreover, T cells purified directly from the islets of NOD mice that had received insulin mimetopes for Treg induction presented with increased frequencies of stable Foxp3⁺Tregs accompanied by a demethylated *Foxp3* TSDR region (Supplementary Fig. 18).

Suppressive potential of induced tregs *in vivo*. For further functional analyses of human CD127^{low}CD25^{high}Tregs purified from humanized mice upon subimmunogenic vaccination we performed *in vitro* suppression assays⁴⁴. Human CD127^{low}CD25^{high}Tregs and conventional T cells were sort-purified from spleens and lymph nodes and first expanded using polyclonal stimulation. Tregs and conventional T cells were rested for 16 h in the absence of IL-2 to force them into synchronous resting states⁴⁴. Suppression of proliferative responses of conventional CD4⁺T cells was then determined by analysing the dilution of their CFSE label in the presence or absence of Tregs. *Ex vivo* human Tregs presented with potent suppressive

capacities (% suppression of responder cell proliferation: Treg: responder 1:2 = 96.1 ± 0.4 ; 1:4 = 64.1 ± 3.8 ; 1:8 = 30.8 ± 3.0 ; Fig. 10b,c).

Next, we performed suppression assays with HLA-DQ8-restricted insulin-specific T-cell clones cloned from children with ongoing islet autoimmunity as responder cells and insulin mimetopes or insulin B:9-23 for stimulation. Induced Tregs from humanized mice suppressed insulin mimetope-specific proliferation (% suppression of insulin-specific responder cells proliferation: Treg: responder 1:1 = 80.3 ± 3.5 ; 1:2 = 62.8 ± 12.7 ; 1:4 = 48.2 ± 8.7 ; 1:8 = 43.2 ± 5.5 ; Fig. 10d). Likewise, such Tregs suppressed proliferation of insulin-specific T-cell clones upon stimulation with insulin B:9–23 (% suppression of insulin-specific responder cells proliferation: Treg: responder 1:1 = 73.5 ± 2.5 ; 1:2 = 64.5 ± 4.4 ; 1:4 = 41.8 ± 2.7 ; and 1:8 = 27.6 ± 1.5 ; Fig. 10e).

Moreover, such induced Tregs from humanized mice suppressed responder T-cell proliferation using effector T cells from T1D patients (% suppression of responder cells proliferation: Treg: responder 1:1 = 46.6 ± 2.3 ; 1:2 = 21.4 ± 2.4 ; 1:4 = 15.6 ± 1.6 ; and 1:8 = 9.5 ± 1.7 , Fig. 10f).

Discussion

Control of autoimmunity through instruction of endogenous regulatory mechanisms is a long envisioned challenging goal of physicians and scientists¹⁸. In man, the development of autoantigen-specific tolerance induction strategies is still in its infancy and currently studies are ongoing. Initial results from clinical trials using natural autoantigens for induction of self-tolerance, for example, natural insulin in T1D showed thus far little benefit^{45–48}. More recently, a first primary

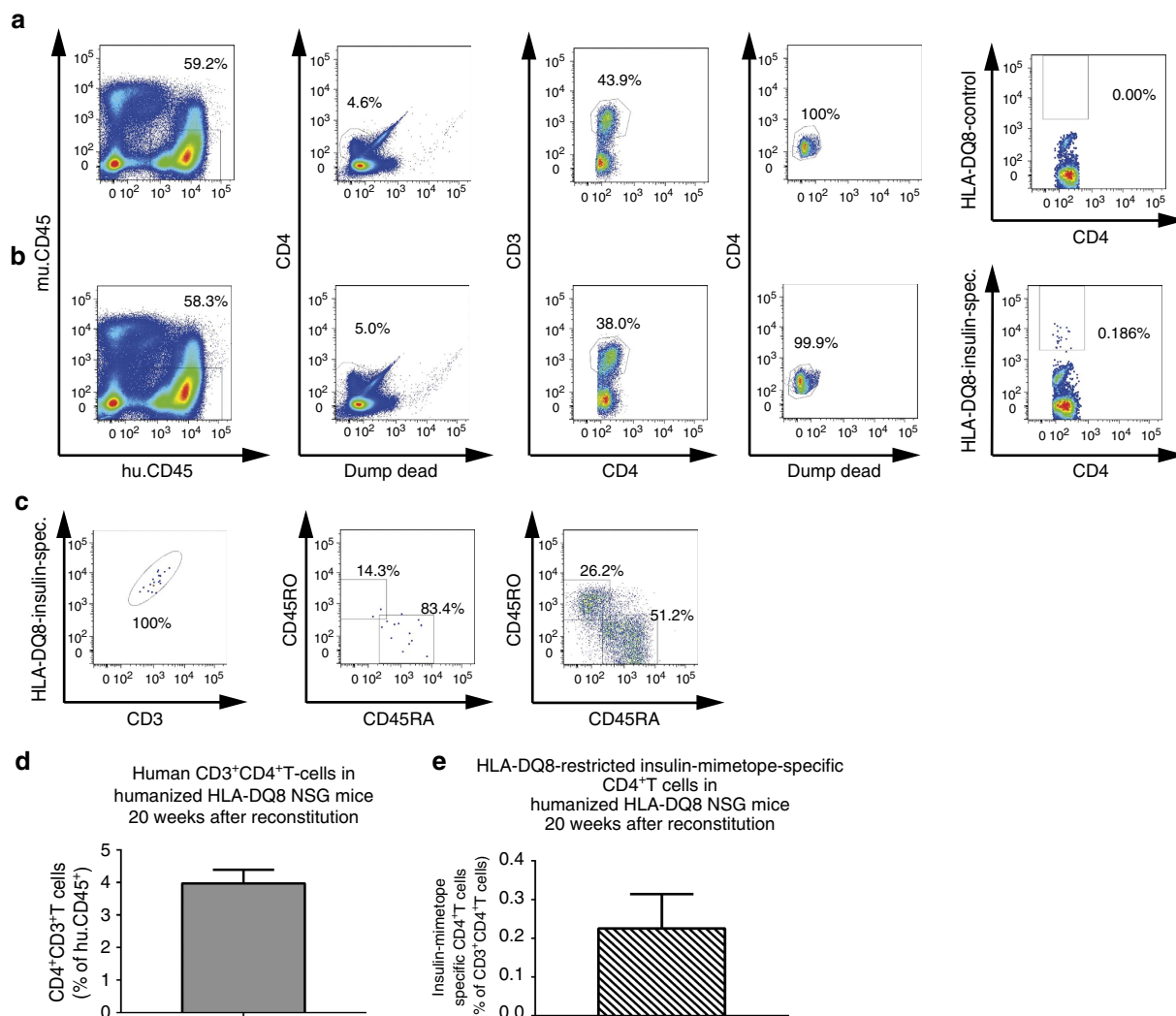


Figure 8 | CD4⁺ T-cell responses in reconstituted humanized NSG-HLA-DQ8 mice. Human immune subsets purified from pooled spleen and lymph nodes of humanized NSG-HLA-DQ8 mice, 20 weeks post reconstitution, were first identified flow cytometrically based on murine versus human CD45 expression. Human CD4⁺ CD3⁺ T cells were characterized upon exclusion of dead cells and additional markers (CD8, CD11b, CD14, CD19). **(a-c)** Representative set of FACS plots for the identification of HLA-DQ8-restricted insulin-specific CD4⁺ T cells. **(a)** Control staining to assess quality and specificity of the tetramer staining by the use of a combination of two control tetramers fused to irrelevant peptides **(a)**; upper row, right plot). **(b)** Representative set of FACS plots for the identification of HLA-DQ8-restricted insulin-specific T cells gating against CD4 **(b)**; lower row, right plot). **(c)** Representative set of FACS plots for the phenotypic characterization of identified HLA-DQ8-restricted insulin-specific CD4⁺ T cells based on gating against CD3 and CD45RA- versus CD45RO-expression (memory-status, insulin-specific versus polyclonal). **(d)** Summary graphs for identified human CD4⁺ T cells purified from spleen and lymph nodes of respective mice, *n* = 8 from two independent experiments. **(e)** Summary graph for identified human HLA-DQ8-restricted insulin-specific CD4⁺ T cells purified from spleen and lymph nodes, *n* = 8 from two independent experiments.

insulin-specific vaccination dose-finding study in children genetically susceptible to T1D was finished⁴⁹ where oral insulin application to children genetically at risk but without ongoing islet autoimmunity supported an immune response.

To further advance the translation of these antigen-specific therapies from bench to bedside it will be critical to investigate whether the choice of antigen, the time point and route of administration induced a tolerogenic response and specifically to study the conditions for efficient human Foxp3⁺Treg induction. It has been suggested that efficacy of tolerance induction may critically depend upon: disease state, antigen dosage, route of administration, the study cohort that is treated and the choice of antigen, for example, insulin versus insulin B chain peptides.

In humans, T1D risk is linked strongly to combinations of the HLA-DR4/DQ8 and DR3/DQ2 haplotypes⁵⁰ with 90% of

T1D patients harbouring DQ8 or DQ2 alleles. HLA-DQ8 shares with I-A^{g7} strikingly similar binding pockets for peptide presentation²⁹. Insulin B:9-23-reactive CD4⁺ T cells are present in the peripheral blood of T1D individuals, the immunogenic register of this peptide has low-affinity binding to HLA-DQ8 (ref. 30) and a strong agonistic variant of the natural insulin epitope established in the murine system⁷ can efficiently stimulate human CD4⁺ T cells³¹.

Here, we identify two novel human insulin mimetopes (ins.mim.1 = 14E-21G-22E and ins.mim.4 = 14E-21E-22E) with increased stimulatory capacities when compared with the natural insulin B:9-23 epitope and previously established insulin variants^{7,17,30,31}. The combination of ins.mim.1 and ins.mim.4 was chosen to use as the best stimulating mimetic within each category of insulin-reactive CD4⁺ T cells, namely type A and type B cells, as suggested in the NOD mouse setting²⁸. However, based

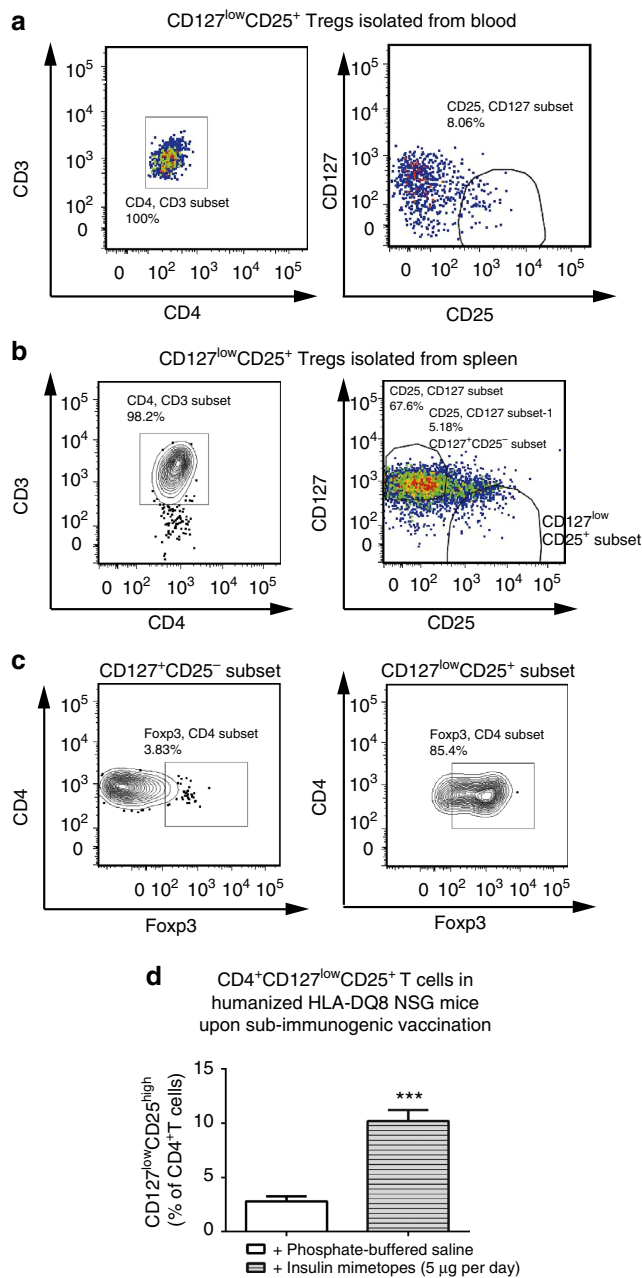


Figure 9 | Identification of CD127^{low}CD25⁺ Tregs in humanized NSG-HLA-DQ8 mice. Human immune subsets isolated from peripheral blood or spleen purified from humanized NSG-HLA-DQ8 mice, 23 weeks post reconstitution, were first identified flow cytometrically based on human CD45 expression. Human CD4⁺CD3⁺T cells were characterized upon exclusion of dead cells and additional markers (CD8, CD11b, CD14 and CD19). **(a)** Representative set of FACS plots for the identification of CD4⁺CD3⁺CD127^{low}CD25⁺ Tregs isolated from blood. **(b)** Representative set of FACS plots identifying CD4⁺CD3⁺CD127^{low}CD25⁺ Tregs purified from spleen. **(c)** Verification of Treg phenotype by intracellular staining for Foxp3 in the CD127⁺CD25⁻ non-Treg-subset and the CD127^{low}CD25⁺ Treg subset as identified in **(b)** (right plot). **(d)** Summary graphs for the quantification of identified CD127^{low}CD25⁺ Tregs purified from peripheral blood and spleen upon subimmunogenic Treg induction *in vivo* using insulin mimetopes by osmotic mini-pumps (ins.mim.1 = 14E-21G-22E; ins.mim.4 = 14E-21E-22E) or control (PBS) in humanized NSG-HLA-DQ8 mice, $n = 8$ from two independent experiments. *** $P < 0.001$ (Student's *t*-test).

on its highest affinity to HLA-DQ8 ins.mim.4 (14E-21E-22E) will probably contribute most to the observed functional effects.

Tetramers using ins.mim.1 and ins.mim.4 permitted for the first time the direct *ex vivo* identification of human insulin mimetope-specific CD4⁺T cells without prior *in vitro* expansion³⁰ and combined with intracellular Foxp3 staining the immediate analysis of insulin mimetope-specific Foxp3⁺Tregs. We have demonstrated that high frequencies of insulin mimetope-specific Tregs were associated with profound delays in T1D progression in children, which supports the rationale for inducing insulin-specific Foxp3⁺Tregs to delay or even prevent human T1D. Moreover, these data are consistent with the observation that children with slowly progressing phenotypes display an accumulation of protective genotypes in T1D susceptibility genes⁵¹ most notably *IL-2*, *IL2-R α* , *INS VNTR* and *IL-10*.

The ability to directly identify human insulin-specific Foxp3⁺Tregs *ex vivo* will be of critical relevance to assess insulin-specific vaccination responses. This is a critical step currently missing in clinical T1D prevention efforts and will support the development of novel T cell-specific biomarkers alongside personalized strategies for efficient prevention of islet autoimmunity and T1D.

The best stimulating human insulin mimetopes when applied at low subimmunogenic doses were also most efficient in inducing human insulin-specific Foxp3⁺Tregs. These results are in accord with observations in NOD mice where subimmunogenic doses of strongly stimulating insulin mimetopes efficiently induced insulin-specific Foxp3⁺Tregs which prevented T1D development⁴⁷. Here, we provide novel conceptual evidence for using low doses of strong-agonistic insulin mimetopes for efficient human Foxp3⁺Treg induction and suppression of human autoimmunity.

With respect to safety aspects of insulin-specific vaccination strategies, recently a first primary insulin-specific vaccination dose-finding study in children genetically susceptible to T1D was completed⁴⁹. Application of high doses of insulin to genetically at-risk healthy children without signs of islet autoimmunity promoted an immune response without hypoglycemia. The incidence and type of adverse events were not different between children who received placebo and children who received insulin, regardless of the insulin dose⁴⁹.

Moreover, insulin peptides have also proved safe at early stages of clinical development, supporting the concept for epitope-based vaccines⁵².

Concerning the time point of vaccination for Treg induction, we show that this process was most efficient in naive T cells from children without ongoing autoimmunity or in non-diabetic children with long-term autoimmunity. It is therefore suggested that insulin mimetope-specific Foxp3⁺Treg induction may be better applied as a primary preventive approach or as a secondary vaccination strategy for non-diabetic children with longer autoimmunity that have successfully passed the critical period of autoimmune development without progression to overt disease (longterm autoimmunity without T1D).

Mechanistically, recent data highlight a critical impact of peptide-MHC quality (stimulation by a strong-agonistic ligand) versus quantity on *in vivo* T-cell responses⁵³. Evidence for ligand discrimination beyond sensing of a cumulative TCR signal in that T cell responses differed between low-density and low-potency weak stimuli^{17,22,53–55} was provided. These findings underline the importance of integrating peptide-MHC quality and quantity in determining the minimal TCR stimulation required for T-cell proliferation *in vivo*⁵³ and support our observations that most efficient stable Foxp3⁺Treg induction is achieved by a subimmunogenic stimulus of a strong-agonistic ligand¹⁷. Accordingly, Tregs induced in humanized NSG mice

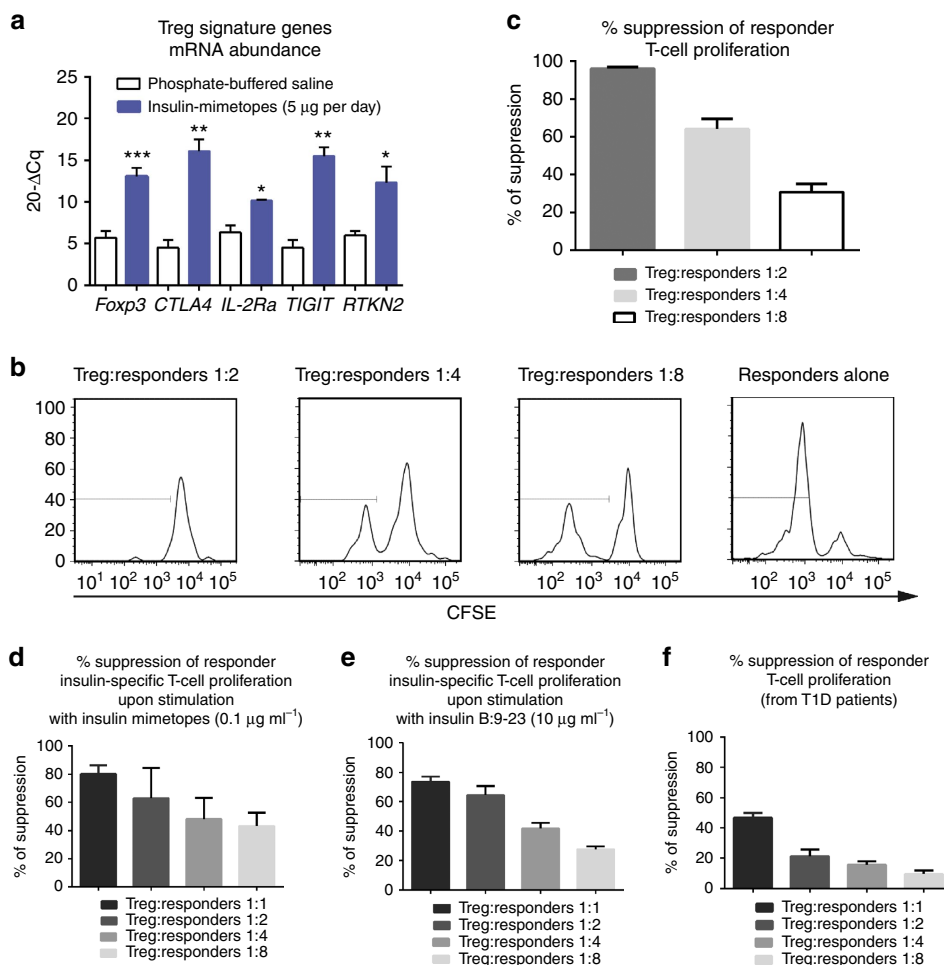


Figure 10 | Treg signatures and suppressive potential in humanized NSG-HLA-DQ8 transgenic mice. (a) Quantitative PCR with reverse transcription analyses of *Foxp3*, *CTLA4*, *IL-2R α* , *TIGIT* and *RTKN2* mRNA abundance in human CD4⁺T cells purified from pooled spleens and lymph nodes of humanized mice after 3 weeks of *in vivo* Treg induction using subcutaneous insulin mimetopes infusion by osmotic mini-pumps (ins.mim.1 = 14E-21G-22E; ins.mim.4 = 14E-21E-22E) in humanized NSG-HLA-DQ8 transgenic mice ($n = 4$). Bars represent the means \pm s.e.m. ($n = 4$ mice per group and experiment, $n = 2$ independent experiments). * $P < 0.05$; ** $P < 0.01$; *** $P < 0.001$ (Student's *t*-test). (b) Analyses of FACS-based suppression assays. Conventional responder CD4⁺T cells or Tregs were purified from pooled spleens and lymph nodes of respective humanized animals. Representative histograms show CFSE dilution profiles of CD4⁺T responder cells alone or in the presence of different ratios of Tregs (1:2; 1:4 and 1:8). (c) Summary graphs for the % suppression of responder cell proliferation in the presence of distinct Treg ratios. Values represent means \pm s.e.m.; $n = 5$ mice per experiment, $n = 2$ independent experiments). (d) Summary graphs for the % suppression of responder cell proliferation using HLA-DQ8-restricted insulin mimetope-specific CD4⁺T-cell clones from children with ongoing islet autoimmunity and stimulation with insulin mimetopes (ins.mim.1 = 14E-21G-22E; ins.mim.4 = 14E-21E-22E, final at 0.1 µg ml⁻¹) in the presence of distinct Treg ratios. Values represent means \pm s.e.m.; $n = 5$ mice per experiment, $n = 2$ independent experiments. (e) Summary graphs for the % suppression of responder cell proliferation using HLA-DQ8-restricted insulin mimetope-specific CD4⁺T-cell clones from children with ongoing islet autoimmunity and stimulation with insulin B:9-23 (at 10 µg ml⁻¹) in the presence of distinct Treg ratios. Values represent means \pm s.e.m.; $n = 5$ mice per experiment, $n = 2$ independent experiments. (f) Summary graphs for the % suppression of responder cell proliferation using responder T cells from T1D patients ($n = 3$) in the presence of distinct Treg ratios. Values represent means \pm s.e.m.; $n = 5$ mice per experiment, $n = 2$ independent experiments.

presented with a demethylated TSDR region and were maintained for prolonged periods of time in the absence of effector cell responses.

More studies are required to gain an improved understanding of how the subimmunogenic application of antigens for the efficient and stable induction of Foxp3⁺Treg cells can be best achieved in human autoimmune diseases. These efforts might include novel strategies for the application of self-antigens—for example, the use of dissolving microneedle patches⁵⁶, which were recently tested for the administration of insulin to individuals with T1D⁵⁷. Such novel application strategies could help to mimic continuous subimmunogenic antigen application promoting efficient Foxp3⁺Treg induction. Safety and efficacy of such

novel devices for vaccination have been recently tested on human skin^{58,59}.

It has been shown that human HSC-engrafted NSG mice harbour a highly-diverse TCR repertoire, which is critical for mounting an efficient yet not self-destructive adaptive immune response⁶⁰. The replacement of mouse MHC molecules by human MHC components has been a major advance in increasing the utility of these 'humanized' mice as this permits the generation and maintenance of robust human T cell responses⁶¹.

In reconstituted NSG-HLA-DQ8 mice we provide first direct evidence for HLA-DQ8-restricted insulin-specific CD4⁺T-cell responses indicating positive selection on human HLA-DQ8

molecules. Moreover, this will allow studying the requirements for human insulin-specific Foxp3⁺Treg induction in further detail.

In sum, in the pre-clinical setting of humanized NSG-HLA-DQ8 transgenic mice we established for the first time subimmunogenic Foxp3⁺Treg induction and demonstrate that subimmunogenic application of insulin mimetopes promotes enhanced levels of insulin-specific Foxp3⁺Tregs in a human immune system *in vivo*. Moreover, such induced Tregs were found to be stable and presented with robust suppressive capacities and increased abundance of Treg signature genes.

It remains challenging to interfere with processes that generate autoimmune T1D in patients; however, defining the requirements for efficient human insulin-specific Foxp3⁺Treg induction *in vivo* as evidenced here by the establishment of subimmunogenic vaccination protocols in humanized mice alongside the development of novel human insulin mimetopes could represent a critical improvement in this challenge.

Methods

Human subjects and blood samples. For the present study blood samples were collected from children or adults who are first degree relatives of patients with T1D. Written consent was obtained for the *Munich Bioresource project* (approval number #5049/11, approval committee: Technische Universität München, Munich, Germany). All subjects have been already enrolled into longitudinal studies with prospective follow-up from birth^{62–64} with the documented age of islet autoantibody seroconversion (initiation of islet autoimmunity). Venous blood was collected using sodium heparin tubes and blood volumes collected were based on EU guidelines with a maximal blood volume of 2.4 ml kg⁻¹ of body weight. Subjects have been stratified based on the presence or absence of multiple islet autoantibodies (= with or without pre-T1D) and based on the duration of islet autoantibody positivity: no autoimmunity: first degree relatives of patients with T1D who are islet autoantibody negative (*n* = 11; median age = 8 years, interquartile range (IQR) = 6–12 years, six males, five females); recent onset of islet autoimmunity: subjects with multiple islet autoantibodies for less than 5 years (*n* = 7, median age = 5 years, IQR = 4–14 years, five males, two females); persistent autoimmunity: subjects with multiple islet autoantibodies for more than 5 but less than 10 years (*n* = 9, median age = 14 years, IQR = 10–17.5 years, 7 males, two females); longterm autoimmunity: subjects with multiple islet autoantibodies for more than a decade who did not yet develop T1D (*n* = 7, median age = 15 years, IQR = 14–25 years, three males, four females). In addition five children with newly diagnosed T1D and very early disease manifestation (disease onset < 5 years) were studied (*n* = 5, median age = 4 years, IQR = 2–8 years, two males, three females) and six children with longterm T1D for > 5 years have been included (*n* = 6, median age = 14, IQR = 11.5–16.5 years, five males, one female). Umbilical cord blood from healthy full-term newborns, acquired immediately after delivery from the clamped umbilical cord was collected in citrate phosphate dextrose, including one from a child of a mother with T1D. Samples (*n* = 6) were provided through the DKMS Cord Blood Bank of the University Hospital Dresden (Germany) or from the Institute of Diabetes Research, Klinikum rechts der Isar, Technische Universität München with informed consent and local ethics committee approval (approval number: #5293/12, Technische Universität München, Munich, Germany).

Mice. NOD.129X1(Cg)-*Foxp3*^{tm2Tch}/DvsJ mice, referred to as NOD Foxp3 GFP reporter mice, were obtained from The Jackson Laboratory. Antigen-specific *in vivo* Treg cell conversion protocols were executed based on established protocols¹⁷: Four weeks-old female NOD Foxp3 GFP reporter mice were implanted subcutaneously with osmotic mini-pumps (Alzet) releasing 5 µg day⁻¹ of insulin mimetopes or the natural insulin-B-chain epitope for 14 days. Mice were randomized to test groups for antigen-specific Treg conversion. No animals were excluded due to illness or outlier results; therefore, no exclusion determination was required. For *ex vivo* analyses of induced insulin-specific Foxp3⁺Tregs, the entire group of mice for treatment with either the natural insulin-epitope or the strong-agonistic mimetope was analysed. NOD.Cg-*Prkdc*^{scid}*H2-Ab1*^{tm1Gru}*Il2rg*^{tm1Wjl} Tg(HLA-DQA1,HLA-DQB1)1Dv1/Sz mice lack mouse MHC class II and transgenically express human HLA-DQ8. These mice were developed by Leonard Shultz at the Jackson Laboratory. To develop this stock, B10M-HLA-DQ8 mice were kindly provided by Dr. Chella David⁶⁵. The DQ8 transgene was backcrossed for 10 generations on the NSG strain background. The NSG-DQ8 mice were then intercrossed with NSG mice lacking mouse MHC class II (NOD.Cg-*Prkdc*^{scid}*H2-Ab1*^{tm1Gru}*Il2rg*^{tm1Wjl}) (ref. 66). The HLA-DQ8 mice were bred and maintained group-housed on a 12-h/12-h light dark cycle at 25 °C with free access to food and water under defined flora at the animal facility of Helmholtz Zentrum München, Munich, Germany and at The Jackson Laboratory according to guidelines established by the Institutional Animal Committees at each institution. These mice were used as hosts for human HSC obtained from human HLA-DQ8

cord blood samples. The sex of the recipient mice was matched for the HSC donor sex. Ethical approval for all mouse experimentations has been received by the District Government of Upper Bavaria, Munich, Germany (approval numbers: #55.2-1-54-2532-81-12 and 55.2-1-54-2532-84-12). The investigators were not blinded to group allocation during the *in vivo* experiments or to the assessment of experimental end points.

Isolation of infiltrating T cells from murine pancreata. Pancreata were digested with collagenase V (1 mg ml⁻¹) in PBS with 0.1 mM HEPES and 0.1% BSA for 4–7 min at 37 °C. The cell suspension was passed through a 100 µm cell strainer and stained for flow-cytometric analysis.

Human cell isolation. Peripheral blood mononuclear cells (PBMC) were isolated by density centrifugation over Ficoll-PLUS (GE Healthcare). HSCs were purified from PBMCs from fresh umbilical cord blood using the CD34⁺ isolation kit (Diamond CD34 Isolation kit human, Miltenyi Biotec) according to the manufacturer's protocols. Human Dendritic cells (DCs) were purified from autologous PBMC samples using the Blood DC Isolation Kit (Blood DC Isolation kit II human, Miltenyi Biotec) according to the manufacturer's instructions. Specifically CD14⁺ and CD19⁺ cells were labelled with magnetic beads and depleted from the PBMC sample by separation on a MACS column. Subsequently the remaining cells were labelled with CD304, CD1c and CD414 magnetic beads and positive selection over a MACS column of CD304⁺ plasmacytoid and CD1c⁺ and CD141⁺ myeloid DCs was performed. Human CD4⁺T cells were isolated from fresh PBMCs via negative magnetic bead enrichment (EasySep Human CD4 T Cell enrichment kit, Stem Cell) following the manufacturer's protocol.

Cell staining for flow cytometry and cell sorting. The following monoclonal antibodies were used for murine fluorescence-activated cell sorting (FACS) staining: From Biologend (San Diego, CA): anti-CD8a Pacific Blue (53–6.7, 1:300); anti-CD11b Pacific Blue (M1/70; 1:300), anti-CD11c Brilliant Violet 421 (N418, 1:300); anti-B220 Pacific Blue (RA3-6B2, 1:300), anti-F4/80 Pacific Blue (BM8, 1:300), anti-CD25 PerCP-Cy5.5 (PC61, 1:200), anti-CD44 PE (IM7, 1:800), anti-CD45 PE-Cy7 (30-F11, 1:200) and Ki67 APC (16A8, 1:200); and from eBioscience (San Diego, CA): anti-CD4 Alexa Fluor 700 (RM4-5; 1:200), anti-CD62L APC (MEL-14, 1:400) and Foxp3 FITC (FJK-16 s, 1:200). Enumeration of cells and acquisition were performed by using FACSARIA and FACSDiva software (BD). Single-cell data analyses are done by the use of the FlowJo software (Tree Star Inc.).

The following monoclonal antibodies were used for human FACS staining: from BD Biosciences (San Jose, CA): anti-CD25 APC (2A3, 1:20), anti-CD45RO APC-H7 (UCHL1, 1:20), anti-CD4 V500 (RPA-T4, 1:20) and anti-HLA-DR PerCP-Cy5.5 (L243, 1:20); from Biologend (San Diego, CA): anti-CD45RA FITC (HI100, 1:20), anti-CD3 PerCP-Cy5.5 (HIT3a, 1:20), anti-CD127 PE-Cy7 (A019D5, 1:20), anti-CD8a Pacific Blue (RPA-T8, 1:50), anti-CD11b Pacific Blue (ICRF44, 1:50), anti-CD14 Pacific Blue (HCD14, 1:50), anti-CD19 Pacific Blue or Alexa Fluor 700 (HIB19, 1:50), anti-CD3 Alexa Fluor 700 (HIT3a, 1:20), anti-CD45 Alexa Fluor 700 (HI30, 1:20), anti-CD34 Brilliant Violet 421 or APC (561, 1:20), anti-CD38 PE (HIT2, 1:20), anti-C-kit PE-Cy7 (104D2, 1:20), anti-lineage cocktail (CD3, CD14, CD16, CD19, CD20, CD56) APC or FITC (UCHT1, HCD14, 3G8, HIB19, 2H7, HCD56, 1:5) anti-CD14 (HCD14), anti-CD33 V500 (WM53, 1:20), anti-Ki67 APC (16A8, 1:200) or anti-Ki67 Brilliant Violet 605 (16A8, 1:400); from eBioscience (San Diego, CA): anti-Foxp3 Alexa Fluor 700 (PCH101, 1:100), anti-Foxp3 PE (236A/E7, 1:100); and from Miltenyi Biotec: anti-CD20 PE (2H7, 1:5).

To detect intracellular protein expression of Foxp3, after surface staining, cells were fixed and permeabilized using the Foxp3 Staining Buffer Set (eBioscience). Cells were acquired on a Becton Dickinson LSR-II or on the BD FACSARIA III cell sorting system flow cytometer using FACSDiva software with optimal compensation and gain settings determined for each experiment based on unstained and single-colour stained samples. Doublets were excluded based on SSC-A versus SSC-W plots. Live cell populations were gated on the basis of cell side and forward scatter and the exclusion of cells positive for 7-AAD (BD Biosciences) for murine stainings and Sytox Blue (Life Technologies) or Fixable Viability Dye eFluor450 (eBioscience) for human stainings. Samples were analysed using FlowJo software version 7.6.1 (TreeStar Inc., OR).

Peptides. Peptides at > 95% purity were synthesized and purified at New England Peptide (Boston, USA) or at JPT Peptides (Berlin, Germany). Peptide sequences. HA₃₀₇₋₃₁₉ epitope: H2N-PKYVKQNTLKLAT-OH, natural insulin B-29-23 epitope: H2N-SHLVEALVLCGERG-OH, four insulin-B-chain-10-23-mimetopes (Supplementary Fig. 1) were employed in studies using human CD4⁺T cells. Peptides were chosen first based on the finding that insulin-B-10-23 peptide variants with a mutation of arginine (R) to glutamic acid (E) at position 22 and/or including a change to glycine (G) at position 21 (ins.mim.2 = 21G-22E; ins.mim.3 = 21E-22E) were indicated to be more potent in stimulating murine insulin-specific CD4⁺T cells^{7,17,28} and also suited to stimulate human insulin-specific CD4⁺T cells^{30,31}.

Second, two novel human insulin mimetopes with mutations at position 22 to glutamic acid (E) together with position 21 being E or G as well as an additional mutation of position 14 from alanine (A) to glutamic acid (E) (ins.mim.1 = 14E-21G-22E; ins.mim.4 = 14E-21E-22E) were set up. The mutation at position 14 was included since structural analyses of a human insulin-peptide-HLA-DQ8 complex had suggested that glutamic acid (= E) is preferred over alanine at the first MHC-anchor²⁹.

Insulin-specific IA⁸⁷-restricted tetramer staining. Tetramer stainings have been performed using established insulin mimetope-specific 22E- and 21G-22E-tetramers²⁸. In brief, untouched CD4⁺T cells were incubated with tetramer reagents for 1 hour at 37 °C in humidified 5% CO₂ with gentle agitation every 30 min followed by direct staining with antibodies for additional surface markers and exclusion of dead cells for 20 min at 4 °C. A set of exclusion markers (CD8, CD11b, CD11c, B220, F4/80 and a dead cell exclusion marker (Sytox Blue)) was used to increase specificity of the staining. As a negative control, we used a tetramer of IA⁸⁷ with the well-characterized peptide from hen egg lysozyme labelled with PE.

Insulin-specific HLA-DQ8-restricted tetramer staining. Fluorescent HLA-DQ8-tetramers based on insulin-B-chain-10-23-mimetopes were developed in collaboration with the NIH tetramer facility. Specifically, two of the insulin-HLA-DQ8-PE-labelled tetramers were combined in stainings: a 14E-21E-22E and a 14E-21G-22E-tetramer were used to identify human insulin-specific CD4⁺T cells. For the HLA-DQ8-restricted insulin-specific tetramer stainings PBMCs were used and CD4⁺T cells were purified by negative MACS selection as described above. To this end, untouched CD4⁺T cells were incubated with insulin-specific HLA-DQ8-tetramers for 1 hour at 37 °C in humidified 5% CO₂ with gentle agitation every 20 min followed by direct staining with antibodies for additional surface markers and exclusion of dead cells (Sytox Blue) for 20 min at 4 °C. A set of exclusion markers (CD8, CD11b, CD19, CD14 and a dead cell exclusion marker (Sytox Blue)) was used to increase specificity of the staining. As negative controls, we used a combination of two HLA-DQ8-tetramers fused to irrelevant peptides (PVSKMRMATPLLQA and QDLELSWNLNGLQADL) and labelled with PE. Virtually no tetramer⁺CD4⁺T cells were detected with the control tetramers. Upon exclusion of unspecific binding, viable CD3⁺CD4⁺tetramer⁺T cells were single-cell sorted for T-cell cloning experiments, expansion, testing of antigen-specificity or used in further downstream assays.

HLA-DQ8-binding assay. Competitive binding assays were carried out according to previously established procedures^{30,67,68}. HLA-DQ8 monomers were kindly provided by R.A.W. from the NIH Tetramer Core Facility (Atlanta, USA). The CLIP peptide of HLA-DQ8 molecules was cleaved off by incubation with thrombin (Novagen) for 2 h (ref. 69).

Specifically, a FITC-labelled GAD65 253-265^{R255F} peptide (IAFFKMFPEVKEK) was used as an indicator peptide (10 μM) for the binding reaction together with thrombin-cleaved HLA-DQ8 monomers (0.4 μM) and increasing concentrations of competitor peptides (natural insulin B:9-23, ins.mim.1,2,3,4, MP185-204). The MP185-204 peptide (TAKAMEQMAGSSEQAAEAME) was used as a positive DQ8-binding control. The indicator peptide incubated with DQ8 monomers in the absence of competitor peptide was used as positive control. For background analysis the binding reaction was performed without HLA-DQ8 monomers. The binding reaction was incubated for 48 h at 37 °C. Assays were then captured using anti-DQ antibody-coated plates (SPV-L3, Abcam, 15 μg ml⁻¹). Detection was performed using anti-FITC HRP (Abcam, 1:1,000) antibodies in combination with TMB substrate (BD Biosciences) and subsequent analysis with the Epoch plate reader (BioTech) at 450 and 405 nm.

Binding curves were fitted by nonlinear regression using log transformed *x* values (*x* = test peptide concentration) with the one-site competitive binding model to extract IC₅₀ values (Prism software, v.6.04, GraphPad Software).

Generation of artificial antigen-presenting cells. Earlier studies had shown that an indirect coating of fluorescently unlabelled HLA-peptide tetramers on beads via an anti-MHCII antibody provides specific and efficient stimulation of antigen-specific CD4⁺T cells³⁴. Therefore, we first coated anti-HLA-DQ antibodies (SPV-L3, Abcam) to antibody-coupling beads (Dynabeads Antibody Coupling Kit, Life Technologies) at 20 μg mg⁻¹ beads followed by coupling with unlabelled HLA-DQ8-tetramers (3 μg per 10 × 10⁶ beads) to the DQ-antibodies. Artificial APCs (aAPCs) using the above described control tetramers were generated accordingly. For stimulation aAPCs were used at a concentration of 230 μg ml⁻¹ corresponding to a tetramer concentration of 5 μg ml⁻¹.

CFSE-T-cell proliferation assays. CD4⁺CD25⁺T cells were labelled with CFSE and incubated with propagated APCs loaded with medium alone, various doses of insulin B:9-23 peptide, or with a titration of various strong-agonistic insulin mimetopes (as described above) for 5 days. In all assays, each condition was performed in triplicate wells. Cells were cultured in X-Vivo15 Medium supplemented with 2 mM glutamine, penicillin (50 U ml⁻¹), streptomycin (50 μg ml⁻¹) and 5%

heat-inactivated human AB serum (Invitrogen) in round bottom 96-well plates. After 5 days, the cell cultures were stained for CD4, CD3, CD25 and CD45RO and processed for FACS analyses. Responsiveness was measured by the presence and quantity of CD4⁺CD25⁺CFSE^{dim}T cells identified by FACS.

Generation of insulin-specific T-cell clones. To perform further phenotyping of insulin-specific CD4⁺T cells and to generate specific T-cell clones 500,000 CFSE-labelled CD4⁺T cells were cultured in the presence of insulin-specific aAPCs or control aAPCs generated as described above for 7 days. At day 7 the cells were analysed and a single viable CFSE^{dim}CD4⁺T cell was sorted into each well of a 96-well plate in the presence of 200 μl of X-Vivo15 medium and 1 × 10⁴ PBMCs of a HLA-DQ8⁻ donor, 1 × 10⁴ PBMCs of a HLA-DQ8⁺ donor as well as 1 × 10⁴ HLA-DQ8⁺ EBV-transformed B cells (Riken Cell Bank, Japan). Feeder cells were irradiated with 40 Gy (PBMCs) or 50 Gy (B cells) before addition to the cultures. Cells were stimulated with 30 ng ml⁻¹ anti-CD3 (OKT3, BioLegend) in the presence of IL-2 (Peprotech, 20 U ml⁻¹) and IL-4 (Peprotech, 10 ng ml⁻¹). Expansion of specific clones was performed by addition of IL-15 (Peprotech, 10 ng ml⁻¹) and IL-21 (Peprotech, 10 ng ml⁻¹) as well as low-dose IL-7 (Peprotech, 0.1 ng ml⁻¹). For expansion of growing clones cells were split into 48-well plates after 2 weeks. Clones were re-tested for antigen-specificity and DQ-restriction by stimulation with natural insulin-peptides or -mimetopes (0.1–10 μg ml⁻¹) in the presence or absence of HLA-DQ blocking antibodies (SPV-L3, Abcam, 10 μg ml⁻¹) and analysis of total CD25 upregulation and CD25⁺⁺⁺ levels after 48 h of stimulation was assessed by FACS analyses.

Analysis of stimulatory potential of insulin mimetopes. Proliferative responses of HLA-DQ8-restricted insulin-specific CFSE-labelled CD4⁺T-cell clones were defined using a titration of individual insulin mimetopes and the natural insulin epitope B:9-23 presented by irradiated T cell depleted PBMCs. Subsequent FACS analyses of CFSE^{dim}CD25⁺CD4⁺T cells were performed as described above. The stimulatory capacity of the insulin mimetopes was assessed as fold of stimulatory capacity of the natural insulin B:9-23 epitope.

Human Treg induction using limited TCR-stimulation *in vitro*. For polyclonal Treg induction, human naive CD4⁺T cells were defined as CD3⁺, CD4⁺, CD45RA⁺, CD45RO⁻, CD127⁺, CD25⁻, HLA-DR⁻ and sorted with the BD FACSAria III for purity (see Supplementary Fig. 6). CD4⁺T cells were cultured for 12 h in a 96-well plate pre-coated with 5 μg ml⁻¹ anti-CD3 (UCHT1, BioLegend) and 5 μg ml⁻¹ anti-CD28 (CD28.2, BioLegend) and 100 U ml⁻¹ IL-2 (Peprotech). Limited TCR stimulation was achieved by pipetting the cells into new, uncoated wells, after 12 h, where they were cultured for additional 36 h without further TCR stimulation. To assess Treg induction using continuous TCR stimulation naive CD4⁺T cells were stimulated in pre-coated wells as described above for a time period of 54 h and analysed accordingly. For antigen-specific Treg induction, human naive CD4⁺T cells were defined as CD3⁺, CD4⁺, CD45RA⁺, CD45RO⁻, CD127⁺, CD25⁻, HLA-DR⁻ and sorted with the BD FACSAria III for purity. Naive CD4⁺T cells were co-cultured with autologous CFSE-labelled DCs isolated as described above in the presence of insulin mimetopes, natural insulin B:9-23 epitope (0.001 and 0.01 ng ml⁻¹). After 12 h APCs were removed by sorting CD4⁺T cells as CFSE⁻ followed by a culture for additional 36 h in new wells without further peptide stimulation.

Restimulation cultures. Upon Treg induction using limited or continuous TCR-stimulation *in vitro* sort-purification of CD127^{low}CD25^{high}CD4⁺Tregs was performed. The Tregs were then stimulated for 36 h in the presence 5 μg ml⁻¹ anti-CD3 (UCHT1, BioLegend) and 5 μg ml⁻¹ anti-CD28 (CD28.2, BioLegend) antibodies without addition of TGFβ followed by the analysis of CD25, CD127 and Foxp3 by intracellular staining and FACS as described above.

Treg suppression assay *in vitro*. Tregs were sort-purified as CD4⁺CD3⁺CD127^{low}CD25^{high}T cells. In control experiments Treg identity of CD4⁺CD3⁺CD127^{low}CD25^{high}T cells was confirmed by intracellular staining for Foxp3. Conventional T cells were sorted as CD4⁺CD3⁺CD127⁺CD25⁻. Tregs were purified from spleens and lymph nodes of humanized mice and first expanded for six days by polyclonal stimulation with anti-CD3 (UCHT1, BioLegend) and anti-CD28 (CD28.2, BioLegend) at 1 μg ml⁻¹ each in the presence of IL-2 (Peprotech, 500 U ml⁻¹) and 20 × 10⁴ irradiated CD4⁻ feeder cells (CD4-depleted PBMCs and EBV-transformed B cells). On day six Tregs and conventional T cells were sort-purified to remove the remaining feeder cells and conventional T cells (responder cells) were labelled with CFSE (0.25 μM). Conventional T cells were expanded accordingly at 50 U ml⁻¹ IL-2. Treg cells and conventional T cells were rested for 16 h in the absence of IL-2 to force them into synchronous resting states⁴⁴. Labelled responder T cells were cultured with or without Tregs (responder: Tregs 1:2; 1:4 and 1:8) for 3 days in the presence of stimulation with anti-CD3 (UCHT1, BioLegend) and anti-CD28 (CD28.2, BioLegend) (1 μg ml⁻¹ each). Analyses were performed on day three on a FACSAria III and suppression of responder cell proliferation was assessed by determining the dilution of their CFSE

label. Suppression of responder cell proliferation is shown in % suppression of the proliferation of the responder cells alone⁴⁴.

For insulin-specific suppression assays, induced Tregs from humanized mice were sort-purified as indicated above. Cells of insulin-specific T-cell clones were used as effector cells labelled with CFSE as described above and co-cultured with induced human Tregs. The cells were stimulated either with insulin mimetopes (100 ng ml⁻¹) or the natural insulin B:9-23 epitope (10 µg ml⁻¹).

Additional experiments were performed using effector T cells from T1D individuals and polyclonal stimulation as outlined above.

Engraftment of NSG mice with human haematopoietic stem cells. Two-week-old NSG-HLA-DQ8 mice were reconstituted with at least 5×10^4 CD34⁺ HSCs from an HLA-DQ8⁺ donor per mouse by intravenous injection in 50 µl PBS into the retro orbital sinus without prior conditioning by irradiation or busulfan treatment. To avoid sex incompatibilities the sex of the NSG-HLA-DQ8 mice for reconstitution was chosen in accordance with the cord blood donor.

Assessment of reconstitution efficacy in NSG-HLA-DQ8 mice. NSG-DQ8 mice were bled 5 and 8 weeks post engraftment and peripheral blood was analysed by FACS to characterize the engraftment of the human immune system using fluorescently labelled-specific human versus murine CD45 antibodies.

Analyses of reconstituted humanized NSG-HLA-DQ8 mice. At various time points after reconstitution humanized NSG-HLA-DQ8 mice were euthanized and whole blood, peripheral lymph nodes, spleen and WAT were analysed for the presence of CD4⁺T cells. CD4⁺T cells were extracted from WAT by collagenase II (Sigma Aldrich, 4 mg ml⁻¹) digestion and peripheral lymph nodes were homogenized by gentle grinding through a cell strainer followed by cellular FACS stainings and analyses as described above.

Human *in vivo* Treg induction in humanized mice. Humanized NSG-HLA-DQ8 mice at 20 weeks post reconstitution were then subjected to *in vivo* Treg induction assays using insulin mimetope peptide infusion by subcutaneous implantation of osmotic mini-pumps, which permit the continuous delivery of minute amounts of peptide for 14 days^{15,17}. Mice were infused with a combination of ins.mim.1 = 14E-21G-22E and ins.mim.4 = 14E-21E-22E at 5 µg day⁻¹. Control animals were infused with PBS. Successfully reconstituted animals were randomized to test groups for antigen-specific Treg induction. No animals were excluded due to illness or outlier results; therefore, no exclusion determination was required. For *ex vivo* T cell analyses, the entire group of mice treated with PBS or the insulin mimetopes was analysed. After 3 weeks, Foxp3⁺Treg induction was assessed upon insulin-specific tetramer stainings as described above and Tregs were identified based on CD4⁺CD3⁺CD127^{low}CD25⁺. Treg identity was verified by intracellular staining for Foxp3 and by analyses of Foxp3 mRNA abundance.

Analysis of Treg signature genes. T cells were sort-purified; cDNA synthesis and subsequent amplification were performed using the SMARTer ultra-low input RNA Kit for sequencing—v3 (Takara Clontech) according to the manufacturer's instructions. cDNA was purified using Agencourt AMPure XP Beads (Beckman Coulter). qPCR was performed on a CFX96 real time system (BioRad) using QuantiTect Primer assays (Qiagen) for Foxp3, CTLA4, IL2-R α , TIGIT, RTKN2, IKZF2, ENTPD1 and FCRL3 and SsoFast Evagreen Supermix (BioRad). Levels of Histone 3 and 18s were used to normalize target gene expression levels (Histone: H3F3A BT020962, primers: fwd: 5'-ACTGGCTACAAAAGCCGCTC-3', rev: 5'-ACTTGCCTCCTGCAAGCAC-3'; 18s: QuantiTect Primer assay, Qiagen).

Analysis of T-cell effector genes. T cell effector genes were analysed on the same cDNA samples used for Treg signature gene analysis described above. qPCR was performed on a CFX96 real time system (BioRad) using QuantiTect Primer assays (Qiagen) for IL17-R α , NFATc2, IL-21, ROR γ t, T-bet and IFN γ and SsoFast Evagreen Supermix (BioRad). Levels of Histone 3 and 18s were used to normalize target gene expression abundance (Histone: H3F3A BT020962, primers: fwd: 5'-ACTGGCTACAAAAGCCGCTC-3', rev: 5'-ACTTGCCTCCTGCAAAGC AC-3'; 18s: QuantiTect Primer assay, Qiagen).

HLA fast genotyping. HLA-genotyping of the children was available. Fast genotyping was used for cord blood experiments and a protocol was developed on the basis of Nguyen *et al.*⁷⁰. In brief, DNA was extracted from whole blood using the Quick-gDNA MiniPrep Kit (Zymo Research) according to the manufacturer's protocol. For qPCR analyses SsoAdvance Universal Probes Supermix (BioRad) was used with 15 ng of gDNA, 250 nM forward and reverse primer and 500 nM of Probes FAM and HEX. Standards were added for subsequent analysis with Bio-Rad CFX Manager 3.1. Primers: rs3104413 fwd 5'-CAGCTGAGCACTGAGTAG-3', rs3104413 rev 5'-GCAGTTGAGAAGTGAGAG-3', rs2854275 fwd 5'-CCAGAA CCAAGCCTAAC-3', rs2854275 rev 5'-GCATCATCTAGTGTCTAAC-3', rs9273363 fwd 5'-GAGGGAGAAAGGAGATG-3', rs9273363 rev 5'-GAAGCTGG TCTACATCTC-3'. Probes: FAM-Probe rs3104413 LPC [6FAM]CAGCCT[+G]

CT[+C]TC[+C]TA[+T]TGG[BHQ1], HEX-Probe rs3104413 LPG [HEX] CAGCCT[+G]CT[+G]TC[+C]TA[+T]TGG[BHQ1], FAM-Probe rs2854275 G [6FAM]TCCACA[+T]TT[+C]AC[+A]AG[+A]AGA[BHQ1], HEX-Probe rs2854275 T [HEX]TCCACA[+T]TT[+A]AC[+A]AG[+A]AGA[BHQ1], FAM-Probe rs9273363 LPC [6FAM]CATGGC[+C]TT[+A]CA[+T]AA[+C] CTC[BHQ1], HEX-Probe rs9273363 LPC [HEX]CATGGC[+C]TT[+C]CA [+T]AA[+C]CTC[BHQ1].

DNA bisulfite conversion and methylation analysis. Because of the reduced nature of available sample material, FACS-sorted CD4⁺T cells (50–2,000 cells) were subjected to a combined sample lysis and bisulfite conversion using the EpiTect Plus LyseAll Bisulfite Kit (Qiagen, Hilden, Germany) or the EZ DNA Methylation-Direct Kit (Zymo Research) according to the manufacturer's instructions. For bias-controlled quantitative methylation analysis, a combination of MS-HRM and subsequent Pyrosequencing was performed as described earlier^{42,43}. Utilizing the PyroMark Assay Design Software 2.0 (Qiagen), PCR primers (human forward: 5'-AAGTTGAATGGGGATGTTTTGGGATA TAGATTATG-3'; human reverse: 5'-CTACCACATCCACCAACACCCATA TCACC-3'; annealing-temperature: 62 °C; murine forward: 5'-TTGGGTTTTGTT GTTATAATTGAATTGG-3'; murine reverse: 5'-ACCTACTAATACACC AACATC-3'; annealing-temperature: 60 °C) and the according sequencing primer (human: 5'-TAGTTTTAGATTGTTTAGATTTT-3'; murine: 5'-AATTT GAATTTGGTTAGATTTT-3') were designed to cover the area of differential methylation in the first Foxp3 intron initially reported by Baron *et al.*⁴² (Supplementary Fig. 14). Pyrosequencing data are presented as means of all CpG-sites analysed due to high homology between methylation levels of the individual sites (Supplementary Fig. 14).

Statistics. Results are presented as mean and s.e.m. or as percentages, where appropriate. For normally distributed data, Student's *t*-test for unpaired values was used to compare means between independent groups and the Student's *t*-test for paired values was used to compare values for the same sample or subject tested under different conditions. The non-parametric Wilcoxon signed-ranks test was applied when data did not show Gaussian distribution. Group size estimations were based upon a power calculation to minimally yield an 80% chance to detect a significant difference in the respective parameter of $P < 0.05$ between the relevant groups. For all tests, a two-tailed *P* value of < 0.05 was considered to be significant. Statistical significance is shown as * = $P < 0.05$; ** = $P < 0.01$; *** = $P < 0.001$, or not significant (ns) $P > 0.05$. Analyses were performed using the programs GraphPad Prism 6 (La Jolla, CA) and the Statistical Package for the Social Sciences (SPSS 19.0; SPSS Inc., Chicago, IL).

References

- Bluestone, J. A., Herold, K. & Eisenbarth, G. Genetics, pathogenesis and clinical interventions in type 1 diabetes. *Nature* **464**, 1293–1300 (2010).
- Patterson, C. C. *et al.* Incidence trends for childhood type 1 diabetes in Europe during 1989–2003 and predicted new cases 2005–20: a multicentre prospective registration study. *Lancet* **373**, 2027–2033 (2009).
- Fairchild, P. J., Wildgoose, R., Atherton, E., Webb, S. & Wraith, D. C. An autoantigenic T cell epitope forms unstable complexes with class II MHC: a novel route for escape from tolerance induction. *Int. Immunol.* **5**, 1151–1158 (1993).
- Garcia, K. C., Teyton, L. & Wilson, I. A. Structural basis of T cell recognition. *Annu. Rev. Immunol.* **17**, 369–397 (1999).
- Hahn, M., Nicholson, M. J., Pyrdol, J. & Wucherpfennig, K. W. Unconventional topology of self peptide-major histocompatibility complex binding by a human autoimmune T cell receptor. *Nat. Immunol.* **6**, 490–496 (2005).
- Liu, G. Y. *et al.* Low avidity recognition of self-antigen by T cells permits escape from central tolerance. *Immunity* **3**, 407–415 (1995).
- Stadinski, B. D. *et al.* Diabetogenic T cells recognize insulin bound to IAg7 in an unexpected, weakly binding register. *Proc. Natl Acad. Sci. USA* **107**, 10978–10983 (2010).
- Ziegler, A. G. *et al.* Seroconversion to multiple islet autoantibodies and risk of progression to diabetes in children. *JAMA* **309**, 2473–2479 (2013).
- Ziegler, A. G. & Nepom, G. T. Prediction and pathogenesis in type 1 diabetes. *Immunity* **32**, 468–478 (2010).
- Fontenot, J. D., Gavin, M. A. & Rudensky, A. Y. Foxp3 programs the development and function of CD4⁺CD25⁺ regulatory T cells. *Nat. Immunol.* **4**, 330–336 (2003).
- Khattry, R., Cox, T., Yasayko, S. A. & Ramsdell, F. An essential role for Scurf in CD4⁺CD25⁺ T regulatory cells. *Nat. Immunol.* **4**, 337–342 (2003).
- Roncador, G. *et al.* Analysis of FOXP3 protein expression in human CD4⁺CD25⁺ regulatory T cells at the single-cell level. *Eur. J. Immunol.* **35**, 1681–1691 (2005).
- Levings, M. K., Sangregorio, R. & Roncarolo, M. G. Human cd25(+)cd4(+) t regulatory cells suppress naive and memory T cell proliferation and can be expanded *in vitro* without loss of function. *J. Exp. Med.* **193**, 1295–1302 (2001).

14. Modigliani, Y. *et al.* Lymphocytes selected in allogeneic thymic epithelium mediate dominant tolerance toward tissue grafts of the thymic epithelium haplotype. *Proc. Natl Acad. Sci. USA* **92**, 7555–7559 (1995).
15. Daniel, C. & von Boehmer, H. Extra-thymically induced regulatory T cells: do they have potential in disease prevention? *Semin. Immunol.* **23**, 410–417 (2011).
16. Daniel, C. & von Boehmer, H. Extrathymic generation of regulatory T cells—chances and challenges for prevention of autoimmune disease. *Adv. Immunol.* **112**, 177–213 (2011).
17. Daniel, C., Weigmann, B., Bronson, R. & von Boehmer, H. Prevention of type 1 diabetes in mice by tolerogenic vaccination with a strong agonist insulin mimetope. *J. Exp. Med.* **208**, 1501–1510 (2011).
18. von Boehmer, H. & Daniel, C. Therapeutic opportunities for manipulating T(Reg) cells in autoimmunity and cancer. *Nat. Rev. Drug Discov.* **12**, 51–63 (2013).
19. Kretschmer, K. *et al.* Inducing and expanding regulatory T cell populations by foreign antigen. *Nat. Immunol.* **6**, 1219–1227 (2005).
20. Daniel, C., Ploegh, H. & von Boehmer, H. Antigen-specific induction of regulatory T cells *in vivo* and *in vitro*. *Methods Mol. Biol.* **707**, 173–185 (2011).
21. Daniel, C., Wennhold, K., Kim, H. J. & von Boehmer, H. Enhancement of antigen-specific Treg vaccination *in vivo*. *Proc. Natl Acad. Sci. USA* **107**, 16246–16251 (2010).
22. Gottschalk, R. A., Corse, E. & Allison, J. P. TCR ligand density and affinity determine peripheral induction of Foxp3 *in vivo*. *J. Exp. Med.* **207**, 1701–1711 (2010).
23. Nakayama, M. *et al.* Prime role for an insulin epitope in the development of type 1 diabetes in NOD mice. *Nature* **435**, 220–223 (2005).
24. Jaeckel, E., Lipes, M. A. & von Boehmer, H. Recessive tolerance to proinsulin 2 reduces but does not abolish type 1 diabetes. *Nat. Immunol.* **5**, 1028–1035 (2004).
25. Alleva, D. G. *et al.* A disease-associated cellular immune response in type 1 diabetics to an immunodominant epitope of insulin. *J. Clin. Invest.* **107**, 173–180 (2001).
26. Daniel, D., Gill, R. G., Schloot, N. & Wegmann, D. Epitope specificity, cytokine production profile and diabetogenic activity of insulin-specific T cell clones isolated from NOD mice. *Eur. J. Immunol.* **25**, 1056–1062 (1995).
27. Wegmann, D. R., Norbury-Glaser, M. & Daniel, D. Insulin-specific T cells are a predominant component of islet infiltrates in pre-diabetic NOD mice. *Eur. J. Immunol.* **24**, 1853–1857 (1994).
28. Crawford, F. *et al.* Specificity and detection of insulin-reactive CD4⁺ T cells in type 1 diabetes in the nonobese diabetic (NOD) mouse. *Proc. Natl Acad. Sci. USA* **108**, 16729–16734 (2011).
29. Lee, K. H., Wucherpfennig, K. W. & Wiley, D. C. Structure of a human insulin peptide-HLA-DQ8 complex and susceptibility to type 1 diabetes. *Nat. Immunol.* **2**, 501–507 (2001).
30. Yang, J. *et al.* Autoreactive T cells specific for insulin B:11–23 recognize a low-affinity peptide register in human subjects with autoimmune diabetes. *Proc. Natl Acad. Sci. USA* **111**, 14840–14845 (2014).
31. Nakayama, M. *et al.* Regulatory versus inflammatory cytokine T-cell responses to mutated insulin peptides in healthy and type 1 diabetic subjects. *Proc. Natl Acad. Sci. USA* **112**, 4429–4434 (2015).
32. Durinovic-Bello, I. *et al.* DRB1*0401-restricted human T cell clone specific for the major proinsulin73–90 epitope expresses a down-regulatory T helper 2 phenotype. *Proc. Natl Acad. Sci. USA* **103**, 11683–11688 (2006).
33. Mannering, S. I. *et al.* Current approaches to measuring human islet-antigen specific T cell function in type 1 diabetes. *Clin. Exp. Immunol.* **162**, 197–209 (2010).
34. Maus, M. V., Riley, J. L., Kwok, W. W., Nepom, G. T. & June, C. H. HLA tetramer-based artificial antigen-presenting cells for stimulation of CD4⁺ T cells. *Clin. Immunol.* **106**, 16–22 (2003).
35. Sauer, S. *et al.* T cell receptor signaling controls Foxp3 expression via PI3K, Akt, and mTOR. *Proc. Natl Acad. Sci. USA* **105**, 7797–7802 (2008).
36. Pearson, T., Greiner, D. L. & Shultz, L. D. In *Current Protocols in Immunology* (eds Coligan, J. E. *et al.*) Ch. 15, Unit 15, 21 (Wiley, 2008).
37. Ferraro, A. *et al.* Interdiversity variation in human T regulatory cells. *Proc. Natl Acad. Sci. USA* **111**, E1111–E1120 (2014).
38. Pfoertner, S. *et al.* Signatures of human regulatory T cells: an encounter with old friends and new players. *Genome Biol.* **7**, R54 (2006).
39. Yu, X. *et al.* The surface protein TIGIT suppresses T cell activation by promoting the generation of mature immunoregulatory dendritic cells. *Nat. Immunol.* **10**, 48–57 (2009).
40. Stanitsky, N. *et al.* The interaction of TIGIT with PVR and PVRL2 inhibits human NK cell cytotoxicity. *Proc. Natl Acad. Sci. USA* **106**, 17858–17863 (2009).
41. Deaglio, S. *et al.* Adenosine generation catalyzed by CD39 and CD73 expressed on regulatory T cells mediates immune suppression. *J. Exp. Med.* **204**, 1257–1265 (2007).
42. Baron, U. *et al.* DNA demethylation in the human FOXP3 locus discriminates regulatory T cells from activated FOXP3(+) conventional T cells. *Eur. J. Immunol.* **37**, 2378–2389 (2007).
43. Floess, S. *et al.* Epigenetic control of the foxp3 locus in regulatory T cells. *PLoS Biol.* **5**, e38 (2007).
44. Collison, L. W. & Vignali, D. A. *In vitro* Treg suppression assays. *Methods Mol. Biol.* **707**, 21–37 (2011).
45. Skyler, J. S. *et al.* Effects of oral insulin in relatives of patients with type 1 diabetes: the Diabetes Prevention Trial--Type 1. *Diabetes Care* **28**, 1068–1076 (2005).
46. Harrison, L. C. *et al.* Pancreatic beta-cell function and immune responses to insulin after administration of intranasal insulin to humans at risk for type 1 diabetes. *Diabetes Care* **27**, 2348–2355 (2004).
47. Nanto-Salonen, K. *et al.* Nasal insulin to prevent type 1 diabetes in children with HLA genotypes and autoantibodies conferring increased risk of disease: a double-blind, randomised controlled trial. *Lancet* **372**, 1746–1755 (2008).
48. Diabetes Prevention Trial--Type 1 Diabetes Study Group. Effects of insulin in relatives of patients with type 1 diabetes mellitus. *N. Engl. J. Med.* **346**, 1685–1691 (2002).
49. Bonifacio, E. *et al.* Effects of high-dose oral insulin on immune responses in children at high risk for type 1 diabetes: the Pre-POINT randomized clinical trial. *JAMA* **313**, 1541–1549 (2015).
50. Shiina, T., Inoko, H. & Kulski, J. K. An update of the HLA genomic region, locus information and disease associations: 2004. *Tissue Antigens* **64**, 631–649 (2004).
51. Achenbach, P. *et al.* Characteristics of rapid vs slow progression to type 1 diabetes in multiple islet autoantibody-positive children. *Diabetologia* **56**, 1615–1622 (2013).
52. Thrower, S. L. *et al.* Proinsulin peptide immunotherapy in type 1 diabetes: report of a first-in-man phase I safety study. *Clin. Exp. Immunol.* **155**, 156–165 (2009).
53. Gottschalk, R. A. *et al.* Distinct influences of peptide-MHC quality and quantity on *in vivo* T-cell responses. *Proc. Natl Acad. Sci. USA* **109**, 881–886 (2012).
54. Singh, N. J. & Schwartz, R. H. The strength of persistent antigenic stimulation modulates adaptive tolerance in peripheral CD4⁺ T cells. *J. Exp. Med.* **198**, 1107–1117 (2003).
55. Stefanova, I. *et al.* TCR ligand discrimination is enforced by competing ERK positive and SHP-1 negative feedback pathways. *Nat. Immunol.* **4**, 248–254 (2003).
56. Sullivan, S. P. *et al.* Dissolving polymer microneedle patches for influenza vaccination. *Nat. Med.* **16**, 915–920 (2010).
57. Gupta, J., Felner, E. I. & Prausnitz, M. R. Rapid pharmacokinetics of intradermal insulin administered using microneedles in type 1 diabetes subjects. *Diabetes Technol. Ther.* **13**, 451–456 (2011).
58. Hirobe, S. *et al.* Development and clinical study of a self-dissolving microneedle patch for transcutaneous immunization device. *Pharm. Res.* **30**, 2664–2674 (2013).
59. Norman, J. J. *et al.* Microneedle patches: usability and acceptability for self-vaccination against influenza. *Vaccine* **32**, 1856–1862 (2014).
60. Marodon, G. *et al.* High diversity of the immune repertoire in humanized NOD.SCID.gamma c-/- mice. *Eur. J. Immunol.* **39**, 2136–2145 (2009).
61. Shultz, L. D., Ishikawa, F. & Greiner, D. L. Humanized mice in translational biomedical research. *Nat. Rev. Immunol.* **7**, 118–130 (2007).
62. Ziegler, A. G., Bonifacio, E. & BABYDIAB-BABYDIET Study Group. Age-related islet autoantibody incidence in offspring of patients with type 1 diabetes. *Diabetologia* **55**, 1937–1943 (2012).
63. Ziegler, A. G., Hummel, M., Schenker, M. & Bonifacio, E. Autoantibody appearance and risk for development of childhood diabetes in offspring of parents with type 1 diabetes: the 2-year analysis of the German BABYDIAB Study. *Diabetes* **48**, 460–468 (1999).
64. Achenbach, P. *et al.* Autoantibodies to zinc transporter 8 and SLC30A8 genotype stratify type 1 diabetes risk. *Diabetologia* **52**, 1881–1888 (2009).
65. Nabozny, G. H. *et al.* HLA-DQ8 transgenic mice are highly susceptible to collagen-induced arthritis: a novel model for human polyarthritis. *J. Exp. Med.* **183**, 27–37 (1996).
66. Covassin, L. *et al.* Human immune system development and survival of non-obese diabetic (NOD)-scid IL2rgamma(null) (NSG) mice engrafted with human thymus and autologous haematopoietic stem cells. *Clin. Exp. Immunol.* **174**, 372–388 (2013).
67. Ettinger, R. A. & Kwok, W. W. A peptide binding motif for HLA-DQA1*0102/DQB1*0602, the class II MHC molecule associated with dominant protection in insulin-dependent diabetes mellitus. *J. Immunol.* **160**, 2365–2373 (1998).
68. Sidney, J. *et al.* In *Current Protocols in Immunology* (eds Coligan, J. E. *et al.*) Ch. 18, Unit 18, 13 (Wiley, 2013).
69. Day, C. L. *et al.* *Ex vivo* analysis of human memory CD4 T cells specific for hepatitis C virus using MHC class II tetramers. *J. Clin. Invest.* **112**, 831–842 (2003).

70. Nguyen, C., Varney, M. D., Harrison, L. C. & Morahan, G. Definition of high-risk type 1 diabetes HLA-DR and HLA-DQ types using only three single nucleotide polymorphisms. *Diabetes* **62**, 2135–2140 (2013).

Acknowledgements

We thank Katharina Warncke for providing umbilical cord blood samples from the Immune Diab Risk Study (IDR); Ruth Chmiel, Melanie Bunk and Susanne Hummel for blood sample collection and patient follow-up; and M.H. Tschöp for critical reading of the manuscript. C.D. is supported by a Junior Research Group at Helmholtz Zentrum München. C.D. received support through an associated membership in the CRC1054 of the Deutsche Forschungsgemeinschaft. The work was supported by grants from the Juvenile Diabetes Research Foundation (JDRF 2-SRA-2014-161-Q-R (C.D., A.-G.Z.), JDRF 17-2012-16 (A.-G.Z.), JDRF 6-2012-20 (A.-G.Z.)), the Kompetenznetz Diabetes mellitus (Competence Network for Diabetes mellitus), funded by the Federal Ministry of Education and Research (FKZ 01GI0805-07, FKZ 01GI0805) and the German Center for Diabetes Research (DZD). L.S. was supported by National Institutes of Health grants U01 DK089572 and the Helmsley Charitable Trust grant 2012PG-T1D018.

Author contributions

I.S. performed *ex vivo*, *in vitro* and *in vivo* experiments for the characterization of human insulin mimetopes and their impact on Treg induction versus T-cell proliferation and -activation, analysed and interpreted data and wrote the manuscript. R.W.F. supported and performed *ex vivo* analyses to assess Treg stability, analysed and interpreted the data. P.A. coordinated islet autoantibody measurements and patient phenotyping. M.G.S. performed *ex vivo* and *in vitro* analyses on Treg induction and -stability, analysed and interpreted the data. F.G. performed *ex vivo* and *in vitro* analyses on insulin-specific T cells, -Tregs and -induction. F.H. coordinated the clinical study centre and patient visits. E.-M.S. designed the HLA-fast genotyping assay.

A.K. prospectively followed patients and families and coordinated study visits and venous blood collection. L.S. provided NSG-HLA-DQ8 mice and supported analyses on humanized mice. R.A.W. conceptualized, designed and produced HLA-DQ8-restricted insulin-specific tetramer reagents. A.-G.Z. advised and co-conceptualized the study design, and is PI of the cohort studies BABYDIAB, DiMelli and the Munich Bioresource, which provided islet autoantibody positive and negative children for the study. C.D. conceptualized, designed, performed *in vivo* experiments with humanized mice, analysed and interpreted all studies and wrote the manuscript.

Additional information

Supplementary Information accompanies this paper at <http://www.nature.com/naturecommunications>

Competing financial interests: The authors declare no competing financial interests.

Reprints and permission information is available online at <http://npq.nature.com/reprintsandpermissions/>

How to cite this article: Serr, I. *et al.* Type 1 diabetes vaccine candidates promote human Foxp3⁺Treg induction in humanized mice. *Nat. Commun.* **7**:10991 doi: 10.1038/ncomms10991 (2016).



This work is licensed under a Creative Commons Attribution 4.0 International License. The images or other third party material in this article are included in the article's Creative Commons license, unless indicated otherwise in the credit line; if the material is not included under the Creative Commons license, users will need to obtain permission from the license holder to reproduce the material. To view a copy of this license, visit <http://creativecommons.org/licenses/by/4.0/>

3.2.1 Supplementary information

Type 1 diabetes vaccine candidates promote human Foxp3(+) Treg induction in humanized mice

Isabelle Serr, Rainer W. Fürst, Peter Achenbach, Martin G. Scherm, Füsün Gökmen, Florian Haupt, Eva-Maria Sedlmeier, Annette Knopff, Leonard Shultz, Richard A. Willis, Anette-G. Ziegler and Carolin Daniel.

Supplementary Figures

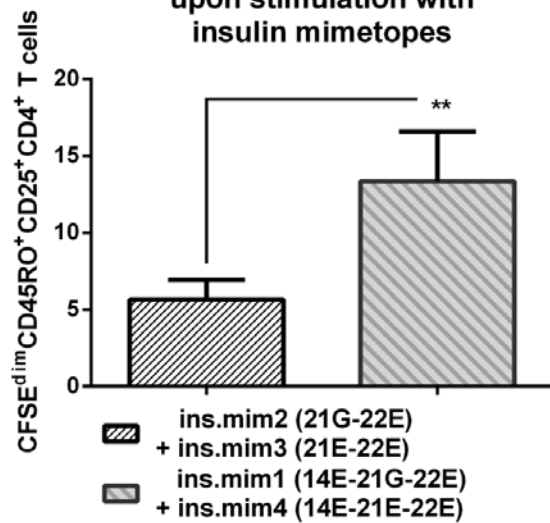
Suppl. Fig.1

ins.mim.1 (14E-21G-22E):	HLVE E LYLVCG GEG
ins.mim.2 (21G-22E):	HLVEALYLVCG GEG
ins.mim.3 (21E-22E):	HLVEALYLVCG E EG
ins.mim.4 (14E-21E-22E):	HLVE E LYLVCG E EG
insulin B chain epitope:	HLVEALYLVCG ERG

Supplementary Figure 1. Shown are peptide sequences of insulin B chain 10-23 mimetopes using one letter amino acid codes.

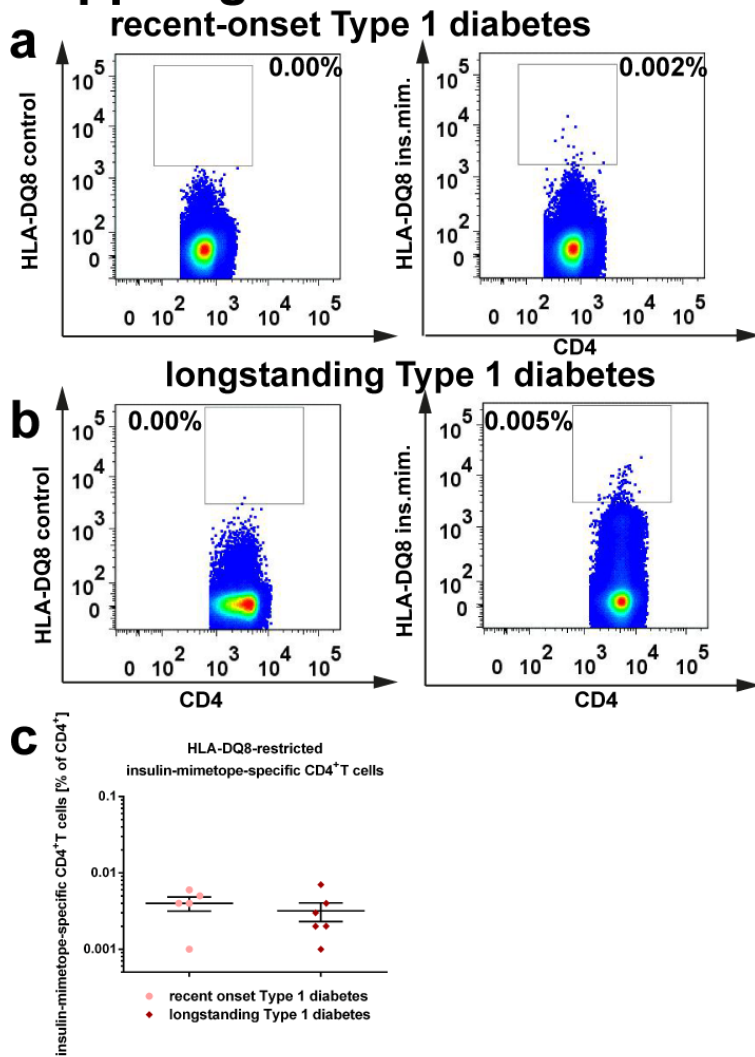
Suppl. Fig.2

proliferation of human CD4⁺T cells
from children without ongoing islet-autoimmunity
upon stimulation with
insulin mimetopes



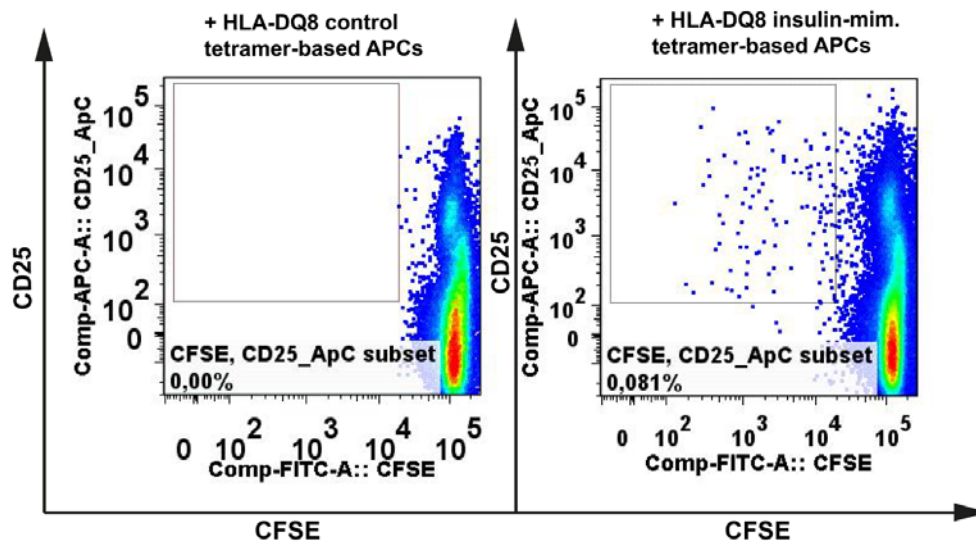
Supplementary Figure 2. Proliferation of human CD4⁺T cells from children without ongoing islet autoimmunity upon stimulation with insulin mimetopes. Percentages of divided human CFSE^{dim}CD4⁺CD45RO⁺T cells upon stimulation with a combination of ins.mim.2= 21G-22E and ins.mim.3=21E-22E or a combination of ins.mim.1= 14E-21G-22E and ins.mim.4=14E-21E-22E. Bars represent the means \pm s.e.m. (n=5) from duplicate wells of five children and four independent experiments. ** $P < 0.01$ (Student's *t*-test).

Suppl.Fig.3



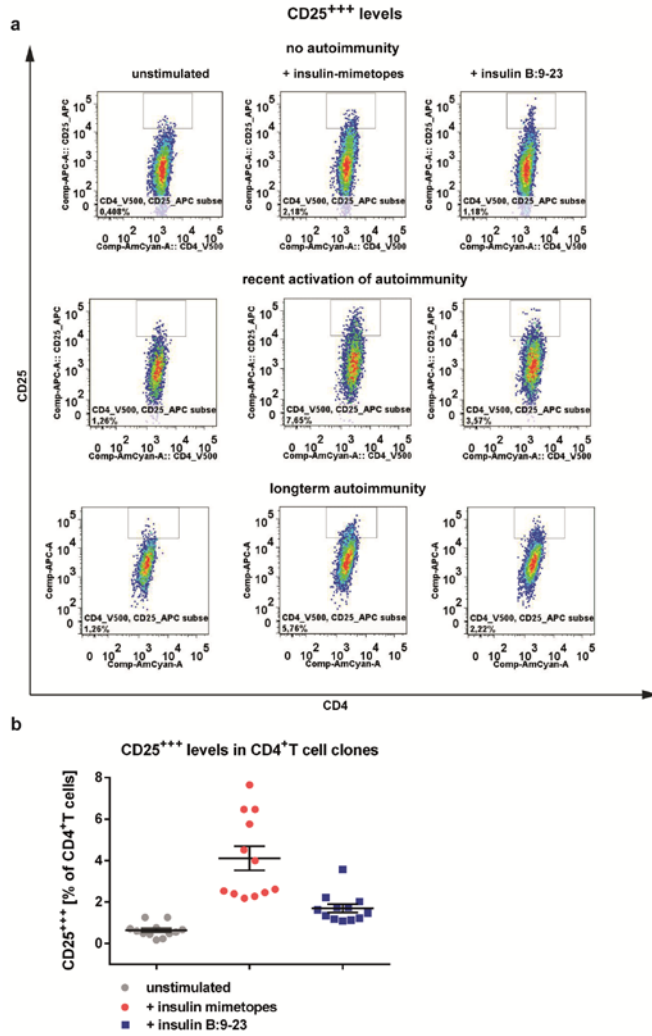
Supplementary Figure 3. Representative FACS plots of HLA-DQ8-restricted insulin mimetope-specific CD4⁺T cells in a child with recent onset of Type 1 diabetes (a) or longterm Type 1 diabetes (b) using tetramer and respective control stainings. (c) Frequencies of HLA-DQ8-restricted insulin mimetope-specific CD4⁺T cells from children with recent onset vs. longstanding Type 1 diabetes. FACS analyses were performed using samples from five children with recent onset of Type 1 diabetes and six children with longterm diabetes in five independent experiments (mean±s.e.m).

Suppl.Fig.4



Supplementary Figure 4. Proliferative responses of CD4⁺T cells from children without ongoing islet autoimmunity to HLA-DQ8-restricted insulin mimetope-specific artificial antigen-presenting cells. Representative FACS plots for CFSE dilution profiles of human CD4⁺T cells from children without autoimmunity (islet autoantibody negative) stimulated with HLA-DQ8 control (left) or HLA-DQ8 insulin mimetope-specific (right) artificial antigen-presenting cells. Responsive CD4⁺T cells were defined as proliferating CFSE^{dim}CD4⁺CD25⁺CD45RO⁺T cells.

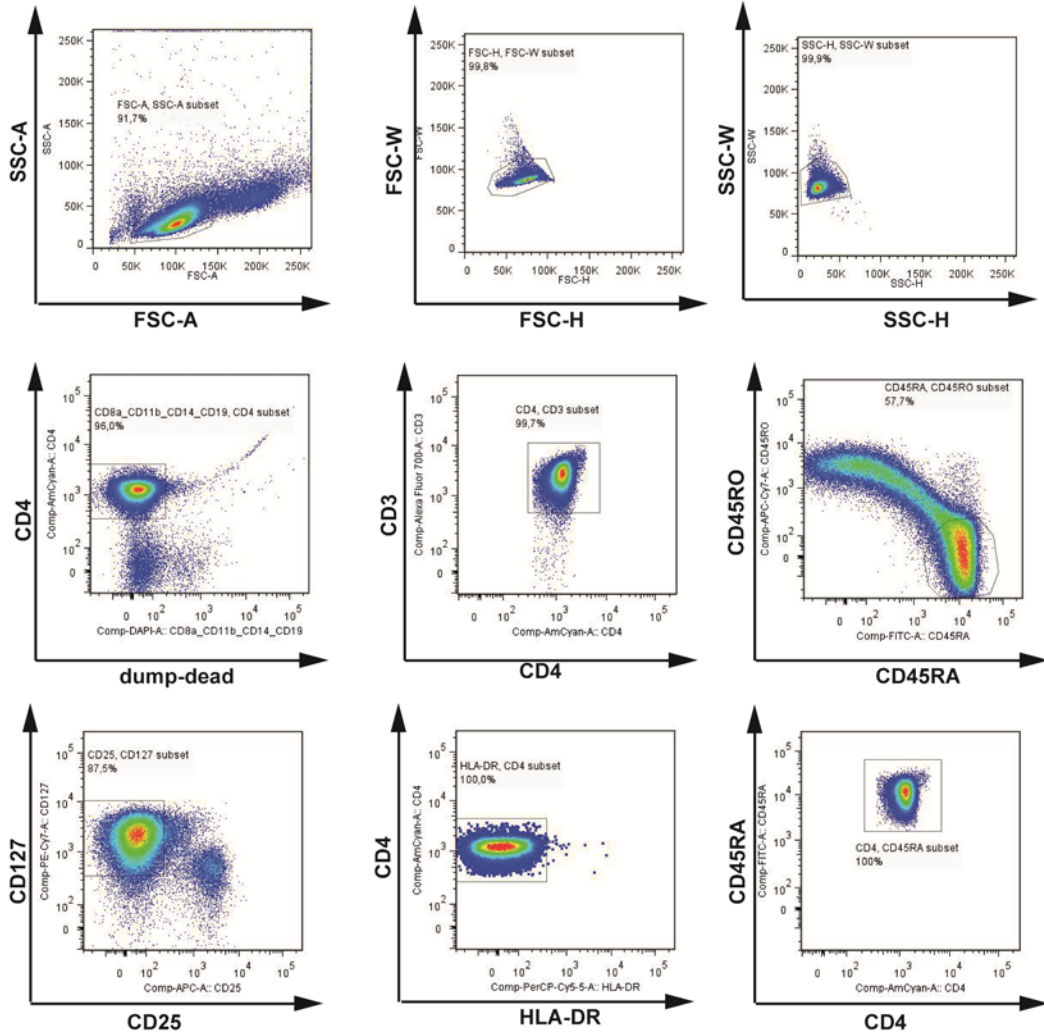
Suppl.Fig.5



Supplementary Figure 5. Agonistic activity of insulin mimetopes in human insulin-specific CD4⁺T cell clones compared to insulin B:9-23. **a)** CD25⁺⁺⁺ levels of insulin-specific CD4⁺T cell clones either left unstimulated (control, left plot) or upon stimulation with insulin mimetopes (ins.mim.1, 2, 3,4 at final 100 ng per ml, middle plot) or with insulin B:9-23 (1000 ng per ml, right plot). Insulin-specific CD4⁺T cell clones from children without ongoing autoimmunity, with recent activation or with longterm autoimmunity. **b)** Summary graph for CD25⁺⁺⁺ levels (mean±s.e.m). Triplicate wells have been analyzed per condition. Four clones from two children without ongoing autoimmunity, four clones from two children with recent activation and four clones from four children with longterm autoimmunity. Four independent experiments have been performed.

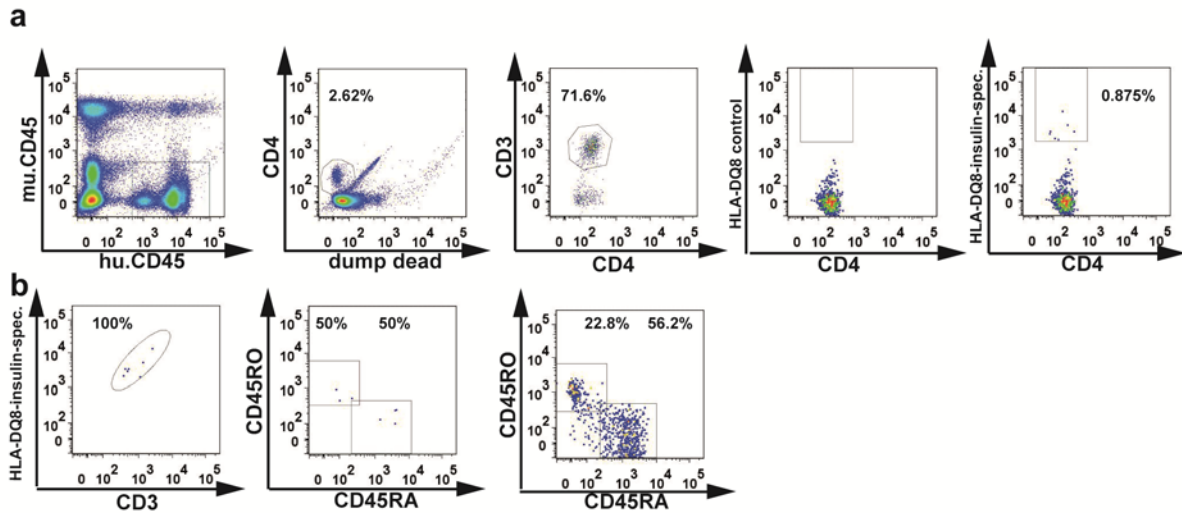
Suppl.Fig. 6

Sorting strategy for human naive CD4⁺T-cells



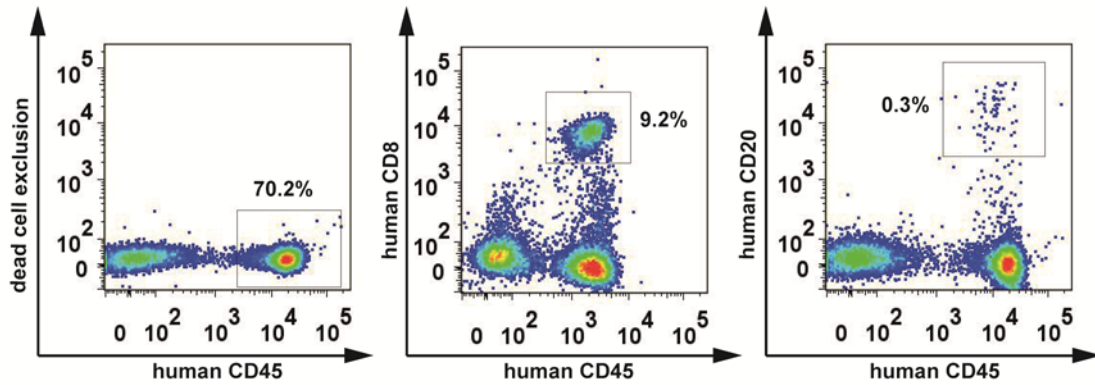
Supplementary Figure 6. Gating strategy for the sort purification of human naive CD4⁺T cells used in *in vitro* Treg induction assays. Human naive CD4⁺T cells were sorted to 99.9% purity as CD4⁺CD3⁺CD45RA⁺CD45RO⁻CD127⁺CD25⁻HLA-DR⁻ T cells using a BD FACSARIA III cell sorting system.

Suppl. Fig.7



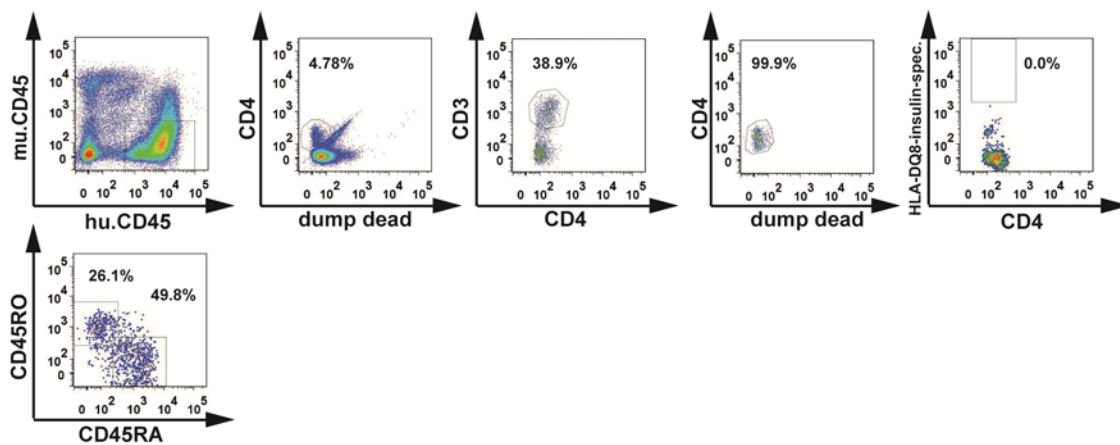
Supplementary Figure 7. Characterization of HLA-DQ8-restricted insulin mimetope-specific CD4⁺T cell responses in NSG-HLA-DQ8 mice. Human immune subsets purified from peripheral blood (a+b) of humanized NSG-HLA-DQ8 mice, 20 weeks post reconstitution, are first identified based on murine vs. human CD45 expression. Human CD4⁺CD3⁺T cells were characterized upon exclusion of dead cells and additional markers (CD8, CD11b, CD14, CD19). (a) Representative set of FACS plots for the identification of HLA-DQ8-restricted insulin-specific CD4⁺T cells. (b) Representative set of FACS plots for the phenotypic characterization of blood-derived HLA-DQ8-restricted insulin-specific CD4⁺T cells based on gating against CD3 and CD45RA vs. CD45RO expression (memory-status, insulin-specific vs. polyclonal).

Suppl.Fig.8



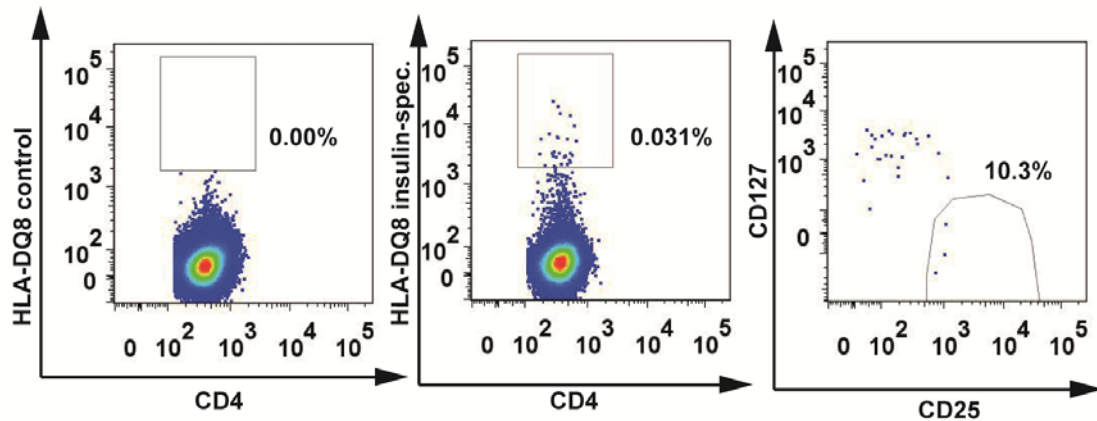
Supplementary Figure 8. Identification of immune subsets in reconstituted NSG-HLA-DQ8 mice. Human immune subsets purified from peripheral blood of NSG-HLA-DQ8 mice, 20 weeks post reconstitution, are first identified based on murine vs. human CD45 expression. Representative set of FACS plots for the identification of human CD8⁺T cells and CD20⁺B cells are shown.

Suppl. Fig.9



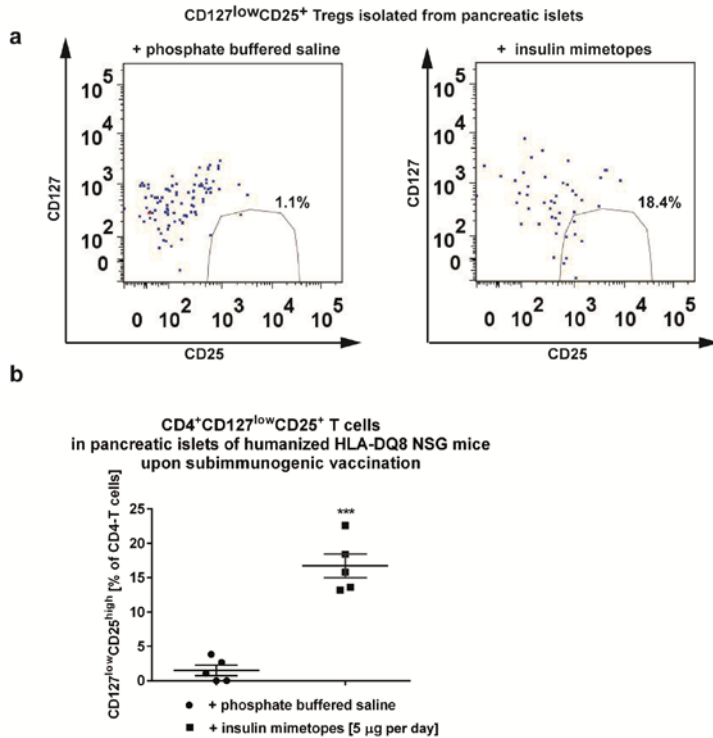
Supplementary Figure 9. Characterization of HLA-DQ8-restricted insulin mimetope-specific CD4⁺T cell responses in NSG-HLA-DQ8 mice. Human immune subsets purified from visceral white fat tissues (a+b). (a) Representative set of FACS plots for the identification of HLA-DQ8-restricted insulin mimetope-specific CD4⁺T cells purified from visceral white fat tissues. (b) Characterization of memory status (CD45RA vs. CD45RO expression) (in polyclonal fat-derived CD4⁺T cells).

Suppl.Fig.10



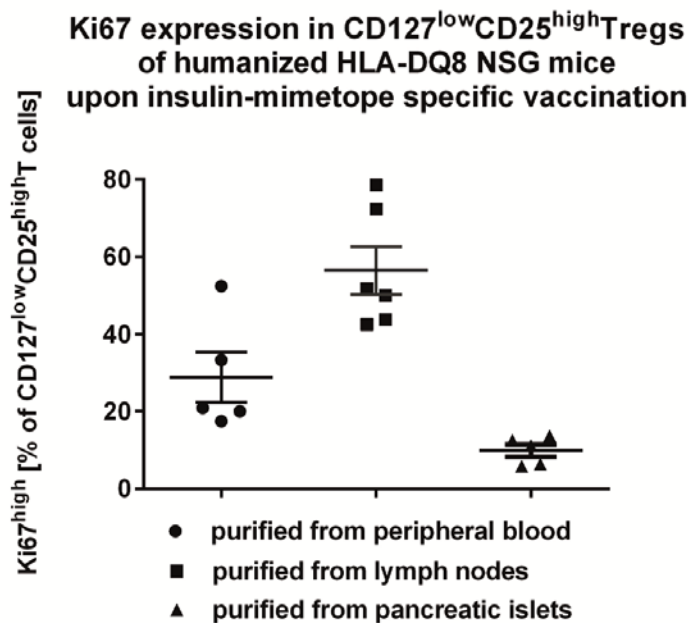
Supplementary Figure 10. Characterization of HLA-DQ8-restricted insulin mimetope-specific CD4⁺T cell responses in NSG-HLA-DQ8 mice upon application of insulin mimetopes to humanized NSG-HLA-DQ8 mice for Treg induction *in vivo*. Treg induction in humanized mice was performed at 20 weeks post reconstitution. Three weeks after Treg induction using insulin mimetopes infusion by osmotic mini-pumps (ins.mim.1= 14E-21G-22E and ins.mim.4=14E-21E-22E) human immune subsets were purified from pancreatic and mesenteric lymph nodes of respective NSG mice. Human CD4⁺CD3⁺T cells were characterized upon exclusion of dead cells and additional markers (CD8, CD11b, CD14, CD19). Representative set of FACS plots for the identification of control- (left plot) and HLA-DQ8-restricted insulin mimetope-specific CD4⁺CD127^{low}CD25^{high}Tregs are shown (total insulin mimetope-specific CD4⁺T cells shown in middle plot, frequencies of CD127^{low}CD25^{high}Tregs in right plot).

Suppl.Fig.11



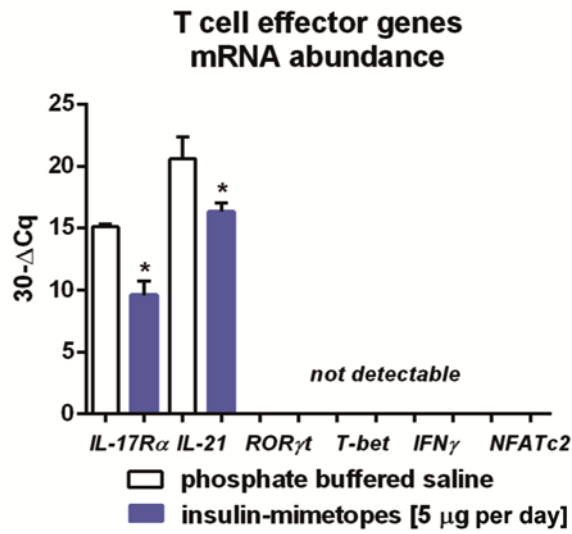
Supplementary Figure 11. Identification of human CD4⁺T cells in pancreatic islets of humanized NSG-HLA-DQ8 mice. Human CD4⁺T cells isolated from pancreatic islets of humanized NSG-HLA-DQ8 mice, 23 weeks post reconstitution were first identified flow cytometrically based on human CD45 expression. Human CD4⁺CD3⁺T cells were characterized upon exclusion of dead cells and additional markers (CD8, CD11b, CD14, CD19). (a) Representative set of FACS plots for the identification of pancreatic islet-infiltrating CD4⁺CD3⁺CD127^{low}CD25⁺Tregs isolated from humanized NSG-HLA-DQ8 mice upon subimmunogenic Treg induction *in vivo* using insulin mimetopes infusion by osmotic mini-pumps (ins.mim1= 14E-21G-22E and ins.mim4=14E-21E-22E) or control (phosphate buffered saline). (b) Summary graph for the frequencies of infiltrating CD4⁺CD3⁺CD127^{low}CD25⁺Tregs upon Treg induction using insulin mimetopes or control (phosphate buffered saline), mean±s.e.m.. n= 5 mice per group from two independent experiments; *** $P < 0.001$ (Student's *t*-test).

Suppl.Fig.12



Supplementary Figure 12. Analysis of Ki67 expression levels in human CD127^{low}CD25^{high} Tregs. Treg induction in humanized mice was performed at 20 weeks post reconstitution. Three weeks after Treg induction using insulin mimetopes infusion by osmotic mini-pumps (ins.mim.1= 14E-21G-22E and ins.mim.4=14E-21E-22E) human immune subsets were purified from peripheral blood, pancreatic and mesenteric lymph nodes or from pancreatic islets of respective NSG mice. Human CD4⁺CD3⁺T cells were first characterized upon exclusion of dead cells and additional markers (CD8, CD11b, CD14, CD19). Summary graphs are shown for the analysis of the proliferative capacity of CD127^{low}CD25^{high}Treg cells by intracellular staining for Ki67 (mean±s.e.m.). n= 8 mice, from two independent experiments.

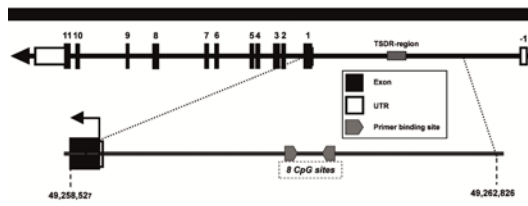
Suppl. Fig.13



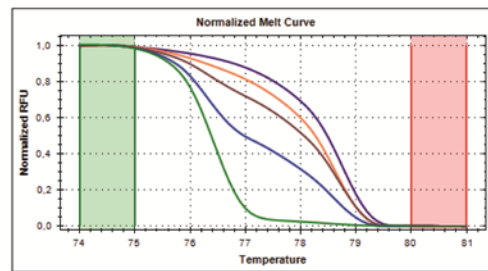
Supplementary Figure 13. Analysis of human T cell effector genes upon subimmunogenic vaccination with human insulin mimetopes in NSG-HLA-DQ8 transgenic mice. Quantitative RT-PCR analyses of *IL-17Rα*, *IL-21*, *RORγt*, *T-bet*, *IFN-γ* and *NFATc2* abundance in human CD4⁺T cells purified from pooled spleens and lymph nodes of humanized mice after three weeks of *in vivo* Treg induction using subcutaneous insulin mimetopes infusion by osmotic mini-pumps (ins.mim.1= 14E-21G-22E and ins.mim.4=14E-21E-22E) in humanized NSG-HLA-DQ8 transgenic mice (n=4). Bars represent the means ± s.e.m. (n=4 mice per group and experiment, n=2 independent experiments). * $P < 0.05$ (Student's *t*-test).

Suppl.Fig.14

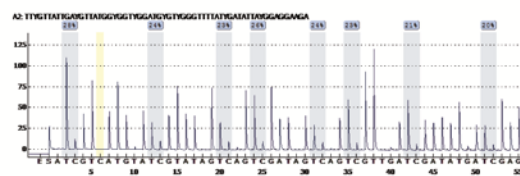
a



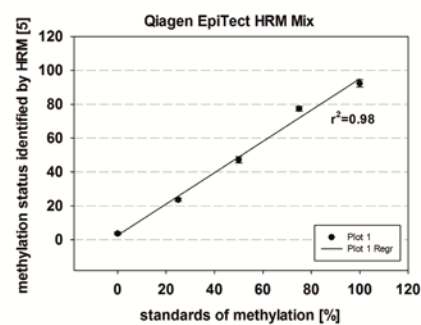
b



c

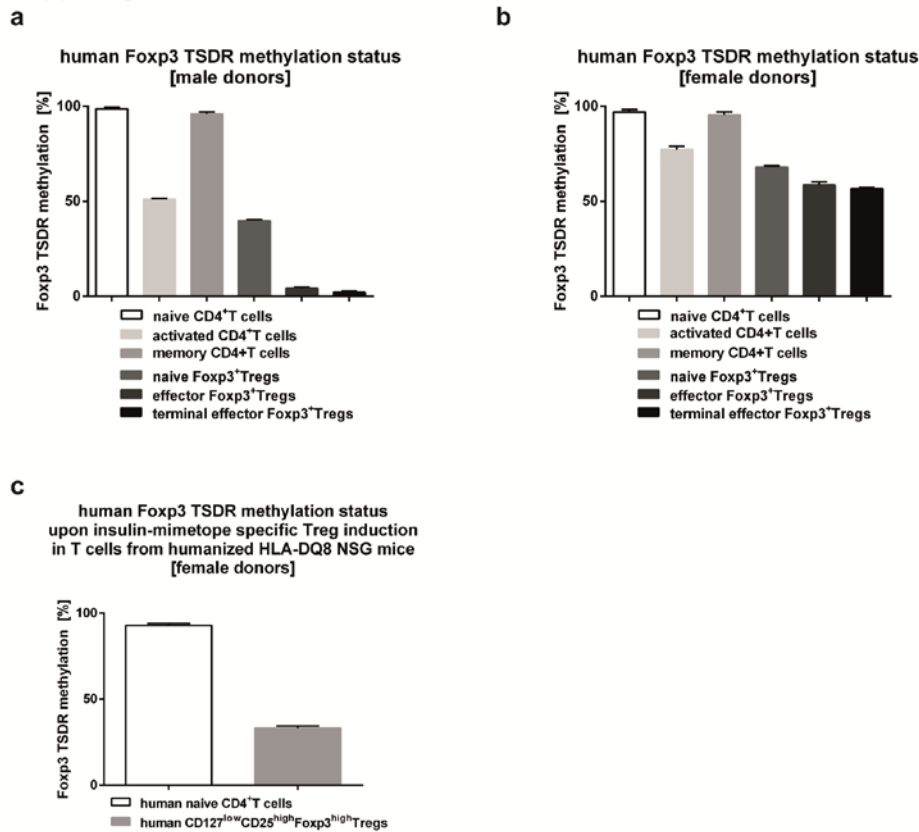


d



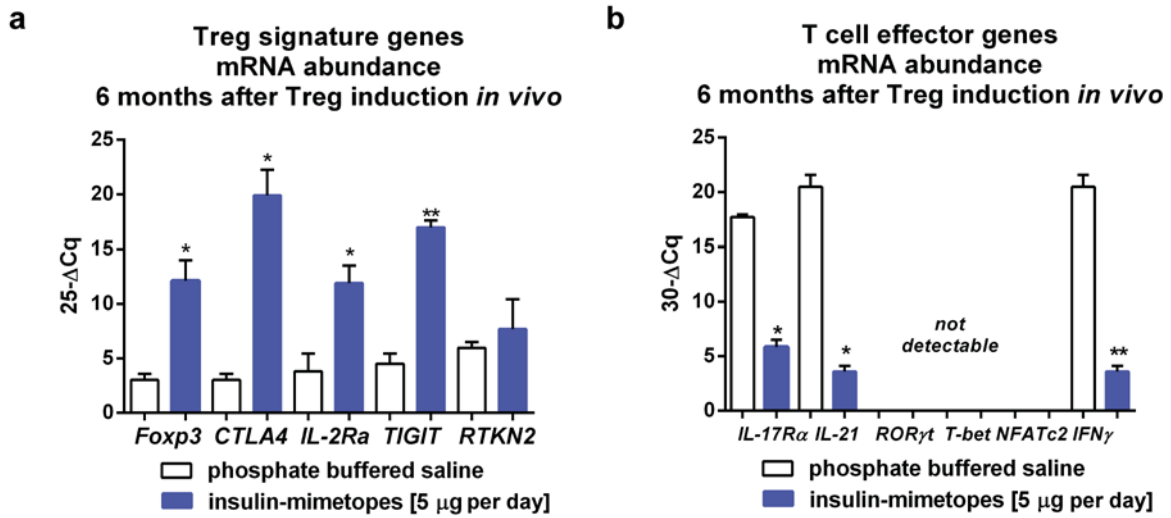
Supplementary Figure 14. DNA-methylation analysis of the human *Foxp3* Treg-specific demethylated region (TSDR). (a) High resolution melting (HRM)-PCR primers were designed to cover the same area in the *Foxp3* locus (displayed transcript variant: ENST00000376207) as originally described by Baron *et al.* (2007). (b) Primers were validated on a standard-series of unmethylated and methylated DNA for unbiased PCR amplification according to their products' uniform high-resolution melting behavior. (c) The obtained amplicons enabled high-quality readouts of eight successive CpG-sites in subsequent pyrosequencing reactions (exemplary file shown). (d) High correlation between methylation levels of input standards and pyrosequencing-readout of PCR products additionally verified the designed assay for even amplification.

Suppl. Fig.15



Supplementary Figure 15. DNA-methylation analysis of the human *Foxp3* Treg-specific demethylated region (TSDR) in human CD4⁺T cell subsets. Pyrosequencing analyses of eight successive CpG-sites in the human *Foxp3* TSDR region as methylation in %. Shown are means \pm s.e.m. from female (**a**) or male (**b**) donors (n=4 each from two independent experiments). Except for the completely methylated cells the methylation levels of the female donor were higher than the levels of the male donor, which is due to the fact, that the *Foxp3* gene is X-linked. (**c**) Human *Foxp3* TSDR methylation status in naïve CD4⁺T cells or CD4⁺CD127^{low}CD25^{high}Tregs purified from pooled lymph nodes and spleens of humanized NSG-HLA-DQ8 transgenic mice (human female donors for reconstitution have been used) upon insulin mimotope-specific Treg induction (ins.mim.1= 14E-21G-22E and ins.mim.4=14E-21E-22E). Bars represent the means \pm s.e.m from six mice and two independent experiments.

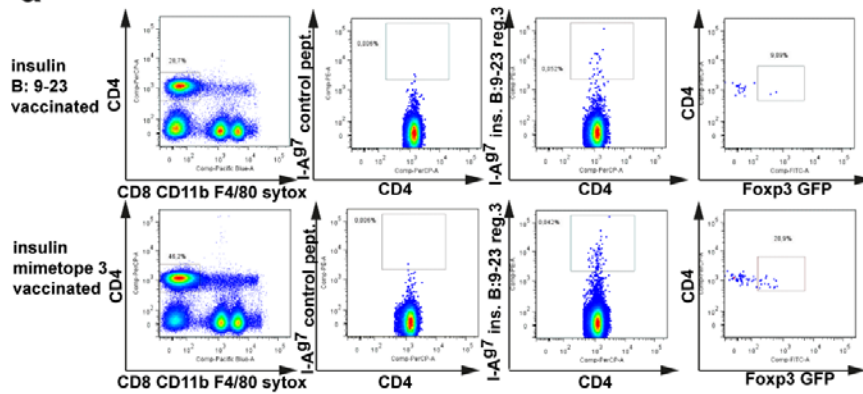
Suppl. Fig.16



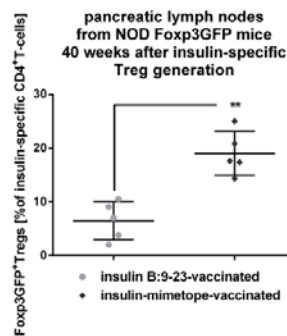
Supplementary Figure 16. Analysis of human Treg signature and T cell effector genes six months after subimmunogenic Treg induction with human insulin mimetopes in NSG-HLA-DQ8 transgenic mice. (a) Quantitative RT-PCR analyses of *Foxp3*, *CTLA4*, *IL-2Rα*, *TIGIT* and *RTKN2* mRNA abundance in human CD4⁺T cells purified from pooled spleens and lymph nodes of humanized mice six months after *in vivo* Treg induction using subcutaneous insulin mimetopes infusion by osmotic mini-pumps (ins.mim.1= 14E-21G-22E and ins.mim.4=14E-21E-22E). Bars represent the means ± s.e.m. (n=5 mice per group). (b) Quantitative RT-PCR analyses of *IL-17Rα*, *IL-21*, *RORγt*, *T-bet*, *IFN-γ* and *NFATc2* abundance in human CD4⁺T cells purified from pooled spleens and lymph nodes of humanized mice six months after *in vivo* Treg induction using subcutaneous insulin mimetopes infusion by osmotic mini-pumps (ins.mim1= 14E-21G-22E and ins.mim4=14E-21E-22E) in humanized NSG-HLA-DQ8 transgenic mice (n=5). Bars represent the means ± s.e.m. (n=5 mice per group). * $P < 0.05$; ** $P < 0.01$ (Student's *t*-test).

Suppl.Fig.17

a



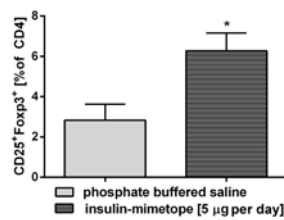
b



Supplementary Figure 17. Maintenance of insulin-specific Foxp3⁺Tregs induced by subimmunogenic TCR stimulation and protection from type 1 diabetes development in Non-obese-diabetic (NOD) mice. Identification of I-A^{g7}-restricted insulin-specific CD4⁺T cells by tetramer staining and flow cytometry, first gating on live, B220⁻, F4/80⁻, CD8⁻, CD11b⁻ and CD4, and then examining the tetramer binding (left panels). Control tetramer staining to assess specificity (second left panel). **(a)** Insulin-specific CD4⁺T cells expressing Foxp3 GFP in pancreatic lymph nodes from 40-wk-old NOD-Foxp3 GFP reporter mice that had received the natural insulin B:9-23 epitope (upper panel) or the strong-agonistic insulin mimetope for Treg induction at 4-6 weeks of age (lower panel). **(b)** Percentages of Foxp3GFP⁺Tregs in insulin-specific CD4⁺T cells purified from pancreatic lymph nodes of 40-weeks-old NOD-Foxp3 GFP reporter mice. Data represent the means \pm s.e.m., n=5 mice per group. ** $P < 0.01$ (Student's t -test).

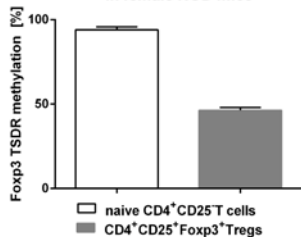
Suppl.Fig.18

a pancreas-residing CD4⁺CD25⁺Foxp3⁺Tregs upon insulin-mimotope-specific Treg induction in NOD mice



b

murine Foxp3 TSDR methylation upon insulin-mimotope Treg induction in female NOD mice



Supplementary Figure 18. Analyses of islet-residing CD4⁺T cells purified from Non-obese-diabetic (NOD) mice upon insulin mimotope-specific Treg induction using subimmunogenic TCR stimulation. (a) Percentages of Foxp3⁺CD4⁺CD25⁺Tregs in islet-infiltrating CD4⁺T cells purified from NOD mice 4 weeks after Treg induction *in vivo*, n=6 mice per group. Data represent the means ± s.e.m., ** $P < 0.01$ (Student's *t*-test). **(b)** Pyrosequencing analyses of eight successive CpG-sites in the murine *Foxp3* TSDR region shown as methylation in %. Shown are means ± s.e.m. of islet-infiltrating naïve or Foxp3⁺CD4⁺CD25⁺Tregs (n=6).

3.2.2 Authors' contributions

Isabelle Serr: Proliferation assays with human CD4⁺T cells stimulated with insulin-mimetopes and FACS analysis (Fig.1a-d, Suppl.Fig.4); Tetramer stainings (FACS) on CD4⁺T cells from children at different stages of islet autoimmunity (Fig.2a-d, Fig.3a-e, Suppl.Fig.3a-c); generation and characterization of insulin-specific CD4⁺T cell clones from children at different stages of islet autoimmunity (Fig.4a-g, Suppl.Fig.2, Suppl.Fig.5a-b); Peptide-HLA-DQ8 binding assays (Fig.4h); insulin-specific Treg induction assays *in vitro* (Fig.5a-c, Suppl.Fig.6); reconstitution and characterization of humanized HLA-DQ8 transgenic mice (Fig.7a-c, Fig.8a-e, Fig.9a-c, Suppl.Fig.7a-b, Suppl.Fig.8, Suppl.Fig.9, Suppl.Fig.10); insulin-specific Treg induction in humanized mice *in vivo* (Fig.9d, Suppl.Fig.11a-b, Suppl.Fig. 12, Suppl.Fig.17a-b, Suppl.Fig.18a), characterization of *in vivo* induced Tregs: gene expression analysis via RT-qPCR (Fig.10a, Suppl.Fig.13, Suppl.Fig.16a-b), Treg suppression assays (Fig.10b-f). Data analysis and interpretation; preparation and editing of the manuscript.

Rainer W. Fürst: Methylation analysis of Tregs via high resolution melting and pyrosequencing.

Peter Achenbach: Autoantibody measurements and patient phenotyping.

Martin G. Scherm: Methylation analysis of Tregs via high resolution melting and pyrosequencing.

Fusun Gökmen: Support of tetramer stainings.

Florian Haupt: Coordination of the clinical study center and patient visits.

Eva-Maria Sedlmeier: HLA-DQ8 fast genotyping.

Annette Knopff: Patient follow-up.

Leonard Shultz: Provision of humanized mice and support of humanized mice analysis.

Richard A. Willis: Conceptualization, design and production of tetramer reagents.

Anette-G. Ziegler: Advisement and co-conceptualization of the study design and principle investigator of cohort studies BABYDIAB, DiMelli and Munich Bioresource, which provided patient samples.

Carolin Daniel: Conceptualization and design of the study, interpretation of data, preparation and editing of the manuscript.

3.3 miRNA92a targets KLF2 and the phosphatase PTEN signaling to promote human T follicular helper precursors in T1D islet autoimmunity

Isabelle Serr, Rainer W. Fürst, Verena B. Ott, Martin G. Scherm, Alexei Nikolaev, Füsün Gökmen, Stefanie Kälin, Stephanie Zillmer, Melanie Bunk, Benno Weigmann, Nicole Kunschke, Brigitta Loretz, Claus-Michael Lehr, Benedikt Kirchner, Bettina Haase, Michael Pfaffl, Ari Waisman, Richard A. Willis, Anette-G. Ziegler and Carolin Daniel.

Published in

Proceedings of the National Academy of Sciences 2016 Oct 25;113(43):E6659–E6668. doi: 10.1073/pnas.1606646113. Epub 2016 Oct 10.

Permission:

PNAS authors need not obtain permission for the following cases: 1) to use their original figures or tables in their future works; 2) to make copies of their papers for their own personal use, including classroom use, or for the personal use of colleagues, provided those copies are not for sale and are not distributed in a systematic way; **3) to include their papers as part of their dissertations;** or 4) to use all or part of their articles in printed compilations of their own works. The full journal reference must be cited and, for articles published in volumes 90–105 (1993–2008), "Copyright (copyright year) National Academy of Sciences."

miRNA92a targets KLF2 and the phosphatase PTEN signaling to promote human T follicular helper precursors in T1D islet autoimmunity

Isabelle Serr^{a,b}, Rainer W. Fürst^{b,c,d}, Verena B. Ott^{b,e,f}, Martin G. Scherm^{a,b}, Alexei Nikolaev^g, Fusun Gökmen^{a,b}, Stefanie Kälin^{b,e,f}, Stephanie Zillmer^{b,c,d}, Melanie Bunk^{b,c,d}, Benno Weigmann^h, Nicole Kunschkeⁱ, Brigitta Loretzⁱ, Claus-Michael Lehr^{i,j}, Benedikt Kirchner^k, Bettina Haase^l, Michael Pfaffl^k, Ari Waisman^g, Richard A. Willis^m, Anette-G. Ziegler^{b,c,d}, and Carolin Daniel^{a,b,1}

^aInstitute for Diabetes Research, Independent Young Investigator Group Immune Tolerance in Type 1 Diabetes, Helmholtz Diabetes Center at Helmholtz Zentrum München, 80939 Munich, Germany; ^bDeutsches Zentrum für Diabetesforschung, 85764 Munich, Germany; ^cInstitute for Diabetes Research, Helmholtz Diabetes Center at Helmholtz Zentrum München, 80939 Munich, Germany; ^dKlinikum rechts der Isar, Technische Universität München, 80939 Munich, Germany; ^eInstitute for Diabetes and Obesity, Helmholtz Diabetes Center at Helmholtz Zentrum München, 80939 Munich, Germany; ^fDivision of Metabolic Diseases, Technische Universität München, 85748 Munich, Germany; ^gInstitute for Molecular Medicine, Universitätsmedizin der Johannes Gutenberg-Universität, 55131 Mainz, Germany; ^hDepartment of Medicine 1, University of Erlangen-Nuremberg, Kussmaul Campus for Medical Research, 91052 Erlangen, Germany; ⁱDepartment of Drug Delivery, Helmholtz Institute for Pharmaceutical Research Saarland, Helmholtz Centre for Infection Research, 66123 Saarbruecken, Germany; ^jDepartment of Pharmacy, Saarland University, 66123 Saarbruecken, Germany; ^kPhysiology Weihenstephan, Technische Universität München, 85354 Freising, Germany; ^lGenomics Core Facility, European Molecular Biology Laboratory, 69117 Heidelberg, Germany; and ^mEmory Vaccine Center, NIH Tetramer Core Facility, Atlanta, GA 30322

Edited by Harvey Cantor, Dana-Farber Cancer Institute, Boston, MA, and approved September 2, 2016 (received for review April 29, 2016)

Aberrant immune activation mediated by T effector cell populations is pivotal in the onset of autoimmunity in type 1 diabetes (T1D). T follicular helper (TFH) cells are essential in the induction of high-affinity antibodies, and their precursor memory compartment circulates in the blood. The role of TFH precursors in the onset of islet autoimmunity and signaling pathways regulating their differentiation is incompletely understood. Here, we provide direct evidence that during onset of islet autoimmunity, the insulin-specific target T-cell population is enriched with a C-X-C chemokine receptor type 5 (CXCR5)⁺CD4⁺ TFH precursor phenotype. During onset of islet autoimmunity, the frequency of TFH precursors was controlled by high expression of microRNA92a (miRNA92a). miRNA92a-mediated TFH precursor induction was regulated by phosphatase and tension homolog (PTEN) - phosphoinositol-3-kinase (PI3K) signaling involving PTEN and forkhead box protein O1 (Foxo1), supporting autoantibody generation and triggering the onset of islet autoimmunity. Moreover, we identify Krueppel-like factor 2 (KLF2) as a target of miRNA92a in regulating human TFH precursor induction. Importantly, a miRNA92a antagomir completely blocked induction of human TFH precursors *in vitro*. More importantly, *in vivo* application of a miRNA92a antagomir to nonobese diabetic (NOD) mice with ongoing islet autoimmunity resulted in a significant reduction of TFH precursors in peripheral blood and pancreatic lymph nodes. Moreover, miRNA92a antagomir application reduced immune infiltration and activation in pancreata of NOD mice as well as humanized NOD Scid IL2 receptor gamma chain knockout (NSG) human leucocyte antigen (HLA)-DQ8 transgenic animals. We therefore propose that miRNA92a and the PTEN-PI3K-KLF2 signaling network could function as targets for innovative precision medicines to reduce T1D islet autoimmunity.

miRNA92a | KLF2 | PTEN-PI3K signaling | T follicular helper cells | type 1 diabetes

Autoimmune type 1 diabetes (T1D) is presumed to result from T-cell-mediated destruction of the pancreatic insulin-secreting islet β cells (1). In children, the development of multiple autoantibodies reacting with the well-established autoantigens (insulin, glutamic decarboxylase, insulinoma antigen, and islet zinc transporter) indicates the onset of islet autoimmunity (pre-T1D) (2, 3). Autoantibodies against insulin are often the first to appear, indicating an essential impact of insulin in the onset of islet autoimmunity (2, 4). In young children, clinically overt T1D can occur within months of the appearance of autoantibodies, but may take more than a decade to occur in some children (5), referring to the

so-called slowly progressing phenotype. Moreover, children with slowly progressing phenotypes can lose some of their earliest islet autoantibodies, especially insulin autoantibodies. Despite these insights, the cellular and molecular mechanisms involved in triggering the onset, as well as the progression, of human islet autoimmunity remain incompletely understood.

T follicular helper (TFH) cells support antibody responses by the induction of B-cell activation. Murine data suggested that islet autoantibodies can enhance the survival of proliferating autoreactive CD4⁺ T cells, whereas blocking Fc γ receptor delayed and reduced the incidence of autoimmune diabetes (6). TFH cells are characterized by a memory phenotype, and thereby retain their capacity to recall their TFH-specific effector functions upon reactivation to provide help for B-cell responses (7). After interactions with dendritic cells in the T-cell zones of secondary lymphoid

Significance

The onset of type 1 diabetes autoimmunity is indicated by the development of multiple islet autoantibodies, produced by B cells with the help of T follicular helper (TFH) cells. MicroRNAs (miRNAs) are small noncoding RNAs that regulate cellular states, as immune activation, making them suitable targets for disease intervention. Here, we show an enrichment of insulin-specific C-X-C chemokine receptor type 5 (CXCR5)⁺CD4⁺ TFH precursors correlating with high miRNA92a abundance during onset of autoimmunity and identify Krueppel-like factor 2 (KLF2) as a target for miRNA92a. We demonstrate that miRNA92a inhibition blocks TFH induction and reduces murine islet autoimmunity *in vivo*. Therefore, we propose miRNA92a and the phosphatase and tension homolog-phosphoinositol-3-kinase-KLF2 signaling network as possible innovative precision medicine targets to interfere with aberrant immune activation in islet autoimmunity.

Author contributions: I.S., R.W.F., B.W., A.-G.Z., and C.D. designed research; I.S., V.B.O., M.G.S., A.N., F.G., S.K., B.W., B.H., and C.D. performed research; S.Z., M.B., N.K., B.L., C.-M.L., M.P., A.W., and R.A.W. contributed new reagents/analytic tools; I.S., V.B.O., M.G.S., B.W., B.K., B.H., and C.D. analyzed data; I.S. and C.D. wrote the paper; and S.Z. and M.B. coordinated human blood samples.

The authors declare no conflict of interest.

This article is a PNAS Direct Submission.

¹To whom correspondence should be addressed. Email: carolin.daniel@helmholtz-muenchen.de.

This article contains supporting information online at www.pnas.org/lookup/suppl/doi:10.1073/pnas.1606646113/-DCSupplemental.

organs, a fraction of activated CD4⁺ T cells migrate toward B-cell follicles by up-regulating C-X-C chemokine receptor type 5 (CXCR5) (8–10). The transcription factor B-cell lymphoma 6 (Bcl6) plays an essential role in initiating TFH-cell differentiation (11). Inducible T-cell costimulator (ICOS) signaling transiently inactivates forkhead box protein O1 (Foxo1), which, in turn, relieves Foxo1-dependent inhibition of Bcl6 expression and promotes TFH differentiation (12). Reduced Foxo1 abundance, either resulting from increased expression of ICOS induced by loss of Foxp1 or due to degradation by the E3 ubiquitin ligase ITCH, may enhance TFH-cell differentiation (13, 14). Moreover, induced deficiency of the zinc finger transcription factor Krueppel-like factor 2 (KLF2) in activated CD4⁺ T cells leads to increased TFH-cell generation and B-cell priming, whereas KLF2 overexpression prevented TFH-cell production (15).

Recent studies in man have provided new insights into the ontogeny of circulating CXCR5⁺CD4⁺ T cells (16–20). In particular, the frequency of circulating TFH precursor C-C chemokine receptor type 7 (CCR7)^{low} programmed cell death protein 1 (PD1)^{high}CXCR5⁺CD4⁺ T cells is associated with active TFH-cell differentiation in secondary lymphoid organs (21).

However, involved signaling pathways that regulate the differentiation of human TFH precursors, as well as their contribution in the initiation and progression of human islet autoimmunity, are incompletely understood (22).

MicroRNAs (miRNAs) function as critical regulators in the mammalian immune system (23–26), and thereby affect complex cellular states, including immune activation and regulation (27, 28). The miRNA17~92 transcript, which is encoded by mouse chromosome 14 and human chromosome 13, is the precursor for six mature miRNAs (miRNA17, miRNA18a, miRNA19a, miRNA20a, miRNA19b, and miRNA92a). Transgenic (Tg) mice overexpressing miRNA17~92 in lymphocytes developed lymphoproliferative disorders and autoimmunity (29), and miRNA92a promoted the generation of TFH cells (30).

In man, the impact of the miRNA17~92 family and its critical targets to the posttranscriptional regulation of human TFH precursor cell induction in the development of human islet autoimmunity are currently unclear. We therefore studied insulin-specific TFH precursors and their signaling pathways during the onset of human islet autoimmunity. We provide direct evidence that during the onset of human islet autoimmunity, the insulin-specific target T-cell population is enriched with a CXCR5⁺CD4⁺ TFH precursor phenotype. The frequency of CCR7^{low}PD1^{high}CXCR5⁺ TFH precursor cells was controlled by high abundance of miRNA92a. miRNA92a-mediated TFH-cell induction was regulated by phosphatase and tension homolog (PTEN) - phosphoinositol-3-kinase (PI3K) signaling involving down-regulation of PTEN, PH domain and leucine-rich repeat protein phosphatase 2 (PHLPP2), and Foxo1. Moreover, we identify KLF2 as a target of miRNA92a and show that upon blockade of KLF2 signaling, miRNA92a-mediated induction of human TFH precursors was severely abolished. Importantly, a miRNA92a antagonist completely blocked human TFH precursor induction in vitro. Of note, in vivo application of a miRNA92a antagonist to nonobese diabetic (NOD) mice significantly lowered TFH precursors. More importantly, application of a miRNA92a antagonist critically reduced pancreatic immune activation. miRNA92a and the PTEN-PI3K-KLF2 signaling network might therefore function as targets for innovative precision intervention that can limit the activation of T1D islet autoimmunity.

Results

Enhancement of Insulin-Specific CXCR5⁺ TFH Precursors During the Onset of Human Islet Autoimmunity. Given the critical role of the autoantigen insulin in initiating islet autoimmunity, we studied the TFH precursor characteristics of the insulin-specific target T-cell population. We used CD4⁺ T cells from nondiabetic children without autoimmunity (islet autoantibody-negative children), with recent onset of autoimmunity (recent activation, multiple autoantibodies for <5 y), persistent autoimmunity (multiple autoantibodies for >5 to <10 y), and long-term autoimmunity (multiple autoantibodies

for >10 y without overt T1D). We applied recently developed fluorescent insulin-specific HLA-DQ8 tetramers (14E-22E and 14E-21G 22E tetramers) based on a set of two insulin B-chain 10–23 mimetopes to identify human HLA-DQ8-restricted insulin-specific CD4⁺ T cells ex vivo directly (31). We detected no tet⁺CD4⁺ T cells using the control tetramers, whereas a population of insulin-specific CD4⁺ T cells was readily identified ex vivo with the insulin-specific tetramers (Fig. 1 *A* and *B*). Frequencies of tet⁺CD4⁺ T cells were correlated with CD3 expression. Importantly, we provide direct evidence that during onset of islet autoimmunity and in the absence of clinically overt T1D, the insulin-specific target T-cell population is enriched with a CXCR5⁺CD4⁺ TFH precursor phenotype (no autoimmunity vs. recent onset of autoimmunity: 14.4 ± 2.9% vs. 42.5 ± 9.2% of tet⁺CD4⁺ T cells; *P* < 0.05; Fig. 1*C*).

Of note, the frequency of these insulin-specific TFH precursors in nondiabetic children with long-term autoimmunity was 14.3 ± 3.0% of tet⁺CD4⁺ T cells, which was significantly lower than in children with recent onset of islet autoimmunity (*P* < 0.05; Fig. 1*C*). These findings are in accordance with the fact that nondiabetic children with latency in progression to clinically overt

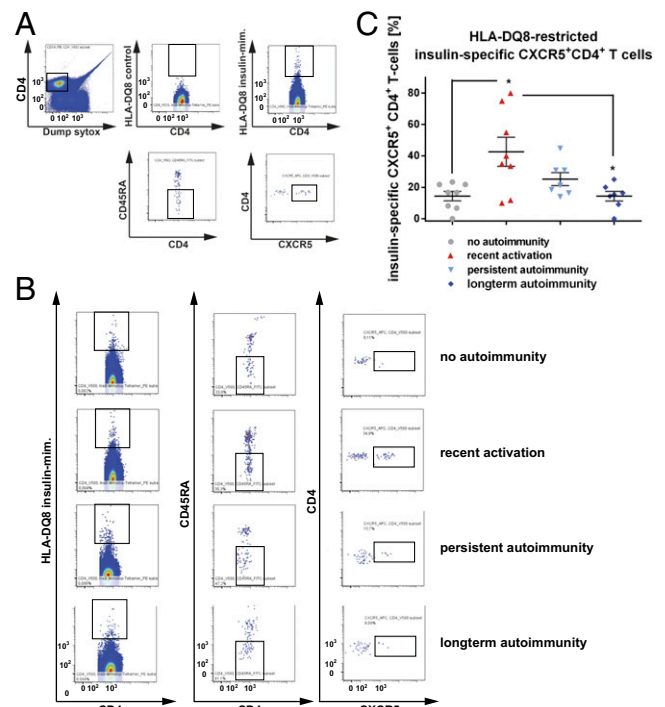


Fig. 1. Ex vivo identification of HLA-DQ8-restricted insulin-specific CXCR5⁺ TFH precursor cells from children with or without ongoing islet autoimmunity. (*A*, Upper Left) Human CD4⁺ T cells were analyzed by flow cytometry, first gating on live, CD19[−], CD14[−], CD8a[−], CD11b[−], CD4⁺, and CD3⁺ cells and then examining the tetramer binding. (*A*, Upper Right) Representative set of FACS plots for the identification of HLA-DQ8-restricted insulin-specific CD4⁺ T cells. mim, mimic. (*A*, Upper Center) Control staining was used to assess the quality and specificity of the tetramer staining using a combination of two control tetramers fused to irrelevant peptides. (*A*, Lower) Insulin-specific CD4⁺ memory TFH precursor cells were then identified by gating on CD45RA[−] and CXCR5⁺. (*B*) FACS plots for insulin-specific memory CXCR5⁺ TFH precursor cells purified from children without autoimmunity (islet autoantibody-negative), with recent onset of autoimmunity (recent activation = multiple autoantibodies for ≤5 y), with persistent autoimmunity (multiple autoantibodies for >5 to ≤10 y), and with long-term autoimmunity (multiple autoantibodies for >10 y without T1D). (*C*) Summary of identified HLA-DQ8-restricted insulin-specific tet⁺CD4⁺CXCR5⁺ TFH precursor cells purified from children without autoimmunity (no autoimmunity, *n* = 8), with recent onset of autoimmunity (recent activation, *n* = 8), with persistent autoimmunity (*n* = 7), and with long-term autoimmunity (*n* = 7). Data represent the mean ± SEM. **P* < 0.05.

disease can lose some of their earliest islet autoantibodies, especially insulin autoantibodies.

Increase of Circulating CCR7^{low}PD1^{high}CXCR5⁺ TFH Precursor Cells During the Onset of Human Islet Autoimmunity. During islet autoimmunity onset, we also identified up-regulated PD1 and ICOS expression levels within circulating CXCR5⁺ T cells, together with increased frequencies of TFH precursors at the polyclonal level (Fig. 2). Specifically, the frequency of CCR7^{low}PD1^{high}CXCR5⁺CD4⁺ T cells (gating example in Fig. 2A, Upper) was significantly greater in children with onset of islet autoimmunity than in children without islet autoimmunity (no autoimmunity vs. recent onset of autoimmunity: 16.8 ± 1.6% vs. 25.8 ± 2.8% of CD4⁺CD45RA⁻ T cells; *P* < 0.01; Fig. 2B), and was significantly reduced in nondiabetic children with long-term autoimmunity (9.0 ± 2.3% of CD4⁺CD45RA⁻ T cells; *P* < 0.01; Fig. 2B) compared with the other two groups of children. The frequency of CXCR5⁺CD4⁺ T cells harboring the highest level of PD1 expression (PD1⁺⁺⁺, gating example in Fig. 2A, Lower) was significantly greater in children with recent onset of islet autoimmunity than in children without autoimmunity (no autoimmunity vs. recent onset of autoimmunity: 0.14 ± 0.03% vs. 0.53 ± 0.11% of CD4⁺ T cells; *P* < 0.01; Fig. 2C and D). The abundance of CXCR5⁺PD1⁺⁺⁺CD4⁺ T cells in nondiabetic children with long-term autoimmunity was 0.16 ± 0.06% of CD4⁺ T cells, which was significantly lower than in children with recent onset of autoimmunity (*P* < 0.05) and similar to the abundance in children without autoimmunity (*P* > 0.05; Fig. 2C and D). CXCR5⁺PD1⁺⁺⁺CD4⁺ T cells also harbored the highest ICOS expression level (ICOS mean fluorescence intensity (MFI) within PD1⁺⁺⁺ subset = 12,600 ± 1,457 vs. ICOS MFI within PD1⁺ subset = 3,919 ± 666; *P* < 0.01; Fig. 2D, Lower Right). These findings therefore support the hypothesis that during the onset of autoimmunity, these circulating CXCR5⁺PD1⁺⁺⁺CD4⁺ T cells with the highest ICOS expression level can boost immune activation and trigger autoantibody production.

To investigate the frequencies of CCR7^{low}PD1^{high} and CXCR5⁺PD1⁺⁺⁺CD4⁺ T cells in children or adolescents near to the diagnosis of clinically overt T1D (newly manifest T1D), we studied T cells from the German new onset diabetes in the young incident cohort study (32, 33). We found the abundance of CCR7^{low}PD1^{high} and CXCR5⁺PD1⁺⁺⁺CD4⁺ T cells in young individuals with newly manifest T1D to be unaltered compared with nondiabetic children with long-term autoimmunity (Fig. 2B and C). Next, we analyzed T helper (Th)-like subtypes within the CXCR5⁺CD4⁺ T-cell population based on the coexpression of CXCR3 and CCR6 (gating example in Fig. 3A). CXCR3⁺CCR6⁻ cells mainly secrete IFN- γ (Th1-like profile) but not Th2 or Th17 cytokines; CXCR3⁻CCR6⁻ cells exclusively secrete Th2 cytokines [interleukin (IL)-4, IL-5, and IL-13]; and CXCR3⁻CCR6⁺ cells secrete Th17 cytokines (IL-17A and IL-22) (17). CXCR5⁺ Th2 cells and CXCR5⁺ Th17 cells were found to induce naive B cells to secrete immunoglobulins via IL-21 but to modulate isotype switching differentially, whereas human CXCR5⁺ Th1 cells were unable to provide B-cell help (17). We found no differences in the frequencies of Th1 cells and Th17 cells within the CXCR5⁺CD4⁺ T-cell compartment between disease groups, including young individuals with new onset T1D (Fig. 3B). However, we observed a significant increase in the TFH-Th2 subset in children with recent onset of islet autoimmunity compared with T cells from children without ongoing autoimmunity or with long-term autoimmunity (no autoimmunity vs. recent onset of autoimmunity vs. long-term autoimmunity: 24.6 ± 2.5% vs. 35.4 ± 3.8%; *P* < 0.05 vs. 23.9 ± 1.4% of CD4⁺CD45RA⁻ T cells; *P* < 0.05; Fig. 3B). In parallel to the increase in the TFH-Th2 subset during onset of islet autoimmunity, we found a significant enhancement in this subset of TFH cells in young individuals with new onset T1D. This increase in TFH-Th2 cells was significant compared with T cells from nondiabetic children with long-term autoimmunity (long-term autoimmunity: 23.9 ± 1.4% vs. with new onset T1D: 50.9 ± 4.4; *P* < 0.05; Fig. 3B).

When we analyzed individual longitudinal samples from nondiabetic children with ongoing islet autoimmunity, we again observed the highest frequencies of Th2-like TFH cells within recent activation of islet autoimmunity (<5 y of islet autoimmunity), whereas frequencies

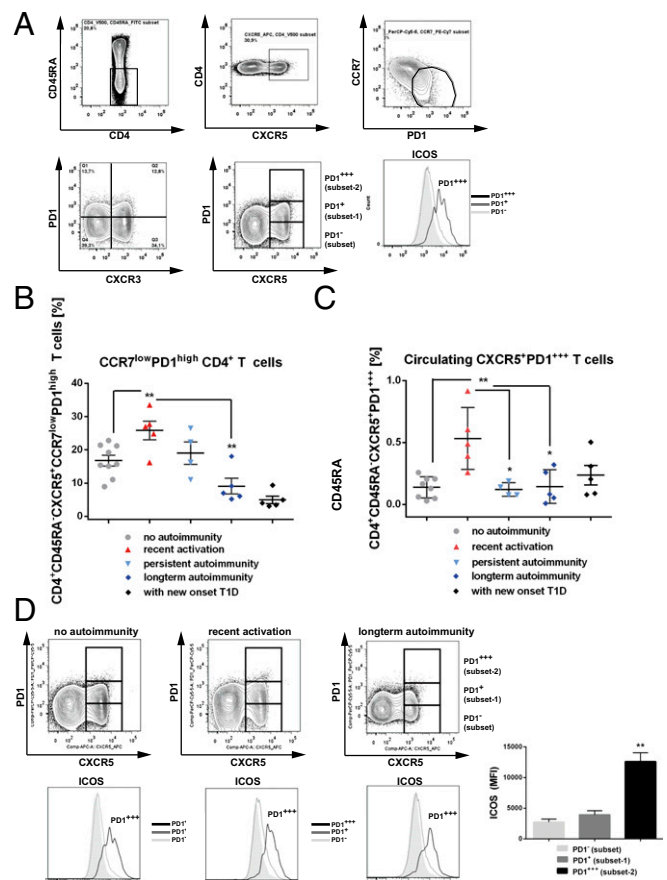


Fig. 2. Identification and characterization of blood-residing CXCR5⁺CCR7^{low}PD1^{high} and CXCR5⁺PD1⁺⁺⁺ cells in CD4⁺ T cells from children with or without ongoing islet autoimmunity or with new onset T1D. (A) Identification of CD4⁺CD45RA⁻CXCR5⁺CCR7^{low}PD1^{high} T cells (Upper) and CXCR5⁺PD1⁻, CXCR5⁺PD1⁺, and CXCR5⁺PD1⁺⁺⁺ T cells (Lower). (Lower Right) Histogram indicates ICOS expression levels in the PD1⁺ subset (light gray line, plot filled), PD1⁺ subset 1 (gray line, plot unfilled), and PD1⁺⁺⁺ subset 2 (black line). (B) Summary graphs for the frequencies of circulating CD4⁺CD45RA⁻CXCR5⁺CCR7^{low}PD1^{high} T cells (no autoimmunity, *n* = 9; recent onset of autoimmunity, *n* = 5; persistent autoimmunity, *n* = 4; long-term autoimmunity, *n* = 5; new onset T1D, *n* = 5). Data represent the mean ± SEM. ***P* < 0.01. (C) Summary graphs for the frequencies of circulating CD4⁺CD45RA⁻CXCR5⁺PD1⁺⁺⁺ T cells (no autoimmunity, *n* = 8; recent onset of autoimmunity, *n* = 5; persistent autoimmunity, *n* = 4; long-term autoimmunity, *n* = 5; new onset T1D, *n* = 5). Data represent the mean ± SEM. **P* < 0.05; ***P* < 0.01. (D, Upper) Identification of CD4⁺CD45RA⁻CXCR5⁺PD1⁺ T cells from children with or without pre-T1D (no autoimmunity, recent activation of autoimmunity, and long-term autoimmunity). (D, Lower) Histograms indicate ICOS expression levels in CXCR5⁺PD1⁻, CXCR5⁺PD1⁺, and CXCR5⁺PD1⁺⁺⁺ subsets. (D, Lower Right) Summary graph shows ICOS MFIs, dependent on the PD1 expression levels. Data represent the mean ± SEM. ***P* < 0.01.

were lower during persistent islet autoimmunity (>5 to <10 y of islet autoimmunity) and further decreased in children with long-term autoimmunity (>10 y of islet autoimmunity; Fig. 3C).

In accordance, the respective T-cell subset presented with an increased abundance of Th2 cytokines, such as IL-4 and IL-13, with no change in IL-10 (Fig. 3D).

Increase of miRNA17~92 Family Abundance in CD4⁺ T Cells from Children with Recent Onset of Islet Autoimmunity.

To define involved signaling pathways, we next examined miRNA92a abundance of CD4⁺ T cells from children with or without islet autoimmunity. Importantly, miRNA92a expression levels were significantly increased in CD4⁺ T cells from children with recent onset of islet autoimmunity (no autoimmunity vs. recent onset of autoimmunity: 7.1 ± 0.6 vs. 11.3 ± 0.7; *P* < 0.05; Fig. 4A). However, its expression was down-regulated

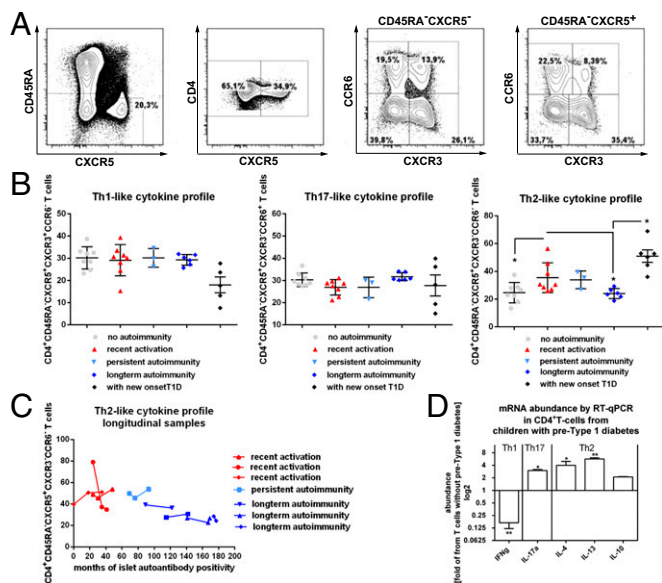


Fig. 3. Identification of circulating CXCR5⁺CD4⁺ T cells and Th1, Th2, or Th17 cytokine expression profiles in CD4⁺ T cells from children with or without ongoing islet autoimmunity or with new onset T1D. (A) Identification of CD4⁺CD45RA⁺CXCR5⁺ T cells and respective CXCR3⁺CCR6⁻ (Th1), CXCR3⁻CCR6⁻ (Th2), or CXCR3⁻CCR6⁺ (Th17) subsets. (B) Summary graphs for the frequencies of circulating CXCR5⁺CD4⁺ T cells with Th1, Th2, or Th17 characteristics (no autoimmunity, $n = 8$; recent onset of autoimmunity, $n = 8$; long-term autoimmunity, $n = 6$; new onset T1D, $n = 5$). Data represent the mean \pm SEM. * $P < 0.05$. (C) Frequencies of the TFH-Th2 subset in longitudinal samples from children with recent activation, persistent islet autoimmunity, or long-term islet autoimmunity. (D) Summary graphs for the mRNA abundance of cytokine expression levels (IFN- γ = Th1; IL-17a = Th17; IL-4, IL-13; and IL-10 = Th2) within respective CD4⁺ T-cell subsets by RT-qPCR from children with islet autoimmunity (pre-T1D). Results are shown in abundance as the fold of T cells from children without ongoing islet autoimmunity (no pre-T1D), with no autoimmunity ($n = 6$), or with ongoing islet autoimmunity ($n = 7$). Data represent the mean \pm SEM. * $P < 0.05$; ** $P < 0.01$.

in nondiabetic children with long-term autoimmunity (6.7 ± 0.7), in accordance with reduced TFH precursor frequencies. These changes in miRNA92a expression levels in relation to duration of islet autoimmunity were not observed within the CD127^{low}CD25^{high} regulatory T (Treg)-cell population (Fig. S14).

The expression profiles of two other members of the miRNA17~92 cluster, miRNA-18a and miRNA-19a, were altered in a similar fashion to the abundance of miRNA92a (Fig. S1 B and C). Of note, we identified a strong correlation between the abundance of miRNA92a and the frequency of CXCR5⁺ TFH precursors. CD4⁺ T cells from children without islet autoimmunity and from nondiabetic children with a slow-progressor phenotype presented with the lowest frequencies of CXCR5⁺ TFH precursors and the lowest abundance of miRNA92a. In contrast, during onset of islet autoimmunity, in states of strong immune activation, more CD4⁺ T cells harbored a CXCR5⁺ TFH precursor phenotype accompanied with increased abundance of miRNA92a ($r^2 = 0.72$; Fig. 4B). In contrast, no correlation was observed between the duration of islet autoimmunity (months of multiple autoantibodies) and the frequencies of CCR7^{low}PD1^{high}CD4⁺ T cells, supporting concepts that point to a relapsing/remitting autoimmunity phenotype (Fig. S24). However, we did find a correlation between miRNA92a abundance in CD4⁺ T cells and levels of insulin autoantibodies (IAA) within disease groups (Fig. S2B).

Reduced Abundance of Predicted Signaling Pathways Regulated by miRNA92a in Human Islet Autoimmunity: PTEN, PHLPP2, and Cytotoxic T-Lymphocyte-Associated Protein 4. We next determined mRNA abundances of predicted signaling pathways regulated by miRNA92a.

As bioinformatics tools, we used miRDB [MirTarget (34)]. Additionally, TargetScan (Human 6.2) was used to predict biological targets for miRNA92a (35). In accordance with the observed enhanced abundance of miRNA92a in CD4⁺ T cells from islet autoantibody-positive children, we found repression of predicted target genes of miRNA92a (Fig. 4C). Specifically, in CD4⁺ T cells from children with ongoing autoimmunity, we observed repression of the phosphatase PTEN, which was outlined as a direct target of the miRNA92a family in mice (29). In our human T-cell setting, we likewise saw reduced abundance of the miRNA92 target PHLPP2 (36), which encodes an Akt phosphatase (37) and functions as a critical negative regulator of the PI3K-Akt signaling pathway as identified in murine studies (Fig. 4C). We also observed reduced mRNA abundance of predicted targets of miRNA92a that negatively regulate T-cell activation, such as cytotoxic T-lymphocyte-associated protein 4 (CTLA4) (Fig. 4C).

miRNA92a Targets the Zinc-Finger Transcription Factor KLF2 During Human Islet Autoimmunity. Next, using TargetScan analyses (35, 38), we identified an evolutionarily conserved binding site for human miRNA92a in the 3' UTR of KLF2. Importantly, abundance of KLF2 was found to be critically repressed in CD4⁺ T cells from children with ongoing islet autoimmunity (Fig. 4C). These findings support a potential role of KLF2 as a target of miRNA92a in human CD4⁺ T cells.

Down-Regulation of PTEN-Foxo1-KLF2 Signaling Network to Promote Human TFH Precursor Cells and Onset of Islet Autoimmunity. To dissect involved signaling pathways relevant for TFH differentiation

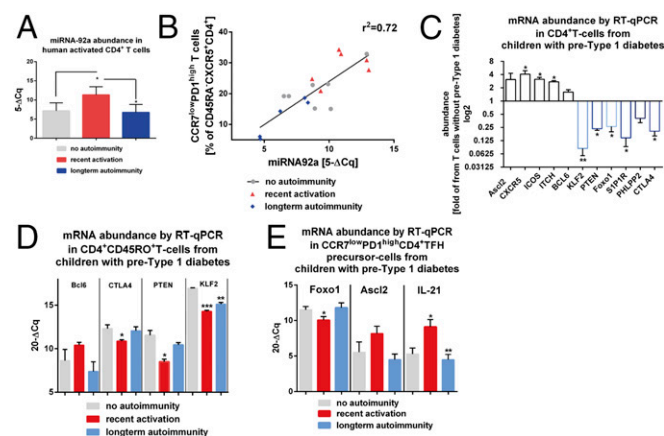


Fig. 4. Enhanced abundance of miRNA92a promotes increased frequencies of circulating CXCR5⁺CD4⁺ T cells during onset of human islet autoimmunity. (A) miRNA92a abundance in human CD4⁺ T cells purified from children with or without pre-T1D (no autoimmunity, $n = 10$; recent onset of autoimmunity, $n = 6$; long-term autoimmunity, $n = 6$) by RT-qPCR analyses. Data represent the mean \pm SEM. * $P < 0.05$. (B) Correlation of CXCR5⁺CCR7^{low}PD1^{high}CD4⁺ T cells with miRNA92a abundance. (C) Abundance of predicted signaling pathways regulated by miRNA92a in human islet autoimmunity. Down-regulation of the PTEN-Foxo1-KLF2 signaling network to promote human TFH precursor cells and onset of islet autoimmunity is shown. mRNA abundance of *Ascl2*, *CXCR5*, *ICOS*, *ITCH*, *Bcl6*, *KLF2*, *PTEN*, *Foxo1*, *PHLPP2*, *CTLA4*, and *S1P1R* from CD4⁺ T cells of individual children with islet autoimmunity (pre-T1D) is shown. Results are shown in abundance as the fold of T cells from children without ongoing islet autoimmunity (no pre-T1D), with no autoimmunity ($n = 6$), and with ongoing islet autoimmunity, $n = 7$. * $P < 0.05$; ** $P < 0.01$. (D) mRNA abundance of genes predictively targeted by miRNA92a in CD4⁺CD45RO⁺ T cells from individual children with or without ongoing pre-T1D as assessed by RT-qPCR analyses (no autoimmunity, $n = 7$; recent onset of autoimmunity, $n = 6$; long-term autoimmunity, $n = 5$). Data represent the mean \pm SEM. * $P < 0.05$; ** $P < 0.01$; *** $P < 0.001$. (E) mRNA abundance of *Foxo1*, *Ascl2*, and *IL-21* in CCR7^{low}PD1^{high}CD4⁺ TFH precursor cells in accordance with the duration of islet autoimmunity (no autoimmunity, $n = 7$; recent onset of autoimmunity, $n = 6$; long-term autoimmunity, $n = 5$). Data represent the mean \pm SEM. * $P < 0.05$; ** $P < 0.01$.

further, we next identified a significantly increased abundance of ICOS in such CD4⁺ T cells from children with ongoing autoimmunity (pre-T1D), whereas expression levels of Foxo1, which represses Bcl6 transcription, as well as PTEN and KLF2, were significantly down-regulated. In accordance with a low abundance of KLF2, we found a high abundance of CXCR5 and low expression of S1PR1 (Fig. 4C) in such CD4⁺ T cells from children with islet autoimmunity compared with children without ongoing islet autoimmunity (no pre-T1D).

When we determined the mRNA abundance of genes involved in T-cell activation and TFH-cell differentiation and function according to the duration of islet autoimmunity, we confirmed that KLF2 abundance was significantly down-regulated, particularly during the onset of islet autoimmunity ($P < 0.001$; Fig. 4D). Moreover, during onset of islet autoimmunity, we likewise observed negative regulators of T-cell activation (e.g., CTLA4, PTEN) to be repressed (Fig. 4D).

Foxo1 expression was significantly reduced in CCR7^{low}PD1^{high} TFH precursors from children with recent onset of islet autoimmunity (Fig. 4E). Additionally, we observed increased levels of Ascl2 and IL-21 in CCR7^{low}PD1^{high} TFH precursors from children with recent onset of islet autoimmunity in contrast to cells from nondiabetic children with long-term autoimmunity (Fig. 4E).

Induction of Human TFH Precursor Cells by miRNA92a in Vitro. We next investigated whether activation of the miRNA92a pathway can induce human TFH precursor cells in vitro. Chitosan-coated poly(D,L-lactide-coglycolide) (PLGA) nanoparticles (39) were used to deliver mature miRNA92a mimics with a triple-RNA strand design (40). The uptake, intracellular localization of labeled nanoparticles, and delivery of fluorescently labeled control miRNAs were verified by confocal microscopy (Fig. S3). Next, we performed in vitro TFH precursor induction experiments (16, 21) with human naive CD4⁺ T cells and autologous memory B cells, sorted as CD20⁺CD27⁺, in the presence or absence of a miRNA92a mimic (Fig. S44). Importantly, the miRNA92a mimic significantly increased the frequencies of CXCR5⁺CD4⁺ TFH precursors in vitro (vehicle + negative control mimic vs. vehicle + miRNA92a mimic: 37.6 ± 1.8 vs. 54.2 ± 3.1 CD45RA⁺CXCR5⁺CD4⁺ T cells; $P < 0.05$; Fig. S4 B and C).

The miRNA92a mimic also significantly enhanced the frequency of CCR7^{low}PD1^{high}CD4⁺ TFH precursor cells using T cells from healthy individuals (vehicle + negative control mimic vs. vehicle + miRNA92a mimic: 1.8 ± 0.2 vs. 4.6 ± 0.8 CCR7^{low}PD1^{high}CD4⁺ T cells; $P < 0.05$; Fig. 5A) and from T1D patients (Fig. 5B). An induction of CCR7^{low}PD1^{high}CD4⁺ TFH precursor cells by miRNA92a mimic was observed already after 3 d of incubation (Fig. S5).

mRNA Abundance of Predicted Signaling Pathways Controlled by miRNA92a During miRNA92a-Mediated TFH Precursor Induction in Vitro. We next studied whether activation of the miRNA92a pathway in vitro can modulate mRNA abundance of signaling pathways predictively targeted by miRNA92a. Upon miRNA92a mimic application, we observed significantly enhanced abundance of ITCH (miRNA92a-mimic: ITCH: 2.6 ± 0.3 , fold of T cells treated with control mimic; $P < 0.05$; Fig. 5C). Bcl6 expression was moderately but significantly up-regulated in line with findings indicating that upon in vitro differentiation, such TFH precursors present with intermediate levels of Bcl6 (41), in contrast to bona fide germinal center TFH cells that harbor high Bcl6 abundance (41). Moreover, expression levels of Foxo1 (miRNA92a mimic: Foxo1: 0.18 ± 0.04 , fold of T cells treated with control mimic; $P < 0.01$) as well as PTEN (miRNA92a mimic: PTEN: 0.27 ± 0.01 , fold of T cells treated with control mimic; $P < 0.05$) were significantly reduced compared with T cells that had been incubated with control mimics (Fig. 5C). In addition, KLF2 mRNA abundance of CD4⁺ T cells from miRNA92a-mediated TFH induction assays was significantly down-regulated compared with T cells treated with control mimics (miRNA92a mimic: KLF2: 0.07 ± 0.02 , fold of T cells treated with control mimic; $P < 0.05$; Fig. 5C). These data further support the concept that KLF2 functions as a target of miRNA92a.

miRNA92a-Mediated Human in Vitro TFH Precursor Induction Is Regulated by PTEN-PI3K Signaling. TFH precursor induction by miRNA92a was further enhanced upon stimulation with phorbol 12-myristate 13-acetate (PMA)/ionomycin in terms of CCR7^{low}PD1^{high}CD4⁺ T cells (Fig. 5D). To analyze the involvement of the PTEN-PI3K signaling network in the regulation of TFH precursor induction, we performed such assays with a miRNA92a mimic in the presence or absence of a PI3K or PTEN inhibitor, respectively. Coapplication of a PI3K inhibitor to the miRNA92a mimic completely abolished TFH precursor induction (CCR7^{low}PD1^{high} T cells: miRNA92a mimic: 13.3 ± 0.3 vs. miRNA92a mimic + PI3K inhibitor: 1.2 ± 0.6 ; $P < 0.01$). In accordance, miRNA92a mimic treatment in the presence of a PTEN inhibitor resulted in a significant boost of TFH precursor cell induction (CCR7^{low}PD1^{high} T cells: miRNA92a mimic: 12.6 ± 0.7 v. miRNA92a mimic + PTEN-inhibitor: 20.6 ± 0.6 ; $P < 0.01$; Fig. 5D).

miRNA92a Targets KLF2 to Promote Human TFH Precursor Induction in Vitro. To underline KLF2 as a target of miRNA92a, we used a specific miRNA92a KLF2 target site blocker (TSB). miRNA TSBs are antisense oligonucleotides that bind to the miRNA target site of an mRNA, thereby preventing miRNAs from gaining access to that site. Application of a miRNA92a mimic in the presence of a control TSB resulted in a significant increase of CCR7^{low}PD1^{high}CD4⁺ TFH precursor cells (vehicle + control TSB: 0.4 ± 0.07 vs. vehicle +

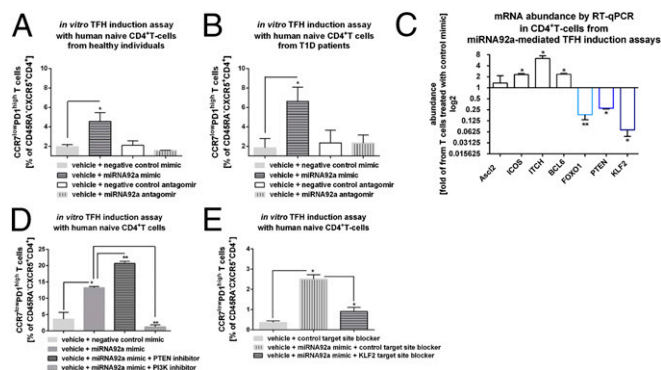


Fig. 5. miRNA92a regulates human TFH precursor induction in vitro. (A) TFH precursor induction using human naive CD4⁺ T cells from healthy individuals in the presence of memory B cells with or without a miRNA92a mimic, a miRNA92a antagomir, or respective negative control mimics or antagomirs. Summary graphs are shown for frequencies of CCR7^{low}PD1^{high} cells presented as percentages of CXCR5⁺CD45RA⁺CD4⁺ T cells. Data represent the mean \pm SEM. $*P < 0.05$. (B) TFH precursor induction as outlined in A using human naive CD4⁺ T cells from T1D individuals. Summary graphs are shown for frequencies of CCR7^{low}PD1^{high} cells presented as percentages of CXCR5⁺CD45RA⁺CD4⁺ T cells. Data represent the mean \pm SEM. $*P < 0.05$. (C) mRNA abundance of predicted signaling pathways controlled by miRNA92a from CD4⁺ T cells of TFH precursor induction assays in the presence of miRNA92a mimic quantified by RT-qPCR analyses. Results are shown in abundance as the fold of T cells treated with negative miRNA mimic controls. Data represent the mean \pm SEM from duplicate wells of four independent experiments. $*P < 0.05$; $**P < 0.01$. (D) TFH induction using human naive CD4⁺ T cells in the presence of memory B cells with or without a miRNA92a mimic or negative miRNA mimic controls. In such assays, PMA (50 ng/mL) and ionomycin (1 μ g/mL) were added for the last 12 h of the experiments, and frequencies of CCR7^{low}PD1^{high}CD4⁺ T cells were analyzed. Experiments were performed in the presence or absence of a PTEN or PI3K inhibitor, respectively. Summary graphs for frequencies of CCR7^{low}PD1^{high} TFH precursor cells (percentage of CD45RA⁺CXCR5⁺CD4⁺ T cells) ($n = 4$). Data represent the mean \pm SEM from duplicate wells of four independent experiments. $*P < 0.05$; $**P < 0.01$. (E) TFH precursor induction using human naive CD4⁺ T cells in the presence of memory B cells with or without a miRNA92a mimic, a control TSB, a miRNA92a KLF2 TSB, or a combination. Summary graphs are shown for frequencies of CCR7^{low}PD1^{high} cells presented as percentages of CXCR5⁺CD45RA⁺CD4⁺ T cells ($n = 4$). Data represent the mean \pm SEM from duplicate wells of four independent experiments. $*P < 0.05$.

miRNA92a mimic + control TSB: 2.5 ± 0.2 ; $P < 0.05$; Fig. 5E) in vitro. In contrast, coapplication of a specific KLF2 TSB significantly reduced the miRNA92a-mediated induction of TFH precursors (vehicle + miRNA92a mimic + control TSB: 2.5 ± 0.2 vs. vehicle + miRNA92a mimic + KLF2 TSB: 0.9 ± 0.2 ; $P < 0.05$; Fig. 5E), further indicating that KLF2 is a target of miRNA92a.

Blockade of Human TFH Precursor Cell Induction by a miRNA92a Antagomir in Vitro. To assess a potential relevance of blocking miRNA92a activity to limit islet autoimmunity, we first performed in vitro TFH induction assays in the presence of a miRNA92a antagomir. Importantly, application of a miRNA92a antagomir completely blocked the induction of human CCR7^{low}PD1^{high}CD4⁺ TFH precursor cells (vehicle + negative control antagomir: 2.1 ± 0.4 vs. vehicle + miRNA92a antagomir: 1.6 ± 0.05 ; Fig. 5A and B) in vitro. The inhibition of human TFH differentiation was seen with CD4⁺ T cells from healthy donors (Fig. 5A), as well as from individuals with T1D (Fig. 5B). Accordingly, in human Treg-cell induction assays using established protocols with naive CD4⁺ T cells and limited T-cell receptor stimulation (31), a miRNA92a antagomir resulted in an increase in induced human CD127^{low}CD25^{high}Foxp3^{high} Treg cells (+ control antagomir: 35.4 ± 0.8 vs. + miRNA92a antagomir: 41.8 ± 0.5 ; $P < 0.01$; Fig. S6).

Inhibition of Murine TFH Precursors by a miRNA92a Antagomir in NOD Mice in Vivo. As a critical model of human autoimmune T1D, NOD mice share many similarities with human T1D, including the presence of specific autoantibodies and autoreactive T cells. In addition, in humans and mice, the T-cell response to insulin is dominated by a major histocompatibility complex II (MHCII) (IA^{g7})-restricted segment of the insulin B chain comprising residues 9–23. In contrast to CD4⁺ T cells from nonautoimmune-prone BALB/c and NOD mice without insulin-specific autoantibodies, CD4⁺ T cells from NOD mice with IAA⁺ autoimmunity presented with significantly increased expression levels of miRNA92a, especially in pancreatic lymph nodes (Fig. 6A and B). Next, to test a possible therapeutic value of blocking miRNA92a activity in halting immune activation in vivo, we used NOD mice with IAA⁺ autoimmunity and a custom-designed locked nucleic acid (LNA) miRNA92a antagomir (Exiqon). Of note, short-term in vivo application of a miRNA92a antagomir (10 mg/kg i.p. on day 0, day 2, and day 6) to NOD mice significantly lowered TFH precursors in peripheral blood compared both with baseline levels assessed before beginning of the treatment and with mice treated with control antagomirs [baseline before miRNA92a antagomir application: CCR7^{low}PD1^{high}CD4⁺ T cells (percentage of CXCR5⁺CD4⁺ T cells): 20.9 ± 1.9 vs. after miRNA92a antagomir application: 10.6 ± 1.0 ; $P < 0.05$; Fig. 6C]. Application of miRNA92a antagomir also resulted in significantly reduced frequencies of CCR7^{low}PD1^{high} TFH precursors in pancreatic lymph nodes [CCR7^{low}PD1^{high}CD4⁺ T cells (percentage of CXCR5⁺CD4⁺ T cells): control antagomir: 48.4 ± 5.9 vs. miRNA92a antagomir: 30.4 ± 3.6 ; $P < 0.05$; Fig. 6D and E]. More importantly, the miRNA92a antagomir application reduced immune activation directly in the pancreas, because frequencies of CD4⁺CD44^{high} T cells were significantly lowered in such treated mice compared with control animals [CD4⁺CD44^{high} T cells (MFI) control antagomir: $2,877 \pm 316$ vs. miRNA92a antagomir: $1,976 \pm 224$; $P < 0.05$; Fig. 6F and G]. Additionally, upon treatment with a miRNA92a antagomir, frequencies of CD4⁺CD25⁺Foxp3⁺ Treg cells were increased in lymph nodes (Fig. 6H and I).

Furthermore, when we treated NOD mice for a longer period of 14 d (with injections four times per week at 5 mg/kg), the miRNA92a antagomir significantly reduced the frequencies of insulin-specific CD4⁺CXCR5⁺ TFH cells in pancreatic lymph nodes (Fig. 6J and K). Additionally, the longer treatment period resulted in a more pronounced reduction of CD4⁺CD44^{high} T cells (Fig. 6L). In contrast, the CD44^{high} T cells within the CD4⁺CD25^{high}Foxp3⁺ Treg-cell population was affected to a lesser extent (Fig. S7). Consistent with a reduced autoimmune activation upon miRNA92a antagomir application, we observed lower levels of proliferating Ki67^{high}CD4⁺ T cells in these NOD mice (Fig. 6M).

Although IAA levels had increased from baseline in control animals, IAA levels were found to be decreased in mice that were given the miRNA92a antagomir (Fig. S8). Accordingly, histopathological evaluation of pancreata from these NOD mice revealed that miRNA92a antagomir application had reduced pancreatic infiltration, resulting in more morphologically intact β cells (Fig. S9A and B). These results were confirmed using analyses by immunofluorescence in pancreatic cryosections of such NOD mice (Fig. S10A–C). NOD pancreata of mice that had received a miRNA92a antagomir showed distinctly reduced CD4⁺ T-cell infiltration accompanied by an enhanced abundance of local CD4⁺Foxp3⁺ Treg cells (Fig. S10A–C).

Next, to assess a potential human in vivo relevance of miRNA92a antagomir application, we investigated human HLA-DQ8-restricted insulin-specific TFH cells in humanized NOD Scid IL2 receptor gamma chain knockout (NSG) human leucocyte antigen (HLA)-DQ8 Tg mice in accordance with previously established procedures (31). Specifically, we focused on human pancreas-infiltrating CD4⁺ T cells upon treatment with a miRNA92a antagomir (1 wk of treatment, with injections three times per week at 10 mg/kg) or a control antagomir. In contrast to humanized mice that were given the control antagomir, mice that received the miRNA92a antagomir showed distinctly reduced frequencies of HLA-DQ8-restricted insulin-specific CD4⁺ T cells in pancreata of humanized NSG HLA-DQ8 mice (Fig. 6N and O). More importantly, miRNA92a antagomir application significantly lowered the frequencies of insulin-specific CD4⁺CXCR5⁺PD1⁺ TFH cells in pancreata of humanized mice (Fig. 6N and P). Overall, these findings further support a role of blocking miRNA92a activity in limiting autoimmune activation.

Discussion

Aberrant immune activation mediated by effector T-cell populations is pivotal in promoting the onset of autoimmunity, as in autoimmune T1D (2, 42). In children with ongoing islet autoimmunity, the time to progression to clinically overt T1D is highly plastic, ranging from a few months to more than two decades (2, 5), which highlights the critical contribution of differences in immune activation and pathways of regulation in disease progression. Therefore, studies of T cells from nondiabetic children according to the duration of islet autoimmunity can provide important insights into the regulation of aberrant immune activation, as well as into the mechanisms involved in triggering the onset of islet autoimmunity.

Currently, the role of TFH cells in promoting the onset of human islet autoimmunity remains unclear, especially concerning their potential function in accelerating progression to clinically overt T1D. Furthermore, our understanding of relevant signaling pathways regulating human TFH induction is limited. This knowledge gap resulted from the fact that previous studies had focused on analyses of TFH-cell characteristics in patients with clinically overt T1D (43, 44), a situation where the main target of the autoimmune attack, the insulin-producing β cells, have been destroyed already. Until now, the role of human TFH precursors during the onset of autoimmunity before clinically manifest T1D and relevant signaling pathways involved in their induction has remained elusive.

To tame aberrant TFH-cell responses specifically (45), the dissection of molecular mechanisms that regulate TFH differentiation and function during the onset of autoimmunity is required. Here, we provide direct evidence that during the onset of human islet autoimmunity, the insulin-specific target T-cell population is enriched with a CXCR5⁺CD4⁺ TFH precursor phenotype.

Mechanistically, we show that miRNA92a is critically involved in the induction of human TFH precursors and links the frequency of CXCR5⁺CD4⁺ T cells and the abundance of miRNA92a with the level of autoimmune activation. Specifically, our findings in CD4⁺ T cells from nondiabetic children with persistent and long-term autoimmunity demonstrate that a reduced frequency of peripheral CXCR5⁺ TFH precursors can be indicative of reduced immune activation in accordance with a slow progression to clinically overt T1D. In line with these results in human CD4⁺ T cells from nondiabetic children with ongoing islet autoimmunity, we identify miRNA92a to be significantly up-regulated in CD4⁺ T cells

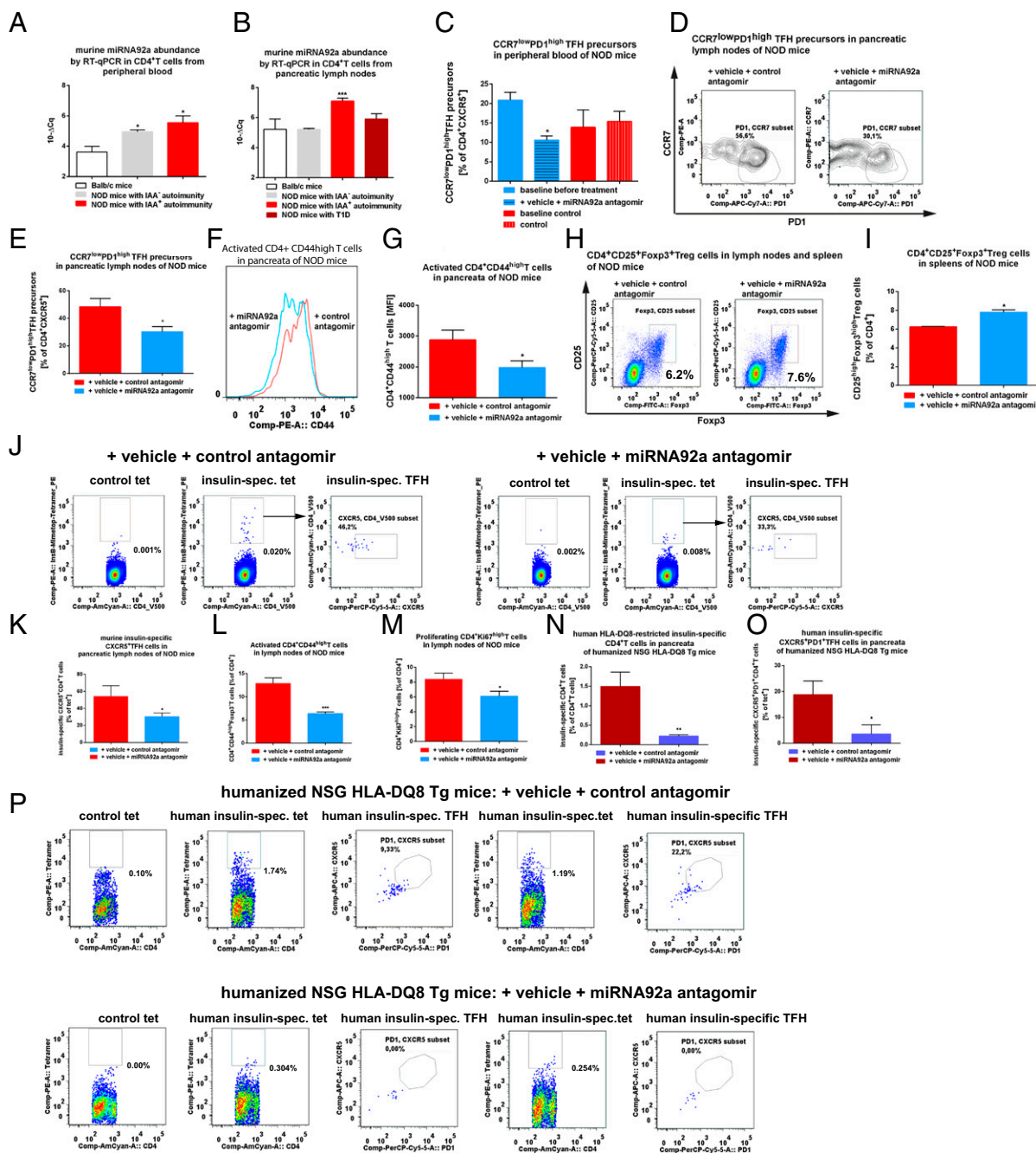


Fig. 6. In vivo miRNA92a antagonist application reduces immune activation in NOD and humanized mice. The miRNA92a abundance in murine CD4⁺ T cells from BALB/c mice and NOD mice with or without ongoing islet autoimmunity, as well as with T1D in peripheral blood (A) or in pancreatic lymph nodes (B), as assessed by RT-qPCR analyses, is shown. Data represent the mean \pm SEM. * P < 0.05; *** P < 0.001. (C) Summary graphs for CCR7^{low}PD1^{high} TFH cells in peripheral blood of NOD mice before and after treatment with either control antagonists or a specific miRNA92a antagonist. Data represent the mean \pm SEM from two independent experiments (n = 4). * P < 0.05. (D) FACS plots for the identification of CCR7^{low}PD1^{high} TFH precursors in pancreatic lymph nodes of NOD mice after treatment with control antagonist or miRNA92a antagonist. (E) Summary graphs for CCR7^{low}PD1^{high} TFH precursors in pancreatic lymph nodes of NOD mice given a control antagonist or a specific miRNA92a antagonist. Data represent the mean \pm SEM from two independent experiments (n = 4). * P < 0.05. (F) FACS histograms for the identification of CD4⁺CD44^{high} T cells of pancreas-infiltrating T cells of NOD mice treated with either control antagonists or a miRNA92a antagonist. (G) Summary graphs for CD4⁺CD44^{high} T cells of pancreas-infiltrating T cells of NOD mice as indicated in F. Data represent the mean \pm SEM from two independent experiments (n = 4). * P < 0.05. (H) Identification of CD4⁺CD25⁺Foxp3⁺ T cells of NOD mice given a control antagonist or a miRNA92a antagonist. (I) Summary graphs for CD4⁺CD25⁺Foxp3⁺ T cells of NOD mice as indicated in H. Data represent the mean \pm SEM from two independent experiments (n = 4). * P < 0.05. (J) Identification of IA^{g7}-restricted, insulin-specific CD4⁺ T cells and CXCR5⁺ TFH cells in pancreatic lymph nodes of NOD mice given a control antagonist or miRNA92a antagonist. (K) Frequencies of insulin-specific TFH cells as in J (mean \pm SEM from two independent experiments; n = 4). * P < 0.05. (L) Frequencies of activated CD44^{high} T cells upon treatment with a control or a miRNA92a antagonist. Data represent the mean \pm SEM from two independent experiments (n = 4). ** P < 0.01. (M) Proliferating CD4⁺Ki67^{high} T cells upon treatment with a control or a miRNA92a antagonist. Data represent the mean \pm SEM from two independent experiments (n = 4). * P < 0.05. (N) Frequencies of human insulin-specific CD4⁺ T cells in pancreata of humanized mice as in P (mean \pm SEM; n = 5). ** P < 0.01. (O) Frequencies of human insulin-specific CXCR5⁺PD1⁺CD4⁺ T cells in pancreata of humanized mice as in P (mean \pm SEM; n = 5). * P < 0.05. (P) Identification of human HLA-DQ8-restricted, insulin-specific CD4⁺ T cells and CXCR5⁺PD1⁺ TFH cells in pancreata of humanized NSG HLA-DQ8 Tg mice given a control antagonist or a miRNA92a antagonist. APC, allophycocyanin; PerCP, peridinin chlorophyll protein; spec., specific.

purified from pancreatic lymph nodes of NOD mice upon initiation of islet autoimmunity.

These findings highlight the importance to study miRNAs in the context of human autoimmunity, particularly in disease-relevant lymphocyte populations, to advance our understanding of gene regulation in autoimmunity, as well as for the identification of novel biomarkers indicative of pathogenic processes (46). Moreover, such miRNAs could function as future drug targets, because sequence-specific miRNA inhibitors were proven to work in patients (47). The delivery of such molecules to immune cells has been challenging; however, there are encouraging results for local or systemic application of miRNA inhibitors in autoimmunity and allergy (48, 49). Of note, *in vivo* application of a miRNA92a antagomir to NOD mice with ongoing islet autoimmunity reduced TFH precursors in peripheral blood and pancreatic lymph nodes. More importantly, application of a miRNA92a antagomir significantly lowered immune activation directly in the pancreas.

The identification of specific miRNA targets and defining their functional relevance remain challenging, because a single miRNA can directly regulate hundreds of genes and the amplitude of control is generally rather modest (50). Here, we provide evidence for repression of PTEN and PHLPP2, thereby permitting a boost of PI3K-Akt kinase signaling to trigger immune activation and TFH differentiation (36). This finding is consistent with an important role of PI3K in the germinal center response (51, 52). Down-regulation of PHLPP2 was shown to be critical for signaling via ICOS-PI3K, which drives the migration of T cells into B-cell follicles (53), a critical part of the TFH differentiation program (51).

We likewise found CTLA4 abundance to be significantly down-regulated during the onset of islet autoimmunity. Accordingly, T cells in CTLA4-deficient mice differentiate spontaneously into TFH cells *in vivo*, supporting a model in which CTLA4 mediates regulation of TFH-cell differentiation by graded control of CD28 engagement (54).

Moreover, during the onset of islet autoimmunity, Foxo1 abundance was significantly reduced. In accordance, murine data showed that Foxo1 negatively regulates Bcl6 and that its enforced nuclear localization prevents TFH-cell differentiation (12). In line with the fact that ICOS coreceptor signaling inactivates Foxo1 (12), we saw here significantly enhanced abundance of ICOS in CD4⁺ T cells from children with recent onset of islet autoimmunity.

In mice, KLF2 functions as a key modulator of homing receptors involved in lymphocyte migration (55, 56). KLF2 serves to restrain murine TFH-cell generation (15), and induced KLF2 deficiency in activated CD4⁺ T cells promotes TFH-cell generation and B-cell priming. Additionally, KLF2 promotes expression of the trafficking receptor S1PR1, and S1PR1 down-regulation was essential for efficient TFH-cell production (15).

Importantly, based on the observed significant down-regulation of KLF2 in CD4⁺ T cells from children with ongoing islet autoimmunity, we demonstrate that reduced KLF2 abundance can promote human TFH precursor induction during the onset of islet autoimmunity. In accordance with a low abundance of KLF2, we found a high abundance of CXCR5 and low expression of S1PR1 in T cells from children with ongoing islet autoimmunity. In addition, ICOS was highlighted to maintain the TFH phenotype by repressing KLF2 (57).

Of note, we highlight KLF2 as a potential target of miRNA92a in the regulation of islet autoimmunity. In accordance, during TFH induction assays, a miRNA92a mimic promoted a significant down-regulation of KLF2 mRNA abundance in CD4⁺ T cells. Moreover, miRNA92a-mediated induction of TFH precursor cells was significantly blunted in the presence of a specific miRNA92a-KLF2 TSB.

In addition, in T cells from such miRNA92a-mediated TFH precursor induction assays, we observed an enhanced abundance of the E3 ubiquitin ligase ITC1, which was found to be essential for the differentiation of TFH cells (13), and a reduced expression of Foxo1. Importantly, KLF2 functions as a direct downstream transcriptional target of Foxo1 (58, 59). Therefore, the reduced abundance of KLF2 could be aligned with the fact that during onset of islet autoimmunity, we observed Foxo1 abundance to be

significantly down-regulated, whereas ICOS and miRNA92a abundance was found to be up-regulated.

With respect to a potential future targeting of TFH cells within the autoimmune disease process, we found CXCR5⁺CD4⁺ TFH cells at higher frequencies in at-risk children with islet autoantibody conversions within the past 5 y (recent onset of islet autoimmunity). Those children with multiple autoantibodies defined as having persistent (5–10 y) and long-term (>10 y) autoimmunity usually harbored frequencies similar to autoantibody-negative children. These observations are in line with concepts that children with a slow-progressor phenotype might have regulated the disease process or might at least be in a transient state of immune regulation. Furthermore, these findings also support the hypothesis that autoimmune T1D might have a relapsing/remitting disease phenotype. The fact that we observed frequencies of TFH cells to be particularly increased in early stages of the disease process is in accordance with a critical role of TFH cells in promoting B-cell activation and autoantibody production, and would therefore suggest that targeting of this population may be important during the very early disease stages. Consistent with this concept, in a limited set of longitudinal samples of children with various durations of islet autoimmunity, we again found the highest frequencies of TFH cells, and particularly Th2-like TFH cells, in early stages of islet autoimmunity. In the future, a more detailed analysis of longitudinal samples from islet autoantibody-positive children will help to clarify further the role of TFH cells in promoting progression to clinical disease.

In conclusion, the findings of this work provide evidence that during the onset of human islet autoimmunity, the insulin-specific target T-cell population is enriched in CXCR5⁺ TFH precursor cells. Moreover, we present a model in which, during the onset of human islet autoimmunity, miRNA92a-mediated TFH precursor cell induction is regulated by PTEN-PI3K signaling involving up-regulation of ICOS and down-regulation of PTEN, PHLPP2, and Foxo1. In addition, we show that KLF2 can function as a target of miRNA92a in promoting induction of TFH precursors. Importantly, miRNA92a antagomir application blocks TFH induction *in vitro* and significantly reduces islet autoimmunity in NOD mice with ongoing islet autoimmunity *in vivo*. Of note, in humanized NSG HLA-DQ8 Tg mice, administration of a miRNA92a antagomir significantly lowered frequencies of pancreas-residing, insulin-specific TFH cells. We therefore propose that manipulating miRNA92a or the PTEN-PI3K-KLF2 signaling network may facilitate the development of innovative regimens for the blockade of human T1D islet autoimmunity.

Materials and Methods

Human Subjects and Blood Samples. Blood samples were collected from first-degree relatives of patients with T1D (children or adults). All subjects have already been enrolled into longitudinal studies with prospective follow-up from birth (60–62). Written informed consent was received from participants before inclusion in the Munich Bioresource Project (approval no. 5049/11; Technische Universität München). The age of islet autoantibody seroconversion (onset of islet autoimmunity) was documented. Blood samples from children with newly manifest T1D were collected from the German new onset diabetes in the young incident cohort study (approval no. 08043; Ethikkommission der Bayerischen Landesärztekammer) (32, 33). Blood samples consisted of venous blood collected in sodium heparin tubes, and blood volumes collected were based on European Union guidelines, with a maximal blood volume of 2.4 mL/kg body weight. Subjects have been stratified based on the presence or absence of multiple islet autoantibodies (with or without pre-T1D) and based on the duration of islet autoantibody positivity as follows: no autoimmunity: first-degree relatives of patients with T1D who are islet autoantibody-negative ($n = 11$, median age = 8 y, interquartile range (IQR) = 6–15 y, six males and five females); recent onset of islet autoimmunity: subjects with multiple islet autoantibodies for less than 5 y ($n = 8$, median age = 7 y, IQR = 4–14 y, six males and two females); persistent autoimmunity: subjects with multiple islet autoantibodies for more than 5 but less than 10 y ($n = 9$, median age = 12 y, IQR = 9.25–17.5 y, seven males and two females); and long-term autoimmunity: subjects with multiple islet autoantibodies for more than a decade who had not yet developed T1D ($n = 7$, median age = 15 y, IQR = 14–25 y, three males and four females). For the blood samples, the investigators were not blinded to the presence and duration of assessed islet autoimmunity of children as described above during analyses of *ex vivo* T-cell phenotypes.

Human Cell Isolation. Peripheral blood mononuclear cells (PBMCs) were isolated by density centrifugation over Ficoll-Paque PLUS (GE Healthcare). For TFH-cell induction assays, human CD4⁺ T cells were isolated from fresh PBMCs via positive magnetic bead enrichment (CD4 microbeads; Miltenyi Biotec) and B cells were isolated from the flow-through using CD19 microbeads (Miltenyi Biotec) following the manufacturer's protocol. For tetramer stainings, human CD4⁺ T cells were isolated by negative enrichment from fresh PBMCs (EasySep Human CD4⁺ T-Cell Isolation Kit; Stemcell).

Cell Staining, Flow Cytometry, and Cell Sorting. A description of monoclonal antibodies used for FACS stainings can be found in *SI Materials and Methods*.

Cells were acquired on a BD FACS Aria III cell sorting system flow cytometer using FACS Diva software (both from BD Biosciences) with optimal compensation and gain settings determined for each experiment based on unstained and single-color-stained samples. Doublets were excluded based on side scatter area (SSC-A) vs. side scatter width (SSC-W) plots. Live-cell populations were gated on the basis of cell side and forward scatter, as well as the exclusion of cells positive for Sytox Blue (Life Technologies). At least 50,000 gated events were acquired for each sample and analyzed using FlowJo Software Version 7.6.1 (TreeStar, Inc.).

Insulin-Specific HLA-DQ8-Restricted Tetramer Stainings. Fluorescent HLA-DQ8 tetramers based on insulin B-chain 10–23 mimetopes were developed in collaboration with the NIH tetramer facility. Specifically, a 14E-22E tetramer and a 14E-21G-22E-HLA-DQ8-phycoerythrin (PE)-labeled tetramer were combined in stainings. Untouched CD4⁺ T cells (as described above) were incubated with tetramers for 1 h at 37 °C in humidified 10% (vol/vol) CO₂ with gentle agitation every 20 min. Surface marker staining was performed directly afterward for 20 min at 4 °C. A set of exclusion markers [CD8, CD11b, CD19, CD14, and a dead cell exclusion marker (Sytox)] was used to increase specificity of the staining. As negative controls, we used a combination of two HLA-DQ8 tetramers fused to irrelevant peptides (PVSKMRMATPLLMQA and QDLELWNLNGLQADL) and labeled with PE. Virtually no CD4⁺ T cells were detected with the control tetramers.

Insulin-Specific IA⁹⁷-Restricted Tetramer Stainings. Fluorescent IA⁹⁷-tetramers based on insulin B-chain 10–23 mimetopes were received from the NIH tetramer core facility. Specifically a 22E tetramer and a 21G-22E-IA⁹⁷-PE-labeled tetramer were combined in stainings. A set of exclusion markers [CD8a, CD11b, CD11c, CD14, B220, F4/80, and a dead cell exclusion marker (Sytox)] was used to increase specificity of the staining. As negative controls, we used one IA⁹⁷ tetramer fused to an irrelevant peptide (AMKRHGLDNYRGYSL) and labeled with PE (31).

Isolation and Processing of Small RNAs/miRNAs. Small RNAs/miRNAs were isolated using the miRNeasy Micro Kit (Qiagen). RNA concentration and purity were determined using a NanoDrop (Epoch; Biotec) and/or RNA Nano Chip and Agilent 2100 Bioanalyzer (Agilent Technologies). For cDNA synthesis, the Universal cDNA Synthesis Kit II (Exiqon) was used according to the instructions. Quantitative PCR (qPCR) was performed using ExiLENT SYBR Green PCR Master Mix (Exiqon) in combination with miRCURY LNA primers for miRNA92a-3p, miRNA19a-3p, and miRNA18a-5p. For normalization, miRCURY LNA primers for the housekeeper 5s rRNA were used (Exiqon). The reaction was run on a CFX96 real-time system (BioRad).

Isolation and Processing of mRNAs. mRNAs were isolated using the miRNeasy Micro Kit (Qiagen). cDNA synthesis was performed with either the SMARTer Ultra Low Input RNA Kit for Sequencing Version 3 (Takara Clontech) when cell material was limited or the iScript cDNA Synthesis Kit (BioRad) when cell material was not limited. For the SMARTer kit, cycle numbers for amplification were adjusted for the lower RNA content of T cells. For qPCR, SsoFast Evagreen Supermix (BioRad) was used (primer information can be found in *SI Materials and Methods*). For normalization, the primers for the housekeeping genes 18s (Quantitect Primer Assay; Qiagen) and Histone (forward: ACT GGC TAC AAA AGC CGC TC, reverse: ACT TGC CTC CTG CAA AGC AC) were used. The reactions were run on a CFX96 Real-Time System.

In Vitro TFH Precursor Cell Induction Assay. Naive T cells were sort-purified as CD4⁺, CD3⁺, CD45RA⁺, CD45RO⁻, and CXCR5⁺, and memory B cells were sorted as CD20⁺ and CD27⁺. Both cell types were cocultured at a ratio of 1:1. The cells were stimulated with 5 µg/mL anti-CD3 (Okt3) and anti-CD28 (CD28.2), both from Biologend; in some experiments, IL-6 and IL-21, both at 50 ng/mL (Peprotech), were added in accordance with previously established procedures (16, 21). On day 5, CD4⁺ T cells were analyzed by flow cytometry on a BD FACS Aria III for expression of CXCR5, PSGL1, PD-1, and CCR7. In some experiments, PMA/ionomycin stimulation (PMA at 50 ng/mL and ionomycin at 1 µg/mL) was added to the assay 12 h before analysis. TFH induction assays have likewise been performed in presence of a PI3K inhibitor (LY294002 at 10 µM) or a PTEN inhibitor (SF1670 at 325 nM), respectively.

Application of miRNA92a Mimic, Antagomir, and KLF2 TSB to Human CD4⁺ T Cells. PLGA-coated nanoparticles, loaded with miRNA92a mimic (miRCURY LNA microRNA Mimic; Exiqon) were added to the wells of the TFH differentiation assay at a ratio of 1:50 mimic/nanoparticles. The final concentration of mimic was 0.75 ng/µL per 100,000 cells (referred to as "high"). Titration was performed, with "medium" referring to 0.375 ng/µL per 100,000 cells and "low" referring to 0.1875 ng/µL per 100,000 cells. For the miRNA92a antagomir, the final concentration was 2 ng/µL per 100,000 cells. Control experiments were performed with nanoparticles and negative miRCURY LNA microRNA Mimic controls. The guide strands were found to have no homology to any known miRNA or mRNA sequences in mouse, rat, or human (63). For investigation of KLF2 as a possible target of miRNA92a, a KLF2 TSB or control TSB (custom-designed by Exiqon) was added to the assay at 2 ng/µL per 100,000 cells.

Mice. For ex vivo analysis of miRNA92a abundance in CD4⁺ T cells, pancreatic lymph nodes from NOD/ShiLtJ mice (The Jackson Laboratory) (according to their insulin autoantibody status; the insulin autoantibody assay protocol is described in *SI Materials and Methods*) or age-matched BALB/c controls were ground through 70-µm cell strainers, stained with antibodies (*Materials and Methods, Cell Staining, Flow Cytometry, and Cell Sorting*), and magnetic activated cell sorting (MACS)-purified using CD4-Biotin and Streptavidin Microbeads (Miltenyi Biotec). Total CD4⁺ T cells were sort-purified, and miRNA abundance was determined as described above.

For the in vivo inhibition of miRNA92a, age-matched, insulin autoantibody-positive female NOD/ShiLtJ mice (The Jackson Laboratory) were randomized into two groups. For short-term treatment, the mice were injected i.p. with 10 mg/kg custom-designed in vivo LNA miRNA92a antagomir (Exiqon) or control antagomir on day 0, day 2, and day 6. Analysis of insulin-specific or polyclonal TFH frequencies was performed from peripheral blood, pancreatic lymph nodes, and all remaining lymph nodes on day 7. In addition, pancreata of the treated mice and control mice were analyzed for the activation status of infiltrating T cells on day 7. Therefore, pancreata were digested in 1 mg/mL Collagenase V for 5 min at 37 °C and passed through a 100 µm cell strainer. For long-term treatment, the mice were injected i.p. with 5 mg/kg in vivo miRNA92a antagomir or control antagomir every second day for 14 d. Insulin-specific or polyclonal TFH frequencies were analyzed in peripheral blood and pancreatic lymph nodes on day 14. To analyze pancreas pathology, pancreata were embedded in Cryomold and frozen on dry ice for cryosections. For analysis of the in vivo effect of miRNA92a on the human immune cells, NOD.Cg-Prkdcscid H2-Ab1tm1Gru Il2rgtm1Wjl Tg (HLA-DQA1, HLA-DQB1)1Dv//Sz (NSG HLA-DQ8 Tg) mice, developed by Leonard Shultz, The Jackson Laboratory, Bar Harbor, ME, were used. These mice lack mouse MHC class II, although they express the human HLA-DQ8 transgenically. NSG HLA-DQ8 mice are immunodeficient and develop a human immune system after reconstitution with human hematopoietic cells. Donors for reconstitution were sex-matched. The treatment of humanized mice with the in vivo miRNA92a antagomir was performed with three i.p. injections of 10 mg/kg over 7 d. No animals were excluded due to illness or outlier results; therefore, no exclusion determination was required.

Ethical approval for all mouse experimentation has been received by the District Government of Upper Bavaria, Munich, Germany (approval nos. 5.2-1-54-2532-81-12 and 55.2-1-54-2532-84-12). The investigators were not blinded to group allocation during the in vivo experiments or to the assessment of experimental end points.

Histopathology of NOD Pancreata. Pancreata were embedded with TissueTek O.C.T. Compound and frozen on dry ice, and serial sections were stained with hematoxylin and eosin. Insulinitis scoring was performed as previously described (64, 65). The following scores were assigned: 0, intact islets/no lesions; 1, perislet infiltrates; 2, <25% islet destruction; 3, >25% islet destruction; and 4, complete islet destruction.

Immunofluorescence. Immunofluorescence staining was done using rabbit-anti-mouse insulin antibodies (Cell Signaling) and donkey-anti-rabbit Alexa⁶⁴⁷ antibodies (Dianova). For CD4 staining, rat-anti-mouse (Becton, Dickinson and Company) antibodies were used, followed by goat-anti-rat AlexaFluor⁴⁸⁸ (Dianova). For FOXP3 staining, cells were incubated with rat-anti-mouse antibodies (eBioscience) and goat-anti-rat^{bio} (Becton, Dickinson and Company) combined with TSA Cyanine3 amplification (PerkinElmer). Nuclei were counterstained with HOECHST 33342 dye (Invitrogen). Negative control slides were incubated with secondary antibodies. Cells were analyzed by confocal microscopy (Olympus).

Statistics. Results are presented as the mean and SEM or as percentages, where appropriate. For normally distributed data, the Student's *t* test for unpaired values was used to compare means between independent groups and the Student's *t* test for paired values was used to compare values for the same

sample or subject tested under different conditions. The nonparametric Wilcoxon signed-ranks test was applied when data did not show a Gaussian distribution. Group size estimations were based upon a power calculation to yield minimally an 80% chance to detect a significant difference in the respective parameter of $P < 0.05$ between the relevant groups. For all tests, a two-tailed P value of < 0.05 was considered to be significant. Statistical significance is shown as $*P < 0.05$, $**P < 0.01$, $***P < 0.001$, or not significant ($P > 0.05$). Analyses were performed using the programs GraphPad Prism 6 and the Statistical Package for the Social Sciences (SPSS 19.0; SPSS, Inc.).

ACKNOWLEDGMENTS. We thank Ruth Chmiel and Susanne Hummel for blood sample collection and patient follow-up; Melanie Spornraft and the European

Molecular Biology Laboratory Genecore facility, especially Vladimir Benes, for providing reagents and analysis tools; Peter Achenbach and Claudia Matzke for supporting IAA measurements in NOD mice; and M. H. Tschöp for critical reading of the manuscript. B.V. is supported by Grant WE 4656/2 and Deutsche Forschungsgemeinschaft (DFG) CRC1811 (B02). C.D. is supported by the Young Investigator Group (Helmholtz Zentrum München) and received support through an associated membership in the CRC1054 of the DFG. The work was supported by grants from the Juvenile Diabetes Research Foundation (JDRF 2-SRA-2014-161-Q-R to C.D. and A.-G.Z.), JDRF 17-2012-16 (to A.G.Z.), and JDRF 6-2012-20 (to A.G.Z.); the Kompetenznetz Diabetes Mellitus (Competence Network for Diabetes Mellitus), funded by the Federal Ministry of Education and Research Grants (FKZ 01GI0805-07 and FKZ 01GI0805); and the German Center for Diabetes Research. A.-G.Z. is Principal Investigator of human birth cohort studies.

- Bluestone JA, Herold K, Eisenbarth G (2010) Genetics, pathogenesis and clinical interventions in type 1 diabetes. *Nature* 464(7293):1293–1300.
- Ziegler AG, Nepom GT (2010) Prediction and pathogenesis in type 1 diabetes. *Immunity* 32(4):468–478.
- Insel RA, et al. (2015) Staging presymptomatic type 1 diabetes: A scientific statement of JDRF, the Endocrine Society, and the American Diabetes Association. *Diabetes Care* 38(10):1964–1974.
- Unanue ER (2014) Antigen presentation in the autoimmune diabetes of the NOD mouse. *Annu Rev Immunol* 32:579–608.
- Ziegler AG, et al. (2013) Seroconversion to multiple islet autoantibodies and risk of progression to diabetes in children. *JAMA* 309(23):2473–2479.
- Silva DG, et al. (2011) Anti-islet autoantibodies trigger autoimmune diabetes in the presence of an increased frequency of islet-reactive CD4 T cells. *Diabetes* 60(8):2102–2111.
- Hale JS, Ahmed R (2015) Memory T follicular helper CD4 T cells. *Front Immunol* 6:16.
- Ansel KM, McHeyzer-Williams LJ, Ngo VN, McHeyzer-Williams MG, Cyster JG (1999) In vivo-activated CD4 T cells upregulate CXCL chemokine receptor 5 and reprogram their response to lymphoid chemokines. *J Exp Med* 190(8):1123–1134.
- Flynn S, Toellner KM, Raykundlia C, Goodall M, Lane P (1998) CD4 T cell cytokine differentiation: The B cell activation molecule, OX40 ligand, instructs CD4 T cells to express interleukin 4 and upregulates expression of the chemokine receptor, Blr-1. *J Exp Med* 188(2):297–304.
- Baumjohann D, et al. (2013) Persistent antigen and germinal center B cells sustain T follicular helper cell responses and phenotype. *Immunity* 38(3):596–605.
- Johnston RJ, et al. (2009) Bcl6 and Blimp-1 are reciprocal and antagonistic regulators of T follicular helper cell differentiation. *Science* 325(5943):1006–1010.
- Stone EL, et al. (2015) ICOS coreceptor signaling inactivates the transcription factor FOXP1 to promote Tfh cell differentiation. *Immunity* 42(2):239–251.
- Xiao N, et al. (2014) The E3 ubiquitin ligase Itch is required for the differentiation of follicular helper T cells. *Nat Immunol* 15(7):657–666.
- Wang H, et al. (2014) The transcription factor Foxp1 is a critical negative regulator of the differentiation of follicular helper T cells. *Nat Immunol* 15(7):667–675.
- Lee JY, et al. (2015) The transcription factor KLF2 restrains CD4⁺ T follicular helper cell differentiation. *Immunity* 42(2):252–264.
- Locci M, et al.; International AIDS Vaccine Initiative Protocol C Principal Investigators (2013) Human circulating PD-1+CXCR3-CXCR5+ memory Tfh cells are highly functional and correlate with broadly neutralizing HIV antibody responses. *Immunity* 39(4):758–769.
- Morita R, et al. (2011) Human blood CXCR5(+)/CD4(+) T cells are counterparts of T follicular cells and contain specific subsets that differentially support antibody secretion. *Immunity* 34(1):108–121.
- Bentebibel SE, et al. (2013) Induction of ICOS+CXCR3+CXCR5+ TH cells correlates with antibody responses to influenza vaccination. *Sci Transl Med* 5(176):176ra32.
- Schmitt N, Bentebibel SE, Ueno H (2014) Phenotype and functions of memory Tfh cells in human blood. *Trends Immunol* 35(9):436–442.
- Ueno H, Bancheau J, Vinuesa CG (2015) Pathophysiology of T follicular helper cells in humans and mice. *Nat Immunol* 16(2):142–152.
- He J, et al. (2013) Circulating precursor CCR7(lo)PD-1(hi) CXCR5⁺ CD4⁺ T cells indicate Tfh cell activity and promote antibody responses upon antigen reexposure. *Immunity* 39(4):770–781.
- Scherin MG, Ott VB, Daniel C (2016) Follicular helper T cells in autoimmunity. *Curr Diab Rep* 16(8):75.
- Xiao S, et al. (2008) Retinoic acid increases Foxp3+ regulatory T cells and inhibits development of Th17 cells by enhancing TGF-beta-driven Smad3 signaling and inhibiting IL-6 and IL-23 receptor expression. *J Immunol* 181(4):2277–2284.
- Kuipers H, Schnorfeil FM, Brocker T (2010) Differentially expressed microRNAs regulate plasmacytoid vs. conventional dendritic cell development. *Mol Immunol* 48(1-3):333–340.
- Kuipers H, Schnorfeil FM, Fehling HJ, Bartels H, Brocker T (2010) Dicer-dependent microRNAs control maturation, function, and maintenance of Langerhans cells in vivo. *J Immunol* 185(11):400–409.
- Turner ML, Schnorfeil FM, Brocker T (2011) MicroRNAs regulate dendritic cell differentiation and function. *J Immunol* 187(8):3911–3917.
- Cobb BS, et al. (2006) A role for Dicer in immune regulation. *J Exp Med* 203(11):2519–2527.
- Cobb BS, et al. (2005) T cell lineage choice and differentiation in the absence of the RNase III enzyme Dicer. *J Exp Med* 201(9):1367–1373.
- Xiao C, et al. (2008) Lymphoproliferative disease and autoimmunity in mice with increased miR-17-92 expression in lymphocytes. *Nat Immunol* 9(4):405–414.
- Baumjohann D, et al. (2013) The microRNA cluster miR-17~92 promotes TFH cell differentiation and represses subset-inappropriate gene expression. *Nat Immunol* 14(8):840–848.
- Serr I, et al. (2016) Type 1 diabetes vaccine candidates promote human Foxp3(+)/Treg induction in humanized mice. *Nat Commun* 7:10991.
- Thümer L, et al. (2010) German new onset diabetes in the young incident cohort study: DiMeIli study design and first-year results. *Rev Diabet Stud* 7(3):202–208.
- Warneke K, et al. (2013) Does diabetes appear in distinct phenotypes in young people? Results of the diabetes mellitus incidence Cohort Registry (DiMeIli). *PLoS One* 8(9):e74339.
- Wong N, Wang X (2015) miRDB: An online resource for microRNA target prediction and functional annotations. *Nucleic Acids Res* 43(Database issue):D146–D152.
- Lewis BP, Burge CB, Bartel DP (2005) Conserved seed pairing, often flanked by adenosines, indicates that thousands of human genes are microRNA targets. *Cell* 120(1):15–20.
- Kang SG, et al. (2013) MicroRNAs of the miR-17-92 family are critical regulators of T (FH) differentiation. *Nat Immunol* 14(8):849–857.
- Jiang P, Rao EY, Meng N, Zhao Y, Wang JJ (2010) MicroRNA-17-92 significantly enhances radiosensitivity in human mantle cell lymphoma cells. *Radiat Oncol* 5:100.
- Friedman RC, Farh KK, Burge CB, Bartel DP (2009) Most mammalian mRNAs are conserved targets of microRNAs. *Genome Res* 19(1):92–105.
- Ravi Kumar MN, Bakowsky U, Lehr CM (2004) Preparation and characterization of cationic PLGA nanospheres as DNA carriers. *Biomaterials* 25(10):1771–1777.
- Bramsén JB, et al. (2007) Improved silencing properties using small internally segmented interfering RNAs. *Nucleic Acids Res* 35(17):5886–5897.
- Ma CS, Deenick EK, Batten M, Tangye SG (2012) The origins, function, and regulation of T follicular helper cells. *J Exp Med* 209(7):1241–1253.
- von Boehmer H, Daniel C (2013) Therapeutic opportunities for manipulating T(Reg) cells in autoimmunity and cancer. *Nat Rev Drug Discov* 12(1):51–63.
- Kenefeck R, et al. (2015) Follicular helper T cell signature in type 1 diabetes. *J Clin Invest* 125(1):292–303.
- Ferreira RC, et al. (2015) IL-21 production by CD4⁺ effector T cells and frequency of circulating follicular helper T cells are increased in type 1 diabetes patients. *Diabetologia* 58(4):781–790.
- Rekers NV, von Herrath MG, Wesley JD (2015) Immunotherapies and immune biomarkers in Type 1 diabetes: A partnership for success. *Clin Immunol* 161(1):37–43.
- Simpson LJ, Ansel KM (2015) MicroRNA regulation of lymphocyte tolerance and autoimmunity. *J Clin Invest* 125(6):2242–2249.
- Janssen HL, et al. (2013) Treatment of HCV infection by targeting microRNA. *N Engl J Med* 368(18):1685–1694.
- Murugaiyan G, et al. (2015) MicroRNA-21 promotes Th17 differentiation and mediates experimental autoimmune encephalomyelitis. *J Clin Invest* 125(3):1069–1080.
- Mattes J, Collison A, Plank M, Phipps S, Foster PS (2009) Antagonism of microRNA-126 suppresses the effector function of TH2 cells and the development of allergic airways disease. *Proc Natl Acad Sci USA* 106(44):18704–18709.
- Bartel DP (2009) MicroRNAs: Target recognition and regulatory functions. *Cell* 136(2):215–233.
- Gigoux M, et al. (2009) Inducible costimulatory promotes helper T-cell differentiation through phosphoinositide 3-kinase. *Proc Natl Acad Sci USA* 106(48):20371–20376.
- Rolf J, et al. (2010) Phosphoinositide 3-kinase activity in T cells regulates the magnitude of the germinal center reaction. *J Immunol* 185(7):4042–4052.
- Xu H, et al. (2013) Follicular T-helper cell recruitment governed by bystander B cells and ICOS-driven motility. *Nature* 496(7446):523–527.
- Du P, Ma X, Wang C (2014) Associations of CTLA4 gene polymorphisms with Graves' ophthalmopathy: A meta-analysis. *Int J Genomics* 2014:537969.
- Sebzda E, Zou Z, Lee JS, Wang T, Kahn ML (2008) Transcription factor KLF2 regulates the migration of naive T cells by restricting chemokine receptor expression patterns. *Nat Immunol* 9(3):292–300.
- Carlson CM, et al. (2006) Kruppel-like factor 2 regulates thymocyte and T-cell migration. *Nature* 442(7100):299–302.
- Weber JP, et al. (2015) ICOS maintains the T follicular helper cell phenotype by down-regulating Kruppel-like factor 2. *J Exp Med* 212(2):217–233.
- Kerdiles YM, et al. (2009) Foxo1 links homing and survival of naive T cells by regulating L-selectin, CCR7 and interleukin 7 receptor. *Nat Immunol* 10(2):176–184.
- Fabre S, et al. (2008) FOXP1 regulates L-Selectin and a network of human T cell homing molecules downstream of phosphatidylinositol 3-kinase. *J Immunol* 181(5):2980–2989.
- Ziegler AG, Bonifacio E; BABYDIAB-BABYDIET Study Group (2012) Age-related islet autoantibody incidence in offspring of patients with type 1 diabetes. *Diabetologia* 55(7):1937–1943.
- Ziegler AG, Hummel M, Schenker M, Bonifacio E (1999) Autoantibody appearance and risk for development of childhood diabetes in offspring of parents with type 1 diabetes: The 2-year analysis of the German BABYDIAB Study. *Diabetes* 48(3):460–468.
- Achenbach P, et al. (2009) Autoantibodies to zinc transporter 8 and SLC30A8 genotype stratify type 1 diabetes risk. *Diabetologia* 52(9):1881–1888.
- Kozomara A, Griffiths-Jones S (2014) miRBase: Annotating high confidence microRNAs using deep sequencing data. *Nucleic Acids Res* 42(Database issue):D68–D73.
- Jaekel E, Lipes MA, von Boehmer H (2004) Recessive tolerance to preproinsulin 2 reduces but does not abolish type 1 diabetes. *Nat Immunol* 5(10):1028–1035.
- Krishnamurthy B, et al. (2006) Responses against islet antigens in NOD mice are prevented by tolerance to proinsulin but not IGRP. *J Clin Invest* 116(12):3258–3265.

3.3.1 Supplementary information

miRNA92a targets KLF2 and the phosphatase PTEN signaling to promote human T follicular helper precursors in T1D islet autoimmunity

Isabelle Serr, Rainer W. Fürst, Verena B. Ott, Martin G. Scherm, Alexei Nikolaev, Füsün Gökmen, Stefanie Kälin, Stephanie Zillmer, Melanie Bunk, Benno Weigmann, Nicole Kunschke, Brigitta Loretz, Claus-Michael Lehr, Benedikt Kirchner, Bettina Haase, Michael Pfaffl, Ari Waisman, Richard A. Willis, Anette-G. Ziegler and Carolin Daniel.

Supporting Information

Serr et al. 10.1073/pnas.1606646113

SI Materials and Methods

Antibodies for Flow Cytometry. The following monoclonal antibodies were used for human FACS staining: anti-CD45RO allophycocyanin (APC)-H7 (UCHL1), anti-CD4 V500 (RPA-T4), anti-PD1 peridinin chlorophyll protein (PerCP)-Cy5.5 (EH12.1), and anti-CD45 APC-H7 (2D1) (all from BD Biosciences) and anti-CD45RA FITC (HI100), anti-CD8a Pacific Blue (RPA-T8), anti-CD11b Pacific Blue (ICRF44), anti-CD14 Pacific Blue (HCD14), anti-CD19 Pacific Blue (HIB19), anti-CCR7 PE-Cy7 (G043H7), anti-CXCR5 APC (J252D4), anti-CD3 Alexa Fluor 700 (HIT3a), anti-CXCR3 APC-Cy7 (G025H7), anti-CXCR3 PerCP-Cy5.5 (G025H7), anti-CCR6 PE-Cy7 (G034E3), anti-ICOS PE (C398.4A), anti-PSGL1 PE (KPL-1), anti-CD20 FITC (2H7), and anti-CD27 APC (M-T271) (all from Biolegend). For murine FACS staining, the following monoclonal antibodies were used: anti-CD4 Biotin (GK1.5), anti-CD14 BD Horizon 450 (rmC5-3), and anti-Bcl6 Alexa Fluor 647 (K112-91) (all from BD Biosciences); anti-CD44 PE (IM7), anti-CD25 PerCP-Cy5.5 (PC61), anti-ICOS FITC (C398.4A), anti-CXCR5 PerCP-Cy5.5 (L138D1), anti-PD-1 Alexa Fluor 780 (J43), anti-CD4 Alexa Fluor 700 (RM4-5), anti-CD8a Pacific Blue (53-6.7), anti-CD11b Pacific Blue (M1/70), anti-B220 Pacific Blue (RA3-6B2), anti-F4/80 Pacific Blue (BM8), and anti-CD11c Brilliant Violet 421 (N418) (all from Biolegend); and anti-CCR7 PE (4B12) and anti-Foxp3 FITC (FJK-16s) (both from eBiosciences).

Primers. For RT-qPCR analysis of gene expression, the following primers were used: QuantiTect Primer Assays (Qiagen) for IFN- γ , IL-13, IL-10, CXCR5, ICOS, ITCH, Bcl6, KLF2, PTEN, Foxo1, S1P1R, PHLPP2, and CTLA4 and PrimePCR PreAmp for SYBR Green Assay (BioRad) for Ascl2, IL-17a, and IL-4. The sequence for the primers for ICOS is as follows: forward (Fwd): GCA CGA CCC TAA CGG TGA AT and reverse (Rev): GAA AAC TGG CCA ACG TGC TT, and the sequence for the primers for IL-21 is as follows: Fwd: CTC CCA AGG TCA AGA TCG CC and Rev: TGG CAG AAA TTC AGG GAC CA.

Chitosan-Coated PLGA Nanoparticle Preparation and Characterization. The nanoparticles were produced following the method described by Ravi Kumar et al. (39) using PLGA Resomer RG 752H (Evonik) and Protasan UP CL 113 Chitosan (NovaMatrix). For confocal imaging, the nanoparticles were produced with a 5-fluoresceinamine (FA)-PLGA conjugate. The measured hydrodynamic diameter was 146.7 ± 0.8 nm (152.8 ± 1.2 nm), the polydispersity index was 0.068 ± 0.009 (0.056 ± 0.007), and the zeta potential was

$+29.6 \pm 0.3$ mV ($+29.6 \pm 0.7$ mV) for the chitosan-coated PLGA nanoparticles and FA-labeled nanoparticles.

Analysis of miRNA/Nanoparticles Uptake by Confocal Imaging of CD4⁺ T-Cell Cytospins. Chitosan-coated PLGA nanoparticles (~130 nm in size) with or without fluorescent label (FA) were obtained from Claus-Michael Lehr at the Department of Drug Delivery, Helmholtz Institute for Pharmaceutical Research Saarland, Saarland University, Germany. Successful uptake and delivery of miRNA to human and murine CD4⁺ T cells was determined: Respective naive CD4⁺ T cells were stimulated with anti-CD3/anti-CD28 for 18 h in the presence of FA-labeled nanoparticles complexed with miRIDIAN miRNA transfection control (Dy547). The uptake was initially confirmed by identification of a clearly distinguishable FA⁺ population using FACS analysis. Additionally the uptake was confirmed by confocal imaging: Human naive CD4⁺ T cells were stimulated as described above for 18 h in the presence or absence of nanoparticles and labeled miRIDIAN miRNA mimic transfection control (Dy547). After the stimulation, CD4⁺ T cells were washed and fixed. Upon generation of cytopins, intracellular localization of nanoparticles and delivered miRNA were assessed by confocal microscopy.

Insulin Autoantibody Assay. Insulin autoantibodies were determined using an ELISA system as described previously. In brief, high-binding, 96-well plates (Costar) were coated with human recombinant insulin (10 μ g/mL; Sigma-Aldrich) overnight at 4 °C. Unspecific blocking was done using PBS containing 2% BSA for 2 h at room temperature. Preincubated serum (diluted 1:10) with or without insulin competition was added and incubated for 2 h at room temperature. After four wash steps, biotinylated anti-mouse IgG1 (Abcam) diluted 1:10,000 in PBS/BSA was added for 30 min at room temperature. After washing the plate, horseradish peroxidase-labeled streptavidin was added for 15 min. The plate was washed five times, and tetramethylbenzidine (TMB) substrate solution was added (OptEIA reagent set; Becton, Dickinson and Company). The reaction was stopped using sulfuric acid, and fluorescent intensity was determined in the Epoch plate reader (Biotech). Each sample was run in duplicate with and without competition using human insulin. For each sample, an index was calculated based on the mean of the results.

To determine levels of IAA in NOD mice, a Protein A/G radiobinding assay based on ¹²⁵I-labeled recombinant human insulin was applied as previously described (62). Serum from non-autoimmune prone BALB/c mice was used as negative control.

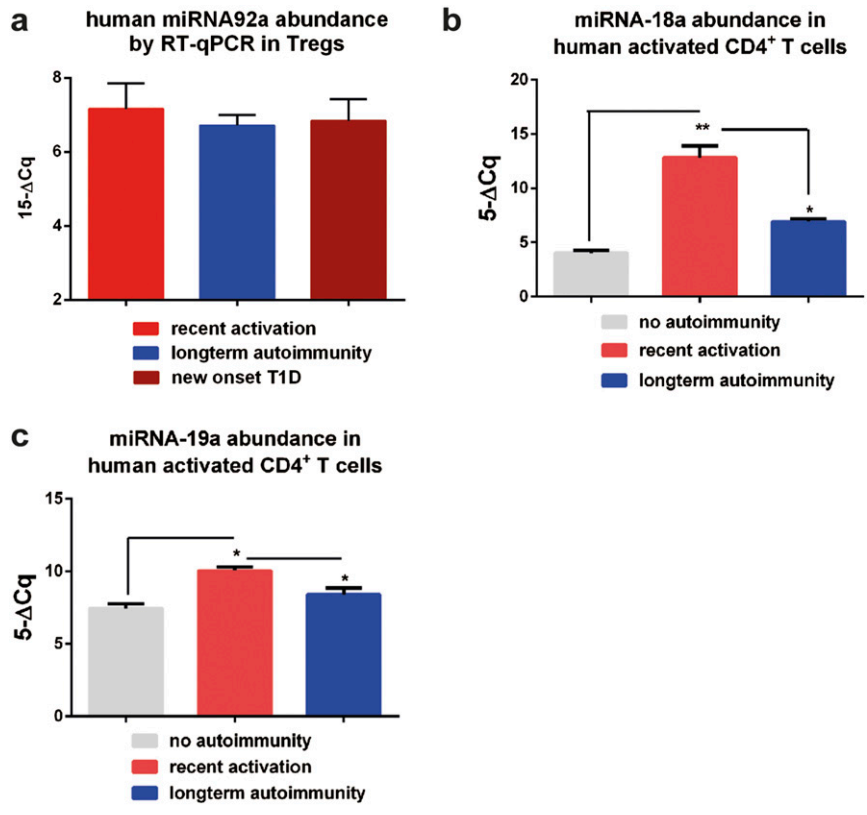


Fig. S1. (A) miRNA92a abundance in CD4⁺CD3⁺CD127^{low}CD25^{high} Treg cells. miRNA18a (B) and miRNA19a (C) abundance in human CD4⁺ T cells purified from children with or without pre-T1D (no autoimmunity, *n* = 10; recent onset of autoimmunity, *n* = 6; long-term autoimmunity, *n* = 6) as assessed by qRT-PCR analyses. Data represent the mean ± SEM. **P* < 0.05; ***P* < 0.01.

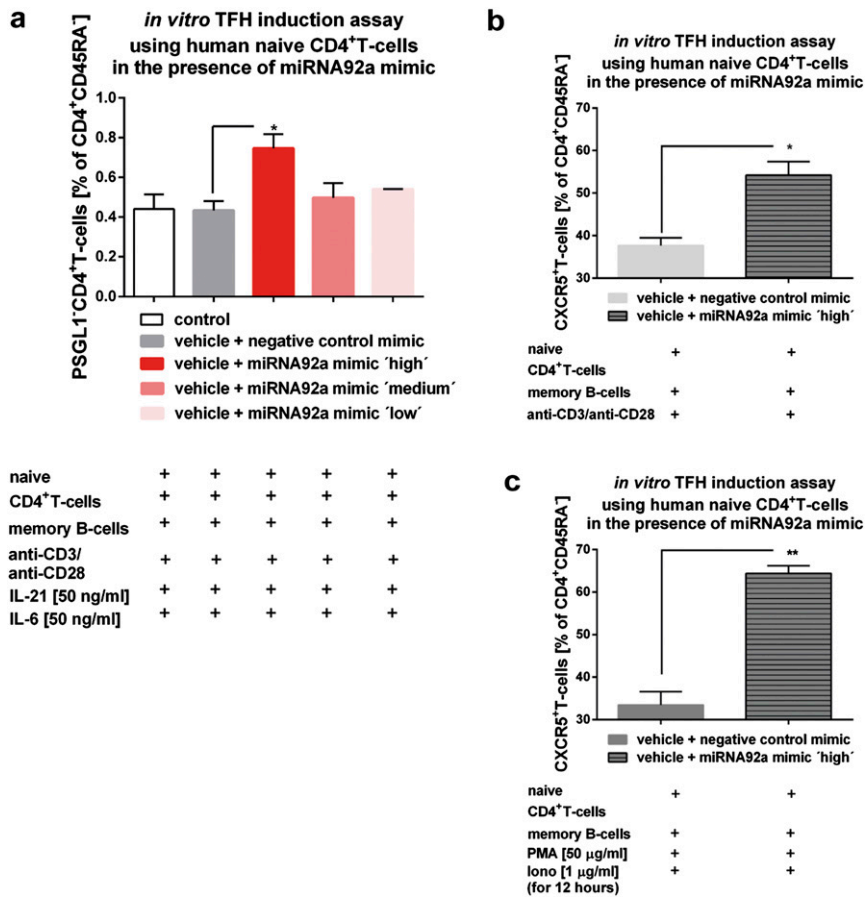


Fig. 54. (A) TFH precursor induction using human naive CD4⁺ T cells in the presence of memory B cells and IL-6, IL-21, and a titration of a miRNA92a mimic (low = 0.0375 µg in 200 µL per 100,000 cells, medium = 0.075 µg in 200 µL per 100,000 cells, and high = 0.15 µg in 200 µL per 100,000 cells) or a negative miRNA mimic control. Summary graph for frequencies of PSGL1⁺CD4⁺ T cells is shown as percentages of CD4⁺CD45RA⁻ T cells (*n* = 4). Data represent the mean ± SEM from duplicate wells per individual. **P* < 0.05. (B) TFH precursor induction using human naive CD4⁺ T cells in the presence of memory B cells and a miRNA92a mimic or a negative miRNA mimic control. Summary graph for frequencies of CXCR5⁺CD4⁺ T cells is shown as percentages of CD4⁺CD45RA⁻ T cells (*n* = 4). Data represent the mean ± SEM from duplicate wells per individual. **P* < 0.05. (C) TFH precursor induction using human naive CD4⁺ T cells in the presence of memory B cells and a miRNA92a mimic or a negative miRNA mimic control. In such assays, PMA (50 ng/mL) and ionomycin (1 µg/mL) were added for the last 12 h of the experiments, and frequencies of CXCR5⁺CD4⁺ T cells shown as percentages of CD4⁺CD45RA⁻ T cells were analyzed (*n* = 4). Data represent the mean ± SEM from duplicate wells per individual. ***P* < 0.01.

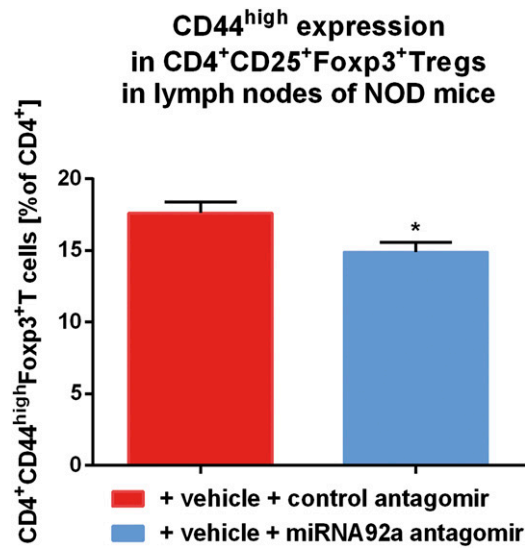


Fig. S7. Summary graph for CD44^{high} expression in CD4⁺CD25⁺Foxp3⁺ Treg cells purified from lymph nodes of NOD mice given a control antagomir or a miRNA92a antagomir (14 d of treatment, with injections four times per week at 5 mg/kg) ($n = 5$ per group). Data represent the mean \pm SEM. * $P < 0.05$.

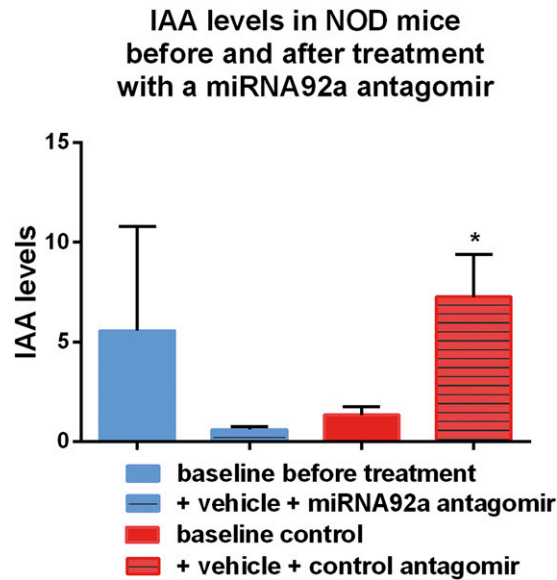


Fig. S8. Summary graphs for IAA levels from NOD mice before and after treatment with either control antagomirs or a specific miRNA92a antagomir (14 d of treatment, with injections four times per week at 5 mg/kg) ($n = 5$ per group). Data represent the mean \pm SEM. * $P < 0.05$.

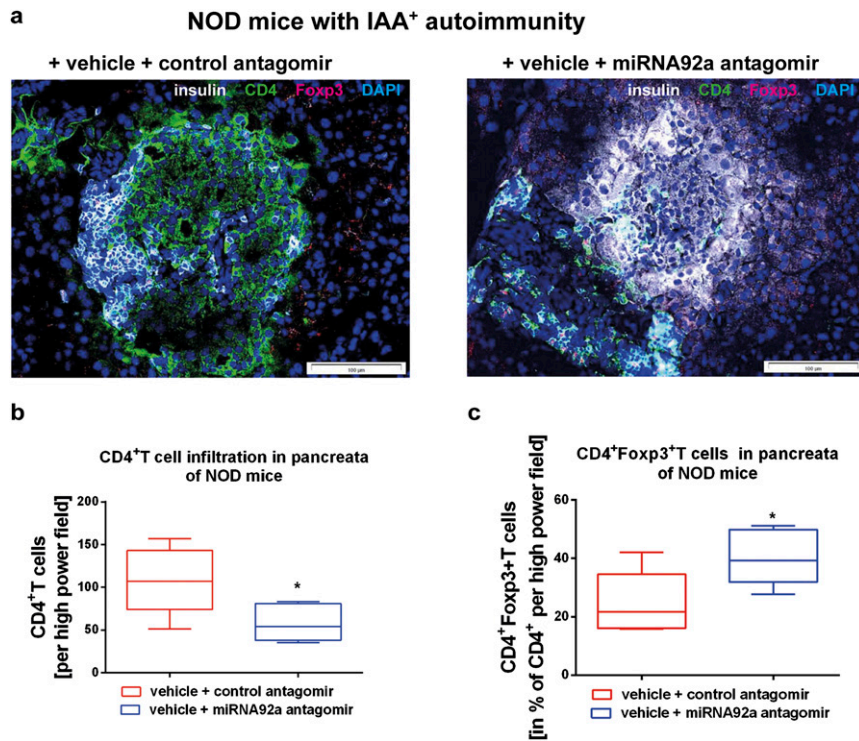


Fig. S10. (A) Immunofluorescence for insulin (white), CD4 (green), and Foxp3 (red) in pancreatic cryosections of NOD mice given a control inhibitor or a miRNA92a inhibitor (14 d of treatment, with injections four times per week at 5 mg/kg). (B) CD4⁺ T cells infiltrating the pancreas as in A. Shown are box and whiskers plots of CD4⁺ T cells per high-power field. (C) CD4⁺Foxp3⁺ T cells in the percentage of infiltrating CD4⁺ T cells per high-power field of mice as in A ($n = 5$ per group).

3.3.2 Authors' contributions

Isabelle Serr: FACS staining and analysis of insulin-specific and polyclonal TFH cells, as well as TFH subpopulations in peripheral blood of children at different stages of islet autoimmunity (Fig.1A-C, Fig.2A-D, Fig.3A-D), gene expression analysis via RT-qPCR for miRNA92a and its target signaling pathways (Fig.4A-E, Suppl.Fig.1A-C), *in vivo* treatment of NOD mice and humanized mice with a miRNA92a antagomir and analysis of T cell activation in pancreas, lymph nodes and blood (Fig.6A-M, Supp.Fig.7, Fig.6N-P), supervision of Verena B. Ott, Data analysis and interpretation; preparation and editing of the manuscript.

Rainer W. Fürst: Support of gene expression analysis.

Verena B. Ott: Human TFH induction assays with miRNA92a, support of gene expression analysis.

Martin G. Scherm: Support of gene expression analysis and support of *in vitro* experiments.

Alexei Nikolaev: Immunofluorescent stainings of pancreatic sections from NOD mice.

Fusun Gökmen: Support of tetramer stainings.

Stefanie Kälin: Support of *in vitro* assays.

Stephanie Zillmer: Blood sample collection.

Melanie Bunk: Blood sample collection.

Benno Weigmann: Histopathological analysis of pancreatic sections from NOD mice with H&E stainings.

Nicole Kunschke: Preparation of nanoparticles for miRNA uptake in T cells.

Brigitta Loretz: Conceptualization, Characterization and Design of nanoparticles.

Claus-Michael Lehr: Conceptualization, Characterization and Design of nanoparticles.

Benedikt Kirchner: Analysis of gene expression data.

Bettina Haase: Analysis of gene expression data.

Michael Pfaffl: Provision of reagents for gene expression analysis.

Ari Waisman: Provision of reagents for immunohistochemical analysis.

Richard A. Willis: Conceptualization, design and production of tetramer reagents.

Anette-G. Ziegler: Advisement and co-conceptualization of the study design and principle investigator of cohort studies BABYDIAB, DiMelli and Munich Bioresource, which provided patient samples.

Carolin Daniel: Conceptualization and design of the study, interpretation of data, preparation and editing of the manuscript.

4. Discussion

Defects in immune tolerance are critical triggers of autoimmune T1D. A better understanding of their molecular basis is therefore pivotal for the development of novel therapeutic strategies aimed at limiting autoimmune activation and progression. The highly variable progression to symptomatic T1D which ranges from a few months to more than two decades in children underscores the plasticity in mechanisms regulating immune activation versus immune tolerance. T cells from children at a pre-symptomatic stage of the disease, who are autoantibody positive but have not yet progressed to symptomatic T1D, offer therefore a valuable resource for studying signaling pathways involved in aberrant immune activation versus immune tolerance.

The launch of prospective follow-up cohort studies in the end of the 1980s and beginning of the 1990s has led to significant improvements in the risk assessment in children genetically at risk for T1D (Achenbach et al., 2009; Näntö-Salonen et al., 2008; Rewers et al., 1996; Thumer et al., 2010; Warncke et al., 2013; Ziegler and Bonifacio, 2012; Ziegler et al., 1999). In combination with advances in the detection and quantification of islet autoantibody titers it has become possible to define the pre-symptomatic stage of T1D more precisely. In this regard it is now clear, that children with two or more islet autoantibodies will develop T1D, however the time of progression is highly variable (Ziegler et al., 2013). Therefore, a stage of the disease without clinical symptoms but with the presence of multiple islet autoantibodies is proposed to be included in the diagnosis of T1D in a new staging strategy (Insel et al., 2015). The heterogeneity in the progression time from seroconversion to symptomatic T1D led to the stratification of children into fast versus slow progressors (Achenbach et al., 2013). Data from cohort studies has revealed that fast and slow progressors differ in many aspects of the disease. For example, slow progressors harbor an accumulation of protective genotypes, whereas fast progressors show increased levels of autoantibodies and a different autoantibody composition at seroconversion (Achenbach et al., 2013; Pöllänen et al., 2017). However, the prediction of progression time from seroconversion to symptomatic T1D remains challenging.

Because of these strong differences in islet autoimmunity development before the onset of the symptomatic disease, the aim of this thesis was to contribute to the dissection of mechanisms of immune activation versus immune tolerance in islet autoimmunity. The focus was set on T cell responses and more specifically on Tregs, because of their pivotal role in regulating immunological tolerance. Insulin epitopes have been demonstrated to be critical targets of the autoimmune attack with insulin autoantibodies being usually the first to appear in humans (Hummel et al., 2004) and the specificity of more than 90% of islet infiltrating T cell clones in NOD mice to the insulin B:9-23 epitope (Alleva et al., 2001; Daniel et al., 1995a). Therefore, the primary aim of this thesis was to investigate insulin-specific CD4⁺T cell responses during islet autoimmunity.

The strong association of many autoimmune diseases with certain HLA haplotypes suggests that peptide presentation is a crucial component of aberrant autoimmune activation and disease development. Weak interactions of important autoantigens with the high-risk HLA molecules have been reported for different autoimmune diseases, including T1D and Multiple Sclerosis (Fairchild et al., 1993; He et al., 2002; Lee et al., 1998; Mason et al., 1995). The weak interaction of MHCII-peptide complexes with the TCR, due to inefficient antigen presentation, can lead to the escape of autoreactive T cells from negative selection in the thymus (Wucherpfennig and Sethi, 2011) and can additionally hinder Treg induction in the periphery. We devised novel strong-agonistic insulin B:9-23 mimetopes, based on work from John Kappler's group (Stadinski et al., 2010b) (Crawford et al., 2011) and the crystal structure (Lee et al., 2001a) of the HLA-DQ8 B:9-23 complex (ins.mim.1 = 14E-21G-22E and ins.mim.4 = 14E-21E-22E) and compared them to the previously established mimetopes used in the NOD mouse model (ins.mim.2 = 21G-22E and ins.mim.3 = 21E-22E) or the natural insulin B:9-23 epitope. The alteration at position 14 led to a significantly improved stimulatory capacity of these novel mimetopes, compared to the ins.mim.2 and ins.mim.3, as highlighted by the increased proliferative response of insulin-specific CD4⁺T cell clones (Serr et al., 2016a). Our findings are in line with the analysis of the crystal structure of the HLA-DQ8 B:9-23 complex: the P1 position of the HLA-DQ8 binding pocket is lined by two positively charged amino acids (arginine and histidine) and a negatively charged glutamic acid at position 14 (14E) of the peptide can form a hydrogen bond network with the P1 pocket (Lee et al., 2001a). Accordingly, we also observed an increased binding affinity of ins.mim.1 and ins.mim.4 to the HLA-DQ8 (Serr et al., 2016a)

Importantly, we likewise aimed to establish novel tools that will permit the direct *ex vivo* analysis of the relevant human insulin-specific Foxp3⁺Treg population – a critical step currently missing in symptomatic T1D prevention efforts. We therefore used these two novel insulin variants for the design of human HLA-DQ8-restricted insulin-specific tetramer reagents. Using these tetramer reagents, we show a decrease in insulin-specific Treg frequencies in children with recent activation of islet autoimmunity (development of autoantibodies within the last 5 years, without progression to symptomatic T1D). In contrast, we observed significantly increased frequencies of insulin-specific Tregs in children which are autoantibody positive for more than 10 years, but have not yet progressed to symptomatic T1D, which indicates that these children are in a transient state of immune tolerance and supports the hypothesis of inducing these cells to prevent or delay the progression from islet autoimmunity to symptomatic T1D (Serr et al., 2016a).

In line with the differences in immune tolerance in these pre-symptomatic children, we also find immune activation to be differently regulated in this early phase of the disease. We focused on immune cells that can promote the development of islet autoantibodies, specifically TFH cells and their precursor population in the blood. In accordance with the

decreased frequencies of insulin-specific Tregs, we also find insulin-specific TFH cells to be increased during recent activation of islet autoimmunity. Intriguingly, this increase in TFH cells is not limited to the insulin-specific target T cell population, but was also observed on a polyclonal level. TFH cells have been studied before in the context of T1D, however their role in accelerating the disease progression is unknown, because up till now, TFH cells have only been studied in patients with symptomatic T1D (Serr et al., 2016b). The increase of TFH precursor frequencies during early phases of the pre-symptomatic disease is in accordance with the involvement of TFH cells in providing B cell help for autoantibody production and highlights, that these cells might be especially important during the early phase of the pre-symptomatic disease. In line with this hypothesis, we find cells of the Th2-like TFH subset to be predominantly increased during recent activation of islet autoimmunity, whereas Th1-like and Th17-like TFH cells are unaltered in their frequencies compared to healthy control children (Serr et al., 2016b). Th2-like TFH cells and Th17-like TFH cells are able to provide help to B cells, whereas Th1-like TFH cells are unable to do so. Th2- and Th17-like TFH cells also impact differentially on the class switching of the B cells, with Th2-like TFH cells promoting more IgG and IgE responses and Th17-like TFH cells promoting IgG and IgA responses (Morita et al., 2011). Recently, in a study of prostate cancer, it was demonstrated that there are also differences between Th2- and Th17-like TFH cells in their ability to induce different subtypes of IgG antibodies (Tan et al., 2015). Regarding T1D various studies suggest that the Ig isotype of the islet autoantibodies and even the IgG subtypes induced in the pre-symptomatic phase of the disease might influence the progression to symptomatic T1D (Hopppu et al., 2006; Hopppu et al., 2004; Petersen et al., 1999).

In accordance with the plasticity in regulation of immune activation versus tolerance in children at different stages of islet autoimmunity, we were interested to understand whether the impairments in immune tolerance in children with recent activation of islet autoimmunity refer also to a defect in Treg induction from naïve CD4⁺T cells.

Therefore, we first went one step back and analyzed mechanisms and requirements of human Treg induction in the steady state. Here we made use of lessons learnt from the murine setting. Specifically, several studies have highlighted that T cell tolerance induction in the peripheral immune system can be achieved or improved by agents or conditions that limit strong TCR signals. These conditions contain, but are not limited to targeting of the immunological synapse by monoclonal antibodies against costimulatory or other molecules like CD28 (Haspot et al., 2005; Laskowski et al., 2002), immature subsets of DCs (Fu et al., 1996; Lutz et al., 2000), or subimmunogenic doses of peptide stimulation (Kretschmer et al., 2005). Stephan Sauer and colleagues have demonstrated that reducing the TCR stimulus by withdrawal after short-term stimulation leads to limited activation of the PI3K/Akt/mTOR pathway and increased Foxp3 induction (Sauer et al., 2008). In accordance with these findings, we demonstrate here, that *in vitro* Treg induction in the absence of TGFβ, when the

TCR stimulation is limited is also possible with human naïve T cells (Serr et al., 2016a). Furthermore, the Foxp3 expression in the human Tregs induced with limited TCR stimulation was more stable than that in Tregs induced with continuous TCR stimulation, which more rapidly lost their Foxp3 expression in restimulation experiments (Serr et al., 2016a).

This observation is in line with findings from several research groups, indicating that for stable Foxp3 expression and maintenance of the Treg phenotype, a complete demethylation of the TSDR of the *Foxp3* locus is indispensable (Baron et al., 2007; Floess et al., 2007; Polansky et al., 2008). Jochen Huehn's group demonstrated moreover, that Tregs induced with TGFβ have a methylated TSDR and are unstable. Additionally, inhibition of the DNA methyltransferase, the enzyme responsible for methylation of 5'-C-phosphate-G-3' (CpG) sites, by azacitidine enabled stable Foxp3 expression in TGFβ induced cells. The *in vivo* induction of Tregs by minute amounts of peptide fused to a DEC-205 antibody, lead to efficient demethylation of the TSDR and stable Foxp3 expression (Polansky et al., 2008). DEC-205 is a receptor on dendritic cells (DCs) that is involved in antigen uptake and presentation on MHC class I and II molecules. Therefore, targeting peptides to DCs by fusing them to DEC-205 antibodies leads to their presentation on MHC molecules on the DC surface. It has been demonstrated previously, that the application of minute amounts of the DEC-205-peptide fusion complexes, to avoid DC maturation, leads to efficient *de novo* Treg induction *in vivo* (Kretschmer et al., 2005). The findings, that demethylation of the TSDR in induced Tregs is observed after Treg induction with minute amounts of DEC-205-peptide complexes and not after Treg induction with TGFβ highlights that TGFβ might use alternative pathways for upregulation of Foxp3 and that subimmunogenic antigen stimulation is suitable to mimic *in vivo* Treg induction (Polansky et al., 2008).

The findings from the murine system that Treg induction is most effective when strong agonistic TCR ligands are supplied under subimmunogenic conditions, prompted us to test the novel insulin mimetopes in an *in vivo* setting in the human immune system. Building up on the findings obtained from human insulin-specific Treg induction *in vitro*, in an *in vivo* setting of humanized mice, we were able to demonstrate the presence of insulin-specific CD4⁺T cells in the periphery, highlighting that these cells were positively selected on HLA-DQ8 molecules in the thymus of these mice (Serr et al., 2016a) and that these mice are a suitable model to study insulin-specific Treg induction *in vivo* in a human immune system. This is in line with previous findings in other, non-NSG, HLA-transgenic mouse models, which were demonstrated to display a TCR repertoire that was selected for in the thymus on human HLA molecules (Chen et al., 2003; Chen et al., 2006). However, the positive selection of autoreactive T cells in the thymus of humanized mice has not been demonstrated before. Importantly for our attempt to induce Tregs, the insulin-specific CD4⁺T cells that we identified in the humanized mice were mostly in a naïve state (Serr et al., 2016a).

In accordance with the improved binding of ins.mim.1 and ins.mim.4 to the HLA-DQ8, we were able to show in antigen-specific Treg induction assays *in vivo* in humanized HLA-DQ8 transgenic NSG mice that these novel mimetopes are capable to induce significantly higher frequencies of Tregs from naïve T cells, compared to the natural insulin B:9-23 epitope, thereby highlighting that efficient human Treg induction, similar to the murine setting, also requires strong-agonistic TCR ligands provided under subimmunogenic conditions (Serr et al., 2016a).

We demonstrated furthermore, that the induced Tregs were suppressive *in vitro* and stable, as indicated by a high degree of demethylation in the TSDR and a long persistence for six months after their induction (Serr et al., 2016a). Importantly, no evidence of effector T cell activation due to the peptide infusion was observed, supporting that the doses used are subimmunogenic and that these doses are safe in regard of inducing unwanted pro-inflammatory responses (Serr et al., 2016a). The optimal subimmunogenic dose for Treg induction in this humanized mouse model needs, however, more detailed investigation. The setup of these investigations was a proof of principle, that the Treg induction strategies from the murine system can also be used in a human setting *in vivo*. However, humanized NSG mice do not develop T1D or islet autoimmunity. Whether the induction of Tregs in this model will be able to halt or reverse islet autoimmunity or symptomatic T1D will need to be investigated in future studies. Additionally, it will be important to define requirements for efficient Treg induction also in settings of ongoing islet autoimmunity.

To answer the question, whether Treg induction is affected during islet autoimmunity given the reduced insulin-specific Treg frequencies we analyzed naïve T cells from children or NOD mice at different stages of islet autoimmunity for the ability to induce Tregs in *in vitro* assays. Indeed, in a manuscript that is currently under revision, we show that the potential to induce Tregs from naïve T cells of children with recent activation of islet autoimmunity is significantly decreased (Serr et al., 2017). We furthermore demonstrate that this is not only true for the insulin-specific generation of Tregs, but also for Treg induction using the non-self antigen hemagglutinin or polyclonal stimulation with anti-CD3, anti-CD28 antibodies (Serr et al., 2017). Similarly Treg induction is impaired in NOD mice with ongoing islet autoimmunity (Serr et al., 2017). In contrast, we observed an at least partial restoration of this Treg induction defect in children with longterm autoimmunity, which highlights that children with a slow progressor phenotype may have regulated the autoimmune response or are in a transient state of tolerance. This is in accordance with studies that identified an accumulation of protective genotypes in T1D susceptibility genes like *IL2*, *IL2Ra*, *INS VNTR* and *IL10* in these slow progressors (Achenbach et al., 2013).

For a mechanistic dissection of reasons for this T cell tolerance induction defect we focused on miRNAs, since they are known to regulate cellular states, like for example T cell activation, rather than single targets. Interestingly, the observed Treg induction defect during recent

activation of islet autoimmunity was accompanied by increased proliferative responses and increased frequencies of activated Foxp3^{intermediate}CD4⁺T cells, indicating differences in the activation threshold of the T cells in these children (Serr et al., 2017).

In line with its implication in the regulation of signal strength of the TCR stimulus in developing lymphocytes, we observed miRNA181a to be upregulated in peripheral CD4⁺T cells in children with recent activation of islet autoimmunity. Our observation, that addition of a miRNA181a mimic to Treg induction assays leads to increased proliferative responses accompanied by impaired Treg induction indicates, that miRNA181a might also be involved in the regulation of differences in activation thresholds in CD4⁺T cells from children at different stages of islet autoimmunity and thereby promote the differences in Treg induction potential (Serr et al., 2017).

Intriguingly, when we inhibited miRNA181a in NOD mice with insulin autoantibody (IAA)⁺ islet autoimmunity, we observed a reduction in islet infiltration (Serr et al., 2017). This is in line with findings that miRNA181a knockout mice develop experimental autoimmune encephalomyelitis (EAE) later and with a lower clinical score than wildtype mice (Schaffert et al., 2015). Whereas Schaffert and colleagues argue, that this effect in miRNA181a KO animals is due to a diminished capacity of autoreactive T cells to enter the central nervous system, our data provide an additional means of explanation. MiRNA181a is known to target negative regulators of T cell activation, such as PTEN and CTLA4 (Li et al., 2007). Accordingly, we observed decreased expression levels of PTEN and CTLA4 in cells treated with a miRNA181a mimic (Serr et al., 2017). This was accompanied by increased expression of CD28 and increased PI3K signaling, highlighting that, in addition to tuning TCR recognition thresholds, miRNA181a also impacts costimulatory signals (Serr et al., 2017).

Interestingly, we observed, that miRNA181a negatively regulates T cell tolerance induction by upregulating nuclear factor of activated T cells 5 (NFAT5) (Serr et al., 2017), a transcription factor originally known for its function in conditions of osmotic stress (Miyakawa et al., 1999). NFAT5 has however been reported to be induced upon TCR stimulation in a calcineurin-dependent manner, independent of osmotic stimuli and to regulate T cell proliferation (Haltermann et al., 2012; Trama et al., 2002). Accordingly, we found a predicted binding site for miRNA181a in the 3'UTR of the *Nfat5* gene. Indeed, we were able to demonstrate in luciferase assays that miRNA181a can directly downregulate *Nfat5* expression via binding to its 3'UTR. The upregulation of NFAT5 by miRNA181a is in contrast to the canonical function of miRNAs, which is the translational silencing or degradation of their target mRNAs (Bagga et al., 2005; Lim et al., 2005; Olsen and Ambros, 1999). There are several possible explanations for this upregulation: the observed induction could result from relief of miRNA181a-mediated repression of NFAT5, or be the consequence of the indirect regulation of a repression pathway. In accordance with this hypothesis, NFAT5 has been demonstrated before to be activated by PI3K signaling (Irrazabal et al., 2006). Since miRNA181a targets PTEN (Li et al.,

2007), a negative regulator of PI3K signaling, the activation of NFAT5 could be indirectly mediated via the inhibition of negative regulators of the PI3K signaling pathway. This is also in line, with the increased CD28 expression in cells treated with a miRNA181a mimic, since costimulatory signals through CD28 increase PI3K signaling.

Alternatively, recent studies have highlighted that in dependence of the cellular state and function, miRNAs can likewise upregulate the translation of their target mRNAs (Bukhari et al., 2016; Truesdell et al., 2012; Vasudevan, 2012; Vasudevan and Steitz, 2007; Vasudevan et al., 2007). Therefore, it is possible that miRNA181a could also directly upregulate NFAT5 translation. Translational upregulation of targets by miRNAs has however only been demonstrated in highly specialized cell types like oocytes (Truesdell et al., 2012) and under certain cellular conditions, especially in quiescent cells or under cell cycle arrest upon serum starvation (Bukhari et al., 2016; Truesdell et al., 2012; Vasudevan, 2012; Vasudevan and Steitz, 2007; Vasudevan et al., 2007). Hence, an indirect upregulation of NFAT5 by miRNA181a through the regulation of repressive pathways is more likely.

In line with our findings of increased NFAT5 levels in children with recent activation of islet autoimmunity (Serr et al., 2017), NFAT5 expression was linked previously to the development of rheumatoid arthritis and its inhibition was demonstrated to ameliorate arthritis in mouse models (Kim et al., 2014; Yoon et al., 2011). Similarly, we demonstrate that NFAT5 inhibition in IAA⁺ NOD mice significantly improves insulinitis scores, immune infiltration in the pancreas and autoantibody levels (Serr et al., 2017). Additionally, NFAT5 inhibition was accompanied by an increased frequency of Tregs in the pancreatic lymph nodes as well as directly in the pancreas of treated mice (Serr et al., 2017). In rheumatoid arthritis, the effect of NFAT5 on disease pathogenesis was demonstrated to be on macrophages (Kim et al., 2014), whereas our data indicate that the miRNA181a – NFAT5 signaling axis inhibits Treg induction in the peripheral immune system, by increasing the sensitivity to the TCR stimulus and might thereby regulate aberrant immune activation and defective T cell tolerance in islet autoimmunity (Serr et al., 2017). The possibility of NFAT5 inhibitors to potentially act beneficially both on innate and adaptive immune cells indicates a more holistic effect for the treatment of autoimmune diseases.

Apart from miRNA181a many other miRNAs target negative regulators of T cell activation and might therefore have a beneficial effect on Treg induction. Because of the important role of the miRNA17~92 cluster in TFH differentiation (Baumjohann et al., 2013a; Kang et al., 2013) and because miRNA92a is known to target PTEN and PHLPP2 signaling, we analyzed the effect of miRNA92a on Treg induction. When we added a miRNA92a antagomir to Treg induction assays *in vitro*, we observed significantly increased frequencies of induced Tregs (Serr et al., 2016b).

In accordance with the apparent opposing signaling requirements for Tregs and TFH cells and the increase in TFH precursor cell frequencies in children with recent activation of islet autoimmunity, we observed significantly enhanced expression of miRNA92a in these children. In contrast, in children with longterm islet autoimmunity, which had not yet progressed to symptomatic T1D, miRNA92a levels were comparable to those in children without autoantibodies. In line with the important role of TFH cells in antibody production, we noticed that miRNA92a expression levels correlated with the insulin autoantibody levels of the children (Serr et al., 2016b).

We verified the role of the miRNA17~92 cluster of miRNAs in TFH differentiation (Baumjohann et al., 2013a; Kang et al., 2013), in *in vitro* TFH induction assays: we observed a significant increase in the frequency of TFH precursors in these assays after addition of the miRNA92a mimic (Serr et al., 2016b). A miRNA92a antagomir on the other hand completely abolished TFH induction (Serr et al., 2016b).

Concerning the mechanism of action of miRNA92a in TFH differentiation, we identified a decreased expression of negative regulators of T cell activation such as PTEN, PHLPP2, Foxo1 and CTLA4 (Serr et al., 2016b), that are confirmed targets of miRNA92a (Jiang et al., 2010; Xiao et al., 2008) in samples from TFH induction assays with miRNA92a mimic. This is in line with findings, that TFH differentiation requires low levels of Foxo1, since Foxo1 represses Bcl6 expression (Stone et al., 2015; Xiao et al., 2014). PTEN and PHLPP2 are repressors of PI3K/Akt signaling and ICOS/PI3K signaling is a crucial component of the TFH differentiation program, and the germinal center reaction (Gigoux et al., 2009; Kang et al., 2013; Rolf et al., 2010). In line with these observations, we found miRNA92a-mediated TFH induction to be significantly impaired when a PI3K inhibitor was added to the culture (Serr et al., 2016b). In contrast, the addition of a PTEN inhibitor increased TFH differentiation, thereby highlighting, that miRNA92a-mediated TFH differentiation is dependent on PI3K signaling (Serr et al., 2016b).

ICOS signaling was also shown to downregulate krueppel-like factor 2 (KLF2), which has been demonstrated to be a key regulator of lymphocyte migration and homing (Carlson et al., 2006; Sebzda et al., 2008). KLF2 deficiency was shown to lead to excessive TFH differentiation, supposedly through regulation of the expression of the trafficking receptor sphingosin 1 phosphate receptor 1 (S1PR1), which inhibits TFH generation (Lee et al., 2015). We were able to link KLF2 to miRNA92a-mediated TFH induction, since a target site blocker that prohibits the binding of miRNA92a specifically to KLF2 abolishes TFH differentiation (Serr et al., 2016b).

Most importantly, we show a beneficial effect of a miRNA92a antagomir *in vivo* in NOD mice: we observed reduced TFH frequencies in the peripheral blood and pancreatic lymph nodes. Additionally, we found reduced numbers of activated T cells directly in the pancreas, accompanied by a decrease in immune infiltration, an improvement in insulinitis score and reduction of insulin autoantibody levels. In accordance with our *in vitro* findings, we also

observed a significant increase in Treg frequencies in lymph nodes and spleen of mice treated with the miRNA92a antagomir (Serr et al., 2016b).

Concerning the clinical application miRNAs are promising new drug targets, because they can be targeted by small, highly specific oligonucleotides. MiRNA inhibitors (also called antagomirs) have already been tested successfully in the clinic for the treatment of hepatitis C virus infections (Janssen et al., 2013). The specific delivery of miRNA inhibitors *in vivo* to target cells, especially immune cells, is however challenging, since miRNAs are negatively charged and thereby do not penetrate the cell membrane (summarized in (Li and Rana, 2014)). Advances have been made concerning the targeted delivery of miRNA inhibitors, especially by encapsulation techniques (summarized in (Li and Rana, 2014)). Nanoparticles for encapsulation have been studied in particular and various nanoparticles have been shown to mediate efficient uptake of small RNAs by lymphocyte populations (Peer et al., 2008). A more specific targeting of T cells was achieved by the use of a single chain CD7 antibody (scFvCD7) fused to a oligonucleotide-nona-arginine peptide (Kumar et al., 2008).

Apart from their potential use as drug targets the stable and easy detection of miRNAs in the serum and also in lymphocyte populations makes them valuable biomarker candidates. The heterogeneity in the progression from islet autoimmunity to symptomatic T1D necessitates the discovery of biomarkers that will enable a better prediction for the time of progression from seroconversion to symptomatic disease. In this regard, TFH cell subset frequencies and miRNA92a levels might function as possible tools to identify children with different progression rates to symptomatic disease or might be useful to predict autoantibody development; however, to obtain conclusive evidence for this, longitudinal samples would need to be analyzed.

In accordance with our findings, miRNA92a was identified to be differentially expressed in the serum of children with and without autoantibodies in a recent study by Alberto Pugliese's group (Snowwhite et al., 2017). That this differential expression was only borderline significant and not significant after further data processing, might be due to the heterogeneous group of autoantibody positive children in the study: these children were not stratified based on the duration of autoantibody positivity (Snowwhite et al., 2017).

Furthermore, according to our data, miRNA181a might be a possible marker to identify children that could benefit from T cell tolerance induction strategies, however we have only analyzed expression levels in lymphocytes and differences in expression in the serum have not been investigated (Serr et al., 2017). The fine tuning of TCR signal strength by miRNA181a also highlights that the definition of subimmunogenic conditions might be different between patients and needs to be determined in a personalized way.

Peptide vaccination for the restoration of tolerance in T1D has been used before in clinical trials and is a long envisioned goal of researches, because it is considered as safe compared

to alternative immunosuppressive therapies. Accordingly, a primary prevention trial for oral insulin treatment in children genetically at risk for T1D (pre-POINT trial) was recently finished and showed no adverse events (Bonifacio et al., 2015).

Since Treg induction is limited in previously activated T cells, translating Treg induction strategies into the clinic would limit these efforts to primary prevention, meaning the prevention of the development of islet autoantibodies in children genetically at risk for developing T1D. In this regard, the pre-POINT study identified an increase in immune cells with a regulatory phenotype after treatment with oral insulin (Bonifacio et al., 2015). However, primary prevention efforts are challenging in the context of T1D, since the peak incidence of seroconversion is very early in life, between 9 months and 2 years of age (Giannopoulou et al., 2015; Ziegler and Bonifacio, 2012). Therefore, many clinical studies have focused on secondary prevention, meaning the prevention of the progression from seroconversion to the symptomatic disease.

However, the broad Treg induction impairment seen in T cells from children with recent activation of islet autoimmunity (Serr et al., 2017) indicates that antigen-specific tolerization strategies might be challenging in this subset of children, which highlights the need of developing combinatorial approaches to interfere with ongoing immune activation while maintaining antigen specificity. Our data indicate additionally, that the effectiveness of antigen-specific tolerance induction strategies in secondary prevention efforts may be beneficial in children with longterm islet autoimmunity, who have passed the critical period after islet autoimmunity onset without progressing to symptomatic T1D. Limiting the immune activation in combination with Treg induction strategies might make the strategy more robust for a broader cohort of children. Our data on the regulation of aberrant immune activation and T cell tolerance defects mediated by miRNA181a and miRNA92a indicate that these might be potential new drug targets suitable for combination therapies.

To optimize Treg induction strategies to interfere with autoimmunity, the subimmunogenic delivery of autoantigenic peptides needs to be optimized and therefore alternative routes of application should also be taken into consideration. Hereof, progress has been made in the use of dissolving microneedle patches. This particular mode of administration might mimic best the subcutaneous implantation of osmotic minipumps from the murine model in a less invasive way and promises success due to the high availability of antigen-presenting cells in the skin. Accordingly, Sean Sullivan and colleagues have used microneedle patches for the administration of influenza vaccines and demonstrated that they are superior in the vaccination efficacy compared to traditional intra muscular injection (Sullivan et al., 2010).

In the regard of clinical studies, the novel insulin-specific tetramer reagents developed in the context of this thesis, offer a helpful tool to better assess the immunological success of Treg

induction strategies and will therefore be useful to optimize Treg induction strategies in the clinic. This is an important step that is currently missing in clinical trials.

In order to develop effective personalized medicines for the treatment or reduction of islet autoimmunity, it is additionally important to overcome the problem of limited translatability from the NOD mouse to the human disease. The use of humanized mouse models offers a useful intermediate and might help to better assess the value of new immune modulatory therapies, before the challenging and elaborate introduction into the clinic. To understand, whether Treg induction defects are also present in pre-symptomatic T1D in the human immune system *in vivo*, mimicking the different stages of islet autoimmunity and also disease progression in humanized mice will be an important step. Therefore, humanized mice can be reconstituted with hematopoietic cells from children at different stages of islet autoimmunity. However, the reconstitution of humanized mice with HSCs from peripheral blood faces important challenges. The reconstitution of humanized mice is most efficient when human hematopoietic stem cells are used, but there is limited availability of these cells in the peripheral blood. PBMCs can be used for reconstitution, however humanized mice reconstituted with PBMCs develop graft versus host disease after a very short time and are not suitable for longterm studies (King et al., 2008). There have however been advances in stem cell research that might enable the reconstitution with HSCs even from adult donors. In this regard two research groups have recently developed protocols for the reprogramming of adult mouse endothelial cells into HSCs (Lis et al., 2017) and the induction of the HSC program in human pluripotent stem cells, respectively (Sugimura et al., 2017). These advances may enable the reconstitution of humanized mice with HSCs even from non-neonate donors and help to establish preclinical models that mimic islet autoimmunity.

In sum, the data presented in this thesis contribute to the understanding of requirements for efficient Treg induction as well as to the mechanistic basis of aberrant immune activation and defective tolerance in islet autoimmunity. Additionally, the introduced novel tetramer reagents and humanized mice are new tools that will help to improve clinical trial readout, as well as the evaluation of translatability of new reagents to the human disease.

5. References

Achenbach, P., Hummel, M., Thumer, L., Boerschmann, H., Hofelmann, D., and Ziegler, A.G. (2013). Characteristics of rapid vs slow progression to type 1 diabetes in multiple islet autoantibody-positive children. *Diabetologia* 56, 1615-1622.

Achenbach, P., Lampasona, V., Landherr, U., Koczwara, K., Krause, S., Grallert, H., Winkler, C., Pfluger, M., Illig, T., Bonifacio, E., and Ziegler, A.G. (2009). Autoantibodies to zinc transporter 8 and SLC30A8 genotype stratify type 1 diabetes risk. *Diabetologia* 52, 1881-1888.

Alleva, D.G., Crowe, P.D., Jin, L., Kwok, W.W., Ling, N., Gottschalk, M., Conlon, P.J., Gottlieb, P.A., Putnam, A.L., and Gaur, A. (2001). A disease-associated cellular immune response in type 1 diabetics to an immunodominant epitope of insulin. *The Journal of clinical investigation* 107, 173-180.

Aly, T.A., Ide, A., Jahromi, M.M., Barker, J.M., Fernando, M.S., Babu, S.R., Yu, L., Miao, D., Erlich, H.A., Fain, P.R., Barriga, K.J., Norris, J.M., Rewers, M.J., and Eisenbarth, G.S. (2006). Extreme genetic risk for type 1A diabetes. *Proceedings of the National Academy of Sciences* 103, 14074-14079.

Apostolou, I., Sarukhan, A., Klein, L., and von Boehmer, H. (2002). Origin of regulatory T cells with known specificity for antigen. *Nature immunology* 3, 756-763.

Apostolou, I., and von Boehmer, H. (2004). In vivo instruction of suppressor commitment in naive T cells. *The Journal of experimental medicine* 199, 1401-1408.

Asao, H., Okuyama, C., Kumaki, S., Ishii, N., Tsuchiya, S., Foster, D., and Sugamura, K. (2001). Cutting Edge: The Common γ -Chain Is an Indispensable Subunit of the IL-21 Receptor Complex. *The Journal of Immunology* 167, 1-5.

Asseman, C., Mauze, S., Leach, M.W., Coffman, R.L., and Powrie, F. (1999). An Essential Role for Interleukin 10 in the Function of Regulatory T Cells That Inhibit Intestinal Inflammation. *The Journal of experimental medicine* 190, 995-1004.

Atkinson, M.A., and Leiter, E.H. (1999). The NOD mouse model of type 1 diabetes: As good as it gets? *Nature medicine* 6, 601-604.

Avery, D.T., Deenick, E.K., Ma, C.S., Suryani, S., Simpson, N., Chew, G.Y., Chan, T.D., Palendira, U., Bustamante, J., Boisson-Dupuis, S., Choo, S., Bleasel, K.E., Peake, J., King, C., French, M.A., Engelhard, D., Al-Hajjar, S., Al-Muhsen, S., Magdorf, K., Roesler, J., Arkwright, P.D., Hissaria, P., Riminton, D.S., Wong, M., Brink, R., Fulcher, D.A., Casanova, J.L., Cook, M.C., and Tangye, S.G. (2010). B cell-intrinsic signaling through IL-21 receptor and STAT3 is required for establishing long-lived antibody responses in humans. *The Journal of experimental medicine* 207, 155-171.

Babaya, N., Liu, E., Miao, D., Li, M., Yu, L., and Eisenbarth, G.S. (2009). Murine high specificity/sensitivity competitive europium insulin autoantibody assay. *Diabetes technology & therapeutics* 11, 227-233.

Baek, D., Villén, J., Shin, C., Camargo, F.D., Gygi, S.P., and Bartel, D.P. (2008). The impact of microRNAs on protein output. *Nature* 455, 64-71.

Baekkeskov, S., Aanstoot, H.-J., Christgai, S., Reetz, A., Solimena, M., Cascalho, M., Folli, F., Richter-Olesen, H., and Camilli, P.-D. (1990). Identification of the 64K autoantigen in insulin-dependent diabetes as the GABA-synthesizing enzyme glutamic acid decarboxylase. *Nature* 347, 151-156.

Bagga, S., Bracht, J., Hunter, S., Massirer, K., Holtz, J., Eachus, R., and Pasquinelli, A.E. (2005). Regulation by let-7 and lin-4 miRNAs Results in Target mRNA Degradation. *Cell* 122, 553-563.

Baron, U., Floess, S., Wiczorek, G., Baumann, K., Grutzkau, A., Dong, J., Thiel, A., Boeld, T.J., Hoffmann, P., Edinger, M., Turbachova, I., Hamann, A., Olek, S., and Huehn, J. (2007). DNA demethylation in the human FOXP3 locus discriminates regulatory T cells from activated FOXP3(+) conventional T cells. *European journal of immunology* 37, 2378-2389.

Barrett, J.C., Clayton, D.G., Concannon, P., Akolkar, B., Cooper, J.D., Erlich, H.A., Julier, C., Morahan, G., Nerup, J., Nierras, C., Plagnol, V., Pociot, F., Schuilenburg, H., Smyth, D.J., Stevens, H., Todd, J.A., Walker, N.M., Rich, S.S., and Type 1 Diabetes Genetics, C. (2009). Genome-wide association study and meta-analysis find that over 40 loci affect risk of type 1 diabetes. *Nature genetics* 41, 703-707.

Baumjohann, D., Kageyama, R., Clingan, J.M., Morar, M.M., Patel, S., de Kouchkovsky, D., Bannard, O., Bluestone, J.A., Matloubian, M., Ansel, K.M., and Jeker, L.T. (2013a). The microRNA cluster miR-17-92 promotes TFH cell differentiation and represses subset-inappropriate gene expression. *Nature immunology* 14, 840-848.

Baumjohann, D., Preite, S., Reboldi, A., Ronchi, F., Ansel, K.M., Lanzavecchia, A., and Sallusto, F. (2013b). Persistent Antigen and Germinal Center B Cells Sustain T Follicular Helper Cell Responses and Phenotype. *Immunity* 38, 596-605.

Bennett, C.L., Christie, J., Ramsdell, F., Brunkow, M.E., Ferguson, P.J., Whitesell, L., Kelly, T.E., Saulsbury, F.T., Chance, P.F., and Ochs, H.D. (2001). The immune dysregulation, polyendocrinopathy, enteropathy, X-linked syndrome (IPEX) is caused by mutations of FOXP3. *Nature genetics* 27, 20-21.

Bentebibel, S.E., Lopez, S., Obermoser, G., Schmitt, N., Mueller, C., Harrod, C., Flano, E., Mejias, A., Albrecht, R.A., Blankenship, D., Xu, H., Pascual, V., Banchereau, J., Garcia-Sastre, A., Palucka, A.K., Ramilo, O., and Ueno, H. (2013). Induction of ICOS+CXCR3+CXCR5+ TH cells correlates with antibody responses to influenza vaccination. *Science translational medicine* 5, 176ra132.

Blazar, B.R., Lindberg, F.P., Ingulli, E., Panoskaltsis-Mortari, A., Oldenborg, P.-A., Iizuka, K., Yokoyama, W.M., and Taylor, P.A. (2001). Cd47 (Integrin-Associated Protein) Engagement of Dendritic Cell and Macrophage Counterreceptors Is Required to Prevent the Clearance of Donor Lymphohematopoietic Cells. *The Journal of experimental medicine* 194, 541-550.

Bonifacio, E., Hummel, M., Walter, M., Schmid, S., and Ziegler, A.-G. (2004). IDDM1 and Multiple Family History of Type 1 Diabetes Combine to Identify Neonates at High Risk for Type 1 Diabetes. *Diabetes care* 27, 2695-2700.

Bonifacio, E., Shattock, M., Dean, B.M., Bottazzo, G.F., Bingley, P.M., Gale, E.A.M., and Dunger, D. (1990). Quantification of islet-cell antibodies and prediction of insulin-dependent diabetes. *The Lancet* 335, 147-149.

Bonifacio, E., Ziegler, A.G., Klingensmith, G., and et al. (2015). Effects of high-dose oral insulin on immune responses in children at high risk for type 1 diabetes: The pre-point randomized clinical trial. *JAMA* 313, 1541-1549.

Bosma, G.C., Custer, R.P., and Bosma, M.J. (1983). A severe combined immunodeficiency mutation in the mouse. *Nature* 301, 527-530.

Bottazzo, G., Florin-Christensen, A., and Doniach, D. (1974). Islet-cell antibodies in Diabetes Mellitus with autoimmune polyendocrine deficiencies *The Lancet* 304, 1279-1283.

Breitfeld, D., Ohl, L., Kremmer, E., Ellwart, J., Sallusto, F., Lipp, M., and Forster, R. (2000). Follicular B helper T cells express CXC chemokine receptor 5, localize to B cell follicles, and support immunoglobulin production. *The Journal of experimental medicine* 192, 1545-1552.

Brognard, J., Sierrecki, E., Gao, T., and Newton, A.C. (2007). PHLPP and a Second Isoform, PHLPP2, Differentially Attenuate the Amplitude of Akt Signaling by Regulating Distinct Akt Isoforms. *Molecular cell* 25, 917-931.

Brunkow, M.E., Jeffery, E.W., Hjerrild, K.A., Paepers, B., Clark, L.B., Yasayko, S.A., Wilkinson, J.E., Galas, D., Ziegler, S.F., and Ramsdell, F. (2001). Disruption of a new forkhead/winged-helix protein, scurfy, results in the fatal lymphoproliferative disorder of the scurfy mouse. *Nature genetics* 27, 68-73.

Brusko, T., Wasserfall, C., McGrail, K., Schatz, R., Viener, H.L., Schatz, D., Haller, M., Rockell, J., Gottlieb, P., Clare-Salzler, M., and Atkinson, M. (2007). No alterations in the frequency of FOXP3+ regulatory T-cells in type 1 diabetes. *Diabetes* 56, 604-612.

Brusko, T.M., Wasserfall, C.H., Clare-Salzler, M.J., Schatz, D.A., and Atkinson, M.A. (2005). Functional Defects and the Influence of Age on the Frequency of CD4+CD25+ T-Cells in Type 1 Diabetes. *Diabetes* 54, 1407-1414.

Bukhari, S.I., Truesdell, S.S., Lee, S., Kollu, S., Classon, A., Boukhali, M., Jain, E., Mortensen, R.D., Yanagiya, A., Sadreyev, R.I., Haas, W., and Vasudevan, S. (2016). A Specialized Mechanism of Translation Mediated by FXR1a-Associated MicroRNP in Cellular Quiescence. *Molecular cell* 61, 760-773.

Cao, X., Cai, S.F., Fehniger, T.A., Song, J., Collins, L.I., Piwnicka-Worms, D.R., and Ley, T.J. (2007). Granzyme B and Perforin Are Important for Regulatory T Cell-Mediated Suppression of Tumor Clearance. *Immunity* 27, 635-646.

Cao, X., Shores, E.W., Hu-Li, J., Anver, M.R., Kelsall, B.L., Russell, S.M., Drago, J., Noguchi, M., Grinberg, A., Bloom, E.T., Paul, W.E., Katz, S.I., Love, P.E., and Leonard, W.J. (1995). Defective lymphoid development in mice lacking expression of the common cytokine receptor γ chain. *Immunity* 2, 223-238.

Carlson, C.M., Endrizzi, B.T., Wu, J., Ding, X., Weinreich, M.A., Walsh, E.R., Wani, M.A., Lingrel, J.B., Hogquist, K.A., and Jameson, S.C. (2006). Kruppel-like factor 2 regulates thymocyte and T-cell migration. *Nature* 442, 299-302.

Chen, D., Ueda, R., Harding, F., Patil, N., Mao, Y., Kurahara, C., Platenburg, G., and Huang, M. (2003). Characterization of HLA DR3/DQ2 transgenic mice: a potential humanized animal model for autoimmune disease studies. *European journal of immunology* *33*, 172-182.

Chen, Z., De Kauwe, A.L., Keech, C., Wijburg, O., Simpfendorfer, K., Alexander, W.S., and McCluskey, J. (2006). Humanized transgenic mice expressing HLA DR4-DQ3 haplotype: reconstitution of phenotype and HLA-restricted T-cell responses. *Tissue Antigens* *68*, 210-219.

Choi, Y.S., Kageyama, R., Eto, D., Escobar, T.C., Johnston, R.J., Monticelli, L., Lao, C., and Crotty, S. (2011a). Bcl6 dependent T follicular helper cell differentiation diverges from effector cell differentiation during priming and depends on the gene Icos. *Immunity* *34*, 932-946.

Choi, Y.S., Kageyama, R., Eto, D., Escobar, T.C., Johnston, R.J., Monticelli, L., Lao, C., and Crotty, S. (2011b). ICOS receptor instructs T follicular helper cell versus effector cell differentiation via induction of the transcriptional repressor Bcl6. *Immunity* *34*, 932-946.

Choi, Y.S., Yang, J.A., Yusuf, I., Johnston, R.J., Greenbaum, J., Peters, B., and Crotty, S. (2013). Bcl6 Expressing Follicular Helper CD4 T Cells Are Fate Committed Early and Have the Capacity To Form Memory. *The Journal of Immunology* *190*, 4014-4026.

Christianson, S.W., Greiner, D.L., Schweitzer, I.B., Gott, B., Beamer, G.L., Schweitzer, P.A., Hesselton, R.M., and Shultz, L.D. (1996). Role of Natural Killer Cells on Engraftment of Human Lymphoid Cells and on Metastasis of Human T-Lymphoblastoid Leukemia Cells in C57BL/6J-scidMice and in C57BL/6J-scid bgMice. *Cellular Immunology* *171*, 186-199.

Cobb, B.S., Hertweck, A., Smith, J., O'Connor, E., Graf, D., Cook, T., Smale, S.T., Sakaguchi, S., Livesey, F.J., Fisher, A.G., and Merckenschlager, M. (2006). A role for Dicer in immune regulation. *The Journal of experimental medicine* *203*, 2519-2527.

Cobb, B.S., Nesterova, T.B., Thompson, E., Hertweck, A., O'Connor, E., Godwin, J., Wilson, C.B., Brockdorff, N., Fisher, A.G., Smale, S.T., and Merckenschlager, M. (2005). T cell lineage choice and differentiation in the absence of the RNase III enzyme Dicer. *The Journal of experimental medicine* *201*, 1367-1373.

Covassin, L., Laning, J., Abdi, R., Langevin, D.L., Phillips, N.E., Shultz, L.D., and Brehm, M.A. (2011). Human peripheral blood CD4 T cell-engrafted non-obese diabetic-scid IL2rgamma(null) H2-Ab1 (tm1Gru) Tg (human leucocyte antigen D-related 4) mice: a mouse model of human allogeneic graft-versus-host disease. *Clinical and experimental immunology* *166*, 269-280.

Crawford, F., Stadinski, B., Jin, N., Michels, A., Nakayama, M., Pratt, P., Marrack, P., Eisenbarth, G., and Kappler, J.W. (2011). Specificity and detection of insulin-reactive CD4+ T cells in type 1 diabetes in the nonobese diabetic (NOD) mouse. *Proceedings of the National Academy of Sciences of the United States of America* 108, 16729-16734.

Daniel, C., Weigmann, B., Bronson, R., and von Boehmer, H. (2011). Prevention of type 1 diabetes in mice by tolerogenic vaccination with a strong agonist insulin mimetope. *The Journal of experimental medicine* 208, 1501-1510.

Daniel, C., Wennhold, K., Kim, H.J., and von Boehmer, H. (2010). Enhancement of antigen-specific Treg vaccination in vivo. *Proceedings of the National Academy of Sciences of the United States of America* 107, 16246-16251.

Daniel, D., Gill, R.G., Schloot, N., and Wegmann, D. (1995a). Epitope specificity, cytokine production profile and diabetogenic activity of insulin-specific T cell clones isolated from NOD mice. *European journal of immunology* 25, 1056-1062.

Daniel, D., Gill, R.G., Schloot, N., and Wegmann, D. (1995b). Epitope specificity, cytokine production profile and diabetogenic activity of insulin-specific T cell clones isolated from NOD mice. *European Journal of Immunology* 25, 1056-1062.

Deenick, E.K., Chan, A., Ma, C.S., Gatto, D., Schwartzberg, P.L., Brink, R., and Tangye, S.G. (2010). Follicular Helper T Cell Differentiation Requires Continuous Antigen Presentation that Is Independent of Unique B Cell Signaling. *Immunity* 33, 241-253.

Delgoffe, G.M., Woo, S.-R., Turnis, M.E., Gravano, D.M., Guy, C., Overacre, A.E., Bettini, M.L., Vogel, P., Finkelstein, D., Bonnevier, J., Workman, C.J., and Vignali, D.A.A. (2013). Stability and function of regulatory T cells is maintained by a neuropilin-1-semaphorin-4a axis. *Nature* 501, 252-256.

DiSanto, J.P., Muller, W., Guy-Grand, D., Fischer, A., and Rajewsky, K. (1995). Lymphoid development in mice with a targeted deletion of the interleukin 2 receptor gamma chain. *Proceedings of the National Academy of Sciences of the United States of America* 92, 377-381.

Ehrlich, P. (1906). *Collected studies on immunity* (J. Wiley & sons).

Emery, L.M., Babu, S., Bugawan, T.L., Norris, J.M., Erlich, H.A., Eisenbarth, G.S., and Rewers, M. (2005). Newborn HLA-DR,DQ genotype screening: age- and ethnicity-specific type 1 diabetes risk estimates. *Pediatric Diabetes* 6, 136-144.

Ettinger, R.A., and Kwok, W.W. (1998). A Peptide Binding Motif for HLA-DQA1*0102/DQB1*0602, the Class II MHC Molecule Associated with Dominant Protection in Insulin-Dependent Diabetes Mellitus. *The Journal of Immunology* 160, 2365-2373.

Fahlén, L., Read, S., Gorelik, L., Hurst, S.D., Coffman, R.L., Flavell, R.A., and Powrie, F. (2005). T cells that cannot respond to TGF- β escape control by CD4⁺ CD25⁺ regulatory T cells. *The Journal of experimental medicine* 201, 737-746.

Fairchild, P.J., Wildgoose, R., Atherton, E., Webb, S., and Wraith, D.C. (1993). An autoantigenic T cell epitope forms unstable complexes with class II MHC: a novel route for escape from tolerance induction. *International immunology* 5, 1151-1158.

Ferreira, R.C., Simons, H.Z., Thompson, W.S., Cutler, A.J., Dopico, X.C., Smyth, D.J., Mashar, M., Schuilenburg, H., Walker, N.M., Dunger, D.B., Wallace, C., Todd, J.A., Wicker, L.S., and Pekalski, M.L. (2015). IL-21 production by CD4⁺ effector T cells and frequency of circulating follicular helper T cells are increased in type 1 diabetes patients. *Diabetologia* 58, 781-790.

Floess, S., Freyer, J., Siewert, C., Baron, U., Olek, S., Polansky, J., Schlawe, K., Chang, H.D., Bopp, T., Schmitt, E., Klein-Hessling, S., Serfling, E., Hamann, A., and Huehn, J. (2007). Epigenetic control of the foxp3 locus in regulatory T cells. *PLoS biology* 5, e38.

Fontenot, J.D., Gavin, M.A., and Rudensky, A.Y. (2003). Foxp3 programs the development and function of CD4⁺CD25⁺ regulatory T cells. *Nature immunology* 4, 330-336.

Fontenot, J.D., Rasmussen, J.P., Williams, L.M., Dooley, J.L., Farr, A.G., and Rudensky, A.Y. (2005). Regulatory T Cell Lineage Specification by the Forkhead Transcription Factor Foxp3. *Immunity* 22, 329-341.

Fu, F., Li, Y., Qian, S., Lu, L., Chambers, F., Starzl, T.E., Fung, J.J., and Thomson, A.W. (1996). Costimulatory molecule-deficient dendritic cell progenitors (MHC class II⁺, CD80dim, CD86⁻) prolong cardiac allograft survival in nonimmunosuppressed recipients. *Transplantation* 62, 659-665.

Garçon, F., Patton, D.T., Emery, J.L., Hirsch, E., Rottapel, R., Sasaki, T., and Okkenhaug, K. (2008). CD28 provides T-cell costimulation and enhances PI3K activity at the immune synapse

independently of its capacity to interact with the p85/p110 heterodimer. *Blood* *111*, 1464-1471.

Giannopoulou, E.Z., Winkler, C., Chmiel, R., Matzke, C., Scholz, M., Beyerlein, A., Achenbach, P., Bonifacio, E., and Ziegler, A.-G. (2015). Islet autoantibody phenotypes and incidence in children at increased risk for type 1 diabetes. *Diabetologia* *58*, 2317-2323.

Gigoux, M., Shang, J., Pak, Y., Xu, M., Choe, J., Mak, T.W., and Suh, W.-K. (2009). Inducible costimulator promotes helper T-cell differentiation through phosphoinositide 3-kinase. *Proceedings of the National Academy of Sciences* *106*, 20371-20376.

Giri, J.G., Ahdieh, M., Eisenman, J., Shanebeck, K., Grabstein, K., Kumaki, S., Namen, A., Park, L.S., Cosman, D., and Anderson, D. (1994). Utilization of the beta and gamma chains of the IL-2 receptor by the novel cytokine IL-15. *The EMBO journal* *13*, 2822-2830.

Goenka, R., Barnett, L.G., Silver, J.S., O'Neill, P.J., Hunter, C.A., Cancro, M.P., and Laufer, T.M. (2011). Cutting edge: dendritic cell-restricted antigen presentation initiates the follicular helper T cell program but cannot complete ultimate effector differentiation. *Journal of immunology* *187*, 1091-1095.

Gondek, D.C., Lu, L.-F., Quezada, S.A., Sakaguchi, S., and Noelle, R.J. (2005). Cutting Edge: Contact-Mediated Suppression by CD4+CD25+ Regulatory Cells Involves a Granzyme B-Dependent, Perforin-Independent Mechanism. *The Journal of Immunology* *174*, 1783-1786.

Gorsuch, A.N., Lister, J., Dean, B.M., Spencer, K.M., McNally, J.M., Bottazzo, G.F., and Cudworth, A.G. (1981). Evidence for a long prediabetic period in Type 1 (insulin-dependent) Diabetes Mellitus. *The Lancet* *318*, 1363-1365.

Gottschalk, R.A., Corse, E., and Allison, J.P. (2010). TCR ligand density and affinity determine peripheral induction of Foxp3 in vivo. *The Journal of experimental medicine* *207*, 1701-1711.

Gottschalk, R.A., Hathorn, M.M., Beuneu, H., Corse, E., Dustin, M.L., Altan-Bonnet, G., and Allison, J.P. (2012). Distinct influences of peptide-MHC quality and quantity on in vivo T-cell responses. *Proceedings of the National Academy of Sciences of the United States of America* *109*, 881-886.

Green, E.A., Gorelik, L., McGregor, C.M., Tran, E.H., and Flavell, R.A. (2003). CD4+CD25+ T regulatory cells control anti-islet CD8+ T cells through TGF- β -TGF- β receptor interactions in type 1 diabetes. *Proceedings of the National Academy of Sciences* *100*, 10878-10883.

Grishok, A., Pasquinelli, A.E., Conte, D., Li, N., Parrish, S., Ha, I., Baillie, D.L., Fire, A., Ruvkun, G., and Mello, C.C. (2001). Genes and Mechanisms Related to RNA Interference Regulate Expression of the Small Temporal RNAs that Control *C. elegans* Developmental Timing. *Cell* 106, 23-34.

Hale, J.S., Youngblood, B., Latner, Donald R., Mohammed, Ata Ur R., Ye, L., Akondy, Rama S., Wu, T., Iyer, Smita S., and Ahmed, R. (2013). Distinct Memory CD4+ T Cells with Commitment to T Follicular Helper- and T Helper 1-Cell Lineages Are Generated after Acute Viral Infection. *Immunity* 38, 805-817.

Haley, B., and Zamore, P.D. (2004). Kinetic analysis of the RNAi enzyme complex. *Nat Struct Mol Biol* 11, 599-606.

Halterman, J.A., Kwon, H.M., and Warnhoff, B.R. (2012). Tonicity-independent regulation of the osmosensitive transcription factor TonEBP (NFAT5). *American Journal of Physiology Cell Physiology* 302, C1-8.

Hammond, S.M., Bernstein, E., Beach, D., and Hannon, G.J. (2000). An RNA-directed nuclease mediates post-transcriptional gene silencing in *Drosophila* cells. *Nature* 404, 293-296.

Hammond, S.M., Boettcher, S., Caudy, A.A., Kobayashi, R., and Hannon, G.J. (2001). Argonaute2, a Link Between Genetic and Biochemical Analyses of RNAi. *Science* 293, 1146-1150.

Hardtke, S., Ohl, L., and Förster, R. (2005). Balanced expression of CXCR5 and CCR7 on follicular T helper cells determines their transient positioning to lymph node follicles and is essential for efficient B-cell help. *Blood* 106, 1924-1931.

Harker, J.A., Lewis, G.M., Mack, L., and Zuniga, E.I. (2011). Late Interleukin-6 Escalates T Follicular Helper Cell Responses and Controls a Chronic Viral Infection. *Science* 334, 825-829.

Harrison, L.C., Honeyman, M.C., Steele, C.E., Stone, N.L., Saruger, E., Bonifacio, E., Couper, J.J., and Colman, P.G. (2004). Pancreatic beta-cell function and immune responses to insulin after administration of intranasal insulin to humans at risk for type 1 diabetes. *Diabetes care* 27, 2348-2355.

Haspot, F., Séveno, C., Dugast, A.-S., Coulon, F., Renaudin, K., Usal, C., Hill, M., Anegón, I., Heslan, M., Josien, R., Brouard, S., Souillou, J.-P., and Vanhove, B. (2005). Anti-CD28

Antibody-Induced Kidney Allograft Tolerance Related to Tryptophan Degradation and TCR–Class II– B7+ Regulatory Cells. *American Journal of Transplantation* 5, 2339-2348.

Hattori, M., Buse, J., Jackson, R., Glimcher, L., Dorf, M., Minami, M., Makino, S., Moriwaki, K., Kuzuya, H., Imura, H., and et, a. (1986). The NOD mouse: recessive diabetogenic gene in the major histocompatibility complex. *Science* 231, 733-735.

Haynes, N.M., Allen, C.D.C., Lesley, R., Ansel, K.M., Killeen, N., and Cyster, J.G. (2007). Role of CXCR5 and CCR7 in Follicular Th Cell Positioning and Appearance of a Programmed Cell Death Gene-1^{High} Germinal Center-Associated Subpopulation. *The Journal of Immunology* 179, 5099-5108.

He, J., Tsai, L.M., Leong, Y.A., Hu, X., Ma, C.S., Chevalier, N., Sun, X., Vandenberg, K., Rockman, S., Ding, Y., Zhu, L., Wei, W., Wang, C., Karnowski, A., Belz, G.T., Ghali, J.R., Cook, M.C., Riminton, D.S., Veillette, A., Schwartzberg, P.L., Mackay, F., Brink, R., Tangye, S.G., Vinuesa, C.G., Mackay, C.R., Li, Z., and Yu, D. (2013). Circulating precursor CCR7(lo)PD-1(hi) CXCR5(+) CD4(+) T cells indicate Tfh cell activity and promote antibody responses upon antigen reexposure. *Immunity* 39, 770-781.

He, X.L., Radu, C., Sidney, J., Sette, A., Ward, E.S., and Garcia, K.C. (2002). Structural snapshot of aberrant antigen presentation linked to autoimmunity: the immunodominant epitope of MBP complexed with I-Au. *Immunity* 17, 83-94.

Hemminki, K., Li, X., Sundquist, J., and Sundquist, K. (2009). Familial association between type 1 diabetes and other autoimmune and related diseases. *Diabetologia* 52, 1820-1828.

Hoppu, S., Härkönen, T., Ronkainen, M.S., Simell, S., Hekkala, A., Toivonen, A., Ilonen, J., Simell, O., and Knip, M. (2006). IA-2 antibody isotypes and epitope specificity during the prediabetic process in children with HLA-conferred susceptibility to type I diabetes. *Clinical and experimental immunology* 144, 59-66.

Hoppu, S., Ronkainen, M.S., Kimpimaki, T., Simell, S., Korhonen, S., Ilonen, J., Simell, O., and Knip, M. (2004). Insulin Autoantibody Isotypes during the Prediabetic Process in Young Children with Increased Genetic Risk of Type 1 Diabetes. *Pediatric research* 55, 236-242.

Hori, S., Nomura, T., and Sakaguchi, S. (2003). Control of Regulatory T Cell Development by the Transcription Factor Foxp3. *Science* 299, 1057-1061.

Hummel, M., Bonifacio, E., Schmid, S., Walter, M., Knopff, A., and Ziegler, A.G. (2004). Brief communication: early appearance of islet autoantibodies predicts childhood type 1 diabetes in offspring of diabetic parents. *Annals of internal medicine* 140, 882-886.

Hutvagner, G., McLachlan, J., Pasquinelli, A.E., Bálint, É., Tuschl, T., and Zamore, P.D. (2001). A Cellular Function for the RNA-Interference Enzyme Dicer in the Maturation of the let-7 Small Temporal RNA. *Science* 293, 834-838.

Hutvagner, G., and Zamore, P.D. (2002). A microRNA in a Multiple-Turnover RNAi Enzyme Complex. *Science* 297, 2056-2060.

Insel, R.A., Dunne, J.L., Atkinson, M.A., Chiang, J.L., Dabelea, D., Gottlieb, P.A., Greenbaum, C.J., Herold, K.C., Krischer, J.P., Lernmark, Å., Ratner, R.E., Rewers, M.J., Schatz, D.A., Skyler, J.S., Sosenko, J.M., and Ziegler, A.-G. (2015). Staging Presymptomatic Type 1 Diabetes: A Scientific Statement of JDRF, the Endocrine Society, and the American Diabetes Association. *Diabetes care* 38, 1964-1974.

International Diabetes Federation (2015). *IDF Diabetes Atlas* (Brussels, Belgium).

Irrazabal, C.E., Burg, M.B., Ward, S.G., and Ferraris, J.D. (2006). Phosphatidylinositol 3-kinase mediates activation of ATM by high NaCl and by ionizing radiation: Role in osmoprotective transcriptional regulation. *Proceedings of the National Academy of Sciences* 103, 8882-8887.

Ishikawa, F., Yasukawa, M., Lyons, B., Yoshida, S., Miyamoto, T., Yoshimoto, G., Watanabe, T., Akashi, K., Shultz, L.D., and Harada, M. (2005). Development of functional human blood and immune systems in NOD/SCID/IL2 receptor γ chain null mice. *Blood* 106, 1565-1573.

Ito, M., Hiramatsu, H., Kobayashi, K., Suzue, K., Kawahata, M., Hioki, K., Ueyama, Y., Koyanagi, Y., Sugamura, K., Tsuji, K., Heike, T., and Nakahata, T. (2002). NOD/SCID/ γ c null mouse: an excellent recipient mouse model for engraftment of human cells. *Blood* 100, 3175-3182.

Jaeckel, E., Lipes, M.A., and von Boehmer, H. (2004). Recessive tolerance to preproinsulin 2 reduces but does not abolish type 1 diabetes. *Nature immunology* 5, 1028-1035.

Janssen, H.L.A., Reesink, H.W., Lawitz, E.J., Zeuzem, S., Rodriguez-Torres, M., Patel, K., van der Meer, A.J., Patock, A.K., Chen, A., Zhou, Y., Persson, R., King, B.D., Kauppinen, S., Levin, A.A., and Hodges, M.R. (2013). Treatment of HCV Infection by Targeting MicroRNA. *New England Journal of Medicine* 368, 1685-1694.

Jiang, P., Rao, E.Y., Meng, N., Zhao, Y., and Wang, J.J. (2010). MicroRNA-17-92 significantly enhances radioresistance in human mantle cell lymphoma cells. *Radiation Oncology* 5, 100.

Johnston, R.J., Poholek, A.C., DiToro, D., Yusuf, I., Eto, D., Barnett, B., Dent, A.L., Craft, J., and Crotty, S. (2009). Bcl6 and Blimp-1 are reciprocal and antagonistic regulators of T follicular helper cell differentiation. *Science* 325, 1006-1010.

Jordan, M.S., Boesteanu, A., Reed, A.J., Petrone, A.L., Hohenbeck, A.E., Lerman, M.A., Najj, A., and Caton, A.J. (2001). Thymic selection of CD4+CD25+ regulatory T cells induced by an agonist self-peptide. *Nature immunology* 2, 301-306.

Kang, S.G., Liu, W.H., Lu, P., Jin, H.Y., Lim, H.W., Shepherd, J., Fremgen, D., Verdin, E., Oldstone, M.B., Qi, H., Teijaro, J.R., and Xiao, C. (2013). MicroRNAs of the miR-17-92 family are critical regulators of T(FH) differentiation. *Nature immunology* 14, 849-857.

Kappler, J.W., Roehm, N., and Marrack, P. (1987). T cell tolerance by clonal elimination in the thymus. *Cell* 49, 273-280.

Kearley, J., Barker, J.E., Robinson, D.S., and Lloyd, C.M. (2005). Resolution of airway inflammation and hyperreactivity after in vivo transfer of CD4+CD25+ regulatory T cells is interleukin 10 dependent. *The Journal of experimental medicine* 202, 1539-1547.

Kenefack, R., Wang, C.J., Kapadi, T., Wardzinski, L., Attridge, K., Clough, L.E., Heuts, F., Kogimtzis, A., Patel, S., Rosenthal, M., Ono, M., Sansom, D.M., Narendran, P., and Walker, L.S.K. (2015). Follicular helper T cell signature in type 1 diabetes. *The Journal of clinical investigation* 125, 292-303.

Ketting, R.F., Fischer, S.E., Bernstein, E., Sijen, T., Hannon, G.J., and Plasterk, R.H. (2001). Dicer functions in RNA interference and in synthesis of small RNA involved in developmental timing in *C. elegans*. *Genes Dev* 15, 2654-2659.

Khattari, R., Cox, T., Yasayko, S.A., and Ramsdell, F. (2003). An essential role for Scurfin in CD4+CD25+ T regulatory cells. *Nature immunology* 4, 337-342.

Kim, C.H., Rott, L.S., Clark-Lewis, I., Campbell, D.J., Wu, L., and Butcher, E.C. (2001). Subspecialization of CXCR5+ T cells: B helper activity is focused in a germinal center-localized subset of CXCR5+ T cells. *The Journal of experimental medicine* 193, 1373-1381.

Kim, N.H., Choi, S., Han, E.J., Hong, B.K., Choi, S.Y., Kwon, H.M., Hwang, S.Y., Cho, C.S., and Kim, W.U. (2014). The xanthine oxidase-NFAT5 pathway regulates macrophage activation and TLR-induced inflammatory arthritis. *European journal of immunology* *44*, 2721-2736.

King, M., Pearson, T., Shultz, L.D., Leif, J., Bottino, R., Trucco, M., Atkinson, M.A., Wasserfall, C., Herold, K.C., Woodland, R.T., Schmidt, M.R., Woda, B.A., Thompson, M.J., Rossini, A.A., and Greiner, D.L. (2008). A new Hu-PBL model for the study of human islet alloreactivity based on NOD-scid mice bearing a targeted mutation in the IL-2 receptor gamma chain gene. *Clinical Immunology* *126*, 303-314.

Kisielow, P., Bluthmann, H., Staerz, U.D., Steinmetz, M., and von Boehmer, H. (1988). Tolerance in T-cell-receptor transgenic mice involves deletion of nonmature CD4+8+ thymocytes. *Nature* *333*, 742-746.

Kondo, M., Takeshita, T., Higuchi, M., Nakamura, M., Sudo, T., Nishikawa, S., and Sugamura, K. (1994). Functional participation of the IL-2 receptor gamma chain in IL-7 receptor complexes. *Science* *263*, 1453-1454.

Kondo, M., Takeshita, T., Ishii, N., Nakamura, M., Watanabe, S., Arai, K., and Sugamura, K. (1993). Sharing of the interleukin-2 (IL-2) receptor gamma chain between receptors for IL-2 and IL-4. *Science* *262*, 1874-1877.

Kretschmer, K., Apostolou, I., Hawiger, D., Khazaie, K., Nussenzweig, M.C., and von Boehmer, H. (2005). Inducing and expanding regulatory T cell populations by foreign antigen. *Nature immunology* *6*, 1219-1227.

Krishnamurthy, B., Dudek, N.L., McKenzie, M.D., Purcell, A.W., Brooks, A.G., Gellert, S., Colman, P.G., Harrison, L.C., Lew, A.M., Thomas, H.E., and Kay, T.W. (2006). Responses against islet antigens in NOD mice are prevented by tolerance to proinsulin but not IGRP. *The Journal of clinical investigation* *116*, 3258-3265.

Kumar, P., Ban, H.-S., Kim, S.-S., Wu, H., Pearson, T., Greiner, D.L., Laouar, A., Yao, J., Haridas, V., Habiro, K., Yang, Y.-G., Jeong, J.-H., Lee, K.-Y., Kim, Y.-H., Kim, S.W., Peipp, M., Fey, G.H., Manjunath, N., Shultz, L.D., Lee, S.-K., and Shankar, P. (2008). T Cell-Specific siRNA Delivery Suppresses HIV-1 Infection in Humanized Mice. *Cell* *134*, 577-586.

Lambert, A.P., Gillespie, K.M., Thomson, G., Cordell, H.J., Todd, J.A., Gale, E.A.M., and Bingley, P.J. (2004). Absolute Risk of Childhood-Onset Type 1 Diabetes Defined by Human Leukocyte Antigen Class II Genotype: A Population-Based Study in the United Kingdom. *The Journal of Clinical Endocrinology & Metabolism* *89*, 4037-4043.

Lan, M.S., Lu, J., Goto, Y., and Notkins, A.L. (1994). Molecular cloning and identification of a receptor-type protein tyrosine phosphatase, IA-2, from human insulinoma. *DNA Cell Biol* 13, 505-514.

Langenkamp, A., Nagata, K., Murphy, K., Wu, L., Lanzavecchia, A., and Sallusto, F. (2003). Kinetics and expression patterns of chemokine receptors in human CD4+ T lymphocytes primed by myeloid or plasmacytoid dendritic cells. *European journal of immunology* 33, 474-482.

Lapidot, T., Pflumio, F., Doedens, M., Murdoch, B., Williams, D., and Dick, J. (1992). Cytokine stimulation of multilineage hematopoiesis from immature human cells engrafted in SCID mice. *Science* 255, 1137-1141.

Laskowski, I.A., Pratschke, J., Wilhelm, M.J., Dong, V.M., Beato, F., Taal, M., Gasser, M., Hancock, W.W., Sayegh, M.H., and Tilney, N.L. (2002). Anti-CD28 monoclonal antibody therapy prevents chronic rejection of renal allografts in rats. *J Am Soc Nephrol* 13, 519-527.

Lee, C., Liang, M.N., Tate, K.M., Rabinowitz, J.D., Beeson, C., Jones, P.P., and McConnell, H.M. (1998). Evidence that the autoimmune antigen myelin basic protein (MBP) Ac1-9 binds towards one end of the major histocompatibility complex (MHC) cleft. *The Journal of experimental medicine* 187, 1505-1516.

Lee, J.-Y., Skon, Cara N., Lee, You J., Oh, S., Taylor, Justin J., Malhotra, D., Jenkins, Marc K., Rosenfeld, M.G., Hogquist, Kristin A., and Jameson, Stephen C. (2015). The Transcription Factor KLF2 Restrains CD4+ T Follicular Helper Cell Differentiation. *Immunity* 42, 252-264.

Lee, K.H., Wucherpfennig, K.W., and Wiley, D.C. (2001a). Structure of a human insulin peptide-HLA-DQ8 complex and susceptibility to type 1 diabetes. *Nature immunology* 2, 501-507.

Lee, K.H., Wucherpfennig, K.W., and Wiley, D.C. (2001b). Structure of a human insulin peptide-HLA-DQ8 complex and susceptibility to type 1 diabetes. *Nature immunology* 2, 501-507.

Lee, Y., Ahn, C., Han, J., Choi, H., Kim, J., Yim, J., Lee, J., Provost, P., Radmark, O., Kim, S., and Kim, V.N. (2003). The nuclear RNase III Drosha initiates microRNA processing. *Nature* 425, 415-419.

Lewis, B.P., Shih, I.h., Jones-Rhoades, M.W., Bartel, D.P., and Burge, C.B. (2003). Prediction of Mammalian MicroRNA Targets. *Cell* 115, 787-798.

Li, Q.J., Chau, J., Ebert, P.J., Sylvester, G., Min, H., Liu, G., Braich, R., Manoharan, M., Soutschek, J., Skare, P., Klein, L.O., Davis, M.M., and Chen, C.Z. (2007). miR-181a is an intrinsic modulator of T cell sensitivity and selection. *Cell* 129, 147-161.

Li, Z., and Rana, T.M. (2014). Therapeutic targeting of microRNAs: current status and future challenges. *Nature reviews Drug discovery* 13, 622-638.

Lim, L.P., Lau, N.C., Garrett-Engele, P., Grimson, A., Schelter, J.M., Castle, J., Bartel, D.P., Linsley, P.S., and Johnson, J.M. (2005). Microarray analysis shows that some microRNAs downregulate large numbers of target mRNAs. *Nature* 433, 769-773.

Lindley, S., Dayan, C.M., Bishop, A., Roep, B.O., Peakman, M., and Tree, T.I.M. (2005). Defective Suppressor Function in CD4+CD25+ T-Cells From Patients With Type 1 Diabetes. *Diabetes* 54, 92-99.

Linterman, M.A., Beaton, L., Yu, D., Ramiscal, R.R., Srivastava, M., Hogan, J.J., Verma, N.K., Smyth, M.J., Rigby, R.J., and Vinuesa, C.G. (2010). IL-21 acts directly on B cells to regulate Bcl-6 expression and germinal center responses. *The Journal of experimental medicine* 207, 353-363.

Lis, R., Karrasch, C.C., Poulos, M.G., Kunar, B., Redmond, D., Duran, J.G.B., Badwe, C.R., Schachterle, W., Ginsberg, M., Xiang, J., Tabrizi, A.R., Shido, K., Rosenwaks, Z., Elemento, O., Speck, N.A., Butler, J.M., Scandura, J.M., and Rafii, S. (2017). Conversion of adult endothelium to immunocompetent haematopoietic stem cells. *Nature* 545, 439-445.

Liu, J., Carmell, M.A., Rivas, F.V., Marsden, C.G., Thomson, J.M., Song, J.-J., Hammond, S.M., Joshua-Tor, L., and Hannon, G.J. (2004). Argonaute2 Is the Catalytic Engine of Mammalian RNAi. *Science* 305, 1437-1441.

Liu, X., Chen, X., Zhong, B., Wang, A., Wang, X., Chu, F., Nurieva, R.I., Yan, X., Chen, P., van der Flier, L.G., Nakatsukasa, H., Neelapu, S.S., Chen, W., Clevers, H., Tian, Q., Qi, H., Wei, L., and Dong, C. (2014). Transcription factor achaete-scute homologue 2 initiates follicular T-helper-cell development. *Nature* 507, 513-518.

Lutz, M.B., Suri, R.M., Niimi, M., Ogilvie, A.L., Kukutsch, N.A., Rossner, S., Schuler, G., and Austyn, J.M. (2000). Immature dendritic cells generated with low doses of GM-CSF in the absence of IL-4 are maturation resistant and prolong allograft survival in vivo. *European journal of immunology* 30, 1813-1822.

Makino, S., Kunimoto, K., Muraoka, Y., Mizushima, Y., Katagiri, K., and Tochino, Y. (1980). Breeding of a non-obese, diabetic strain of mice. *Jikken dobutsu Experimental animals* 29, 1-13.

Marodon, G., Desjardins, D., Mercey, L., Baillou, C., Parent, P., Manuel, M., Caux, C., Bellier, B., Pasqual, N., and Klatzmann, D. (2009). High diversity of the immune repertoire in humanized NOD.SCID.gamma c^{-/-} mice. *European journal of immunology* 39, 2136-2145.

Martinez, J., and Tuschl, T. (2004). RISC is a 5' phosphomonoester-producing RNA endonuclease. *Genes Dev* 18, 975-980.

Mason, K., Denney, D.W., Jr., and McConnell, H.M. (1995). Kinetics of the reaction of a myelin basic protein peptide with soluble IAu. *Biochemistry* 34, 14874-14878.

Maus, M.V., Riley, J.L., Kwok, W.W., Nepom, G.T., and June, C.H. (2003). HLA tetramer-based artificial antigen-presenting cells for stimulation of CD4⁺ T cells. *Clinical Immunology* 106, 16-22.

McCune, J., Namikawa, R., Kaneshima, H., Shultz, L., Lieberman, M., and Weissman, I. (1988). The SCID-hu mouse: murine model for the analysis of human hematolymphoid differentiation and function. *Science* 241, 1632-1639.

Meister, G., Landthaler, M., Patkaniowska, A., Dorsett, Y., Teng, G., and Tuschl, T. (2004). Human Argonaute2 Mediates RNA Cleavage Targeted by miRNAs and siRNAs. *Molecular cell* 15, 185-197.

Mellanby, R.J., Thomas, D., Phillips, J.M., and Cooke, A. (2007). Diabetes in non-obese diabetic mice is not associated with quantitative changes in CD4⁺ CD25⁺ Foxp3⁺ regulatory T cells. *Immunology* 121, 15-28.

Mestas, J., and Hughes, C.C.W. (2004). Of mice and not men - differences between mouse and human immunology. *Journal of immunology* 172, 2731-2738.

Miller, A., Lider, O., and Weiner, H.L. (1991). Antigen-driven bystander suppression after oral administration of antigens. *The Journal of experimental medicine* 174, 791-798.

Misra, N., Bayry, J., Lacroix-Desmazes, S., Kazatchkine, M.D., and Kaveri, S.V. (2004). Cutting Edge: Human CD4+CD25+ T Cells Restrain the Maturation and Antigen-Presenting Function of Dendritic Cells. *The Journal of Immunology* 172, 4676-4680.

Miyakawa, H., Woo, S.K., Dahl, S.C., Handler, J.S., and Kwon, H.M. (1999). Tonicity-responsive enhancer binding protein, a Rel-like protein that stimulates transcription in response to hypertonicity. *Proceedings of the National Academy of Sciences* 96, 2538-2542.

Morita, R., Schmitt, N., Bentebibel, S.E., Ranganathan, R., Bourdery, L., Zurawski, G., Foucat, E., Dullaers, M., Oh, S., Sabzghabaei, N., Lavecchio, E.M., Punaro, M., Pascual, V., Banchereau, J., and Ueno, H. (2011). Human blood CXCR5(+)CD4(+) T cells are counterparts of T follicular cells and contain specific subsets that differentially support antibody secretion. *Immunity* 34, 108-121.

Mosier, D.E., Gulizia, R.J., Baird, S.M., and Wilson, D.B. (1988). Transfer of a functional human immune system to mice with severe combined immunodeficiency. *Nature* 335, 256-259.

Nakayama, M., Abiru, N., Moriyama, H., Babaya, N., Liu, E., Miao, D., Yu, L., Wegmann, D.R., Hutton, J.C., Elliott, J.F., and Eisenbarth, G.S. (2005). Prime role for an insulin epitope in the development of type 1 diabetes in NOD mice. *Nature* 435, 220-223.

Nanto-Salonen, K., Kupila, A., Simell, S., Siljander, H., Salonsaari, T., Hekkala, A., Korhonen, S., Erkkola, R., Sipila, J.I., Haavisto, L., Siltala, M., Tuominen, J., Hakalax, J., Hyoty, H., Ilonen, J., Veijola, R., Simell, T., Knip, M., and Simell, O. (2008). Nasal insulin to prevent type 1 diabetes in children with HLA genotypes and autoantibodies conferring increased risk of disease: a double-blind, randomised controlled trial. *Lancet* 372, 1746-1755.

Näntö-Salonen, K., Kupila, A., Simell, S., Siljander, H., Salonsaari, T., Hekkala, A., Korhonen, S., Erkkola, R., Sipilä, J.I., Haavisto, L., Siltala, M., Tuominen, J., Hakalax, J., Hyöty, H., Ilonen, J., Veijola, R., Simell, T., Knip, M., and Simell, O. (2008). Nasal insulin to prevent type 1 diabetes in children with HLA genotypes and autoantibodies conferring increased risk of disease: a double-blind, randomised controlled trial. *The Lancet* 372, 1746-1755.

National Institute of Environmental Health Sciences (2012). NIEHS Autoimmune Diseases fact sheet (North Carolina, USA).

Nerup, J., Platz, P., Andersen, O.O., Christy, M., Lyngse, J., Poulsen, J.E., Ryder, L.P., Thomsen, M., Nielsen, L.S., and Svejgaard, A. (1974). HL-A antigens and Diabetes Mellitus. *The Lancet* 304, 864-866.

Nguyen, C., Varney, M.D., Harrison, L.C., and Morahan, G. (2013). Definition of high-risk type 1 diabetes HLA-DR and HLA-DQ types using only three single nucleotide polymorphisms. *Diabetes* 62, 2135-2140.

Nistico, L., Buzzetti, R., Pritchard, L.E., Van der Auwera, B., Giovannini, C., Bosi, E., Larrad, M.T., Rios, M.S., Chow, C.C., Cockram, C.S., Jacobs, K., Mijovic, C., Bain, S.C., Barnett, A.H., Vandewalle, C.L., Schuit, F., Gorus, F.K., Tosi, R., Pozzilli, P., and Todd, J.A. (1996). The CTLA-4 gene region of chromosome 2q33 is linked to, and associated with, type 1 diabetes. *Belgian Diabetes Registry. Human molecular genetics* 5, 1075-1080.

Noguchi, M., Nakamura, Y., Russell, S., Ziegler, S., Tsang, M., Cao, X., and Leonard, W. (1993). Interleukin-2 receptor gamma chain: a functional component of the interleukin-7 receptor. *Science* 262, 1877-1880.

Nurieva, R.I., Chung, Y., Hwang, D., Yang, X.O., Kang, H.S., Ma, L., Wang, Y.H., Watowich, S.S., Jetten, A.M., Tian, Q., and Dong, C. (2008). Generation of T follicular helper cells is mediated by interleukin-21 but independent of T helper 1, 2, or 17 cell lineages. *Immunity* 29, 138-149.

Nurieva, R.I., Chung, Y., Martinez, G.J., Yang, X.O., Tanaka, S., Matskevitch, T.D., Wang, Y.-H., and Dong, C. (2009). Bcl6 Mediates the Development of T Follicular Helper Cells. *Science* 325, 1001-1005.

Odegard, J.M., Marks, B.R., DiPlacido, L.D., Poholek, A.C., Kono, D.H., Dong, C., Flavell, R.A., and Craft, J. (2008). ICOS-dependent extrafollicular helper T cells elicit IgG production via IL-21 in systemic autoimmunity. *The Journal of experimental medicine* 205, 2873-2886.

Ohbo, K., Suda, T., Hashiyama, M., Mantani, A., Ikebe, M., Miyakawa, K., Moriyama, M., Nakamura, M., Katsuki, M., Takahashi, K., Yamamura, K., and Sugamura, K. (1996). Modulation of hematopoiesis in mice with a truncated mutant of the interleukin-2 receptor gamma chain. *Blood* 87, 956-967.

Okazawa, H., Motegi, S.-i., Ohyama, N., Ohnishi, H., Tomizawa, T., Kaneko, Y., Oldenborg, P.-A., Ishikawa, O., and Matozaki, T. (2005). Negative Regulation of Phagocytosis in Macrophages by the CD47-SHPS-1 System. *The Journal of Immunology* 174, 2004-2011.

Oldenborg, P.-A., Zheleznyak, A., Fang, Y.-F., Lagenaur, C.F., Gresham, H.D., and Lindberg, F.P. (2000). Role of CD47 as a Marker of Self on Red Blood Cells. *Science* 288, 2051-2054.

Olsen, P.H., and Ambros, V. (1999). The lin-4 Regulatory RNA Controls Developmental Timing in *Caenorhabditis elegans* by Blocking LIN-14 Protein Synthesis after the Initiation of Translation. *Developmental Biology* 216, 671-680.

Onishi, Y., Fehervari, Z., Yamaguchi, T., and Sakaguchi, S. (2008). Foxp3⁺ natural regulatory T cells preferentially form aggregates on dendritic cells in vitro and actively inhibit their maturation. *Proceedings of the National Academy of Sciences* 105, 10113-10118.

Ouyang, W., Beckett, O., Ma, Q., Paik, J.H., DePinho, R.A., and Li, M.O. (2010). Foxo proteins cooperatively control the differentiation of Foxp3⁺ regulatory T cells. *Nature immunology* 11, 618-627.

Palmer, J., Asplin, C., Clemons, P., Lyen, K., Tatpati, O., Raghu, P., and Paquette, T. (1983). Insulin antibodies in insulin-dependent diabetics before insulin treatment. *Science* 222, 1337-1339.

Pandiyan, P., Zheng, L., Ishihara, S., Reed, J., and Lenardo, M.J. (2007). CD4⁺CD25⁺Foxp3⁺ regulatory T cells induce cytokine deprivation-mediated apoptosis of effector CD4⁺ T cells. *Nature immunology* 8, 1353-1362.

Patterson, C.C., Dahlquist, G.G., Gyurus, E., Green, A., Soltesz, G., and Group, E.S. (2009). Incidence trends for childhood type 1 diabetes in Europe during 1989-2003 and predicted new cases 2005-20: a multicentre prospective registration study. *Lancet* 373, 2027-2033.

Peer, D., Park, E.J., Morishita, Y., Carman, C.V., and Shimaoka, M. (2008). Systemic Leukocyte-Directed siRNA Delivery Revealing Cyclin D1 as an Anti-Inflammatory Target. *Science* 319, 627-630.

Petersen, J.S., Kulmala, P., Clausen, J.T., Knip, M., Dyrberg, T., and the Childhood Diabetes in Finland Study, G. (1999). Progression to Type 1 Diabetes Is Associated with a Change in the Immunoglobulin Isotype Profile of Autoantibodies to Glutamic Acid Decarboxylase (GAD65). *Clinical Immunology* 90, 276-281.

Poholek, A.C., Hansen, K., Hernandez, S.G., Eto, D., Chandele, A., Weinstein, J.S., Dong, X., Odegard, J.M., Kaech, S.M., Dent, A.L., Crotty, S., and Craft, J. (2010). In vivo regulation of Bcl6 and T follicular helper cell development. *Journal of immunology* 185, 313-326.

Polansky, J.K., Kretschmer, K., Freyer, J., Floess, S., Garbe, A., Baron, U., Olek, S., Hamann, A., von Boehmer, H., and Huehn, J. (2008). DNA methylation controls Foxp3 gene expression. *European journal of immunology* 38, 1654-1663.

Pöllänen, P.M., Lempainen, J., Laine, A.-P., Toppari, J., Veijola, R., Vähäsalo, P., Ilonen, J., Siljander, H., and Knip, M. (2017). Characterisation of rapid progressors to type 1 diabetes among children with HLA-conferred disease susceptibility. *Diabetologia* 60, 1284-1293.

Pontesilli, O., Carotenuto, P., Gazda, L.S., Pratt, P.F., and Prowse, S.J. (1987). Circulating lymphocyte populations and autoantibodies in non-obese diabetic (NOD) mice: a longitudinal study. *Clinical and experimental immunology* 70, 84-93.

Prochazka, M., Leiter, E., Serreze, D., and Coleman, D. (1987). Three recessive loci required for insulin-dependent diabetes in nonobese diabetic mice. *Science* 237, 286-289.

Pugliese, A., Zeller, M., Fernandez Jr., A., Zalcberg, L.J., Bartlett, R.J., Ricordi, C., Pietropaolo, M., Eisenbarth, G.S., Bennett, S.T., and Patel, D.D. (1997). The insulin gene is transcribed in the human thymus and transcription levels correlate with allelic variation at the *INS-VNTR-IDDM2* susceptibility locus for type 1 diabetes. *Nat Genet* 15, 293-297.

Rabin, D.U., Pleasic, S.M., Shapiro, J.A., Yoo-Warren, H., Oles, J., Hicks, J.M., Goldstein, D.E., and Rae, P.M. (1994). Islet cell antigen 512 is a diabetes-specific islet autoantigen related to protein tyrosine phosphatases. *The Journal of Immunology* 152, 3183-3188.

Rewers, M., Bugawan, T.L., Norris, J.M., Blair, A., Beaty, B., Hoffman, M., McDuffie, R.S., Jr., Hamman, R.F., Klingensmith, G., Eisenbarth, G.S., and Erlich, H.A. (1996). Newborn screening for HLA markers associated with IDDM: diabetes autoimmunity study in the young (DAISY). *Diabetologia* 39, 807-812.

Rewers, M., and Ludvigsson, J. (2016). Environmental risk factors for type 1 diabetes. *The Lancet* 387, 2340-2348.

Rolf, J., Bell, S.E., Kovesdi, D., Janas, M.L., Soond, D.R., Webb, L.M., Santinelli, S., Saunders, T., Hebeis, B., Killeen, N., Okkenhaug, K., and Turner, M. (2010). Phosphoinositide 3-kinase activity in T cells regulates the magnitude of the germinal center reaction. *Journal of immunology* 185, 4042-4052.

Roncador, G., Brown, P.J., Maestre, L., Hue, S., Martinez-Torrecuadrada, J.L., Ling, K.L., Pratap, S., Toms, C., Fox, B.C., Cerundolo, V., Powrie, F., and Banham, A.H. (2005). Analysis of FOXP3

protein expression in human CD4+CD25+ regulatory T cells at the single-cell level. *European journal of immunology* 35, 1681-1691.

Russell, S., Johnston, J., Noguchi, M., Kawamura, M., Bacon, C., Friedmann, M., Berg, M., McVicar, D., Witthuhn, B., Silvennoinen, O., and et, a. (1994). Interaction of IL-2R beta and gamma c chains with Jak1 and Jak3: implications for XSCID and XCID. *Science* 266, 1042-1045.

Russell, S., Keegan, A., Harada, N., Nakamura, Y., Noguchi, M., Leland, P., Friedmann, M., Miyajima, A., Puri, R., Paul, W., and et, a. (1993). Interleukin-2 receptor gamma chain: a functional component of the interleukin-4 receptor. *Science* 262, 1880-1883.

Sakaguchi, S., Sakaguchi, N., Asano, M., Itoh, M., and Toda, M. (1995). Immunologic self-tolerance maintained by activated T cells expressing IL-2 receptor alpha-chains (CD25). Breakdown of a single mechanism of self-tolerance causes various autoimmune diseases. *Journal of immunology* 155, 1151-1164.

Sauer, S., Bruno, L., Hertweck, A., Finlay, D., Leleu, M., Spivakov, M., Knight, Z.A., Cobb, B.S., Cantrell, D., O'Connor, E., Shokat, K.M., Fisher, A.G., and Merckenschlager, M. (2008). T cell receptor signaling controls Foxp3 expression via PI3K, Akt, and mTOR. *Proceedings of the National Academy of Sciences of the United States of America* 105, 7797-7802.

Schaerli, P., Willimann, K., Lang, A.B., Lipp, M., Loetscher, P., and Moser, B. (2000). CXC chemokine receptor 5 expression defines follicular homing T cells with B cell helper function. *The Journal of experimental medicine* 192, 1553-1562.

Schaffert, S.A., Loh, C., Wang, S., Arnold, C.P., Axtell, R.C., Newell, E.W., Nolan, G., Ansel, K.M., Davis, M.M., Steinman, L., and Chen, C.-Z. (2015). mir-181a-1/b-1 Modulates Tolerance through Opposing Activities in Selection and Peripheral T Cell Function. *The Journal of Immunology* 195, 1470-1479.

Schenker, M., Hummel, M., Ferber, K., Walter, M., Keller, E., Albert, E.D., Janka, H.-U., Kastendiek, C., Sorger, M., Louwen, F., and Ziegler, A.-G. (1999). Early expression and high prevalence of islet autoantibodies for DR3/4 heterozygous and DR4/4 homozygous offspring of parents with Type I diabetes: The German BABYDIAB study. *Diabetologia* 42, 671-677.

Schuler, W., Weiler, I.J., Schuler, A., Phillips, R.A., Rosenberg, N., Mak, T.W., Kearney, J.F., Perry, R.P., and Bosma, M.J. (1986). Rearrangement of antigen receptor genes is defective in mice with severe combined immune deficiency. *Cell* 46, 963-972.

Sebzda, E., Zou, Z., Lee, J.S., Wang, T., and Kahn, M.L. (2008). Transcription factor KLF2 regulates the migration of naive T cells by restricting chemokine receptor expression patterns. *Nature immunology* 9, 292-300.

Selbach, M., Schwanhausser, B., Thierfelder, N., Fang, Z., Khanin, R., and Rajewsky, N. (2008). Widespread changes in protein synthesis induced by microRNAs. *Nature* 455, 58-63.

Serr, I., Furst, R.W., Achenbach, P., Scherm, M.G., Gokmen, F., Haupt, F., Sedlmeier, E.M., Knopff, A., Shultz, L., Willis, R.A., Ziegler, A.G., and Daniel, C. (2016a). Type 1 diabetes vaccine candidates promote human Foxp3(+)Treg induction in humanized mice. *Nature communications* 7, 10991.

Serr, I., Fürst, R.W., Ott, V.B., Scherm, M.G., Nikolaev, A., Gökmen, F., Kälin, S., Zillmer, S., Bunk, M., Weigmann, B., Kunschke, N., Loretz, B., Lehr, C.-M., Kirchner, B., Haase, B., Pfaffl, M., Waisman, A., Willis, R.A., Ziegler, A.-G., and Daniel, C. (2016b). miRNA92a targets KLF2 and the phosphatase PTEN signaling to promote human T follicular helper precursors in T1D islet autoimmunity. *Proceedings of the National Academy of Sciences*, 201606646.

Serr, I., Scherm, M.G., Zahm, A.M., Schug, J., Flynn, V.K., Hippich, M., Kälin, S., Becker, M., Achenbach, P., Nikolaev, A., Gerlach, K., Kunschke, N., Loretz, B., Lehr, C.M., Kirchner, B., Spornraft, M., Haase, B., Segars, J.H., Küper, C., Palmisano, R., Waisman, A., Willis, R.A., Kim, W.-U., Weigmann, B., Kaestner, K.H., Ziegler, A.G., and Daniel, C. (2017). A miRNA181a/NFAT5 axis links impaired T cell tolerance induction with autoimmune Type 1 diabetes. *Science Translational Medicine*, *in revision*.

Shultz, L.D., Ishikawa, F., and Greiner, D.L. (2007). Humanized mice in translational biomedical research. *Nature reviews Immunology* 7, 118-130.

Shultz, L.D., Lyons, B.L., Burzenski, L.M., Gott, B., Chen, X., Chaleff, S., Kotb, M., Gillies, S.D., King, M., Mangada, J., Greiner, D.L., and Handgretinger, R. (2005). Human Lymphoid and Myeloid Cell Development in NOD/LtSz-scid IL2R null Mice Engrafted with Mobilized Human Hemopoietic Stem Cells. *The Journal of Immunology* 174, 6477-6489.

Shultz, L.D., Schweitzer, P.A., Christianson, S.W., Gott, B., Schweitzer, I.B., Tennent, B., McKenna, S., Mobraaten, L., Rajan, T.V., and Greiner, D.L. (1995). Multiple defects in innate and adaptive immunologic function in NOD/LtSz-scid mice. *The Journal of Immunology* 154, 180-191.

Sidney, J., Southwood, S., Moore, C., Oseroff, C., Pinilla, C., Grey, H.M., and Sette, A. (2013). Measurement of MHC/peptide interactions by gel filtration or monoclonal antibody capture. *Current protocols in immunology* / edited by John E Coligan [et al] *Chapter 18*, Unit 18 13.

Singal, D.P., and Blajchman, M.A. (1973). Histocompatibility (HL-A) Antigens, Lymphocytotoxic Antibodies and Tissue Antibodies in Patients with Diabetes Mellitus. *Diabetes* 22, 429-432.

Skyler, J.S., Krischer, J.P., Wolfsdorf, J., Cowie, C., Palmer, J.P., Greenbaum, C., Cuthbertson, D., Rafkin-Mervis, L.E., Chase, H.P., and Leschek, E. (2005). Effects of oral insulin in relatives of patients with type 1 diabetes: The Diabetes Prevention Trial--Type 1. *Diabetes care* 28, 1068-1076.

Snowwhite, I.V., Allende, G., Sosenko, J., Pastori, R.L., Messinger Cayetano, S., and Pugliese, A. (2017). Association of serum microRNAs with islet autoimmunity, disease progression and metabolic impairment in relatives at risk of type 1 diabetes. *Diabetologia*, 1-14.

Stadinski, B.D., Zhang, L., Crawford, F., Marrack, P., Eisenbarth, G.S., and Kappler, J.W. (2010a). Diabetogenic T cells recognize insulin bound to IAg7 in an unexpected, weakly binding register. *Proceedings of the National Academy of Sciences* 107, 10978-10983.

Stadinski, B.D., Zhang, L., Crawford, F., Marrack, P., Eisenbarth, G.S., and Kappler, J.W. (2010b). Diabetogenic T cells recognize insulin bound to IAg7 in an unexpected, weakly binding register. *Proceedings of the National Academy of Sciences of the United States of America* 107, 10978-10983.

Stambolic, V., Suzuki, A., de la Pompa, J.L., Brothers, G.M., Mirtsos, C., Sasaki, T., Ruland, J., Penninger, J.M., Siderovski, D.P., and Mak, T.W. (1998). Negative Regulation of PKB/Akt-Dependent Cell Survival by the Tumor Suppressor PTEN. *Cell* 95, 29-39.

Steiner, D.J., Kim, A., Miller, K., and Hara, M. (2010). Pancreatic islet plasticity: interspecies comparison of islet architecture and composition. *Islets* 2, 135-145.

Stone, Erica L., Pepper, M., Katayama, Carol D., Kerdiles, Yann M., Lai, C.-Y., Emslie, E., Lin, Yin C., Yang, E., Goldrath, Ananda W., Li, Ming O., Cantrell, Doreen A., and Hedrick, Stephen M. (2015). ICOS Coreceptor Signaling Inactivates the Transcription Factor FOXO1 to Promote Tfh Cell Differentiation. *Immunity* 42, 239-251.

Strowig, T., Rongvaux, A., Rathinam, C., Takizawa, H., Borsotti, C., Philbrick, W., Eynon, E.E., Manz, M.G., and Flavell, R.A. (2011). Transgenic expression of human signal regulatory protein

alpha in Rag2^{-/-}γc^{-/-} mice improves engraftment of human hematopoietic cells in humanized mice. *Proceedings of the National Academy of Sciences* 108, 13218-13223.

Sugimura, R., Jha, D.K., Han, A., Soria-Valles, C., da Rocha, E.L., Lu, Y.-F., Goettel, J.A., Serrao, E., Rowe, R.G., Malleshaiah, M., Wong, I., Sousa, P., Zhu, T.N., Ditadi, A., Keller, G., Engelman, A.N., Snapper, S.B., Doulatov, S., and Daley, G.Q. (2017). Haematopoietic stem and progenitor cells from human pluripotent stem cells. *Nature* 545, 432-438.

Sullivan, S.P., Koutsonanos, D.G., Del Pilar Martin, M., Lee, J.W., Zarnitsyn, V., Choi, S.O., Murthy, N., Compans, R.W., Skountzou, I., and Prausnitz, M.R. (2010). Dissolving polymer microneedle patches for influenza vaccination. *Nature medicine* 16, 915-920.

Takenaka, K., Prasolava, T.K., Wang, J.C., Mortin-Toth, S.M., Khalouei, S., Gan, O.I., Dick, J.E., and Danska, J.S. (2007). Polymorphism in Sirpa modulates engraftment of human hematopoietic stem cells. *Nature immunology* 8, 1313-1323.

Takeshita, T., Asao, H., Ohtani, K., Ishii, N., Kumaki, S., Tanaka, N., Munakata, H., Nakamura, M., and Sugamura, K. (1992). Cloning of the gamma chain of the human IL-2 receptor. *Science* 257, 379-382.

Tan, J., Jin, X., Zhao, R., Wei, X., Liu, Y., and Kong, X. (2015). Beneficial effect of T follicular helper cells on antibody class switching of B cells in prostate cancer. *Oncol Rep* 33, 1512-1518.

Thornton, A.M., and Shevach, E.M. (1998). CD4(+)CD25(+) Immunoregulatory T Cells Suppress Polyclonal T Cell Activation In Vitro by Inhibiting Interleukin 2 Production. *The Journal of experimental medicine* 188, 287-296.

Thumer, L., Adler, K., Bonifacio, E., Hofmann, F., Keller, M., Milz, C., Munte, A., and Ziegler, A.G. (2010). German new onset diabetes in the young incident cohort study: DiMelli study design and first-year results. *Rev Diabet Stud* 7, 202-208.

Todd, J.A., Bell, J.I., and McDevitt, H.O. (1987). HLA-DQ beta gene contributes to susceptibility and resistance to insulin-dependent diabetes mellitus. *Nature* 329, 599-604.

Todd, J.A., Walker, N.M., Cooper, J.D., Smyth, D.J., Downes, K., Plagnol, V., Bailey, R., Nejentsev, S., Field, S.F., Payne, F., Lowe, C.E., Szeszko, J.S., Hafler, J.P., Zeitels, L., Yang, J.H., Vella, A., Nutland, S., Stevens, H.E., Schuilenburg, H., Coleman, G., Maisuria, M., Meadows, W., Smink, L.J., Healy, B., Burren, O.S., Lam, A.A., Ovington, N.R., Allen, J., Adlem, E., Leung, H.T., Wallace,

C., Howson, J.M., Guja, C., Ionescu-Tirgoviste, C., Genetics of Type 1 Diabetes in, F., Simmonds, M.J., Heward, J.M., Gough, S.C., Wellcome Trust Case Control, C., Dunger, D.B., Wicker, L.S., and Clayton, D.G. (2007). Robust associations of four new chromosome regions from genome-wide analyses of type 1 diabetes. *Nature genetics* 39, 857-864.

Trama, J., Go, W.Y., and Ho, S.N. (2002). The Osmoprotective Function of the NFAT5 Transcription Factor in T Cell Development and Activation. *The Journal of Immunology* 169, 5477-5488.

Truesdell, S.S., Mortensen, R.D., Seo, M., Schroeder, J.C., Lee, J.H., LeTonqueze, O., and Vasudevan, S. (2012). MicroRNA-mediated mRNA translation activation in quiescent cells and oocytes involves recruitment of a nuclear microRNP. *Sci Rep* 2, 842.

Vafiadis, P., Bennett, S.T., Todd, J.A., Nadeau, J., Grabs, R., Goodayer, C.G., Wickramasinghe, S., Colle, E., and Polychronakos, C. (1997). Insulin expression in human thymus is modulated by *INS* VNTR alleles at the *IDDM2* locus. *nat Genet* 15, 289-292.

Vasudevan, S. (2012). Posttranscriptional upregulation by microRNAs. *Wiley interdisciplinary reviews RNA* 3, 311-330.

Vasudevan, S., and Steitz, J.A. (2007). AU-Rich-Element-Mediated Upregulation of Translation by FXR1 and Argonaute 2. *Cell* 128, 1105-1118.

Vasudevan, S., Tong, Y., and Steitz, J.A. (2007). Switching from repression to activation: microRNAs can up-regulate translation. *Science* 318, 1931-1934.

Vella, A., Cooper, J.D., Lowe, C.E., Walker, N., Nutland, S., Widmer, B., Jones, R., Ring, S.M., McArdle, W., Pembrey, M.E., Strachan, D.P., Dunger, D.B., Twells, R.C.J., Clayton, D.G., and Todd, J.A. (2005). Localization of a Type 1 Diabetes Locus in the *IL2RA/CD25* Region by Use of Tag Single-Nucleotide Polymorphisms. *American Journal of Human Genetics* 76, 773-779.

Verginis, P., McLaughlin, K.A., Wucherpfennig, K.W., von Boehmer, H., and Apostolou, I. (2008). Induction of antigen-specific regulatory T cells in wild-type mice: visualization and targets of suppression. *Proceedings of the National Academy of Sciences of the United States of America* 105, 3479-3484.

Warncke, K., Krasmann, M., Puff, R., Dunstheimer, D., Ziegler, A.G., and Beyerlein, A. (2013). Does diabetes appear in distinct phenotypes in young people? Results of the diabetes mellitus incidence Cohort Registry (DiMelli). *PloS one* 8, e74339.

Wenzlau, J.M., Juhl, K., Yu, L., Moua, O., Sarkar, S.A., Gottlieb, P., Rewers, M., Eisenbarth, G.S., Jensen, J., Davidson, H.W., and Hutton, J.C. (2007). The cation efflux transporter ZnT8 (Slc30A8) is a major autoantigen in human type 1 diabetes. *Proceedings of the National Academy of Sciences* *104*, 17040-17045.

Wucherpfennig, K.W., and Sethi, D. (2011). T cell receptor recognition of self and foreign antigens in the induction of autoimmunity. *Seminars in immunology* *23*, 84-91.

Xiao, C., Srinivasan, L., Calado, D.P., Patterson, H.C., Zhang, B., Wang, J., Henderson, J.M., Kutok, J.L., and Rajewsky, K. (2008). Lymphoproliferative disease and autoimmunity in mice with increased miR-17-92 expression in lymphocytes. *Nature immunology* *9*, 405-414.

Xiao, N., Eto, D., Elly, C., Peng, G., Crotty, S., and Liu, Y.-C. (2014). The E3 ubiquitin ligase Itch is required for the differentiation of follicular helper T cells. *Nature immunology* *15*, 657-666.

Xu, H., Li, X., Liu, D., Li, J., Zhang, X., Chen, X., Hou, S., Peng, L., Xu, C., Liu, W., Zhang, L., and Qi, H. (2013). Follicular T-helper cell recruitment governed by bystander B cells and ICOS-driven motility. *Nature* *496*, 523-527.

Yang, J., Chow, I.-T., Sosinowski, T., Torres-Chinn, N., Greenbaum, C.J., James, E.A., Kappler, J.W., Davidson, H.W., and Kwok, W.W. (2014). Autoreactive T cells specific for insulin B:11-23 recognize a low-affinity peptide register in human subjects with autoimmune diabetes. *Proceedings of the National Academy of Sciences of the United States of America* *111*, 14840-14845.

Yoon, H.-J., You, S., Yoo, S.-A., Kim, N.-H., Kwon, H.M., Yoon, C.-H., Cho, C.-S., Hwang, D., and Kim, W.-U. (2011). NFAT5 is a critical regulator of inflammatory arthritis. *Arthritis and rheumatism* *63*, 10.1002/art.30229.

You, S., Belghith, M., Cobbold, S., Alyanakian, M.-A., Gouarin, C., Barriot, S., Garcia, C., Waldmann, H., Bach, J.-F., and Chatenoud, L. (2005). Autoimmune Diabetes Onset Results From Qualitative Rather Than Quantitative Age-Dependent Changes in Pathogenic T-Cells. *Diabetes* *54*, 1415-1422.

Yu, D., Rao, S., Tsai, L.M., Lee, S.K., He, Y., Sutcliffe, E.L., Srivastava, M., Linterman, M., Zheng, L., Simpson, N., Ellyard, J.I., Parish, I.A., Ma, C.S., Li, Q.J., Parish, C.R., Mackay, C.R., and Vinuesa, C.G. (2009). The transcriptional repressor Bcl-6 directs T follicular helper cell lineage commitment. *Immunity* *31*, 457-468.

Zamore, P.D., Tuschl, T., Sharp, P.A., and Bartel, D.P. (2000). RNAi: Double-Stranded RNA Directs the ATP-Dependent Cleavage of mRNA at 21 to 23 Nucleotide Intervals. *Cell* 101, 25-33.

Ziegler, A.-G., and Bonifacio, E. (2012). Age-related islet autoantibody incidence in offspring of patients with type 1 diabetes. *Diabetologia* 55, 1937-1943.

Ziegler, A.G., Hummel, M., Schenker, M., and Bonifacio, E. (1999). Autoantibody appearance and risk for development of childhood diabetes in offspring of parents with type 1 diabetes: the 2-year analysis of the German BABYDIAB Study. *Diabetes* 48, 460-468.

Ziegler, A.G., and Nepom, G.T. (2010). Prediction and pathogenesis in type 1 diabetes. *Immunity* 32, 468-478.

Ziegler, A.G., Rewers, M., Simell, O., Simell, T., Lempainen, J., Steck, A., Winkler, C., Ilonen, J., Veijola, R., Knip, M., Bonifacio, E., and Eisenbarth, G.S. (2013). Seroconversion to Multiple Islet Autoantibodies and Risk of Progression to Diabetes in Children. *JAMA* 309, 2473-2479.

Zotos, D., Coquet, J.M., Zhang, Y., Light, A., D'Costa, K., Kallies, A., Corcoran, L.M., Godfrey, D.I., Toellner, K.M., Smyth, M.J., Nutt, S.L., and Tarlinton, D.M. (2010). IL-21 regulates germinal center B cell differentiation and proliferation through a B cell-intrinsic mechanism. *The Journal of experimental medicine* 207, 365-378.

Danksagung

Zu allererst möchte ich mich bei Carolin Daniel bedanken, für die außergewöhnliche Betreuung und Förderung und den regen Ideenaustausch. Danke für deine immer offene Tür und Unterstützung und für deine ansteckende und motivierende Art. Ich sage nur: „Passion for Science“!

Ich bedanke mich außerdem herzlich bei Prof. Dr. Anette-Gabriele Ziegler für die Möglichkeit meine Doktorarbeit an ihrem Institut durchzuführen. Vielen Dank für die vielen hilfreichen Diskussionen und für das Patientenmaterial!

Vielen Dank auch an Prof. Dr. Martin Hrabé-de-Angelis für die Betreuung meiner Doktorarbeit als Zweitbetreuer, für den Input in den Thesis Committee Meetings und für das Interesse!

Ich danke auch allen Kollaborationspartnern, die Reagenzien oder Mäuse bereitgestellt haben und mit den Experimenten geholfen haben. Insbesondere bedanke ich mich ganz herzlich bei Benno Weigmann und seiner Arbeitsgruppe für die Unterstützung der Immunhistochemie!

Vielen Dank ebenfalls an alle Mitarbeiter des IDF1 für die tolle Zusammenarbeit! Insbesondere bedanke ich mich bei allen Studienbetreuern und den Ärzten für das Sammeln der Proben und natürlich bei allen Studienteilnehmern für das Bereitstellen des Probenmaterials. Ohne sie wäre diese Arbeit so nicht möglich gewesen. Ein herzliches Dankeschön auch an alle Technischen Assistenten und das TEDDY Team für eure offene Art und dafür, dass ihr mich von Anfang an willkommen geheißen habt.

Ein ganz besonderes Dankeschön geht an die gesamte Arbeitsgruppe Ag Daniel und alle gegenwärtigen und früheren Mitarbeiter. Besonders bedanke ich mich bei Maike Becker, Victoria Flynn und Verena Ott. Ihr habt die Zeit hier für mich unvergesslich gemacht und eine tolle Arbeitsatmosphäre geschaffen. Vielen Dank, dass ihr immer mit angepackt habt, wenn mal Not am Mann war, dass ihr immer ein offenes Ohr hattet und vielen Dank für die vielen hilfreichen Diskussionen.

Zuletzt möchte ich mich bei meiner Familie bedanken für ihre Unterstützung und insbesondere bei Till für sein Verständnis für die vielen Nachtschichten und durchgearbeiteten Wochenenden. Ohne dich hätte ich das nicht geschafft!